



**HAL**  
open science

# Electrogenerated divalent samarium for CO activation: applications in carboxylic acid synthesis

Sakna Bazzi

► **To cite this version:**

Sakna Bazzi. Electrogenerated divalent samarium for CO activation : applications in carboxylic acid synthesis. Catalysis. Université Paris Saclay (COMUE), 2019. English. NNT : 2019SACLS397 . tel-03917104

**HAL Id: tel-03917104**

**<https://theses.hal.science/tel-03917104>**

Submitted on 1 Jan 2023

**HAL** is a multi-disciplinary open access archive for the deposit and dissemination of scientific research documents, whether they are published or not. The documents may come from teaching and research institutions in France or abroad, or from public or private research centers.

L'archive ouverte pluridisciplinaire **HAL**, est destinée au dépôt et à la diffusion de documents scientifiques de niveau recherche, publiés ou non, émanant des établissements d'enseignement et de recherche français ou étrangers, des laboratoires publics ou privés.

# Electrogenerated divalent samarium for CO<sub>2</sub> activation: applications in carboxylic acid synthesis.

Thèse de doctorat de l'Université Paris-Saclay  
préparée à l'Université Paris-Sud

École doctorale n°571 Sciences chimiques : molécules, matériaux,  
instrumentation et biosystèmes (2MIB)  
Spécialité de doctorat : Chimie

Thèse présentée et soutenue à Orsay, le 13 Novembre 2019, par

**Mme Sakna Bazzi**

Composition du Jury :

M. A. Aukauloo Professeur, Université Paris-Sud (ICMMO UMR 8182)	Président
M. D. J. Procter Professeur, University of Manchester	Rapporteur
Mme. E. Metay Chargée de recherche, Université de Lyon (CASYEN-ICBMC)	Rapporteur
M. E. Leonel Professeur, Université Paris Est Créteil (ICMPE-ESO)	Examineur
M M. Mellah Maître de conférence, Université Paris-Sud (ICMMO UMR 8182)	Directeur de thèse
Mme. E. Schulz Directrice de recherche, Université Paris-Sud (ICMMO UMR 8182)	Invitée



---

# French Summary

---

La nature constitue le système le plus harmonisé sur cette terre. Au fil des ans, elle a toujours réussi à maintenir l'équilibre entre tous les écosystèmes tout en fournissant à l'être humain ce dont il a besoin. Cependant, l'énorme croissance de la population a déclenché des productions industrielles massives pour satisfaire les besoins, en particulier au cours des dernières décennies. En conséquence, des menaces écologiques sont apparues suite à la surexploitation des ressources naturelles et au rejet des déchets nocifs, principalement dans l'air, mais également dans l'eau et le sol.

Rapidement, la pollution de l'air a renforcé le réchauffement climatique (vagues de chaleur répétitives, désertification, pluies acides...) causé principalement par les gaz à effet de serre, et en particulier le dioxyde de carbone.

Face à ces crises environnementales, les scientifiques ont été les premiers à déclencher l'alerte sur les conséquences de ce changement climatique brusque si les niveaux de pollution de l'environnement sont maintenus à un niveau aussi élevé. Par la suite, des efforts prometteurs pour réduire les normes du principal responsable, le CO<sub>2</sub>, dans l'atmosphère ont commencé à se développer en tentant, par exemple, de le stocker sous terre ou de le capturer par des membranes sélectives.

Les chimistes ont réfléchi différemment en proposant d'exploiter ce gaz en le transformant en des composés chimiques d'intérêts, la fixation du CO<sub>2</sub> s'est alors vite développée et de nouvelles stratégies basées sur le concept du CO<sub>2</sub> comme brique de synthèse ont fourni des de nombreuses molécules de haute valeur ajoutée dans les domaines pharmaceutiques, agrochimiques et en chimie fine. Malheureusement, les nombreuses approches proposées ajoutent plus de complications qu'elles ne permettent de résoudre le dilemme principal en exigeant des températures trop élevées ou trop basses, une importante pression de CO<sub>2</sub>, voire pire en produisant plus de déchets tels que des déchets métalliques.

Depuis son utilisation en chimie de synthèse, l'électrochimie s'est révélée être un outil de choix pour réaliser des réactions chimiques dans des conditions plus douces. C'est pourquoi, la fixation du CO<sub>2</sub> en s'appuyant sur les avantages qu'apporte l'électrochimie a trouvé très vite été envisagée comme alternative aux additifs métalliques, voire mieux, comme moyen prometteur de synthèse de produits chimiques précieux tels que les acides carboxyliques, sans production de déchets supplémentaires. En dépit d'avancées significatives, le principal inconvénient demeure le potentiel électrochimique élevé requis pour la synthèse de composés visés, en plus du faible rendement et de la faible sélectivité.

Dans notre groupe, nous avons utilisé l'électrochimie pour mettre en oeuvre une méthode de génération *in situ* de complexes de samarium divalents réputés être des réducteurs suffisamment puissants pour initier des transformations radicalaires, grâce au transfert monoélectronique. Plus récemment, nous avons mis au point des réactions électrocatalytiques en utilisant une quantité

---

catalytique de ces complexes pour obtenir des résultats surprenants, souvent difficiles à obtenir avec d'autres réactifs ou nécessitant l'utilisation d'une quantité sur-stoechiométrique d'un co-réducteur.

Dans cette thèse, nous nous intéressons à explorer la réactivité de ces complexes de samarium divalents (réducteurs puissants) pour réaliser réduction efficace du CO<sub>2</sub>, en utilisant l'électrochimie comme source d'électrons afin de synthétiser des acides carboxyliques à partir de substrats commerciaux.

Après une introduction générale et un état de l'art autour de la problématique du CO<sub>2</sub>, dans le premier chapitre, nous aborderons la carboxylation de chlorures et de bromures aromatiques sous atmosphère de CO<sub>2(g)</sub> avec un complexe de samarium divalent électrogénéré. L'espèce active Sm (II) est électrogénérée en continu à partir d'une électrode de samarium métallique dans le diméthylformamide DMF comme solvant en présence de tétrafluoroborate de tétrabutylammonium (*n*Bu<sub>4</sub>NBF<sub>4</sub>) servant à la fois d'électrolyte support et de source de ligands du samarium. Les études mécanistiques ont révélés que dans le cas des bromures, le mécanisme de la réaction a lieu suivant un couplage radicalaire alors dans le cas des chlorures, c'est une substitution radicalaire.

Dans le deuxième chapitre, nous avons étudié la carboxylation des dérivés du chlorure de benzyle, dans l'acétonitrile, afin d'obtenir des acides phénylacétiques en utilisant cette fois une quantité catalytique de 20 mol% de SmI<sub>2</sub> précisément électrogénérée avant l'addition du produit de départ. Dans cette réaction, l'utilisation de carboglace comme source de CO<sub>2</sub> s'est révélé être avantageuse. Il est également nécessaire d'utiliser le chlorure de triméthylsilyle TMSCl comme agent oxophile pour dissocier l'espèce trivalent de Sm du produit de la réaction et régénérer l'espèce divalente active. Des expériences de contrôle ont montrés que le mécanisme se fait aussi suivant un processus de substitution radicalaire et que la formation du radical benzylique n'est jamais observée sous nos conditions électrochimiques. L'ensemble de ces résultats confirment une réelle activation du CO<sub>2</sub> en radical carboxylate correspondant pour initier la carboxylation.

Le troisième chapitre concerne l'hydrocarboxylation des dérivés de styrène et de phénylacétylène, catalysée par 10 mol% de SmCl<sub>2</sub> généré in situ par l'électroréduction de sels de SmCl<sub>3</sub>, en présence de *ter*-butanol et bien sûr, TMSCl dans l'acétonitrile. Sous ces conditions, les alcynes ont fournis un mélange de acide carboxylique aliphatique et acide acrylique alors que les alcynes protégés ont réagis pour produire exclusivement les correspondants acides acryliques. L'ensembles des acides ainsi obtenus montre une selectivité totale pour une addition anti-Markovnikov du CO<sub>2</sub>, ce qui est tout à fait en accord avec un processus radicalaire de fixation du CO<sub>2</sub>. Les études mécanistiques, nous ont permis de mettre en évidence que l'acétonitrile (CH<sub>3</sub>CN) utilisée comme solvant est la source de proton dans cette transformations d'hydrocarboxylation.





---

# Acknowledgement

---

*Four years ago, my feet landed in Paris, but my mind remained up in the sky, with all my dreams and goals. Now, I am more than happy to say that most of these dreams have been accomplished, thanks to many God's blessings I had in the last couple of years.*

*First of all, I will start with my supportive loving family. **Dad, Mom, my sisters (Farah, Zeinab, Jana, Hala), my brother (Mohamed Ali), and the tiny cute creatures (Jawad, Fatima, Ali, Ali El Reda, Zeinab)**, words are not enough to express how much I love you and count on you. Thank you for being the wind under my wings and the source of joy in the darkest days. To my fiancé, **Hassan**, you were and still my backbone and the shoulder that I lean on whenever I am tired to rise again full of confidence and energy to conquer the world. Thank you for pushing me every day and for bringing out the best in me.*

*I would like to deeply acknowledge the **IDEX-Paris Saclay International Master's Scholarship Program** that allowed me to start my journey in France. For her belief in me and her continuous support, I cannot be thankful enough for Dr. Nada Jaber who inspired me and knew that I am fully capable of taking the responsibility of representing the Lebanese University in the academic year 2015-2016. I would also take a moment to thank **Dr. David Bonnaffé** for accepting my Master 2 application, but also **Dr. Cyrille Kouklovsky** for his help during this year.*

*A few months later, I was thrilled to find myself in the **Molecular Catalysis Laboratory** where I was not just a student, I was a member of this loving family. Starting from **Dr. Emmanuelle Schulz** ( I hope I wrote it for once correctly!), thank you, "mère" Schulz, for being the nicest, most honest and caring person during my Master's and my Ph.D. As you enriched my personality in many ways, I hope I also added something to you that will always remind you of me.*

*For **Dr. Mohamed Mellah**, I owe you countless things. Thank you for introducing me to the Samarium and electrochemistry world, where I learned that everything is possible, and nothing is as you expect. Thank you for trusting me with this project that I represented for the **Ministry of Education thesis funding** that I would endlessly be thankful for providing me with enough money to deliver this work. Thank you, Momo, for, in your way, helping me to become the independent, confident and strong research that I am now. And lastly, thank you for not only being my supervisor but also for being a good friend of mine.*

*Molecular catalysis family was generous enough to introduce me to such great people that I will always remember. For all the permanent members, thank you for your advice and kindness, in some days, it was just what I need to survive the bad times. Special thanks to **Marie, Lucile, Clément**, and **Nicolas** who were there to support me during my first baby steps in the lab. Each one of you contributed somehow to what I became today, and I wish you all the best. To **Mariam, Sandra, Alexandre, Guillaume, Zhilong, Zhiwei** you were more like sisters and brothers than colleagues, the moments we shared will always be alive in my heart. Best of luck with your Ph.D. journey, don't worry, you will survive, believe me! For all the young members in this family, know*



---

*that you are in good hands and everything will turn out just fine. Most of all, do not forget to have fun, because Chemistry is fun!*

*I dedicate a special part to **Dr. Sara Patricia Morcillo**. You are an amazing person and I am more than proud to call you a friend even if we have not seen each other since the first year of my Ph.D., still, your wisdom guided me in my journey and for that, I will always be thankful for.*

*Another blessing I had in 2018-2019 was meeting **Dr. Thomas Castanheiro**, an intelligent and creative researcher who changed my point of thinking in chemistry. May you accomplish, my “bro”, all your goals and dreams.*

*For her selfless acts and help, I express my sincere admiration to **Emilie Kolodziej**. I believe that the **ECM** is so lucky to have you, Wonder Woman.*

*Special acknowledgment for **Prof. Ally Aukauloo**, our discussions always filled me up with a great dose of creativity. Thank you for devoting this time to hear my concerns and my ideas.*

*I kept for the last the greatest people ever, my third family, my Lebanese friends. My heartfelt gratitude for **Fatima, Moussa, Zahraa, Alaa, Mohamad, Marwa, Issa, Ali and Lama**, I had an amazing time knowing you and being part of your lives. Thank you for your support and most of all for your availability whenever I needed help. You are an excellent example of Lebanese kindness, generosity, and culture. I wish you all a great successful life.*

*For their shiny heart-warming smile; I tend to deeply thank **Mansoura and Nelly**.*

*Finally, huge thanks for all the members of **Institut de Chimie Moleculaire et des Matériaux d’Orsay**. It was my great pleasure to meet you all.*

*With love,*

*Sakna BAZZI*





---

# Table of Contents

---

General Introduction.....	1
Carbon Dioxide.....	7
1. Generality about the increasing carbon dioxide problematic.....	7
a. Sources and role of CO <sub>2</sub> in nature.....	7
b. Global warming .....	8
c. Consequences and solutions.....	9
2. Chemical properties of CO <sub>2</sub> .....	11
a. The structure of CO <sub>2</sub> and its existing forms in solution.....	11
b. CO <sub>2</sub> fixation: insertion vs. activation.....	13
c. Reported synthesis of R-COOH using CO <sub>2</sub> as C <sub>1</sub> -building block.....	17
Samarium (II): a powerful reducing agent.....	22
1. Complexes of divalent samarium and their applications .....	22
a. The synthesis of SmI <sub>2</sub> .....	22
b. Other complexes of divalent samarium .....	23
c. The influence of additives on Sm(II) complexes reactivity .....	24
d. The challenge behind developing processes catalyzed by Sm(II).....	27
e. Electrogenerated Samarium complexes .....	29
f. Electrocatalysis using Sm(II) complexes.....	31
g. Carbon dioxide activation using divalent Sm in the literature.....	33
Summary.....	37
Carboxylation of aryl halides using electrogenerated samarium(II) complex via CO <sub>2</sub> activation.....	43
1. Aryl carboxylic acids: state of the art .....	43
2. Synthesis of benzoic acids using stoichiometric organometallic and metal-based catalysis .....	44
3. The advance achieved by electrochemistry in the synthesis of benzoic acids .....	49
4. Carboxylation of aryl halides via CO <sub>2</sub> activation using electrogenerated Sm(II) complexes.....	51
5. Mechanistic studies.....	55
a. Control experiments.....	55
b. Kagan's reagent vs. the electrogenerated Sm(II).....	56
c. Radical trapping experiment .....	57
6. Electrochemical Studies.....	58
a. The oxidation of samarium: a noteworthy interaction .....	58
b. Sm(II)+ CO <sub>2</sub> = CO <sub>2</sub> activation.....	59
7. Proposed mechanism .....	59
8. Attempts to perform a catalytic reaction.....	60
9. Conclusion and Perspectives.....	61
Experimental Part .....	65

Electrogenerated Sm(II)-catalyzed the carboxylation of benzyl chloride derivatives .....	75
1. Phenylacetic acids: state of the art .....	75
2. Catalytic carboxylation of organic (pseudo)halides.....	76
a. Using benzyl halides as starting material.....	76
b. Using benzyl esters derivatives as starting material .....	78
c. Using ammonium salts as starting material .....	79
d. Photocarboxylation of benzylic C–H bonds .....	80
3. Electrocarboxylation of benzyl chlorides.....	81
b. Direct Electrocarboxylation .....	81
b. Indirect electrocarboxylations of benzyl chloride derivatives .....	83
4. Carboxylation of benzyl chlorides .....	84
5. Sm(II)-catalyzed carboxylation of benzyl chlorides via CO <sub>2</sub> activation.....	86
a. Optimization & Scope of the catalytic carboxylation .....	86
b. Mechanistic studies .....	88
c. Electrochemical studies of the catalytic carboxylation of benzyl chloride .....	91
6. Conclusion and perspectives .....	92
Experimental Part .....	95
Electrogenerated Sm(II)-catalyzed the hydrocarboxylation of styrene and phenylacetylene derivatives.....	107
1. Hydrocarboxylation of styrene and phenylacetylene derivatives: state of the art.....	107
2. Catalytic $\beta$ -hydrocarboxylation of styrene and phenylacetylene derivatives .....	109
a. The use of organoboranes .....	109
b. The use of organozinc and Grignard reagent .....	111
c. Ligand-controlled hydrocarboxylation .....	112
d. Site-selectivity controlled by the substrate .....	114
3. $\beta$ -Selective hydrocarboxylation initiated by CO <sub>2</sub> <sup>-</sup> .....	115
4. Electrocarboxylation of styrene and phenylacetylene derivatives .....	116
a. Electrocarboxylation using sacrificial anodes.....	116
b. Carboxylations via chemical mediators .....	119
5. Catalytic hydrocarboxylation of styrene and phenylacetylene derivatives mediated by electrogenerated Sm(II) .....	121
a. Hydrocarboxylation of styrene derivatives .....	121
b. Hydrocarboxylation of phenylacetylene derivatives.....	124
c. Mechanistic studies .....	128
6. Conclusion and Perspectives.....	136
General conclusion .....	141
Experimental Part .....	145





---

# Table of Figures

---

Figure 1: Carbon dioxide cycle.....	7
Figure 2: Chart shows observed monthly temperatures (grey line), estimated human-caused warming (red), and idealized potential pathways to meeting 1.5°C limit in 2100 (grey, blue, and purple). All relative to 1850-1900. ....	8
Figure 3: The required soil composition to store the carbon dioxide underground.....	10
Figure 4: Carbon dioxide uses. ....	10
Figure 5: Different binding modes of carbon dioxide with a transition metal center. ....	12
Figure 6: Possible mechanistic pathways for the carboxylation of halogenated reagents. ....	14
Figure 7: Reduction of carbon dioxide to the corresponding radical anion. ....	15
Figure 8: Carbon dioxide reduction to oxalic acid, formic acid, methanol or methane.....	16
Figure 9: Carboxylation of substituted and unsaturated substrates showing the possible products.....	16
Figure 10: The role of Lewis acid in the CO <sub>2</sub> insertion step. ....	17
Figure 11: The mechanism of carboxylation depending on the substrate nature and the additives.....	18
Figure 12: Oxidative and reductive quenching mechanisms in a photochemical reaction .....	19
Figure 13: The difference between the electrocarboxylation using inert anode ( <i>on the left</i> ) and sacrificial anode ( <i>on the right</i> ).....	21
Figure 14: The reported optimization of the synthesis and the electrolysis of SmI <sub>2</sub> between 1907 and 2012. ...	23
Figure 15: Sm(II)-based reductants. ....	23
Figure 16: Applications of the divalent SmI <sub>2</sub> in the literature. ....	24
Figure 17: Lewis Base reagents used with SmI <sub>2</sub> chemistry.....	25
Figure 18: Stereoselective cyclization of $\gamma, \delta$ -unsaturated ketones mediated by SmI <sub>2</sub> according to the alcohol cosolvent. <sup>36</sup> .....	26
Figure 19: Comparison between the redox potential of SmI <sub>2</sub> , SmBr <sub>2</sub> , and SmCl <sub>2</sub> ( <i>on the left</i> ); The redox potential of inorganic additives compared with the Sm(II) ( <i>on the right</i> ). ....	27
Figure 20: Pinacolisation mechanism catalyzed by SmI <sub>2</sub> . ....	28
Figure 21: The proposed mechanism for the cyclization cascades catalyzed by SmI <sub>2</sub> . ....	28
Figure 22: Samarium(II) complexes prepared by electrolysis from Sm anode. ....	30
Figure 23: The reduction of aliphatic chloride by divalent samarium complexes. ....	31
Figure 24: Reduction of aliphatic ketones mediated by electrogenerated SmI <sub>2</sub> .....	31
Figure 25: Electrogeneration (on the left) and electrocatalysis (on the right) processes with SmX <sub>2</sub> .....	32
Figure 26: The synthesis of azobenzene derivatives catalyzed by electrogenerated SmI <sub>2</sub> . <sup>45</sup> .....	32
Figure 27: The formation of the oxalate complex issued from the reaction of (Cp <sup>*</sup> ) <sub>2</sub> Sm(THF) <sub>2</sub> derivatives with CO <sub>2</sub> reported by Evans. <sup>15, 46</sup> .....	33
Figure 28: The proposed pathway for the reaction of the Cp <sup>*</sup> <sub>2</sub> Sm complex with CO <sub>2</sub> . <sup>47</sup> .....	34
Figure 29: Photoinduced reductive carboxylation of alkyl halides reported by Ogawa's group. <sup>49</sup> .....	34
Figure 30: Reductive coupling of nitrones with CO <sub>2</sub> . <sup>50</sup> .....	35



Figure 31: Representative examples of benzoic acids in the pharmaceutical and agrochemical industry.....	43
Figure 32: Synthesis of benzoic acids using stoichiometric organometallic species.....	44
Figure 33: Ni-catalyzed carboxylations of various electrophilic C-O bonds.....	45
Figure 34: Preparation of different organometallic compounds prior to the carboxylation reactions.....	46
Figure 35: Carboxylation of aryl bromide reported by Osakada in 1994 ( <i>top</i> ) and the first catalytic carboxylation of the same compounds described by Martin in 2009 ( <i>bottom</i> ).....	46
Figure 36: Ni-catalyzed carboxylation of aryl chlorides. <sup>58</sup> .....	47
Figure 37: The proposed mechanism of photoinduced carboxylation of aryl bromide and chloride mediated by Pd/Ir dual catalysts. <sup>18e</sup> .....	48
Figure 38: König's light promoted carboxylation of aryl sulfonates and bromides.....	49
Figure 39: Carboxylation of C-H acidic bonds (A); directed carboxylation (B); non-directed carboxylation (C). .....	49
Figure 40: Reported mechanism for the electrocarboxylation of aryl halides.....	50
Figure 41: Detection of oxalic acid after 15 min of Sm(II) electrolysis under CO <sub>2</sub> atmosphere.....	51
Figure 42: Carboxylation of 1a using electrogenerated divalent samarium.....	52
Figure 43: Scope of the carboxylation of aryl bromide using electrogenerated Sm(II) in DMF under CO <sub>2</sub> atmosphere.....	53
Figure 44: Proposed mechanism for halogen elimination mediated by Sm(II).....	54
Figure 45: Carboxylation of aryl chlorides by electrogenerated Sm(II) in DMF under CO <sub>2</sub> atmosphere.....	55
Figure 46: CO <sub>2</sub> only ( <i>on the left</i> ); Ph-Br ( <i>in the middle</i> ) and Ph-Cl ( <i>on the right</i> ) without CO <sub>2</sub> .....	56
Figure 47: Experimental tests using Kagan's reagent.....	57
Figure 48: Radical trapping experiment with TEMPO.....	57
Figure 49: Samarium anode oxidation: Sm electrode surface 20 mm <sup>2</sup> , scanning potential between -1.5 and 0.9 V vs. SCE in DMF with <i>n</i> Bu <sub>4</sub> NPF <sub>6</sub> [0.1 M]. Scan rate : 100 mV.s-1. (a) blue line: without additive; (b) green line: in the presence of chlorobenzene 0.025 M; (c) Red line: after bubbling CO <sub>2</sub> in the solution for 5 min.....	58
Figure 50: Cyclic voltammetry of SmCl <sub>2</sub> before and after adding CO <sub>2</sub> : Glassy carbon electrode surface 20 mm <sup>2</sup> , and platinum wire as counter electrode scanning potential between -0.5 and -3 V vs. SCE in CH <sub>3</sub> CN with <i>n</i> Bu <sub>4</sub> NPF <sub>6</sub> [0.1 M]. Scan rate: 100 mV/s. (a): 0.1 M <i>n</i> Bu <sub>4</sub> NPF <sub>6</sub> ; (b): 0.1 M SmCl <sub>2</sub> in CH <sub>3</sub> CN; (c): 0.1 M SmCl <sub>2</sub> + CO <sub>2</sub> .....	59
Figure 51: Proposed mechanism for the carboxylation of aryl bromides via radical coupling.....	60
Figure 52: Proposed mechanisms for the carboxylation of aryl chlorides via radical substitution.....	60
Figure 53: Screening catalytic carboxylation of aryl chloride reaction conditions.....	61
Figure 54: required further investigation for the carboxylation of aromatic halides.....	62
Figure 55: Carboxylation of activated alkenes by electrogenerated Sm(II).....	63
Figure 56: Examples of NSAIDs containing the phenylacetic acid motif.....	75
Figure 57: Proposed mechanism for the carboxylation of benzyl halides described by Martin's group.....	76
Figure 58: Pd-catalyzed the carboxylation of benzyl chlorides. <sup>81</sup> .....	77
Figure 59: Mechanistic pathway for the carboxylation of benzyl halides with formic acid. <sup>82</sup> .....	78
Figure 60 Ni-catalyzed the carboxylation of C <sub>sp3</sub> -O bonds. <sup>79a</sup> .....	78
Figure 61: Proposed hypothesis for the different behavior observed according to the substrates. <sup>79a</sup> .....	79

Figure 62: First cross-electrophile coupling reaction via unconventional C-N bond cleavage/CO <sub>2</sub> insertion. <sup>79b</sup>	80
Figure 63: Plausible mechanism for the photocarboxylation of benzylic C <sub>sp3</sub> -H bonds. <sup>86</sup>	81
Figure 64: Developed systems for direct electrocarboxylation of benzyl chlorides.	82
Figure 65: Carboxylation of benzyl halides using transition metal catalysts (TM) as chemical mediators.	83
Figure 66: General mechanistic pathway for the carboxylation of benzyl chloride.	84
Figure 67: Carboxylation of benzyl chloride using a stoichiometric amount of electrogenerated divalent Sm in different solvents and different CO <sub>2</sub> source.	85
Figure 68: Scope of the carboxylation of benzyl chlorides with electrogenerated Sm(II)	85
Figure 69: Divalent Sm(II)-catalyzed carboxylation of primary and secondary benzyl chlorides.	87
Figure 70: Blank tests: (1) without Sm(II); (2) without TMSCl; (3) without benzyl chloride; (4) without CO <sub>2</sub> .	88
Figure 71: Investigating the role of ion exchange.	89
Figure 72: Radical trapping attempt using TEMPO as a radical scavenger.	90
Figure 73: Radical trapping experiment using β-pinene as a radical scavenger.	90
Figure 74 Cyclic voltammetry analysis of the carboxylation of benzyl chloride: Glassy carbon electrode surface 20 mm <sup>2</sup> , and platinum wire as counter electrode scanning potential between -0.5 and -2 V vs. SCE in CH <sub>3</sub> CN with <i>n</i> Bu <sub>4</sub> NPF <sub>6</sub> [0.1 M]. Scan rate: 100 mV/s. (a): 0.1 M <i>n</i> Bu <sub>4</sub> NPF <sub>6</sub> ; (b): (a) + 0.2 M SmCl <sub>2</sub> ; (c): (b) + CO <sub>2</sub> ; (d): (c) + 0.5 mL solution of BnCl:TMSCl 1:1.5 in CH <sub>3</sub> CN; (e): (d) + 0.5 mL solution of BnCl:TMSCl 1:1.5.	91
Figure 75 Proposed mechanism for the carboxylation of benzyl chlorides catalyzed by SmI <sub>2</sub>	92
Figure 76 Comparison between the aromatic carboxylic acid and phenyl carboxylic acid	93
Figure 77 Enantioselective carboxylation of benzyl chlorides by chiral Sm(II) complex	93
Figure 78: The hydrocarboxylation outcome depending on the reactional conditions.	107
Figure 79: Described protocols leading to the anti-Markovnikov hydrocarboxylation	108
Figure 80: Höberg's work on the carboxylation of styrene derivatives	109
Figure 81: Hydrocarboxylation of alkenes catalyzed by Cu-complexes. <sup>104, 105</sup>	110
Figure 82: Skydrup's hydrocarboxylation of alkynes to produce malonic acids. <sup>106</sup>	111
Figure 83: Products of the hydrocarboxylation of 1-phenyl-1-propyne using Ma's conditions. <sup>107</sup>	111
Figure 84: Effect of the hydride source on the regioselectivity. <sup>13b</sup>	112
Figure 85: Ni-catalyzed selective hydrocarboxylation of alkynes to yield acrylic acids. <sup>100</sup>	112
Figure 86: Ligand controlled photo-hydrocarboxylation of styrene derivatives reported by König and his co-workers. <sup>77b</sup>	113
Figure 87: Synthesis of lactones via the hydrocarboxylation of alkynes mediated by Ni catalysis	114
Figure 88: Hydrocarboxylation of ynamides to produce β-amino-α,β-unsaturated esters. <sup>109,110</sup>	114
Figure 89: <i>p</i> -Terphenyl catalyzed the photocatalytic hydrocarboxylation of styrene derivatives.	115
Figure 90: Possible transformations of styrene and carbon dioxide in an electrochemical process. S= styrene, D-H: proton donor. <sup>112</sup>	117
Figure 91: Electrocarboxylation of phenylacetylene derivatives using a Ni-cathode. <sup>113</sup>	118
Figure 92: The effect of adding CuI on the electrocarboxylation of alkynes. <sup>114</sup>	119

Figure 93: Fe-catalyzed carboxylation of styrene derivatives via CO <sub>2</sub> activation. <sup>115</sup> .....	119
Figure 94: Carboxylation of phenylpropene and the isolated mixture of carboxylic acids reported by Périchon's group. <sup>117</sup> .....	120
Figure 95: Substrate scope of styrene derivatives.....	123
Figure 96: hydrocarboxylation of bromovinyl benzene as a substrate. ....	123
Figure 97: Substrate scope of 1,2 disubstituted styrene derivatives. ....	124
Figure 98: Scope of the hydrocarboxylation of phenylacetylene derivatives .....	126
Figure 99: Scope of the hydrocarboxylation of protected alkynes .....	127
Figure 100: Hydrocarboxylation with strong electron-rich substrates.....	128
Figure 101: Blank experiments with styrene and phenylacetylene derivatives. ....	129
Figure 102: Stoichiometric tests starting from 4-ethynyltoluene.....	130
Figure 103: Deuterium labeling experiments with styrene derivatives .....	130
Figure 104: Deuterium labeling experiments with phenylacetylene. ....	131
Figure 105: Suggested intermediates interpreting the D-labeling results .....	132
Figure 106: Radical clock experiment. ....	132
Figure 107: Radical trapping experiments of indene and 4-ethynyltoluene with TEMPO.....	133
Figure 108: Cyclic Voltammetry analysis of hydrocarboxylation of alkenes: Glassy carbon electrode surface 20 mm <sup>2</sup> , and platinum wire as counter electrode scanning potential between – 0.5 and -2 V vs. SCE in CH <sub>3</sub> CN with <i>n</i> Bu <sub>4</sub> NPF <sub>6</sub> [0.1 M]. Scan rate: 100 mV/s. (a): 0.1 M electrogenerated SmCl <sub>2</sub> in 0.1 M <i>n</i> Bu <sub>4</sub> NPF <sub>6</sub> in CH <sub>3</sub> CN; (b): (a) + CO <sub>2</sub> ; (c): (b) + 1 mL <i>t</i> BuOH:TMSCl:indene (10:8:1) .....	134
Figure 109: Cyclic voltammetry study of hydrocarboxylation of phenylacetylene: Glassy carbon electrode surface 20 mm <sup>2</sup> , and platinum wire as counter electrode scanning potential between – 0.5 and -2 V vs. SCE in CH <sub>3</sub> CN with <i>n</i> Bu <sub>4</sub> NPF <sub>6</sub> [0.1 M]. Scan rate: 100 mV/s. (a): 0.1 M <i>n</i> Bu <sub>4</sub> NPF <sub>6</sub> ; (b): (a) + 0.1 M electrogenerated SmCl <sub>2</sub> ; (c): (b) + CO <sub>2</sub> ; (d): (c) + 1 mL <i>t</i> BuOH:TMSCl:phenylacetylene (20:6:1) .....	135
Figure 110: Suggested mechanism for the carboxylation of alkenes catalyzed by SmCl <sub>2</sub> complex .....	136
Figure 111: Carboxylation of aryl halides mediated by electrogenerated Sm(II) complex. ....	141
Figure 113: Catalytic carboxylation of benzyl chloride derivatives initiated by Sm(II) complexes.....	142
Figure 114: Carboxylation of styrene and phenylacetylene derivatives catalyzed by electrogenerated Sm(II) complexes. ....	142





# General Introduction

---

Nature crowns this world as the most harmonized system on this Earth. Over the years, it always succeeded to maintain the balance between all the ecosystems and to provide, on the other hand, to human creatures what they want. However, the increasing number of populations demanded massive industrial investments to satisfy their needs, especially during the past decades. Consequently, the industrial expansion started to threaten this balance by taking extensively from nature's resources and giving back nothing but harmful wastes, mainly in the air but also in water and soil.

Air pollution was not a huge problem until we began to notice the global warming effects (repetitive heatwaves, desertification, acid rain) caused by greenhouse gases, primarily carbon dioxide.

Facing these consequences, Scientists were the first to start the alert about what are we going to face from ecological crises to fatal diseases if the level of brutal abuse of the environment is kept as high. Subsequently, promising efforts to reduce the standards of the main responsible, CO<sub>2</sub>, in the atmosphere started to grow by trying to store it underground or capture it by selective membranes.

Chemists thought differently by proposing the transformation of this gas into daily used compounds and encouraged the concept of CO<sub>2</sub> fixation. Since then, a revolution in chemistry started and opened the way for novel strategies based on CO<sub>2</sub> insertion to deliver valuable materials in pharmaceutical, agrochemical, and fine chemistry. Still, many of these protocols add more complications than solving the main dilemma by requiring high or low temperatures, important CO<sub>2</sub> pressure, or even worst, create more wastes such as metallic ones.

Since its establishment, the electrochemistry was the tool of choice to develop affordable chemical reactions under safer conditions. It did not take long before its use reunites with the CO<sub>2</sub> fixation and it was commercialized as the alternative to metallic additives or even better, as a promising way to synthesize valuable chemicals such as carboxylic acids, without the production of unnecessary wastes. Despite this significant breakthrough, the principal drawback was the high overpotential required for the preparation of carboxylic acids in addition to the low efficiency and poor selectivity.

In our group, we took advantage of the electrochemistry to produce divalent samarium as a reductant powerful enough to initiate radical transformations, thanks to its monoelectronic reductive behavior. More recently, we established electrocatalytic reactions allowing the use of a catalytic loading of this complex to yield amazing results that were not possible with other reagents or necessitated the use of an over-stoichiometric amount of a co-reducing agent.

In this thesis, we are interested in exploring the reactivity of the divalent samarium complexes to achieve the CO<sub>2</sub> activation, relying on the electrochemistry as a green source of electrons, to obtain carboxylic acids from commercially available substrates.

After a general introduction and state of the art around the CO<sub>2</sub> problematic, in the first chapter, we discuss the carboxylation of **aromatic chlorides** and bromides under **CO<sub>2(g)</sub> atmosphere** using electrogenerated divalent samarium complex. The active Sm (II) species is *continuously* electrogenerated from a metallic samarium rod in the presence of tetrabutylammonium tetrafluoroborate **nBu<sub>4</sub>NBF<sub>4</sub>** as electrolyte and source of ligands, in dimethylformamide **DMF** as a solvent for this transformation.

In the second chapter, we investigate the carboxylation of **benzyl chloride** derivatives, in **acetonitrile**, to obtain **phenylacetic acids** using this time a **catalytic amount of SmI<sub>2</sub>** precisely electrogenerated *before* the addition of the starting material. This reaction requires the presence of trimethylsilyl chloride **TMSCl** to regenerate the catalyst and the use of **dry ice** as a source of CO<sub>2</sub> in the medium.

The third chapter concerns the hydrocarboxylation of **styrene and phenylacetylene** derivatives via *anti-Markovnikov addition* of CO<sub>2</sub> (**dry ice**), catalyzed by 10 mol% of **SmCl<sub>2</sub>** generated *in situ* from the electroreduction of SmCl<sub>3</sub>, in the presence of *ter*-butanol **t-BuOH** as a proton source and of course, **TMSCl** in acetonitrile.

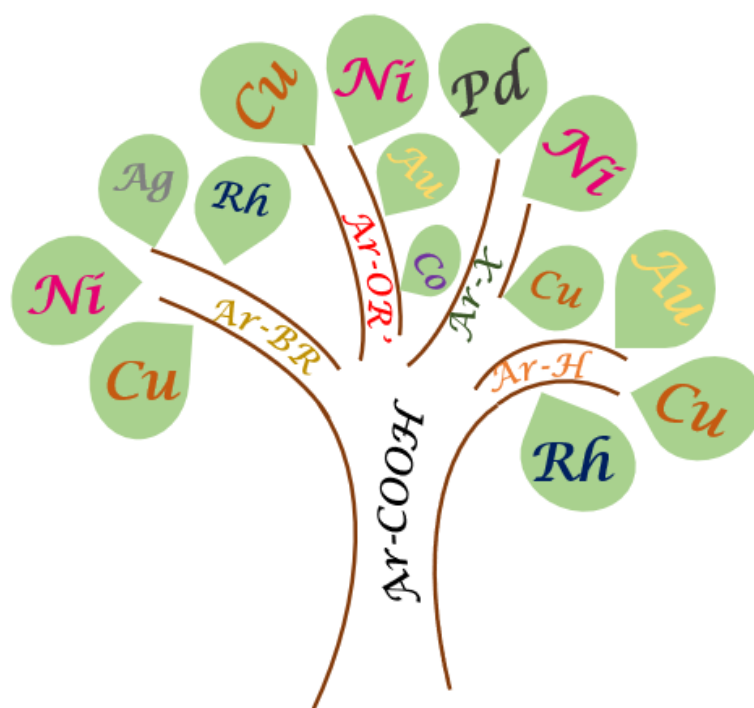








## Literature overlook





# Carbon Dioxide

## 1. Generality about the increasing carbon dioxide problematic

### a. Sources and role of CO<sub>2</sub> in nature

As simple as it can be, a carbon dioxide molecule is formed via the combination of three atoms: one carbon and two oxygens. The central atom in this compound is the carbon, presented in its most oxidized form (+4). However, this small molecule of CO<sub>2</sub> plays a major role in life (**Figure 1**) and it is considered as the main carbon source in the atmosphere.

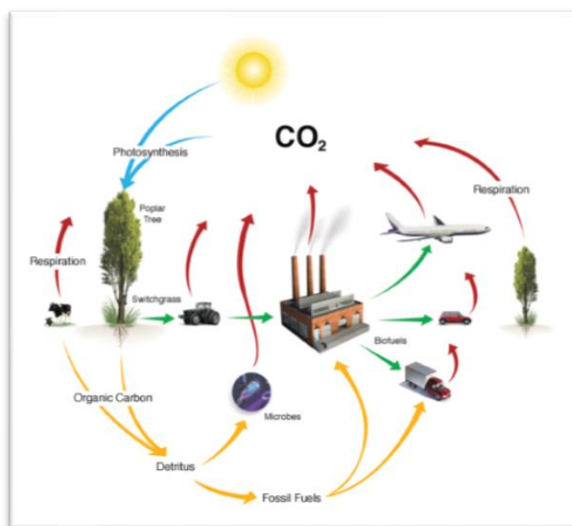


**Figure 1:** Carbon dioxide cycle.

For example, the plants absorb the CO<sub>2</sub> to produce glucose and release dioxygen O<sub>2</sub> during the day via photosynthesis, and the opposite during the night. Besides, the oceans are one of the largest reservoirs of this gas after its dissolution and transformation to bicarbonate CO<sub>3</sub><sup>2-</sup> in deep cold water. This process is yet reversible on the surface due to the temperature rise leading to the decrease of CO<sub>2</sub> solubility in water.

On the other hand, the respiration, erupting volcano, and economic growth are inherently producing the CO<sub>2</sub>, especially this latter due to the continuous burning of fossil fuels.<sup>1</sup> On top of this category, the production of cement contributes to almost 6% of the total CO<sub>2</sub> emission,

<sup>1</sup> a) S. Chu, Y. Cui, N. Liu, *Nat. Mater.* **2017**, *16*, 16; b) N. S. Lewis, *Science* **2016**, *351*, 1920; c) B. Obama, *Science* **2017**, *355*, 126; d) A. Schoedel, Z. Ji, O. M. Yaghi, *Nat. Energy* **2016**, *1*, 16034; e) Z. Han, R. Kortlever, H. Y. Chen, J. C. Peters, T. Agapie, *ACS Cent. Sci.* **2017**, *3*, 853.

including those coming from the raw material. Although the development of many alternatives, fossil fuels remain on the top of energy sources, essential for many sectors.

Consequently, this balance between absorbed and generated CO<sub>2</sub> is strongly disrupted, causing the most discussed crisis, *global warming*.

### b. Global warming

The term *warming* signifies the temperature rise compared to normal levels, but why the CO<sub>2</sub> increasing levels are going to warm the Earth?

The carbon dioxide and other gases (N<sub>2</sub>O, H<sub>2</sub>O<sub>(g)</sub>, CH<sub>4</sub> & O<sub>3</sub>), are together called the greenhouse gases (**GHGs**). These gases can absorb infrared photons, unlike others in the atmosphere (e.g., N<sub>2</sub> and O<sub>2</sub> cannot absorb infrared energy). The gained energy is likely to be re-released as an infrared emission as a crucial phenomenon keep the global temperature in a reasonable range.

*The Intergovernmental Panel on Climate Change (IPCC)*'s special report published in **October 2018** drawing the attention to the increasing levels of carbon dioxide, exceeding 414 ppm in May 2019,<sup>2</sup> which is responsible for over warming the Earth's climate to a serious problematic point.

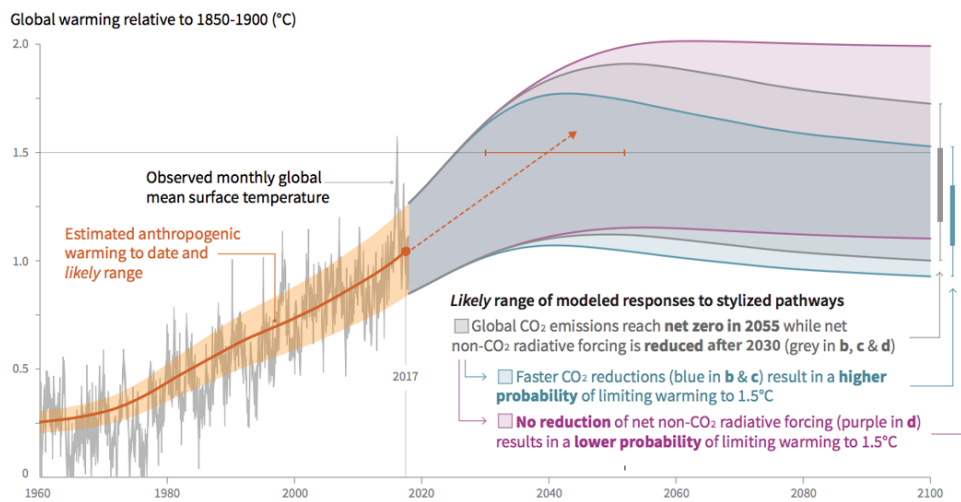


**Figure 2:** Chart shows observed monthly temperatures (grey line), estimated human-caused warming (red), and idealized potential pathways to meeting 1.5°C limit in 2100 (grey, blue, and purple). All relative to 1850-1900.<sup>3</sup>

Furthermore, this report highlighted the importance of limiting global temperature rise to **1.5°C** by the mid-century (2040-2050) and declaring that the precedent limit to **2°C** is no longer enough to avoid the disastrous impact of climate change arising each day. According to the report, the human activities are responsible for adding **0.2°C** to global average temperatures each decade, and the CO<sub>2</sub> emissions are on the top of the list (**Figure 2**).

<sup>2</sup> <https://www.co2.earth/>

<sup>3</sup> <https://www.ipcc.ch/sr15/>

To resolve the crisis, the 91 scientists agreed that the global CO<sub>2</sub> emissions need to drop to net-zero by 2050 so we can remain below 1.5°C.

By the end of the report, the main conclusion is: if innovative new technologies for CO<sub>2</sub> removal do not find its way shortly, all the proposed scenarios are threatening to fail, and the consequences on a global scale will be severe.

### *c. Consequences and solutions*

Extreme weather, floods, biodiversity loss, deforestation... these are among the climate change consequences. So, as mentioned in the previous section, creating new methods to remove the carbon dioxide is a must to achieve the goal.

The *Carbon Capture, Storage, and Utilisation (CCSU)* constitute a new technology opening the pathway for the reduction of CO<sub>2</sub> emissions and meeting climate and energy goals.<sup>4</sup> It's mainly based on three concepts:

- i- **Capture:** The separation of CO<sub>2</sub> before, during, or after the fuel combustion process depends on the used technology. For example, the separation of CO<sub>2</sub> known as **post-combustion capture** requires an amine-based adsorption system. Besides the high cost of this latter, the corrosion is one of the problems encountered by the process due to acid gases (mainly CO<sub>2</sub> and H<sub>2</sub>S) which reduces subsequently its lifetime and limits its use.
- ii- **Storage:** The CO<sub>2</sub> is injected under the ground which leads to its condensation into a liquid and to its safe storage eventually. Still, its sequestration necessitates a unique geological overlay of porous rocks and seal, especially this last layer as it forms an impermeable barrier to avoid CO<sub>2</sub> migration toward the surface. This technique presents some complications, mainly the untraceable CO<sub>2</sub> evolution over time, so in case of leaks, for example, it is hard to react immediately and solve the problem (**Figure 3**).

---

<sup>4</sup> a) Q-W. Song, Z-H. Zhou, L-N. He, *Green Chem.*, **2017**, *19*, 3707 ; b) G. Cui, J. Wang, S. Zhang, *Chem. Soc. Rev.*, **2016**, *45*, 4307; c) N.V.D. Assen, P. Voll, M. Peters, A. Bardow, *Chem. Soc. Rev.*, **2014**, *43*, 7982

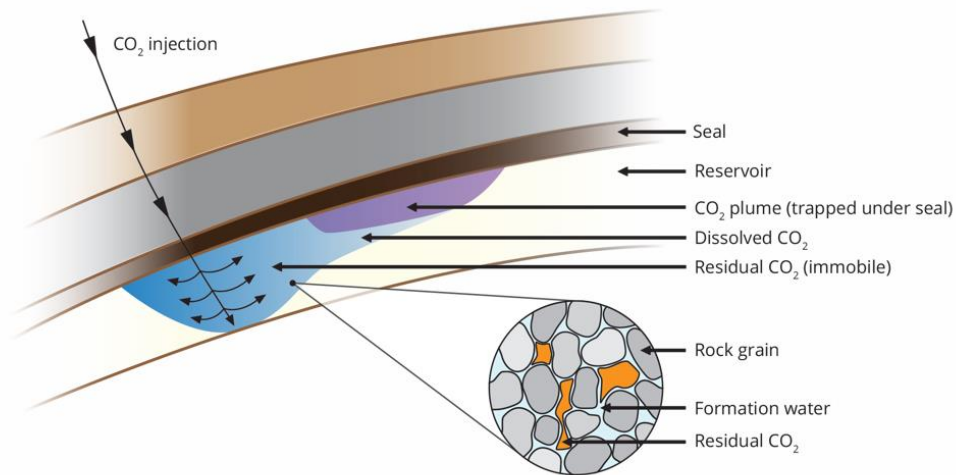


**Figure 3:** The required soil composition to store the carbon dioxide underground

iii- *Utilization:* The number of publications regarding CO<sub>2</sub> usage in the last ten years has increased significantly, targeting two main applications (**Figure 4**):

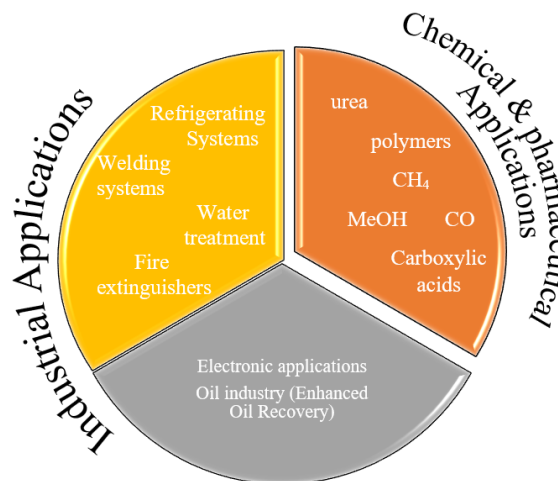


**Figure 4:** Carbon dioxide uses.

**A. Industrial applications:** This category does not show usually any conversion of carbon dioxide. As an example, the CO<sub>2</sub>-based fire extinguishers for the fires caused by solvents, fuels, and oils.

Another technical illustration is *Enhanced oil recovery (EOR)*. It is based on injecting the CO<sub>2</sub> under high pressure into an oil reservoir. Enough pressure will allow the oil circulation through the pipes and arrive at the surface of the ground. The main advantage of CO<sub>2</sub> here is reducing the viscosity of the oil, facilitating its recovery.

However, these applications demand a vast amount of energy so, by the end of the process, there will be somehow CO<sub>2</sub> emissions and resources depletion.

**B. Chemical and pharmaceutical applications:** These applications are not considered as the main path to reduce carbon dioxide levels, yet in most cases, they don't either involve any increase in its emission. The CO<sub>2</sub> transformation into methanol or methane or another hydrocarbon is well studied and although the great advance in this field, it appears to be critical from an economic point of view considering their low market value.<sup>5</sup>

On the other hand, these methods can yield valuable compounds (polymers, carbamates, urea, carboxylic acids...) extensively consumed. Notably, the carboxylic acids form a quite interesting category by itself. This functional group exists not only in drugs but also in paints, cosmetics, plastics..., products that established a great market and endless daily need translated into an expected gain of 5% in the carboxylic acid market by 2024.<sup>6</sup>

The critical question to ask here is how we can use carbon dioxide, especially in chemistry, a gas known for its thermodynamic stability and kinetic inertia? To answer this inquiry, the chemical properties of CO<sub>2</sub> should be identified and discussed first.

## 2. Chemical properties of CO<sub>2</sub>

### a. The structure of CO<sub>2</sub> and its existing forms in solution

The carbon dioxide is a non-toxic, noninflammable, renewable, abundant gas. The boiling point of CO<sub>2</sub> is - 51 °C, and it is present in a gaseous state under atmospheric pressure and room temperature. In the atmosphere, the density of CO<sub>2</sub> is 1.98 Kg/m<sup>3</sup>, almost 1.65 times higher than the air density.

Dissolved in water, the carbon dioxide exists in three forms depending on the pH: carbonate CO<sub>3</sub><sup>2-</sup> (pH >10), hydrogen carbonate HCO<sub>3</sub><sup>-</sup> (6.5 < pH <10) and dissolved CO<sub>2</sub> (pH < 6.5).

In organic solvents, the CO<sub>2</sub> solubility is much higher than in aqueous solution.<sup>7</sup> Interestingly, it strongly depends on the polarity and the protic character of the solvent (**Table 1**).

**Table 1:** CO<sub>2</sub> solubility in different organic solvents.<sup>7</sup>

Solvents	The concentration of dissolved CO <sub>2</sub> (mol/L) at 25°C
<i>Dimethyl sulfoxide</i>	0.138 ± 0,003
<i>Dimethylformamide</i>	0.199 ± 0,006
<i>Tetrahydrofuran</i>	0.205 ± 0,008
<i>Acetonitrile</i>	0.279 ± 0,008
<i>Methanol</i>	0.330 ± 0,01

<sup>5</sup> A. Tortajada, F. J. Hernandez, M. Borjesson, R. Martin, *Angew. Chem. Int. Ed.* **2018**, 57, 15948.

<sup>6</sup> <https://www.gminsights.com/industry-analysis/carboxylic-acid-market>

<sup>7</sup> C. M. Sanchez-Sanchez, V. Montiel, D. A. Tryk, A. Aldaz, A. Fujishima, *P. App. Chem* **2001**, 12, 73, 1917



Under low temperature ( $< -78^{\circ}\text{C}$ ), this gas will transform immediately via a condensation process to form the “dry ice.” This solid will gradually convert to the gas state if stored at room temperature. Easy to transport and overpressure risk-free are the main advantages of the  $\text{CO}_{2(\text{s})}$  compared to the case of using  $\text{CO}_{2(\text{g})}$  bottles.

From another point of view, this linear molecule with a  $D_{\infty\text{h}}$  symmetry has no dipole moment, yet the electronegativity difference between the oxygen and carbon attracts the electrons towards the former and thus creating a partial positive charge on the latter. This electronic distribution rules the  $\text{CO}_2$  interaction in a chemical medium; the carbon center is electron-poor thus possessing a Lewis acid character while the oxygen reacts as a Lewis base.

Moreover, the frontier molecular orbital theory indicates the same electronic behavior.<sup>8</sup> As expected, the Highest Occupied Molecular Orbital HOMO lies on the oxygen atom while the Lowest Unoccupied Molecular Orbital LUMO is found on the carbon atom. Based on this fact, the coordination of a metal center and carbon dioxide was classified in 24 binding modes depending on how many metal center and  $\text{CO}_2$  molecule are involved.<sup>9</sup> In the case of a transitional metal, there are mainly four binding modes (**Figure 5**):<sup>5</sup>

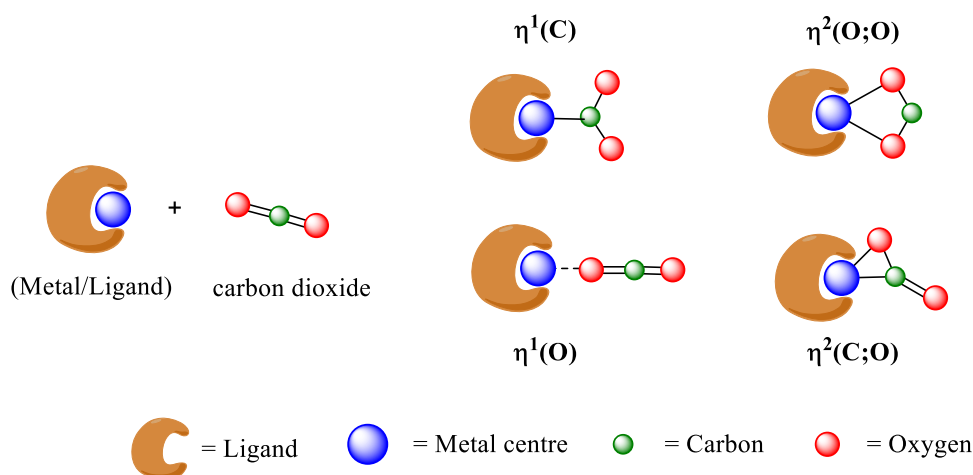


**Figure 5:** Different binding modes of carbon dioxide with a transition metal center.

**i-  $\eta^1(\text{C})$ :** This interaction requires an electron-rich metal center to coordinate to the deficient carbon atom. In this case, the orbital  $d_{z^2}$  of the metal will react with the LUMO of  $\text{CO}_2$  via a charge transfer, stabilizing the formation of this type of complexes.

**ii-  $\eta^1(\text{O})$  and  $\eta^2(\text{O};\text{O})$ :** The metal center is in this case electron-poor thus it coordinated to the electron-rich site of carbon dioxide which is the oxygen atom. An example of this type is the alkali metals, known for their low oxidation potential.

<sup>8</sup> M. Aresta, A. Dibenedetto, E. Quaranta, *Reaction Mechanisms in Carbon Dioxide Conversion*, Springer-Verlag: Berlin Heidelberg 2016.

<sup>9</sup> A. Behr, *Angew. Chem. Int. Ed. Engl.* 1988, 27, 661.

iii-  $\eta^2(\text{C}; \text{O})$ : as the most common binding mode, it demonstrates a double interaction between the metal and the  $\text{CO}_2$ . The oxygen transfers the electrons into the empty  $d_{z^2}$  of the metal. This latter responds by transferring a part of the  $d_{xy}$  charge via “ $\pi$ -back bonding” to the LUMO localized on the carbon. For example, the Nickel exhibited this type of binding mode in the first Ni- $\text{CO}_2$  complex reported by Aresta *et al.*<sup>10</sup>

After its coordination to the metal center, the  $\text{CO}_2$  fixation to the substrate is the next step, and generally, the typical metal catalysis goes through a  $\text{CO}_2$  insertion mechanism while the unusual path, and commonly described in photochemical and electrochemical reactions, is the  $\text{CO}_2$  activation.

### b. $\text{CO}_2$ fixation: insertion vs. activation

#### A. $\text{CO}_2$ insertion:

The  $\text{CO}_2$  is well known to be a stable molecule ( $\Delta G = -396$  kJ/mol) with a high redox potential (-2.21 V/SCE in DMF). To encounter this great stability, transition metals perform usually at first an *oxidative addition* with the available reagent in the medium (alkenes, alkynes, aryl or aromatic halides ...) to produce highly reactive organometallics.

Nevertheless, the **14/16 VE rule** controls the transition metal catalysis. Indeed, the metal goes from 14 VE to 16 VE during the oxidative addition. So, there are three options determined by the experimental conditions:

(1) In the case of halogenated substrates, a **co-reductant** must be added in the medium to reduce the metal center to **15 VE (Figure 6, path 1)**. After this monoelectronic reduction, the coordinated  $\text{CO}_2$  will then follow an insertion step in the M-R bond to form the insertion adduct holding the same number of electrons (15). Finally, to regenerate the catalyst, another equivalent of the reducing agent is necessary to give back the initial active catalyst and consequently, to play the role of a cation of the carboxylate anion. A perfect example will be the nickel catalyst described by Martin's group, for the carboxylation of pseudo(halide) bonds, involving the three oxidation states of Ni(0/I/II).<sup>11</sup>

(2) Another possible path is when only two oxidation states are concerned during the catalytic cycle. In this case, after the  $\text{CO}_2$  insertion, an alkyl carbanion donor like diethylzinc **Et<sub>2</sub>Zn** as a terminal reducing agent will eliminate the carboxylated product, releasing a metal-alkyl species (**Figure 6, path 2**). After the elimination of an alkyl halide, the original complex will be recovered to catalyze the reaction.<sup>12</sup>

<sup>10</sup> S. Z. Tasker, E. A. Standley, T. F. Jamison, *Nature* **2014**, 509, 299.

<sup>11</sup> A. Correa, T. Léon, R. Martin, *J. Am. Chem. Soc.* **2013**, 135, 1221.

<sup>12</sup> A. Correa, R. Martin, *J. Am. Chem. Soc.* **2009**, 131, 15974.

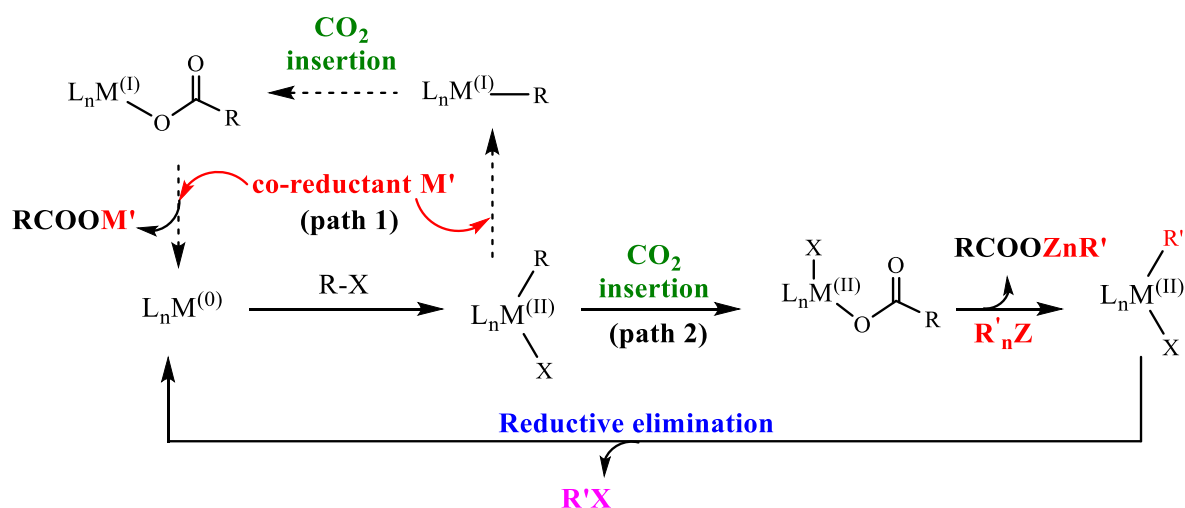


**Figure 6:** Possible mechanistic pathways for the carboxylation of halogenated reagents.

(3) When the used substrate contains an unsaturated bond (alkenes, alkynes, imines ...), the reaction requires the addition of a hydrogen donor or a hydride source. Furthermore, the catalyst is under the control of steric hindrance due to the presence of two possibilities, which are the Markovnikov or anti-Markovnikov addition, and therefore, the ligand choice plays a significant role. This point will be detailed in the third chapter, but the major product arises from the Markovnikov addition<sup>13</sup> where the hydrogen is on the less substituted carbon. The rest of the mechanism depends strongly on the substrate nature, the ligand, and the additives in the medium.

The  $CO_2$  insertion has been reported in many metal-based catalyses and thus widely investigated.<sup>5</sup> While it offers low catalyst loading and good selectivity, the transition metal-based route possesses significant drawbacks:

**i- The over stoichiometric amount of additives:** The metal-based additives are mainly needed to reduce the catalyst and regenerate the active oxidation state. Some of these reagents interfere with the mechanism, facilitating the insertion by lowering the  $CO_2$  activation energy; others are whether toxic or air-sensitive, thus making the reaction manipulation much harder.

**ii- The expensive ligands:** Although the block-d are cheap, abundant metals, yet their combination with costly ligands, specifically designed to enhance the selectivity, decreases the possibility of their use for future industrial applications. Moreover, few of these ligands are commercially available, which adds a pre-additional synthetic step to the reaction.

**iii- The designed substrate:** Designing means adding structural modifications to the starting material, essential for the reaction to work. The organozinc and organoboranes reagents constitute a right example in this case, mostly used instead of the unfunctionalized substrates due to their high reactivity. Also, having these functional groups will increase the reaction selectivity leading to the direct insertion at the selected position.

<sup>13</sup> a) C. M. Williams, J. B. Johnson, T. Rovis, *J. Am. Chem. Soc.* **2008**, *130*, 14936; b) M. D. Greenhalgh, S. P. Thomas, *J. Am. Chem. Soc.* **2012**, *134*, 11900; c) P. Shao, S. Wang, C. Chen, C. Xi, *Org. Lett.* **2016**, *18*, 2050; d) S. Kawashima, K. Aikawa, K. Mikami, *Eur. J. Org. Chem.* **2016**, 3166.

**iv- The selectivity issues:** Specifically, in the case of unsaturated products, the selectivity during the insertion is based on the ligand and the substrate. Under ligand-control, most of these reactions show high selectivity, yet a slight change in the substrate's structure yields a considerable drop of selectivity indicating the critical structure dependence of the developed system.

**v- The long reaction time and the crucial role of temperature:** Up to 36 hrs are sometimes required under very high (150°C) or on the contrary, low temperature (-70°C), causing side products and low reaction efficiency.

## **B. CO<sub>2</sub> activation**

To activate the CO<sub>2</sub> means generating an active species from this stable molecule, in most common active form of this compound is the radical anion [CO<sub>2</sub>]<sup>•-</sup>, formed via an electron transfer mechanism, mainly using electrochemistry and photochemistry. As previously discussed, the LUMO lies on the carbon center so any additional electron will likely reside in this anti-bonding orbital, leading to the CO<sub>2</sub> reduction resistance ( $E_{red} = -2.21 V$ ). After a successful electron transfer, this additional radical affects the CO<sub>2</sub> structure significantly. First, the carbon oxidation state decreases from (+4) to (+3) and the previous electrophilic center gains a strong nucleophilic character. Secondly, the symmetry changes from  $D_{\infty h}$  to  $C_{2v}$ , translated by going from linear to bent geometry ( $\widehat{OCO} = 180^\circ$  to  $138^\circ$ ). And lastly, the additional electron is added on the carbon atom and the oxygen atom bears the negative charge. This latter occupies a  $\pi$ -orbital on the oxygen atom while the transferred electron takes place in the  $\sigma$ -orbital of the carbon center. Furthermore, the C-O bond increases to 1.24 Å (compared to 1.16 Å before) (**Figure 7**).

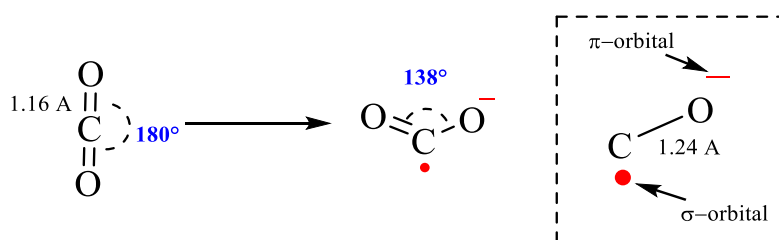


**Figure 7:** Reduction of carbon dioxide to the corresponding radical anion.

Once generated, this radical anion is very unstable, so the next steps depend strongly on the medium and the experimental conditions:

- In protic solvent:* without any substrate and under high concentration, the [CO<sub>2</sub>]<sup>•-</sup> will probably dimerize to give the oxalate and furtherly, the **oxalic acid** in the presence of traces of water. Low concentration can lead to the formation of **formic acid** instead after a **hydrogen transfer** and protonation of the carboxylate anion. Further reduction is also possible to obtain carbon monoxide, formaldehyde, methanol, and methane, but these reactions require harsh conditions and thus a highly reactive reagent (**Figure 8**).

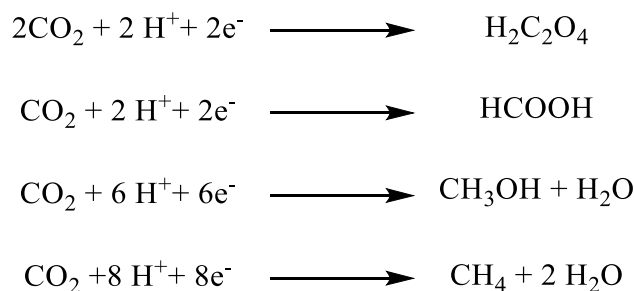


**Figure 8:** Carbon dioxide reduction to oxalic acid, formic acid, methanol or methane

2. *In aprotic solvent:* in this case, the formation of the oxalic acid is still probable but in case of adding a substrate, the whole pathway changes to yield much more valuable products via C-C bond formation. The reaction begins with the radical anion that is strong enough to activate the substrate in the medium, performing a **radical addition**, in the case of an unsaturated substrate (e.g alkenes), to generate another stable radical, or a **radical substitution** if the substrate has a good leaving group (I, Br, Cl, OTf). During the **radical addition** path, the obtained radical can undergo a further reduction, a dimerization or the addition of another radical anion  $[\text{CO}_2]^-$ . Finally, in both pathways, we get the corresponding products are obtained after protonation (**Figure 9**).

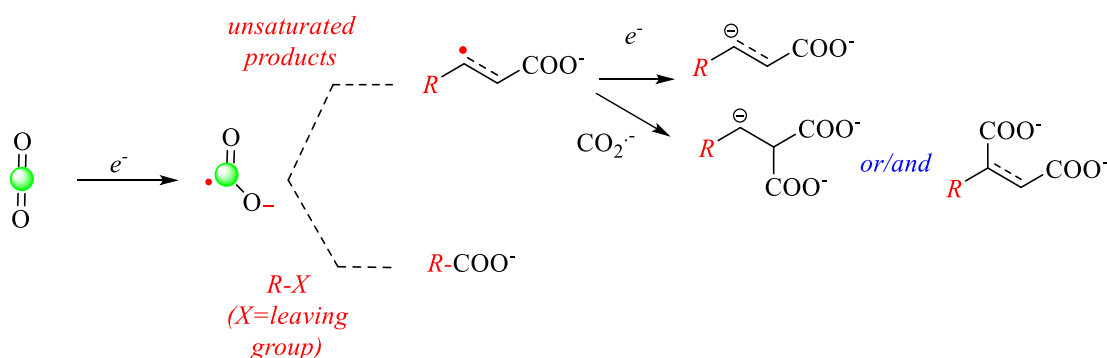


**Figure 9:** Carboxylation of substituted and unsaturated substrates showing the possible products.

This method presents the future of using carbon dioxide because it doesn't need a designed substrate nor an additive to activate the  $\text{CO}_2$ , most importantly, any heat. The primary issue with this path is selectivity. Having a free radical in the medium implies that it can add to the position that generates the most stable radical and also, it can furtherly combine with this latter to isolate  $\alpha,\beta$ -difunctionalized products or even produce the  $\alpha,\alpha$ -product via a second radical addition on the same position. So, at the end of the reaction, a mixture of at least three products is obtained.

To control the reaction, significant optimization and profound knowledge of radical chemistry and carbon dioxide reactivity are crucial to overcoming these problems.

As indicated before, this type of reactivity is known using electrochemistry and photochemistry. We will discuss in detail these two methods in the next section.

Due to the importance of carboxylic acids and their wide applications with respect to the work described in this manuscript, the next section will only highlight the reported examples in the literature using CO<sub>2</sub> fixation methods (CO<sub>2</sub> insertion and CO<sub>2</sub> activation) to generate these valuable compounds.

### c. Reported synthesis of R-COOH using CO<sub>2</sub> as C<sub>1</sub>-building block

#### A. Over stoichiometric organometallics

Reported with many transitional metals (Ni, Ti, Zn, Mo, Nb) in addition to Grignard and organolithium reagents,<sup>14</sup> this method consists of using an over stoichiometric amount of a metal complex to activate the CO<sub>2</sub>. In most cases, this reaction goes through a CO<sub>2</sub> insertion into the metal-carbon bond to afford the corresponding carboxylic acid. In some examples, an excess amount of additives (MgCl<sub>2</sub>, LiCl, R<sub>2</sub>Zn) (**Figure 10**) or harsh conditions are crucial to overcoming the energy-demanding CO<sub>2</sub> insertion step.

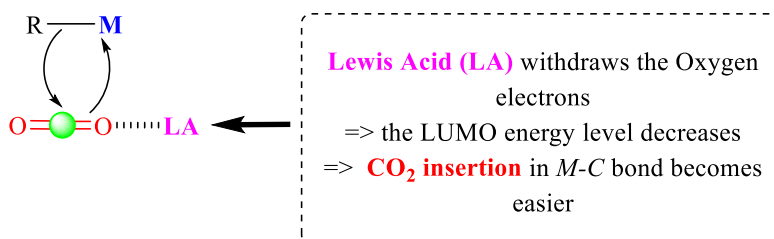


**Figure 10:** The role of Lewis acid in the CO<sub>2</sub> insertion step.

Interestingly, there were only a few examples regarding the carboxylation using lanthanides, mainly limited to the samarium, ytterbium, and europium complexes. Evans group reported carboxylation example using divalent organosamarium complex (Cp\*)<sub>2</sub>Sm(η<sup>3</sup>-CH<sub>2</sub>CH=CHR) (R= H, Me, Et).<sup>15</sup> The authors suggested that the carboxylation goes through a CO<sub>2</sub> insertion path in the Sm - C bond to obtain the unbranched carboxylic acid. Of note, this unique reactivity will be clarified subsequently in the samarium reactivity chapter.

#### B. Transition metal-based catalysis

After developing the stoichiometric reactions, the chemists started investigating the possibility to go a step further by trying to establish catalytic carboxylation as an economically better alternative. In 1997 when Nicholas and Shi reported the first catalytic system based on using Pd (0) to transform the allyl stannanes in the corresponding allyl tin esters.<sup>16</sup> This example offered a simple

<sup>14</sup> J. Luo, I. Larrosa, *ChemSusChem*. **2017**, *10*, 3317

<sup>15</sup> W.J. Evans, C.A. Seibel, J.W. Ziller, R.J. Doedens, *Organometallics* **1998**, *17*, 2103

<sup>16</sup> M. Shi, K. M. Nicholas, *J. Am. Chem. Soc.* **1997**, *119*, 5057

transformation, but the conditions were quite harsh, requiring high CO<sub>2</sub> pressure (33 atm) and high temperature (70°C) and consequently limiting its application in organic synthesis.

Afterwards, many catalysts were investigated, taking advantage of numerous transition metals characteristics (Ni, Pd, Cu, Ti, Co, Rh, Ag, Fe, Au)<sup>5</sup> to develop new reactivity and most importantly, to improve the conditions by lowering the catalyst loading, the temperature, the CO<sub>2</sub> pressure or by widening the reaction scope to obtain more interesting carboxylic acids (**Figure 11**).

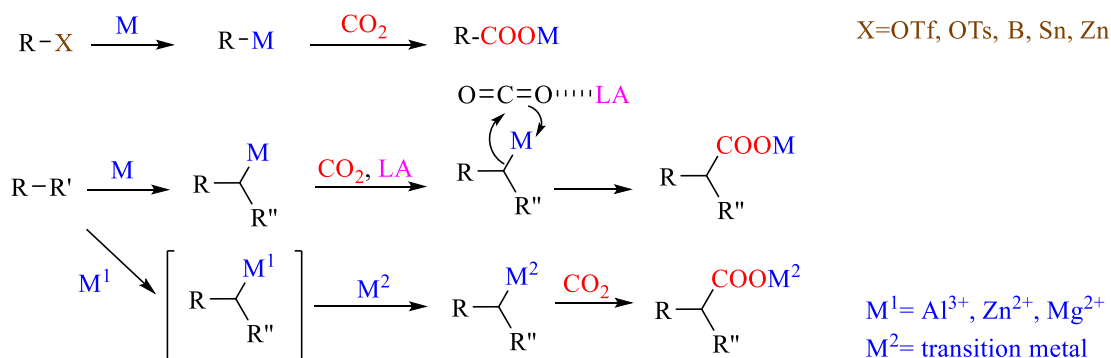


**Figure 11:** The mechanism of carboxylation depending on the substrate nature and the additives.

Although the remarkable advance, new problems arose:

- (1) The overuse of reducing reagents added to regenerate the catalyst initial oxidation state and in some other cases, to enhance the reductive elimination step at the end.
- (2) The organoboranes and organozinc reagents, used to achieve the carboxylation, require at least one additional step. The former is used not only to increase the reactivity but also to control the selectivity while the latter mainly due to its good functional tolerance. Additionally, the organoaluminium intermediates were also investigated in some examples, but the reactions turned to be less general with these species.<sup>17</sup>
- (3) The expensive ligands associated with these catalysts limit their further industrial application and even decrease the probability of future academic use. Moreover, most of these ligands are not commercially available, so an additional synthetic step is necessary before trying the reaction.

<sup>17</sup> M. Takimoto, Z. Hou, *Chem., Eur. J.* **2013**, *19*, 11439; A. Ueno, M. Takimoto, W. N. O. Wylie, M. Nishiura, T. Ikariya, Z. Hou, *Chem. Asian J.* **2015**, *10*, 1010; A. Ueno, M. Takimoto, Z. Hou, *Org. Biomol. Chem.* **2017**, *15*, 2370.

### C. Photochemistry

One of the chemist's tools recently developed to generate carboxylic acids is the carboxylation using photochemistry.<sup>18</sup> Generally, the photocatalyst is capable of absorbing light in a spectral range that neither the solvents nor the common organic substrates usually absorb. It's a new method opening the way to access a high level of selectivity by adjusting the redox potentials.

A typical photocatalytic system is based on three components (

**Figure 12):**

(a) **Photosensitizer:** It is a chemical compound that has light sensitivity and can absorb it to form the excited state. Its addition is needed when the catalyst is not sensitive to the light, and so, it requests an intermediate to transfer the energy. Usually, the added amount of this compound exceeds slightly the amount of the catalyst.

(b) **Sacrificial electron donor:** Present in excessive amount, a sacrificial electron donor is required to whether retrieve the original photosensitizer (*oxidative quenching mechanism*) or to perform the reduced state from its excited form (*reductive quenching mechanism*). Tertiary amines present this kind of reactivity as a rich electron donor species.

(c) **The catalyst:** As the only component interacting with the carbon dioxide via coordination, it is thus responsible for its subsequent reduction. The catalyst mainly interacts with the photosensitizer via an electron transfer process to produce the active radical anion  $[\text{Cat}]^-$ .

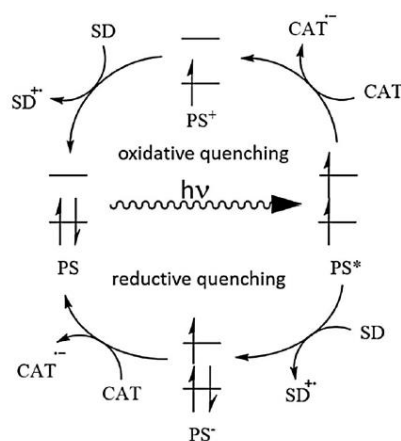


**Figure 12:** Oxidative and reductive quenching mechanisms in a photochemical reaction

This method proved its efficiency in different types of carboxylation: the carboxylation of aryl halides, hydrocarboxylation (Markovnikov and anti-Markovnikov), thiocarboxylate formation, carboxylation of  $C_{sp^3}$ -H and  $C_{sp^2}$ -H bonds, carbocarboxylation, dicarbofunctionalization and finally, the synthesis of the amino acids via  $\text{CO}_2$  activation.<sup>5</sup>

<sup>18</sup> a) C.S. Yeung, *Angew. Chem. Int. Ed.* **2019**, 58, 5492; b) A. Paul, M. D. Smith, A. K Vannucci, *J.Org. Chem.* **2017**, 82, 1996; c) K. N. Lee, Z. Lei, M.-Y. Nagai, *J. Am. Chem. Soc.* **2017**, 139, 5003; d) M. Chen, X. Zhao, C. Yang, W. Xia, *Org. Lett.* **2017**, 19, 3807; e) K. Shimomaki, K. Murata, R. Martin, N. Iwasawa, *J. Am. Chem. Soc.* **2017**, 139, 9467.



If  $E_{\text{redox catalyst}} > E_{\text{redox CO}_2}$ , the catalyst can activate the  $\text{CO}_2$  and reduce it to the corresponding radical anion. On the other hand, if  $E_{\text{redox substrate}} < E_{\text{redox catalyst}} < E_{\text{redox CO}_2}$ , it reduces the substrate in the medium to generate the radical strong enough to reduce the carbon dioxide

Although the future of photochemistry looks promising, yet it suffers from many drawbacks:

- (1) The excessive amount of electron donor.
- (2) The need for a substoichiometric quantity of base ( $\text{K}_2\text{CO}_3$ ,  $\text{Cs}_2\text{CO}_3$ ) in the medium to buffer a produced acid or to facilitate the reductive elimination step.
- (3) the repetitive use of activated substrates which limits the scope investigation.
- (4) The crucial role of electron-rich ligands needed to avoid the formation of side products.

#### **D. Electrochemistry**

Known since decades ago, electrochemistry offers a great alternative to the existing methods by replacing excessive quantities of reducing reagents with clean electrons.<sup>19</sup> Gladly, the reduction of carbon dioxide requires a single electron transfer, therefore the electrochemistry seems to be the right choice for this kind of transformation. Although it can be used for an efficient pathway to obtain biofuels such as formic acid, methanol, and methane via electron transfer mechanism (**Figure 8**), the electrocarboxylation of commercially available organic substrates permits to access valuable products like carboxylic acids.<sup>20</sup>

In the 1960s, Loveland *et al.* described the first electrocarboxylation of 1,3-butadiene using a platinum anode and a mercury cathode in a two-compartment cell, initially used to eliminate any side products.<sup>21</sup> However, a mixture of mono and dicarboxylic acids were obtained due to the manipulation under a low  $\text{CO}_2$  pressure, which plays a significant role in the selectivity, in addition to the high cost of used membranes.

The use of a sacrificial anode (e.g., Mg, Al) instead of an inert anode combined with other cathode materials (e.g., Ni, stainless steel) can work efficiently in an undivided cell (**Figure 13**). This modification allowed the use of high  $\text{CO}_2$  pressure and consequently, provided higher reaction selectivity.<sup>22</sup>

As in photochemistry, the metal- $\text{CO}_2$  interaction depends on the redox potential of the metal center. If the metal complex has a higher  $E_{\text{redox}}$  than the  $E_{\text{redox CO}_2}$  (-2.21 V vs. SCE in DMF),  $\text{CO}_2$  activation yields the formation of the corresponding radical anion. However, organic frameworks characterized by a reduction potential in this window can also be reduced. On the opposite case ( $E_{\text{redox metal complex}} < E_{\text{redox CO}_2}$ ), the metal will likely undergo a reduction of the substrate in the

<sup>19</sup> P.S. Baran, Y. Kawamata, M. Yan, *Chem. Rev.* **2017**, *117*, 13230

<sup>20</sup> D.E. De Vos, K. Binnemans, J. Fransaer, R. Matthessen, *Beilstein J. Org. Chem.* **2014**, *10*, 2484

<sup>21</sup> J. W Loveland, *U.S. Patent* 3,032,489, May 1, 1962

<sup>22</sup> G. Silvestri, S. Gambino, G. Filardo, *Acta Chem. Scand.* **1991**, *45*, 987

medium to form a strong nucleophile (Grignard type reagent) that will eventually reduce the CO<sub>2</sub> delivering the expected carboxylic acid.

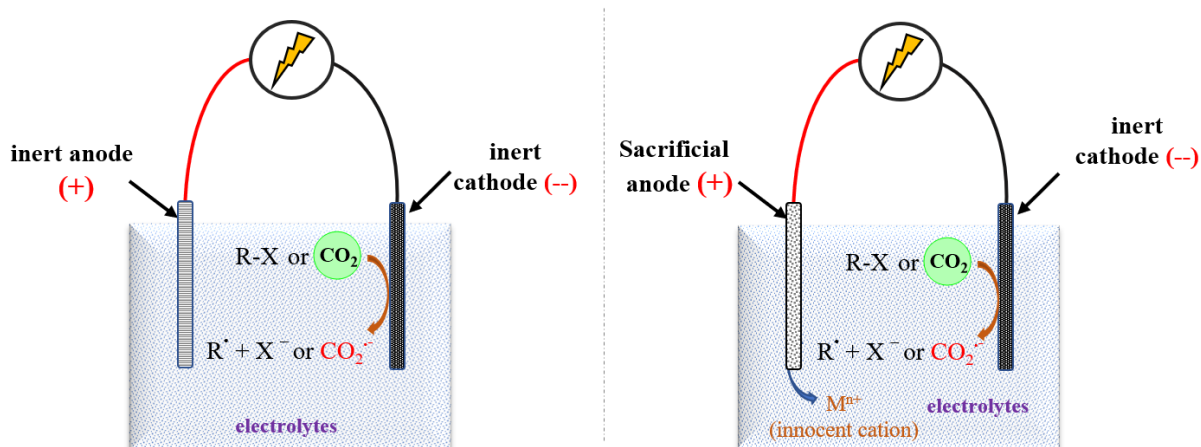


**Figure 13:** The difference between the electrocarboxylation using inert anode (*on the left*) and sacrificial anode (*on the right*)

Based on these points, many systems were developed with different sacrificial anodes aiming to extend the reactivity and to transform diverse substrates (organic halides, alkenes, dienes, alkynes, imines, ketones, aldehydes, amino acids...).<sup>19</sup> Furthermore, many attempts to increase the selectivity by adding redox mediators, proton scavengers, different ammonium salts, etc.... were performed and well investigated.<sup>19</sup> Still, large amount of waste generated from the significant consumption of metal (the anode), remained a considerable drawback besides the use of toxic lead and expensive platinum as cathodes.

After 35 years, the electrocatalytic reduction of CO<sub>2</sub> still suffers from these problems and needs much more attention to fulfill its goal. It reflects the immense challenge behind the development of an electrochemical system capable of overcoming the high thermodynamic stability and kinetic inertia of this gas without demanding harsh conditions or an additional additive.

In our group, we have developed recently a new electrochemical method based on using samarium electrode as the anode to generate *in situ* divalent samarium complexes, known as active monoelectronic reductive reagents,<sup>23</sup> and widely used since their simple and easy preparation developed by Professor Henri Kagan in 1977.<sup>24</sup>

This electrochemical intervention allowed not only to access a broader application for these complexes but also to prepare *in situ* this air-sensitive reagent under mild conditions and without extreme precautions.

Inspired by the literature and relying on our expertise in the divalent samarium domain, we decided to investigate its affinity towards the CO<sub>2</sub> and to elaborate a new strategy to activate the carbon dioxide using catalytic amounts of Sm(II) electrogenerated complexes.

<sup>23</sup> a) M. Mellah, K. Sahloul, *Chem. Eur. J.*, **2012**, 11205; b) M. Mellah, L. Sun *Organometallics*, **2014**, 33, 4625.

<sup>24</sup> P. Girard, J.-L. Namy, H.B. Kagan, *New. J. Chem.* **1977**, 1, 5; P. Girard, J.-L. Namy, H.B. Kagan, *J. Am. Chem. Soc.* **1980**, 102, 2693; J.-L. Namy, P. Girard, H.B. Kagan, *Nouv. J. Chim.* **1981**, 5, 479.

---

# Samarium (II): a powerful reducing agent

---

## 1. Complexes of divalent samarium and their applications

### a. The synthesis of $\text{SmI}_2$

The synthesis of  $\text{SmI}_2$  has gone through a long series of optimization before becoming a commercially available solution today.

In 1906, Matignon and Cazès successfully reduced  $\text{SmI}_3$  to the  $\text{SmI}_2$  by using metallic samarium as a reductant or dihydrogen gas under very high temperature (between 600-900°C).<sup>25</sup> However, these harsh conditions impede their future applications in fine chemistry.

Seventy years later, Professor Kagan introduced the first synthesis of  $\text{SmI}_2$  under mild conditions, and since then, the  $\text{SmI}_2$  in solution is called “Kagan’s reagent”. A dark blue solution of  $\text{SmI}_2$  was obtained, after 1h, in anhydrous THF containing a mixture of samarium powder and 1,2-diiodoethane under an inert atmosphere, ready to use in organic synthesis.

Kagan’s work on divalent samarium encouraged other chemists to develop a more efficient synthesis of  $\text{SmI}_2$ . The use of some protocols replaced  $\text{ICH}_2\text{CH}_2\text{I}$  with  $\text{I}_2$ ,<sup>26</sup> others described later the use of sophisticated systems such as ultrasounds<sup>27</sup> and microwaves<sup>28</sup> to produce more efficiently this reagent (**Figure 14**).

The limitations of these synthetic protocols were the poor  $\text{SmI}_2$  solubility in THF in addition to the air sensitivity of this complex. For this reason, the manipulation using this reagent was possible only under inert atmosphere and in anhydrous solvents to achieve the desired results. Moreover, most of the transformations mediated by  $\text{SmI}_2$  required an over stoichiometric amount of this reagent to furnish the targeted product according to the number of transferred electrons.

---

<sup>25</sup> C.A. Matignon, Cazès, *Ann. Chim. Et de Phys.*, **1906**, 8ème série, t. VIII, 417

<sup>26</sup> a) T. Imamoto, M. Ono, *Chem. Lett.*, **1987**, 501; b, Y. Nishiyama, Y. Kanagawa, N. Akane, Y. Ishii, *Chem. Lett.*, **1992**, 2431; c) Y. Nishiyama, H. Kusui, T. Hatano, N. Akane, Y. Ishii, *J. Org. Chem.*, **1994**, 59, 7902.

<sup>27</sup> a) J.M. Concellon, H. Rodríguez-Solla, E. Bardales, M. Huerta, *J. Org. Chem.*, **2003**, 1775; R.A. Flowers, E.N. Pesciotta, E. Prasad, P.K.S. Antharjanam, J.A. Teprovich, *Inorg. Chem.*, **2008**, 5015.

<sup>28</sup> a) G. Hilmersson, A. Dahlén, *J. Inorg. Chem.*, **2004**, 3020; b) G. Hilmersson, R.A. Flowers, E. Prasad, A. Dahlén, *Chem. Eur. J.*, **2005**, 11, 3279

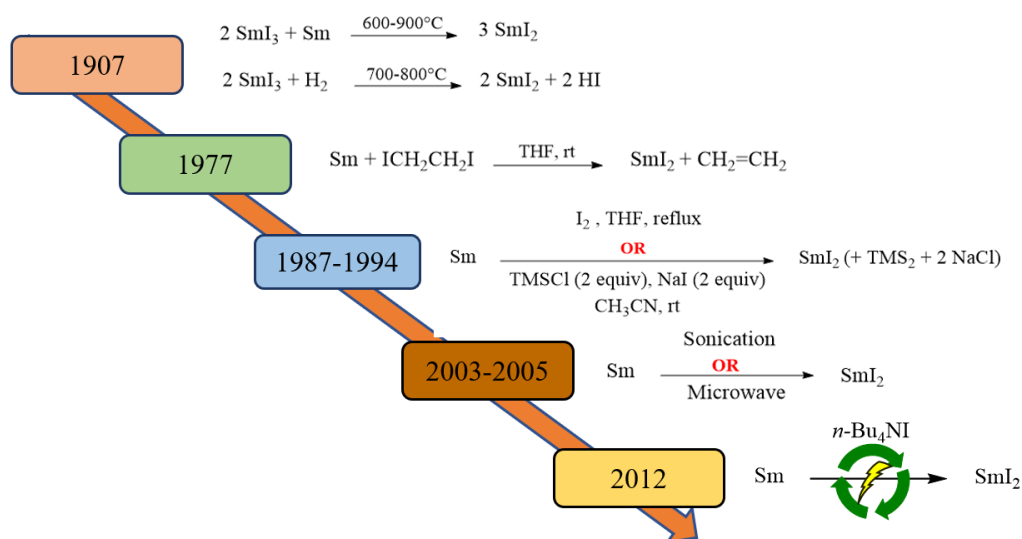


**Figure 14:** The reported optimization of the synthesis and the electrolysis of  $\text{SmI}_2$  between 1907 and 2012.<sup>29</sup>

These critical points encouraged the chemists to investigate other samarium complexes, aiming to enhance not only the solubility of these species but also their reactivity and the resulting selectivity.

### b. Other complexes of divalent samarium

To modulate the reactivity of samarium, different complexes were prepared, generally starting from  $\text{SmI}_2$  through salt metathesis (**Figure 15**):

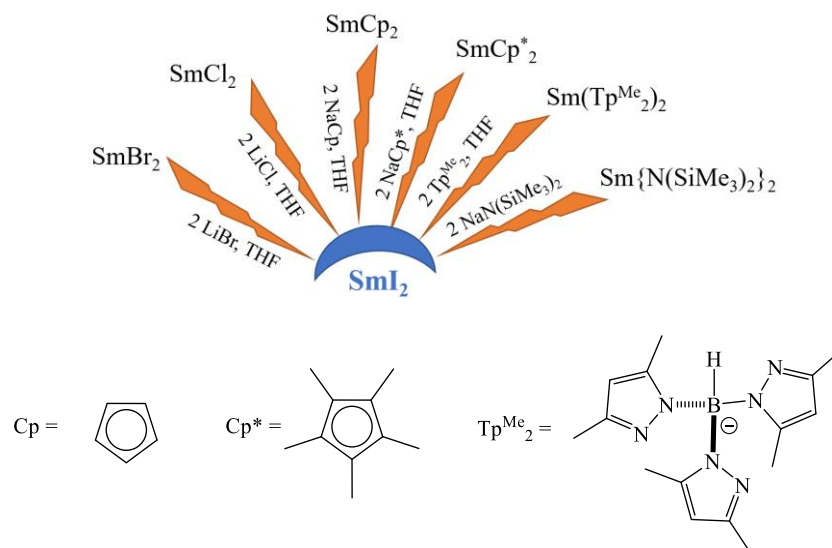


**Figure 15:** Sm(II)-based reductants.

<sup>29</sup> M. Szostak, M. Spain, D. J. Procter, *J. Org. Chem.* **2012**, 77, 3049

The obtained Sm(II) complexes were subject for extensive reactivity investigations to study their potentials in radical chemistry, especially the SmI<sub>2</sub> (**Figure 16**).<sup>30</sup> Consequently, many applications arose over the years from the reduction of diverse functional groups to C-C, C-N and very recently, N-N bond formation.<sup>31</sup>

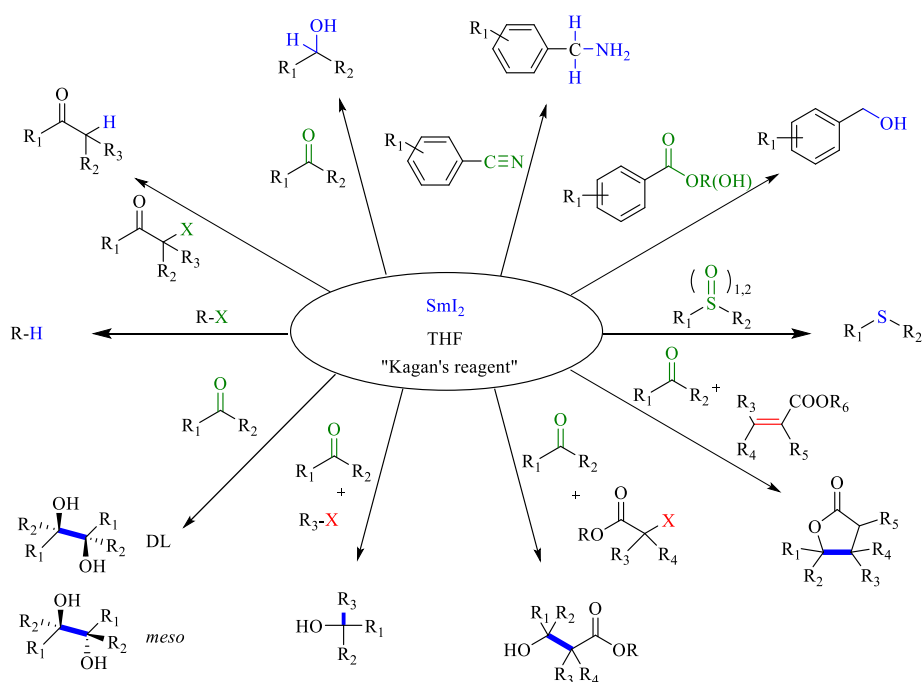


**Figure 16:** Applications of the divalent SmI<sub>2</sub> in the literature.

Since the reactivity of the Sm(II)-based complexes is quite extraordinary, and it took many years to uncover the secret behind this particular behavior of the metal center. The primary concern is how to control such reactivity to obtain the desired selectivity in a chemical transformation.

### c. The influence of additives on Sm(II) complexes reactivity

The Sm(II) center presents a unique monoelectronic reactivity, due to the high stability of its (+3) oxidation state. The redox potential of the corresponding complexes depends on many factors, and particularly the associated ligand. The ligand choice indeed modulates the reductive power of these colorful complexes and controls thus their selectivity.<sup>30,32</sup>

Interestingly, these species show a high affinity for the oxygen and nitrogen atoms. Therefore, their air sensitivity is attributed to their affinity to the oxygen in the atmosphere. Any manipulation using Sm(II) complexes should be conducted under an inert atmosphere, otherwise, the oxidation to the (+3) state can occur rapidly, evidenced by an immediate change of the color of the solution.

<sup>30</sup> M. Szostak, M. Spain, D. J. Procter, *Chem. Soc. Rev.* **2013**, *42*, 9155; M. Szostak, N. J. Fazakerley, D. Parmar, D. J. Procter, *Chem. Rev.* **2014**, *114*, 5959.

<sup>31</sup> D. Procter, R.A. Flowers, T. Skrydstrup, *Organic Synthesis Using Samarium Diodide: A Practical Guide*, RSC Publishing: Cambridge, U.K., **2010**.

<sup>32</sup> S. Maity, R.A. Flowers, *J. Am. Chem. Soc.* **2019**, *141*, 3207

The SmI<sub>2</sub> remained representative for the divalent Sm complexes over the past decade. Many radical transformations were mediated by this reagent with considerable selectivity. After studying the literature, the main parameters to manipulate the redox potential of the divalent samarium species are summarized below:

**i. Lewis Base:** These additives are characterized by high electron density, and therefore, their coordination to the divalent metal center enhances its redox potential. The most common example is the use of hexamethylphosphoramide (**HMPA**) introduced by Inanaga in 1987, who proved its effect on the reduction rate of alkyl and aryl halides allowing alkyl chlorides to react at room temperature.<sup>33</sup> By adding HMPA, not only the reaction rate increased but also a remarkable gain in selectivity towards the desired product was reported by Molander in 1992 in a reductive cyclization of unactivated unsaturated ketones.<sup>34</sup> This selectivity was subsequently explained by a formation of a sterically encumbered reductant Sm-HMPA responsible for limiting the side reactions (hydrogen atom abstraction from THF), stabilizing the radical intermediates and boosting the diastereoselectivity.<sup>35</sup>

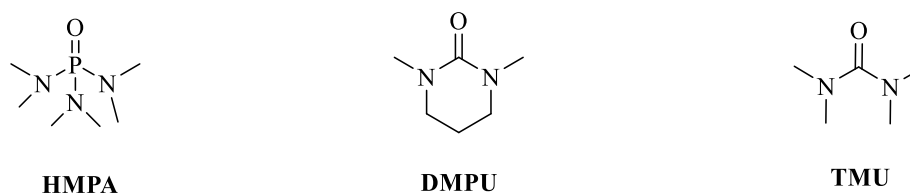


**Figure 17:** Lewis Base reagents used with SmI<sub>2</sub> chemistry

For toxicity reasons, HMPA was afterward substituted by other nitrogen-containing reagents such as 1,3-dimethyl-3,4,5,6-tetrahydro-2(1H)-pyrimidinone (**DMPU**) and 1,1,3,3-tetramethylurea (**TMU**) that demonstrated a similar reactivity in different transformations (**Figure 17**).

**ii. Proton donor:** The proton source offers an opportunity to modulate the reaction rate and the selectivity at the same time, as reported in previous examples.<sup>31</sup> The reduction of ketones was successfully performed to the corresponding alcohols using a combination of SmI<sub>2</sub> and proton donors. This latter has a considerable impact on the mechanistic pathway as described by Procter's group in 2003. In this work, two different cyclization products were independently obtained by only varying the proton source, with either methanol or *t*-butanol (**Figure 18**).<sup>36</sup> Using the former permitted the isolation of the spiro compound while the latter gave the four-membered ring, clearly from another mechanistic route. To explain this difference, the authors proposed that MeOH reacted as a ligand to the metal center which made the protonation step much faster. Whereas, in *t*-BuOH, a noncoordinating bulky proton donor, the samarium was coordinated by THF. As a result, the radical anion intermediate underwent a radical cyclization to form the cyclobutanol derivatives.

<sup>33</sup> J. Inanaga, M. Ishikawa, M. Yamaguchi, *Chem. Lett.* **1987**, 1485.

<sup>34</sup> G.A. Molander, J.A. Mckie, *J. Org. Chem.* **1992**, 57, 3132.

<sup>35</sup> K.A. Choquette, D.V. Sadasivam, R. A. Flowers, *J. Am. Chem. Soc.* **2010**, 132, 17396.

<sup>36</sup> T.K. Hutton, K.W. Muir, D.J. Procter, *Org. Lett.*, **2003**, 5, 25, 4811.

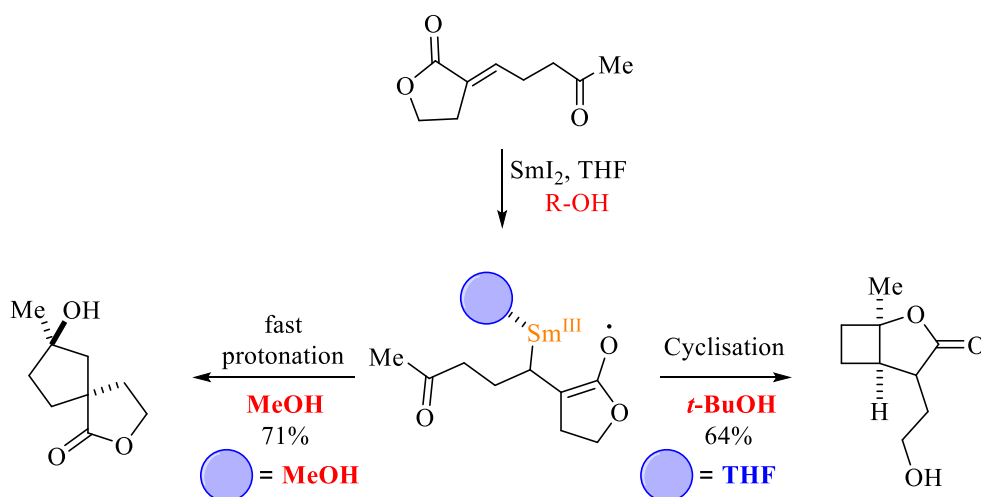


**Figure 18:** Stereoselective cyclization of  $\gamma$ ,  $\delta$ -unsaturated ketones mediated by  $\text{SmI}_2$  according to the alcohol cosolvent.<sup>36</sup>

In this context, water can also be used as a proton donor as Procter and co-workers described for the reduction of aliphatic esters that remained a great challenge since many years ago, by using a  $\text{SmI}_2\text{-H}_2\text{O}$  system.<sup>37</sup> Interestingly, this duo allowed many difficult reactions to work efficiently.

This distinct behavior of the alcohols, known as weak acids, is attributed to the ability of  $\text{Sm(II)}$  to withdraw the oxygen electrons, which enhances the ionic character of the O-H bond and results in an important drop in pKa.

**iii. Inorganic additives:** Mineral salts are considered key components in some reactions mediated by  $\text{SmI}_2$ . While some of them stimulate a ligand exchange to form *in situ* a stronger reductive samarium complex (e.g.,  $\text{LiBr}_2$ ,  $\text{LiCl}_2$  to generate  $\text{SmBr}_2$  and  $\text{SmCl}_2$  from  $\text{SmI}_2$ , respectively) (**Figure 19, on the left**),<sup>38</sup> others like  $\text{FeCl}_3$  and  $\text{NiI}_2$  can interfere in the mechanism of the reaction.<sup>30,39</sup> The evaluation of the  $E^\circ$  value of these transition metals proves that samarium easily reduces  $\text{Ni(II)}$  to  $\text{Ni(0)}$  and  $\text{Fe(III)}$  to  $\text{Fe(II)}$  or  $\text{Fe(0)}$  (**Figure 19, on the right**). As a result, a new type of reactivity can arise that usually does not exist in the unique presence of  $\text{SmI}_2$ .

<sup>37</sup> M. Szostak, M. Spain, A.J. Eberhart, D. J. Procter, *J. Org. Chem.* **2014**, *79*, **24**, 11988.

<sup>38</sup> A. Dahlén, G. Hilmersson, *Eur. J. Inorg. Chem.* **2004**, 3393.

<sup>39</sup> H.B. Kagan, *J. Alloys Compd.* **2006**, *408*, 421.

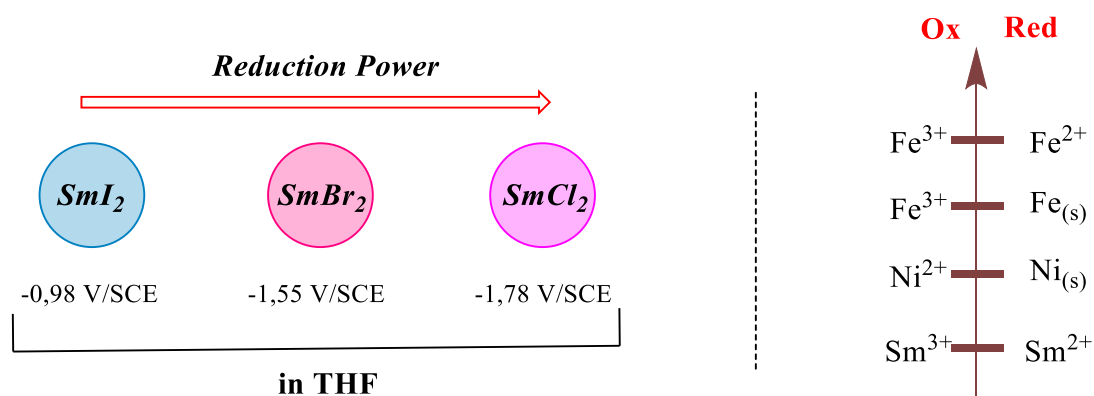


**Figure 19:** Comparison between the redox potential of  $SmI_2$ ,  $SmBr_2$ , and  $SmCl_2$  (on the left); The redox potential of inorganic additives compared with the  $Sm(II)$  (on the right).

In conclusion, depending on the desired reactivity, the samarium chemistry offers a wide range of applications for the reduction of many functional groups and for C-C bond formations. Whether it is a cyclization to trigger a simple reduction or to produce a complex product, the additives are an important option to consider, according to their enormous effect on the rate, the yield, and the selectivity of a reaction.

These complexes were continuously used in an over stoichiometric amount until the establishment of catalytic conditions by Endo and co-workers in 1996.<sup>40</sup>

#### *d. The challenge behind developing processes catalyzed by $Sm(II)$*

Elaborating catalytic reactions with  $Sm(II)$  complexes requires thinking about different critical aspects. Firstly, exploring a reaction with 1/10 of the original amount of  $Sm(II)$  could not work as with an over stoichiometric quantity of this latter, like the reduction of some challenging functional group usually necessitating harsh conditions to induce the expected reactivity. Furthermore and most importantly, the use of catalytic amount of samarium requires finding a technique to cleave the  $Sm(III)$  from the product, especially those holding an oxygen atom. Therefore, an oxophilic reagent must be used to regenerate the  $Sm(II)$ .

Endo's group found an answer to all these concerns in a pinacol coupling reaction, by adding trimethylsilyl chloride  $TMSCl$  as an oxophilic reagent to dissociate the trivalent samarium and magnesium in the solid-state as a co-reductant.<sup>40</sup> The reaction led to moderate to good yields.

<sup>40</sup> R. Nomura, T. Matsuno, T. Endo, *J. Am. Chem. Soc.* **1996**, *118*, 11666.



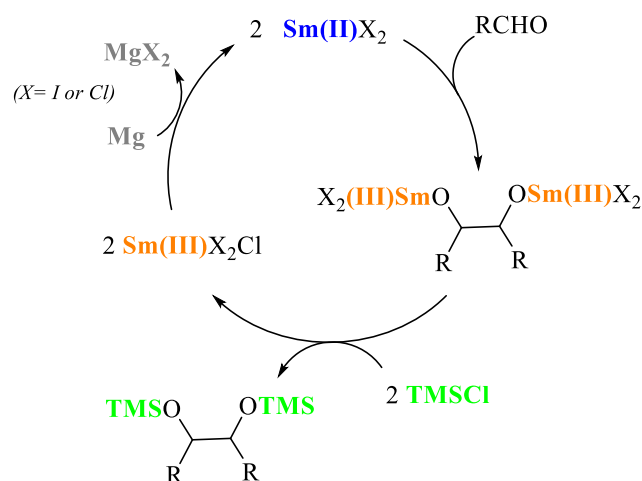


**Figure 20:** Pinacolisation mechanism catalyzed by  $\text{SmI}_2$ .

Based on this concept, several conditions were developed with different reactions, involving various oxyphilic reagents (TMSOTf) and reductants (Zn-Hg, mischmetal).<sup>41</sup> The main problem was the excessive amount of co-reductant required for each transformation in addition to the absence of general conditions to apply for different types of reactions.

Very recently, Procter's group published the first radical cyclization reaction catalyzed by  $\text{SmI}_2$  with no need for a reductant or an oxyphilic additive (**Figure 21**).<sup>42</sup>

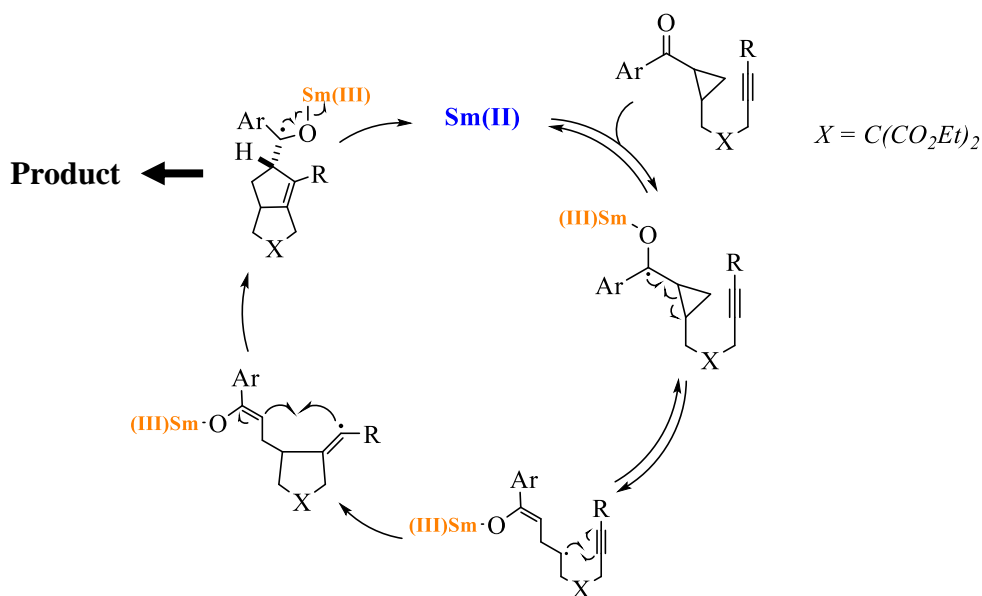


**Figure 21:** The proposed mechanism for the cyclization cascades catalyzed by  $\text{SmI}_2$ .

In this reaction, a cyclopropane substituent is mandatory on the  $\alpha$ -position of the ketyl radical to open and subsequently form another radical. This latter then undergoes a radical addition on the

<sup>41</sup> a) E.J. Corey, G.Z. Zheng, *Tetrahedron Lett.* **1997**, 38, 2045; b) F. Héllion, J.-L. Namy, *J. Org. Chem.* **1999**, 64, 2944; c) M.-I. Lannou, F. Héllion, J.-L. Namy, *Tetrahedron* **2003**, 59, 10551

<sup>42</sup> H.-M. Huang, J.J.W. McDouall, D.J. Procter, *Nature Catalysis* **2019**, 2, 11

alkyne leading to the formation of the first cycle and a vinyl radical that performs 1,2-radical addition to the Sm(III) enolate and form the ketyl radical again. The critical step lies in the regeneration of Sm(II) and which is due to the thermodynamic stability of the final product, allowing a back-electron transfer process to Sm(III).

Despite the great presented work, this protocol is based on specifically designed substrates and does not offer a general protocol for catalytic Sm(II) mediated reactions.

With no doubt, the efforts involved to develop catalytic conditions have achieved a great advance since the first preparation of Sm(II) complexes. The main difficulty resides in finding the optimal system to regenerate the (+2) oxidation state of samarium without using a large quantity of a non-innocent co-reductant. Besides, the oxyphilic additive remains an essential addition to the reaction, even though it is frequently used in an over-stoichiometric quantity. Nevertheless, it does not interfere at least in the mechanism.

In this context, electrochemistry appears to be an excellent substitute for the co-reductants, as an efficient clean-electron source to regenerate the Sm(II) without producing any metallic wastes. Périchon's group applied this idea by using a magnesium or aluminum sacrificial anode and a nickel cathode in the presence of SmCl<sub>3</sub> for radical coupling of aldehydes and ketones,<sup>43a</sup> and later on for direct reductive dimerization of aromatic esters.<sup>43b</sup> Under these electrochemical conditions, the Sm(II) is generated *in situ* from the electroreduction of SmCl<sub>3</sub>. Moreover, the Mg<sup>2+</sup> or Al<sup>3+</sup> cations served as oxyphilic reagents to dissociate the Sm(III) from the final product. Although the amazing advance reported in this work, the continuous generation of additional active metallic salts in the reaction remains a considerable disadvantage from a mechanistic and ecologic point of view.

#### *e. Electrogenerated Samarium complexes*

The work of our group is based on using a samarium sacrificial anode in the presence of ammonium salts, as the source of anions/ligands for samarium (I<sup>-</sup>, Br<sup>-</sup>, Cl<sup>-</sup> ...). The electricity allows the *in situ* oxidation of Sm(s) anode to access the divalent samarium complexes and on the other hand, the cathodic reduction transforms the tetrabutyl ammonium cations to a mixture of tributylamine, butane, and n-butene.<sup>24</sup>

---

<sup>43</sup> a) E. Léornard, E. Duñach, J. Périchon, *J. Chem. Soc., Chem. Commun.* **1989**, 276; b) H. Hébré, E. Duñach, M. Heintz, M. Troupel, J. Périchon, *Synlett.* **1991**, 901.

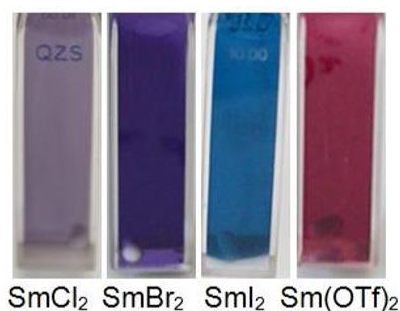


**Figure 22:** Samarium(II) complexes prepared by electrolysis from Sm anode.

The equivalents of samarium generated in the solution are calculated using the equations below. During a *chronopotentiometry* experiment, the quantity of electricity  $Q$  (in Coulomb C) is proportional to the current value  $i$  (in Ampere A) and the electrolysis time  $t$  (in seconds s), so:

$$Q = i \times t$$

Also, Faraday's first law states that:

$$Q = z \times n \times F$$

$z$ : the valency number of ions of the substance (electrons transferred per ion)

$n$ : number of moles of the electrogenerated species.

$F$ : Faraday's constant =  $96485 \text{ C}\cdot\text{mol}^{-1}$

Depending on the dielectric constant of the solvent, the electrons circulation suffers from more or less medium resistance, and thus, the quantity of electricity is never the exact as the calculated one, so we finally obtain this equation:

$$\eta \times i \times t = z \times n \times F$$

$\eta$ : Faraday efficiency (calculated by titration around 70% in THF).

Fixing the current value and adding a determined quantity of the substrate allows the calculation of the reaction time  $t$  to electrogenerate the desired number of Sm(II) equivalents in the medium.

Additionally, this method demonstrated that the *in situ* generation of this monoelectronic reductant does not only increase the reactivity of the divalent complex but also facilitates the manipulation of such sensitive species. As an example, the reduction of alkyl chloride derivatives was only possible with a chemically prepared  $\text{SmI}_2$  solution containing 8 equivalent of HMPA under  $60^\circ\text{C}$  for 8 hours (**Figure 23, Condition A**).<sup>33</sup> Under electrochemical conditions, and after only 2 hours, the reduction afforded 77% of the product in the presence of *t*-BuOH as a proton source, at room temperature (**Figure 23, Condition B**).<sup>23b</sup>

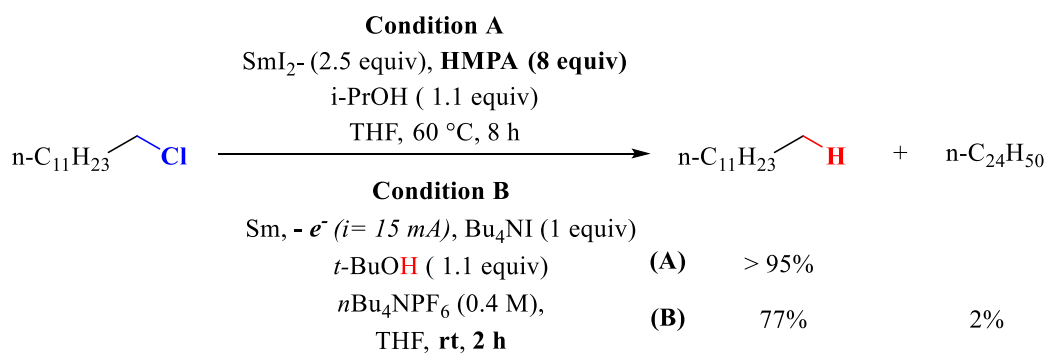


**Figure 23:** The reduction of aliphatic chloride by divalent samarium complexes.

Another representative example is the reduction of aliphatic ketones, known for their high reduction potential. In batch, these compounds are only accessible with SmBr<sub>2</sub>, while electrogenerated SmI<sub>2</sub> achieved the reduction using mild conditions (**Figure 24**).<sup>23a</sup>

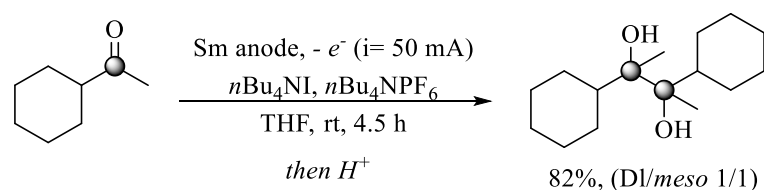


**Figure 24:** Reduction of aliphatic ketones mediated by electrogenerated SmI<sub>2</sub>.

#### f. Electrocatalysis using Sm(II) complexes

The primary goal of this electrochemical method was always the elaboration of catalytic applications using the divalent Sm complexes. After several optimizations, the addition of 1.5 equiv of TMSCl allowed decreasing the amount of the electrogenerated Sm(II) to 10 mol% in the previous reactions (pinacolization and Barbier-type reactions).<sup>44</sup> Furthermore and to regenerate the Sm(II), the polarity of the electrodes was reversed after the electrogeneration of the calculated catalytic amount. Thus, the samarium electrode becomes the cathode where the reduction takes place and the glassy carbon (GC) or the stainless steel (SS) anode for the oxidation. After the electron transfer, the Sm(III) dissociation from the intermediate or the product assisted by the TMSCl, permits its reduction on the Sm cathode and the regeneration of the active Sm(II) species.

The figure below illustrates the process in detail:

<sup>44</sup> L. Sun, K. Sahloul, M. Mellah, *ACS Catal.* **2013**, 3, 256.

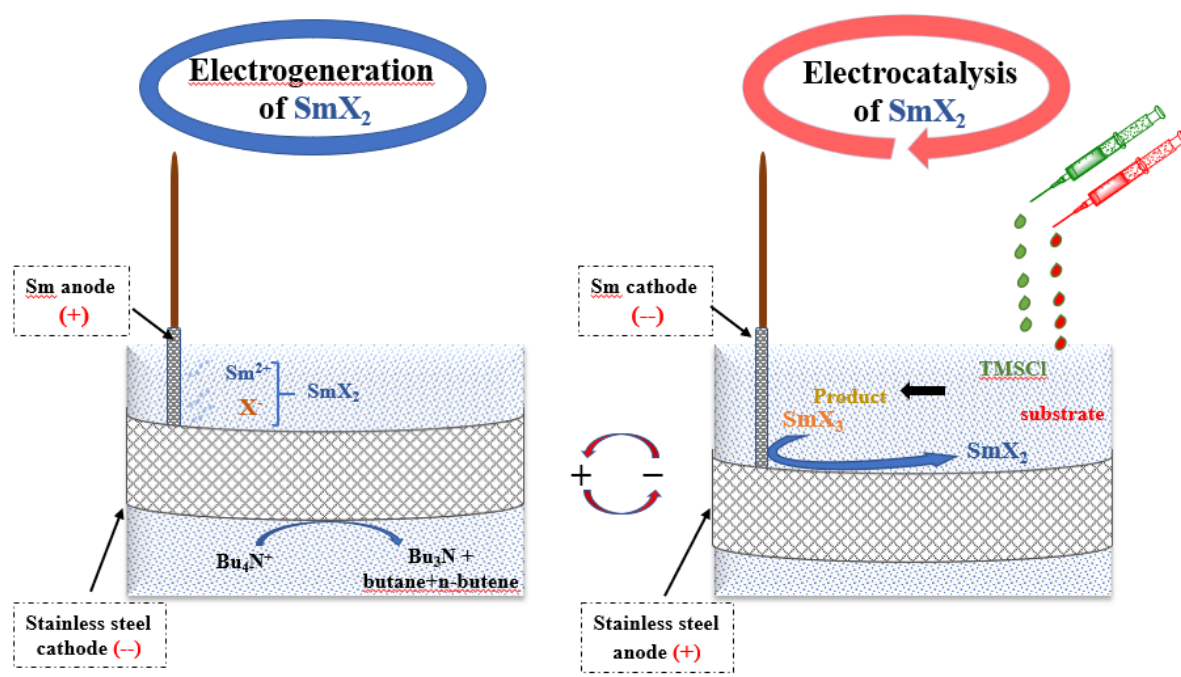


**Figure 25:** Electrogeneration (on the left) and electrocatalysis (on the right) processes with  $\text{SmX}_2$ .

Under these conditions, a reducing agent is no more needed during the electrocatalysis process and thus, metallic wastes are consequently not produced leading to a reaction clearly mediated by the unique catalyst in the mixture, the divalent samarium.

Using this process, the synthesis of symmetric and dissymmetric azobenzene derivatives was reported by our group, starting from the corresponding nitrobenzenes (**Figure 26**).<sup>45</sup> In the literature, the reduction of nitrobenzenes is achieved only under harsh conditions using expensive catalysts.

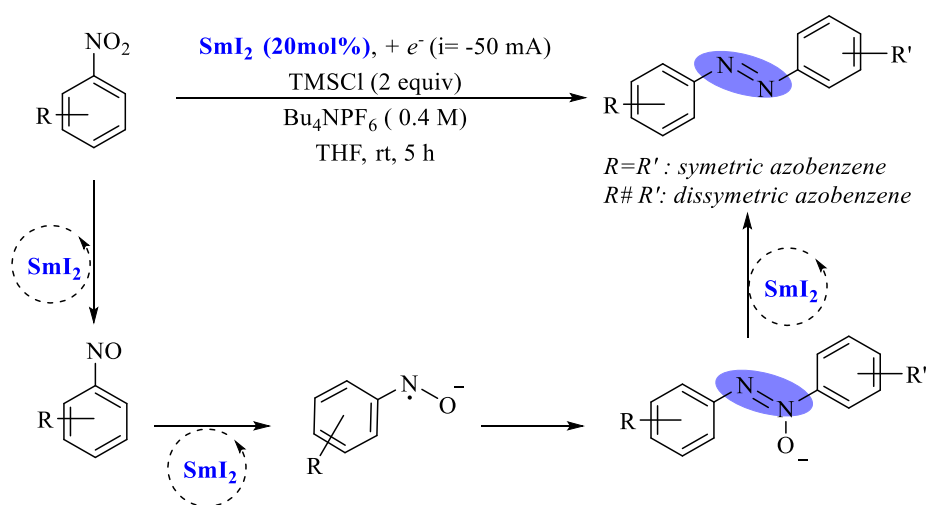


**Figure 26:** The synthesis of azobenzene derivatives catalyzed by electrogenerated  $\text{SmI}_2$ .<sup>45</sup>

Furthermore, the challenging reduction of phthalimides and sulfoxides was also viable using our method (unpublished results).

Undoubtedly, our electrocatalytic procedure offers a promising tool to widen the catalytic applications of divalent samarium complexes. Nowadays, the reduction of carbon dioxide and its use as a C<sub>1</sub>-building block is one of the most discussed topics in chemistry. While our method was successful for the reduction of challenging functional groups, we wondered if it can be applied in the case of CO<sub>2</sub>, known for its high thermodynamic and kinetic stability.

In this context, the reported examples combining the use of divalent samarium complexes with CO<sub>2</sub> are reported in the next section.

### g. Carbon dioxide activation using divalent Sm in the literature

The first CO<sub>2</sub> reduction to oxalate using Cp\*<sub>2</sub>Sm(THF)<sub>2</sub> complex was described in 1998 by Evans's group.<sup>15</sup> Under CO<sub>2</sub> atmosphere and after only 6 min in THF, the authors demonstrated that the oxidation of Sm(II) to Sm(III) occurred based on the Cp\* chemical shift in <sup>13</sup>C NMR spectra and the presence of a carboxylate carbon shift at 200 ppm indicating the reduction of carbon dioxide. Crystals could be recovered and they surprisingly showed a bimetallic complex with an oxalate molecule bridging the two centers to form the orange [(C<sub>5</sub>Me<sub>5</sub>)<sub>2</sub>Sm]<sub>2</sub>(μ-η<sup>2</sup>: η<sup>2</sup>-O<sub>2</sub>CCO<sub>2</sub>) complex (**Figure 27, top**). In this complex, each metal center is attached to two oxygen atoms to create a five-membered ring instead of a four-membered ring.

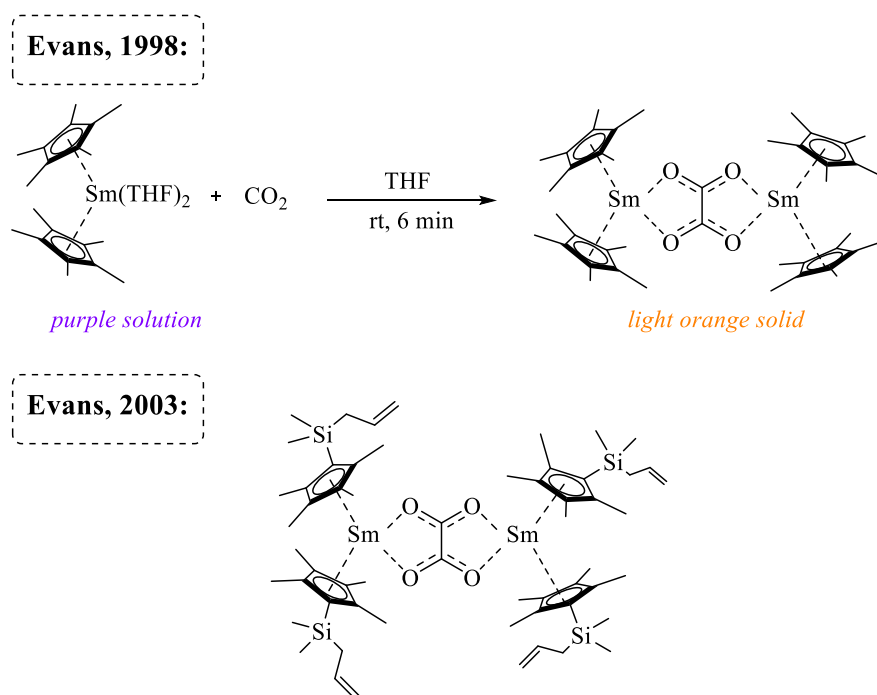


**Figure 27:** The formation of the oxalate complex issued from the reaction of (Cp\*)<sub>2</sub>Sm(THF)<sub>2</sub> derivatives with CO<sub>2</sub> reported by Evans.<sup>15, 46</sup>

Notably, the same group and others published a few years later another Sm(II) complexes just by changing the ligand and exhibiting an analog reactivity (**Figure 27, bottom**).<sup>46</sup>

After more than 15 years, a DFT study to explain the Cp\*<sub>2</sub>Sm - CO<sub>2</sub> interaction was reported.<sup>47</sup> The calculation demonstrated that the oxalate product is thermodynamically favorable, and its formation is a two-step process: First, the Cp\*<sub>2</sub>Sm<sup>II</sup> reduces the CO<sub>2</sub> to form not the mononuclear radical, anionic species [Cp\*<sub>2</sub>Sm<sup>III</sup>(CO<sub>2</sub><sup>•-</sup>)] but the dinuclear complex found to be much more stable than the first. Second, by the elongation of the Sm<sup>I</sup>-C bond with a shortening of the Sm<sup>I</sup>-O one allows the insertion of a second molecule of CO<sub>2</sub> to yield the bridged oxalate complex (**Figure 28**).

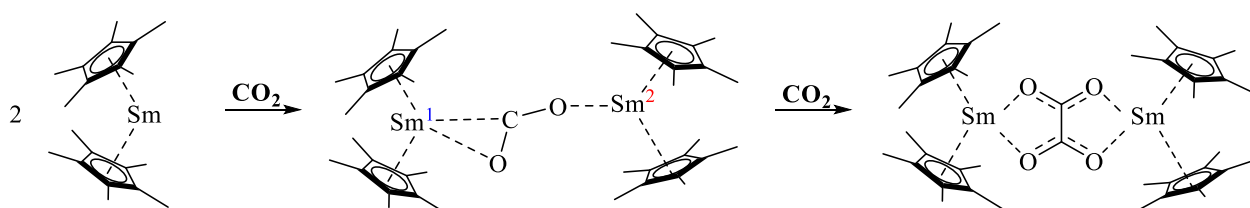


**Figure 28:** The proposed pathway for the reaction of the Cp\*<sub>2</sub>Sm complex with CO<sub>2</sub>.<sup>47</sup>

Besides the reductive disproportionation of carbon dioxide,<sup>48</sup> examples targeting C-C bond formation via CO<sub>2</sub> activation using divalent samarium as a reductive reagent, are limited, as far as we know, to one report by Ogawa's group describing a photoinduced reductive carboxylation of alkyl halides (**Figure 29**).<sup>49</sup> The authors described two mechanistic pathways. **Path A** proposed the formation of an organosamarium in the medium that attacks the CO<sub>2</sub> moiety to furnish the corresponding carboxylic acid. Whereas the **path B** suggested that after the formation of alkyl radical species and the coordination of CO<sub>2</sub> to SmI<sub>2</sub>, a photoinduced electron transfer to the CO<sub>2</sub> triggers the formation of the corresponding radical anion and finally, the radical coupling yields the desired carboxylic acid.

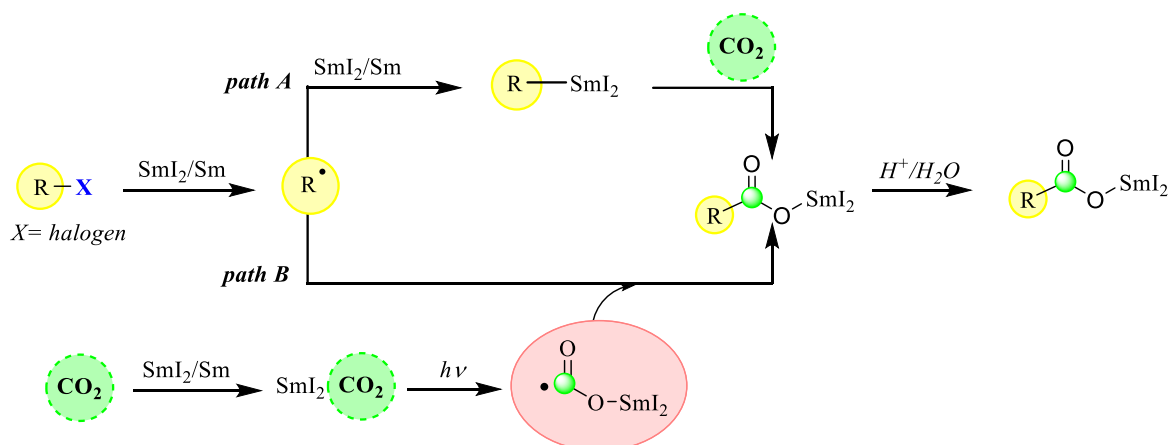


**Figure 29:** Photoinduced reductive carboxylation of alkyl halides reported by Ogawa's group.<sup>49</sup>

<sup>46</sup> W.J. Evans, J.M. Perotti, J.C. Brady, J.W. Ziller, *J. Am. Chem. Soc.* **2003**, *125*, 5204.

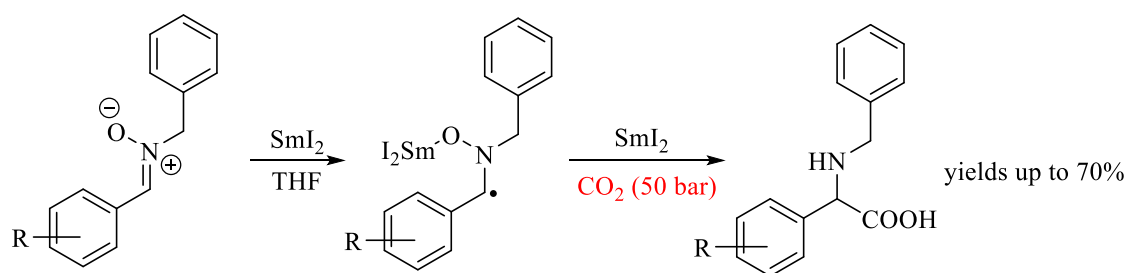
<sup>47</sup> L. Castro, S. Labouille, D.R. Kindra, J.W. Ziller, F. Nief, W. J. Evans, L. Maron, *Chem. Eur. J.* **2012**, *18*, 7886.

<sup>48</sup> M. Mazzanti, M. Laurent, Y. Yang, F. Fadaei-Tirani, D. Toniolo, A.R. Willauer, *Dalton Trans.* **2019**, *48*, 6100

<sup>49</sup> A. Nomoto, Y. Kojo, G. Shiino, Y. Tomisaka, I. Mitani, M. Tatsumi, A. Ogawa, *Tetrahedron Lett.* **2010**, *51*, 6580.

However, the reduction of CO<sub>2</sub> does not occur without the light, and thus, the SmI<sub>2</sub> reductive power is not strong enough to activate the CO<sub>2</sub>. Moreover, without the light, the transformation takes another route, leading to the reduced product R-H.

Other strategies based on the classic organosamarium reactivity were illustrated. For example, Py's group highlighted an interesting pathway to obtain  $\alpha$ -amino acids mediated by SmI<sub>2</sub> starting from nitrones (**Figure 30**).<sup>50</sup> Under 50 bar pressure of CO<sub>2</sub> and an excess amount of SmI<sub>2</sub>, this latter interacts firstly with the nitrones to generate a radical intermediate. After a second electron transfer, the anionic species was produced that was capable to perform a nucleophilic addition with the CO<sub>2</sub> and yielded the desired amino acid.



*side products:*

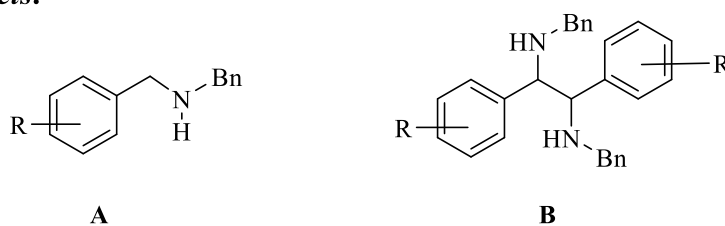


**Figure 30:** Reductive coupling of nitrones with CO<sub>2</sub>.<sup>50</sup>

Despite the various molecules synthesized in this publication, the carboxylation competes with two side reactions, limiting thus the efficiency of this method: the reduced product **A**, obtained after proton abstraction from the solvent and the radical homocoupling leading to the dimer **B**.

<sup>50</sup> A. Prikhod'ko, O. Walter, T.A. Zevaco, J.Garcia-Rodriguez, O. Mouhtady, S. Py, *Eur. J. Org. Chem.* **2012**, 3742.





---

## Summary

---

This concise state of the art serves as an introductory guide for the general impact of carbon dioxide on this life generally and its utilization in fine chemistry. Our aim is to convert it into valuable compounds like pharmaceuticals, polymers, and valuable compounds.

At this stage, the current strategies involve mostly expensive catalysts, strong metal-based reductant, harsh reaction conditions (temperature, pressure)... these drawbacks clearly emphasize the urge to create new routes that avoid these processes and remain efficient and eco-friendly.

Low valent samarium complexes are known since the seminal Kagan's work in 1977. These species are acknowledged for their active monoelectronic redox potentials. Over the past few years, a large variety of transformations were reported with these complexes, but their use was limited to over stoichiometric conditions while the catalytic procedures emerged only after the addition of a reducing agent.

Targeting these flaws, a new electrochemical protocol was developed in our group, allowing the generation *in situ* of these divalent complexes. Generally, the divalent electrogenerated species appear to be powerful and more selective than "classical SmI<sub>2</sub>". This electrochemical approach for SmX<sub>2</sub> chemistry opened a new way for catalytic application and made the catalysis more ecological by replacing the metallic reductant by electricity, as a clean source of electrons.

However, in the literature, we rarely find these two branches of chemistry (carbon dioxide and divalent samarium) combined together for C-C bond formation purposes. Apparently, the Sm (II) species is powerful enough to reduce the CO<sub>2</sub> and on the other hand, we have a rich literature in the C-C coupling mediated by samarium complexes.<sup>51</sup> Still, as far as we know, an example in which the CO<sub>2</sub> is undoubtedly reduced by Sm(II) to consequently promote a radical transformation is not addressed before.

For this reason, the subject of this thesis targets this major field to elaborate carboxylation reactions via CO<sub>2</sub> activation mediated by electrogenerated Sm(II) complexes. We aim to combine our knowledge in divalent samarium chemistry and in electrochemistry to create a new reductive carboxylation procedure. This type of protocols can allow not only the elaboration of reductant-free reactions but also the synthesis of valuable compounds such as carboxylic acids under mild conditions.

---

<sup>51</sup> a) M. Szostak, N.J. Fazakerley, D. Parmar, D.J. Procter, *Chem. Rev.* **2014**, *114*, 5959; b) M. Szostak, D.J. Procter, *Angew. Chem., Int. Ed.* **2012**, *51*, 9238.









---

Carboxylation of aryl halides  
using electrogenerated  
samarium(II) complex via CO<sub>2</sub>  
activation

---



# Carboxylation of aryl halides using electrogenerated samarium(II) complex via CO<sub>2</sub> activation

## 1. Aryl carboxylic acids: state of the art

Aryl carboxylic acids (benzoic acids) and their derivatives are found not only in many natural, medicinal (drugs, radiolabeled tracers, inhibitors) and agrochemical products (herbicides) (**Figure 31**) but also in polymers, detergents, cosmetics, etc. In other words, this class of carboxylic acids is essential and used daily in a large amount, justifying thus the need for efficient, economical, and fast strategies to synthesize these valuable motifs.

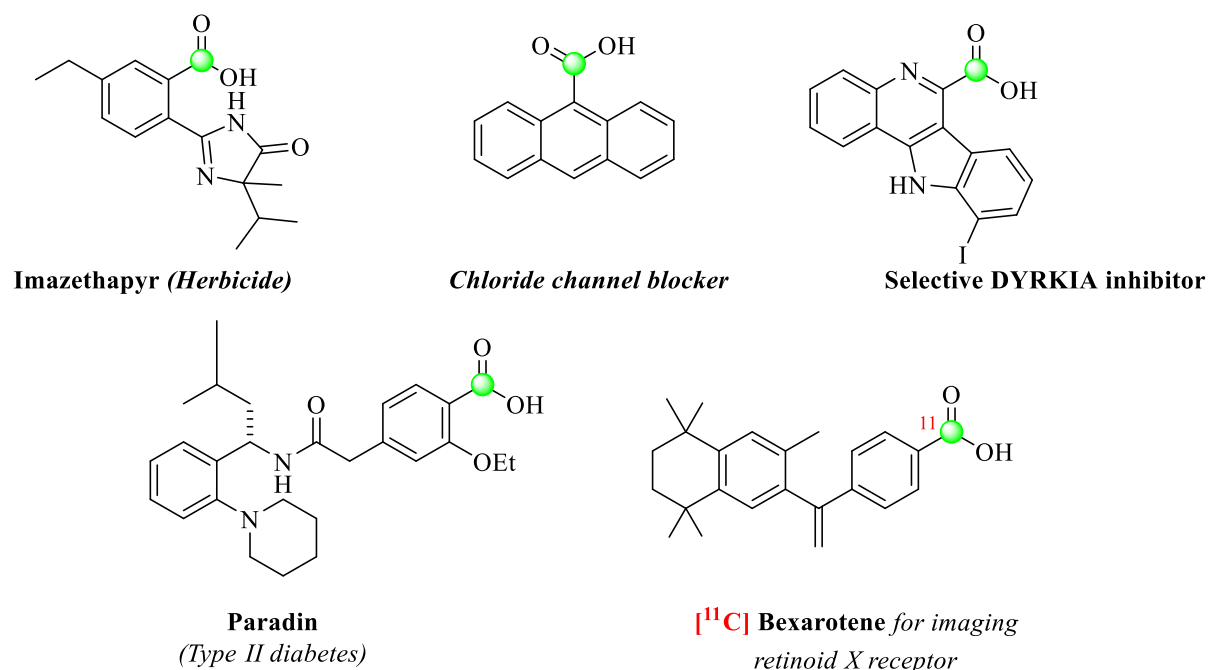


**Figure 31:** Representative examples of benzoic acids in the pharmaceutical and agrochemical industry.

In this context, the use of carbon dioxide as a cheap, abundant, and non-toxic reagent stands as the best ecologic and economic candidate to satisfy the industrial urge for these compounds. Therefore, different carboxylation reactions were indeed developed exploiting stoichiometric organometallics, transition metal catalysis, and also electrochemistry.



## 2. Synthesis of benzoic acids using stoichiometric organometallic and metal-based catalysis

The treatment of Grignard, arylzinc, and aryllithium reagents with CO<sub>2</sub> allowed the carboxylation of numerous aromatic moiety. Though the remarkable efficiency of these stoichiometric transformations, yet they suffered from many constraints, especially due to the short lifetime and the air/moisture sensitivity of these species. Furthermore, these metal-based compounds exhibited an incompatibility with electrophilic functional groups like cyano, nitro, and carbonyl moieties. This significant drawback made the synthesis of a variety of carboxylic acids not possible using these organometallics (**Figure 32**).<sup>52</sup>

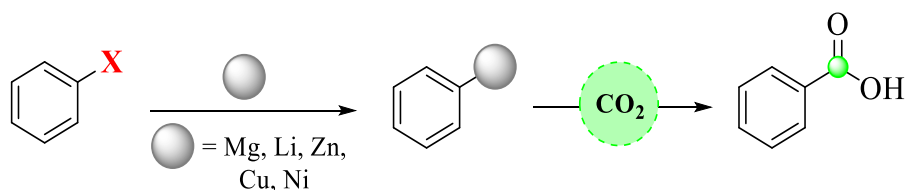


**Figure 32:** Synthesis of benzoic acids using stoichiometric organometallic species.

On the other hand, transition metals are characterized by a good functional group tolerance, and consequently, their use was the key to synthesize aryl carboxylic acid with high selectivity and under mild conditions.<sup>53</sup> Therefore, catalytic carboxylation reactions were rapidly developed with these metals, such as reductive carboxylation, which provides a promising method to access aryl carboxylic acids using CO<sub>2</sub>.<sup>5, 18a</sup>

For example, the reductive carboxylation of aryl sulfonates (e.g., OTf, OTs), aryl esters, and more recently, aryl fluorosulfates<sup>54</sup> furnished a wide range of aryl carboxylic acids (**Figure 33**). Various methods are reported to cleave the strong C<sub>sp2</sub>-O bond, but they mostly require an additional source of energy (heat up to 100°C) for the catalyst to overcome the high activation energy of the C-O bond. Furthermore, an excessive amount of reductants, like Mn powder, must be added in these procedures which can limit their future industrial use.

<sup>52</sup> M. Ahamed, J. Verbeek, U. Funke, J. Lecina, A. Verbruggen, G. Bormans, *ChemCatChem*, **2016**, 8,3692; A. Nagaki, Y. Takahashi, J. Yoshida, *Chem. -Eur. J.* **2014**, 20, 793; I. Mutule, E. Suna, *Tetrahedron*, **2005**, 61, 11168.

<sup>53</sup> a) K. Osakada, R. Sato, T. Yamamoto, *Organometallics* **1994**, 13, 4645; b) H. Sugimoto, Y. Fujiwara, I. Kawata, H. Taniguchi, *J. Organomet. Chem.* **1984**, 266, 44; c) G.W. Ebert, W.L. Juda, R.H. Kosakowski, B. Ma, L. Dong, K. E. Cummings, M.V.B. Phelps, A.E. Mostafa, J. Luo, *J. Org. Chem.* **2005**, 70, 4314.

<sup>54</sup> C. Ma, C.Q. Zhao, X.-T. Xu, Z.-M. Li, X.-Y. Wang, K. Zhang, T.-S. Mei, *Org. Lett.* **2019**, 21, 2464

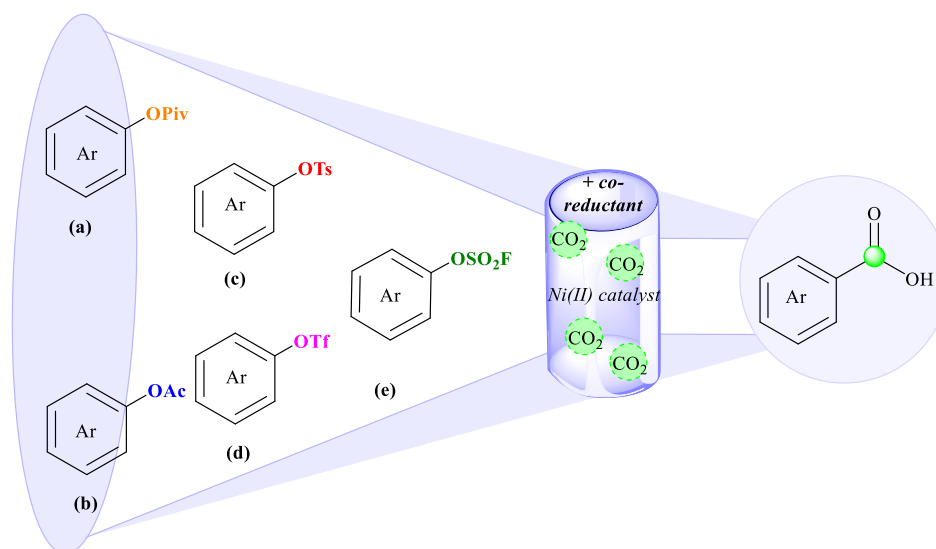


**Figure 33:** Ni-catalyzed carboxylations of various electrophilic C-O bonds.

The carboxylation of phenylboronic esters was also investigated with different catalysts (Cu, Ni, Ag or Rh). Remarkably, DFT calculations proved that a transmetalation, between the boron and the active catalyst, precedes and facilitates the CO<sub>2</sub> insertion step.<sup>55</sup>

Later on, interesting CO<sub>2</sub> fixation systems based on using aryl zinc reagents emerged, showing a comparable reactivity with the boron-containing substrates. Of note, these transformations required a large number of additives (base and metallic salts like CsF) whether to accelerate the transmetalation step or to enhance the nucleophilicity of the organometallic species by creating four-coordinate boronate complexes allowing a smooth CO<sub>2</sub> insertion.<sup>56</sup>

Besides the additives, ligand choice played a crucial role in some protocols by allowing to decrease the catalytic loadings and to expand the applicability of the reaction as reported by Hou and co-workers using IPr as a ligand for Cu catalyst.<sup>57</sup>

Since the synthesis of aryl boronate and aryl zinc reagents starts from the corresponding aryl halides, carboxylation strategies starting directly from aryl halides, known as cheap and commercially available products, arose rapidly to produce aryl carboxylic acids (**Figure 34**).

<sup>55</sup> L. Dang, Z. Lin, T. B. Marder, *Organometallics* **2010**, 29, 917

<sup>56</sup> K. Ukai, M. Aoki, J. Takaya, N. Iwasawa, *J. Am. Chem. Soc.* **2006**, 128, 8706

<sup>57</sup> T. Ohishi, M. Nishiura, Z. Hou, *Angew. Chem.* **2008**, 127, 5876; *Angew. Chem., Int. Ed.* **2008**, 47, 5792.

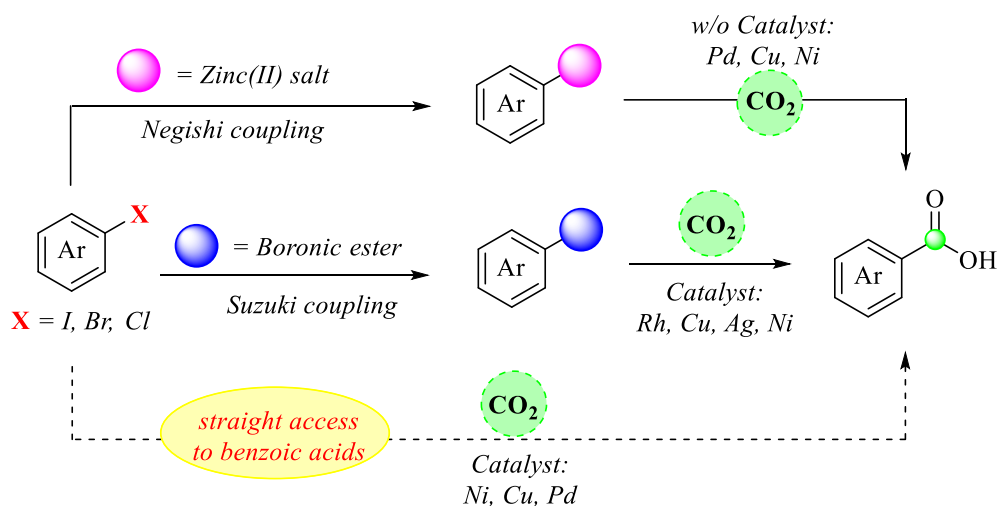


**Figure 34:** Preparation of different organometallic compounds prior to the carboxylation reactions.

In 1994, Osakada and his coworkers succeeded to produce benzoic acids from aryl bromides in good yields (up to 55%), using a stoichiometric amount of a Ni complex.<sup>53a</sup> Strangely, this strategy did not trigger further investigation until 2009, when Martin's group published a Pd-catalyzed carboxylation of aryl bromides (**Figure 35**).<sup>12</sup>

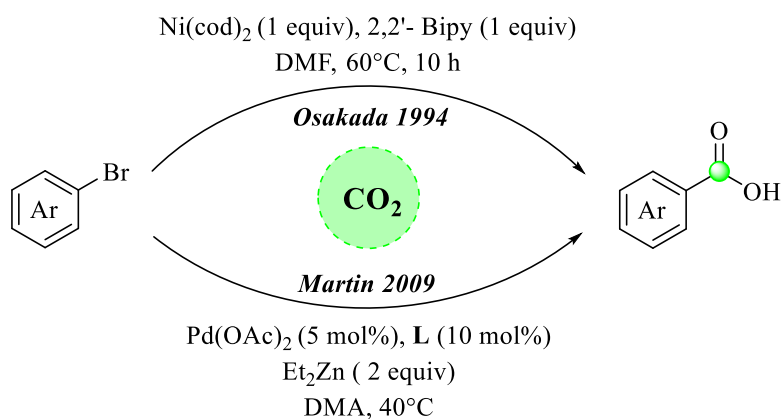


**Figure 35:** Carboxylation of aryl bromide reported by Osakada in 1994 (*top*) and the first catalytic carboxylation of the same compounds described by Martin in 2009 (*bottom*).

The reaction conditions exhibited an excellent functional tolerance and furnished various carboxylic acids in satisfying yields (40-82%). However, the addition of the pyrophoric diethylzinc  $\text{Et}_2\text{Zn}$  was crucial for this transformation in addition to the use of an electron-rich phosphine ligand to decrease the Negishi-type cross-coupling side product, and thus to enhance the selectivity of the reaction.

Pioneered by this example, several groups published the carboxylation of aryl bromide and iodide substrates but not of the more challenging aryl chlorides. Tsuji and Fujihara were the first to overcome this challenge by combining a Ni-catalyst with Mn powder as a reducing reagent and

ammonium salts ( $\text{Et}_4\text{NI}$ ) to achieve the carboxylation of aryl chlorides (**Figure 36**).<sup>58</sup> In this protocol, the Mn facilitated the regeneration of the Ni(I) intermediate after the oxidative addition by performing a SET to the Ni(II) center. The active Ni(I) underwent then a  $\text{CO}_2$  insertion followed by a second SET and a transmetalation step that allowed the regeneration of Ni(0) complex. On the other side, the authors suggested that the addition of  $\text{Et}_4\text{NI}$  enhanced the electron transfer steps between Mn and nickel via an “*Mn - I - Ni*” bridge, a hypothesis inspired from Iyoda’s approach in 1990.<sup>59</sup>

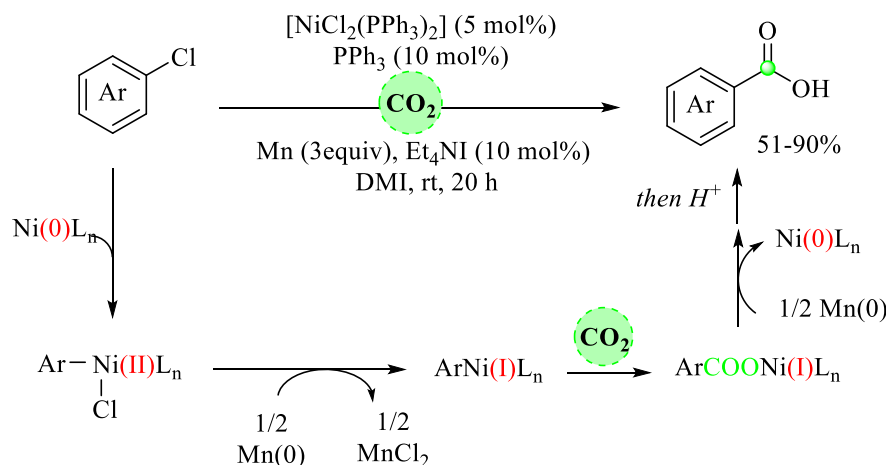


**Figure 36:** Ni-catalyzed carboxylation of aryl chlorides.<sup>58</sup>

A light-promoted carboxylation of aryl bromides and chlorides was reported in 2017 by Iwasawa and Martin using Pd/photoredox dual catalysts, allowing to replace the metallic reducing agent by a tertiary amine as an electron donor.<sup>18e</sup> As is the previous example with Pd catalyst,<sup>12</sup> the electron-rich phosphine ligand tBuXPhos was necessary for the carboxylation of aryl chlorides, while the addition of  $\text{Cs}_2\text{CO}_3$  reduced the formation of the hydrohalogenated side product.

However, electrochemical studies provided additional information regarding the mechanistic pathway. The cyclic voltammetry of the  $\text{ArPd}^{\text{II}}\text{Br}(\text{XPhos})$  indicated that its reduction potential ( $-2.28$  V vs.  $\text{Fc}/\text{Fc}^+$ ) is lower than the  $\text{Ir}^{\text{II}}$  complex ( $-1.87$  V vs.  $\text{Fc}/\text{Fc}^+$ ). This observation signifies that the  $\text{Ir}^{\text{II}}$ -based reducing agent cannot trigger the regeneration of  $\text{Pd}^{\text{(I)}}$  intermediate, responsible for the  $\text{CO}_2$  insertion step. However, a new peak at  $-1.4$  V vs.  $\text{Fc}/\text{Fc}^+$  was observed in the CV of the same complex under  $\text{CO}_2$  atmosphere. The authors suggested that a Pd- $\text{CO}_2$  adduct is formed in the medium, exhibiting a lower redox potential than the initial complex, and consequently, allow to be reduced by the  $\text{Ir}^{\text{II}}$  complex. However, the  $^{31}\text{P}$  NMR spectra did not support this theory and no significant shift was observed. So based on these data, the authors proposed two mechanistic pathways (**Figure 37**):

<sup>58</sup> T. Fujihara, K. Nogi, T. Xu, J. Terao, Y. Tsuji, *J. Am. Chem. Soc.* **2012**, *134*, 9106

<sup>59</sup> H. Otsuka, K. Sato, N. Nisato, M. Oda, M. Iyoda, *Bull. Chem. Soc. Jpn.* **1990**, *63*, 80; M. Sakaitani, H. Otsuka, M. Oda, M. Iyoda, *Chem. Lett.* **1985**, 127

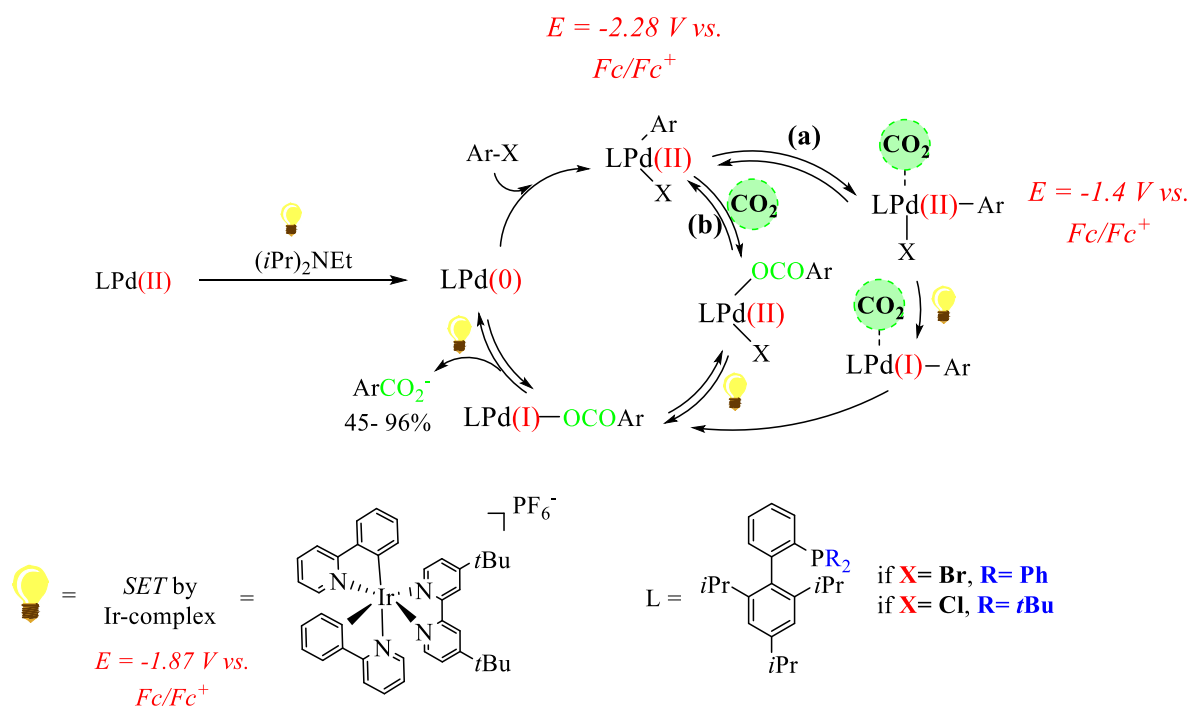


**Figure 37:** The proposed mechanism of photoinduced carboxylation of aryl bromide and chloride mediated by Pd/Ir dual catalysts.<sup>18e</sup>

The **path (a)** proposes the coordination of  $CO_2$  to  $ArPd^{II}X(XPhos)$  to form a new  $Pd^{II} - CO_2$  species. This adduct has a lower reduction potential than the  $ArPdX(XPhos)$ , and thus, it undergoes the electron transfer from the  $Ir^{II}$  catalyst. After a  $CO_2$  insertion step followed with another SET, the initial catalyst is regenerated.

The **path (b)** favors first the formation of a  $CO_2$  insertion product  $(ArCOO)PdX(XPhos)$  while the electron transfer step comes at last to furnish the  $Pd(I)$  intermediate. Notably, the  $^{31}P$  NMR showed only the peak corresponding to the oxidative addition intermediate  $ArPdX(XPhos)$  and thus, no additional proof for the formation of  $(ArCOO)PdX(XPhos)$  was provided by the authors.

Another important photoredox system developed by König, but with a  $Ni^{II}$  - complex, described the carboxylation of aryl as well as alkyl bromides.<sup>60</sup> In this case, a mixture of the organic photosensitizer 1,2,3,5-tetrakis(carbazol-9-yl)-4,6-dicyanobenzene (4CzIPN), a Hantzsch ester (HEH) as a sacrificial reductant, and neocuproine offered the right combination to generate aryl carboxylic acids. Although the significant advancement presented by this method, the number of additives required for this approach cannot be ignored (**Figure 38**).

<sup>60</sup> Q.-Y. Meng, S. Wang, B. König, *Angew.Chem. Int. Ed.* **2017**, *56*, 13426.

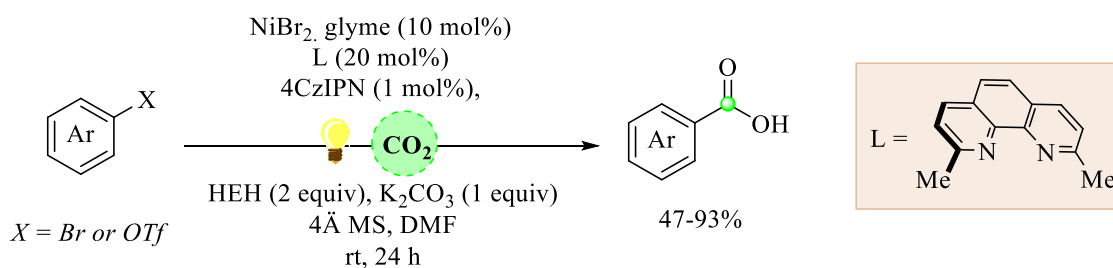


**Figure 38:** König's light promoted carboxylation of aryl sulfonates and bromides.

Direct  $C_{sp^2}$ -H activation was also very recently reported for the carboxylation of aryl compounds to produce benzoic acids.<sup>61</sup> Still, its application remained limited to acidic  $sp^2$  C-H bonds such as polyfluorinated arenes (**Figure 39, A**). In addition, some Rh-catalyzed carboxylation of benzene derivatives were efficient when they hold a directing group (**Figure 39, B**). It is essential to guarantee a selective  $\text{CO}_2$  fixation, otherwise, the reaction yielded a mixture of carboxylated products, as shown in Iwasawa's work (**Figure 39, C**).<sup>62</sup> And finally, the presence of the metallic reducing agent in a great amount, similarly to the previously reported methods, persisted as a significant drawback.

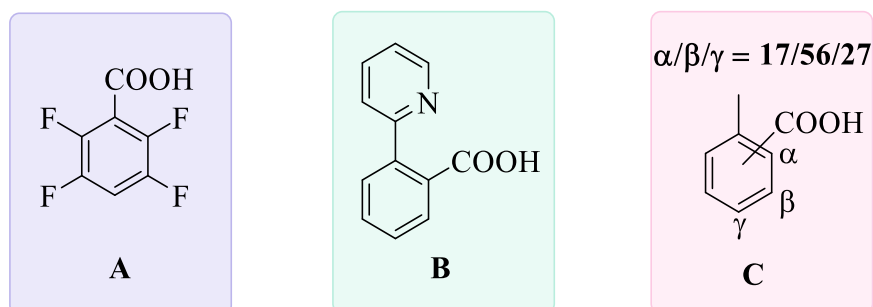


**Figure 39:** Carboxylation of C-H acidic bonds (**A**); directed carboxylation (**B**); non-directed carboxylation (**C**).

Noteworthy, several base and Lewis acid-mediated carboxylation reactions exist in the literature, but they will not be discussed in this introduction.<sup>13</sup>

### 3. The advance achieved by electrochemistry in the synthesis of benzoic acids

<sup>61</sup> J. Hong, M. Li, J. Zhang, B. Sun, F. Mo, *ChemSusChem*, **2019**, *12*, 6.

<sup>62</sup> T. Suga, H. Mizuno, J. Takaya, N. Iwasawa, *Chem. Commun.* **2014**, *50*, 14360

Since its discovery, the electrochemistry has been introduced as the perfect tool to synthesize fine chemicals under mild and safe conditions. But over the last decade, it gained an additional advantage by being an eco-friendly option as it substitutes the redox reagent essential in many transformations, thereby fulfilling most of the green chemistry principles.

However, the electrocarboxylation reactions, mainly those starting from aryl halides, are still under-investigated and deserves more attention.

In 1984, preliminary studies conducted by Silvestri and Perichon, independently, revealed that using sacrificial Al or Mg anodes in an undivided cell setup, led to the carboxylation of aryl halides under a CO<sub>2</sub> atmosphere.<sup>63</sup> In these cases, the metal played mainly two roles: (1) it delivered the electrons and (2) it stabilized the reduced fragments. Noteworthy, the electrogenerated Al<sup>3+</sup> and Mg<sup>2+</sup> cations display no significant reductive power. However, these methods require high overvoltages, which consequently affect the efficiency of the carboxylation.

Targeting this problematic point, catalytic electrocarboxylation mediated by Pd,<sup>64</sup> Ni<sup>65</sup> and Co<sup>66</sup> complexes emerged and enabled the carboxylation of aromatic halides under low overvoltage, which subsequently improved the chemoselectivity. Still, a sacrificial anode was required in these examples to avoid the oxidation of the catalyst and then lose its reactivity.

Concerning the mechanism, most of the reported approaches were based on one proposed pathway (**Figure 40**): the generated electrons reduced the aryl halide to the corresponding radical. This radical species was then reduced to the corresponding carbanion or the organometallic intermediate that underwent then a nucleophilic addition with the CO<sub>2</sub> and delivered the benzoic acid.

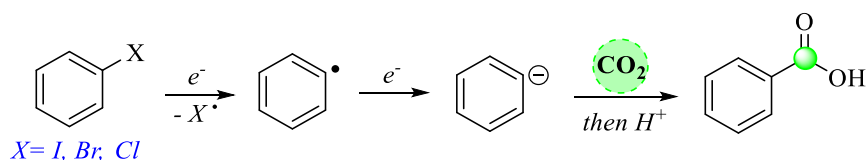


**Figure 40:** Reported mechanism for the electrocarboxylation of aryl halides.

Of note, the formation of [CO<sub>2</sub>]<sup>-•</sup> radical anion was not reported, and the electrocarboxylation followed a typical CO<sub>2</sub> fixation mechanism with a metal-based reagent/catalyst.

Within our continuous efforts to expand the reactivity of electrogenerated divalent samarium complexes, the CO<sub>2</sub> activation for C-C bond formation seemed an attractive, yet challenging mission to begin. The challenge lies in these following points:

**I- Stability:** The electrochemical conditions established by our group involve the use of simple ligands **X** ( I<sup>-</sup>, Cl<sup>-</sup>, Br<sup>-</sup>, BF<sub>4</sub><sup>-</sup>, OTf<sup>-</sup> . . . ) deriving from the electrolytes (like ammonium salts

<sup>63</sup> G. Silvestri, S. Gambino, G. Filardo, A. Gulotta, *Angew. Chem. Int. Ed.* **1984**, 23, 979; O. Sock, M. Troupel, J. Périchon, *Tetrahedron Lett.* **1985**, 26, 1509.

<sup>64</sup> C. Amatore, A. Jutand, *J. Am. Chem. Soc.* **1991**, 113, 2819; M. Troupel, Y. Rollin, J. Périchon, J. F. Fauvarque *Nouv. J. Chim.* **1981**, 2, 621.

<sup>65</sup> C. Amatore, A. Jutand, *J. Am. Chem. Soc.* **1992**, 114, 7076.

<sup>66</sup> H. Senboku, A. Katayama, *Cur. Opin. Green Sustain. Chem.* **2017**, 3, 50.

$n\text{Bu}_4\text{NX}$ ) to coordinate the samarium for its dissolution from the anode. As for the reported examples, the  $\text{CO}_2$  reduction by divalent samarium complexes was possible only when it is coordinated to very electron-rich ligands such as  $\text{Cp}^*$  derivatives.

**II- Solubility:** The  $\text{CO}_2$  is a polar molecule, so its solubility increases in polar solvents like DMF, acetonitrile, water. The utilization of such solvents is unusual in the  $\text{Sm}(\text{II})$  chemistry.

**III- Reactivity:** The  $\text{CO}_2$  radical anion can initiate many side reactions in the medium. For example, the  $\text{CO}_2$  dimerization to produce the oxalate species is thermodynamically the most favorable reaction as mentioned previously.<sup>46</sup> Furthermore, the generated carboxylic acid presents a higher reactivity than the initial substrate and can thus undergo a second  $\text{CO}_2$  addition to yield a dicarboxylated product. These two hypotheses can influence the efficiency of the reaction, which is a key parameter towards successful electrochemical transformations.

In the next part, our results concerning the activation of  $\text{CO}_2$  using electrogenerated  $\text{Sm}(\text{II})$  complexes will thus be described, keeping in mind these challenges.

#### 4. Carboxylation of aryl halides via $\text{CO}_2$ activation using electrogenerated $\text{Sm}(\text{II})$ complexes

To start our investigation, a solution of  $n\text{Bu}_4\text{NBF}_4$  (0.2 equiv) in 100 mL of DMF was introduced in a one-compartment cell containing a stainless steel grid as the cathode and a cylindric samarium rod as the anode. Choosing to work in a chronopotentiometry mode, the current was fixed at 100 mA. The reaction was then started to electrogenerate *in situ* the  $\text{SmI}_2$  following the electrolysis conditions explained in the introduction chapter. During the reaction time, the  $\text{CO}_2$  was continuously bubbled via a fritted glass (**Figure 41**).

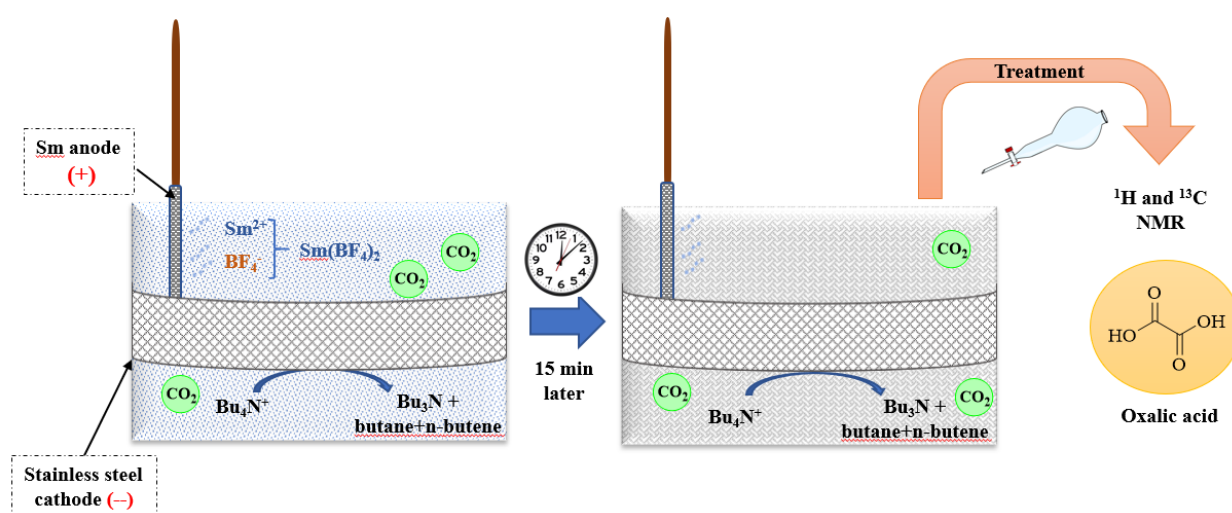


**Figure 41:** Detection of oxalic acid after 15 min of  $\text{Sm}(\text{II})$  electrolysis under  $\text{CO}_2$  atmosphere.



During the electrolysis, the accumulation of a white precipitate was observed, and after 15 min, the solution turned entirely white. The  $^{13}\text{C}$  NMR analysis showed one signal at 161.12 ppm, in  $d_6$ -DMSO, which corresponded to a carboxylic acid shift. The obtained spectra matched perfectly the one obtained from a commercial oxalic acid. This result confirms that, under our conditions, the electrogenerated samarium can effectively reduce the  $\text{CO}_2$  into the corresponding radical anion, and produce after radical homocoupling, the oxalate species.

Next, another solution of  $n\text{Bu}_4\text{NBF}_4$  was prepared, and the 1-bromo-4-methoxybenzene **1a** was added as the substrate, the electrolysis was started following the previous electrolytic conditions (**Figure 42**). Interestingly, the white precipitation did not appear during the transformation, indicating that the addition of the aryl bromide inhibited somehow the  $\text{CO}_2$  dimerization. After 4 hours of electrolysis, the 4-methoxy benzoic acid **1'a** was isolated with a 71% yield.

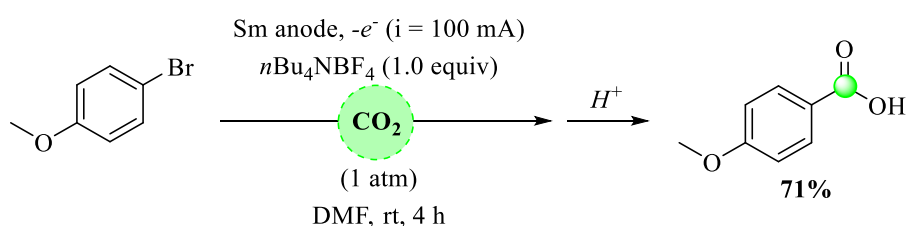


**Figure 42:** Carboxylation of **1a** using electrogenerated divalent samarium.

To validate this particular behavior of divalent samarium, the samarium rod was replaced by a magnesium or a nickel one. None of them presented the same capacity to reduce the  $\text{CO}_2$  or to form the carboxylated products.

With these results in hand, we turned our attention to the scope of the reaction to confirm the efficiency of our approach and to also evaluate the effect of various substituents on the starting material (**Figure 43**). The carboxylation of aryl bromide occurred nicely with electron-donating (**1a-e**), and electron-withdrawing groups (**1g-i**) except for the nitro group (**1k**). In this case, a mixture of products was isolated, none of it corresponding to the carboxylic acid. We attributed this result to the reduction of the nitro group by Sm(II), a reactivity which was recently reported by our group.<sup>45</sup>

Furthermore, the substrate **1j** was totally recovered, an expected behavior due to the high-affinity of the samarium for oxygen atoms. The hydroxyl group probably trapped the Sm(II) during the reaction and subsequently inhibited its interaction with the  $\text{CO}_2$ .

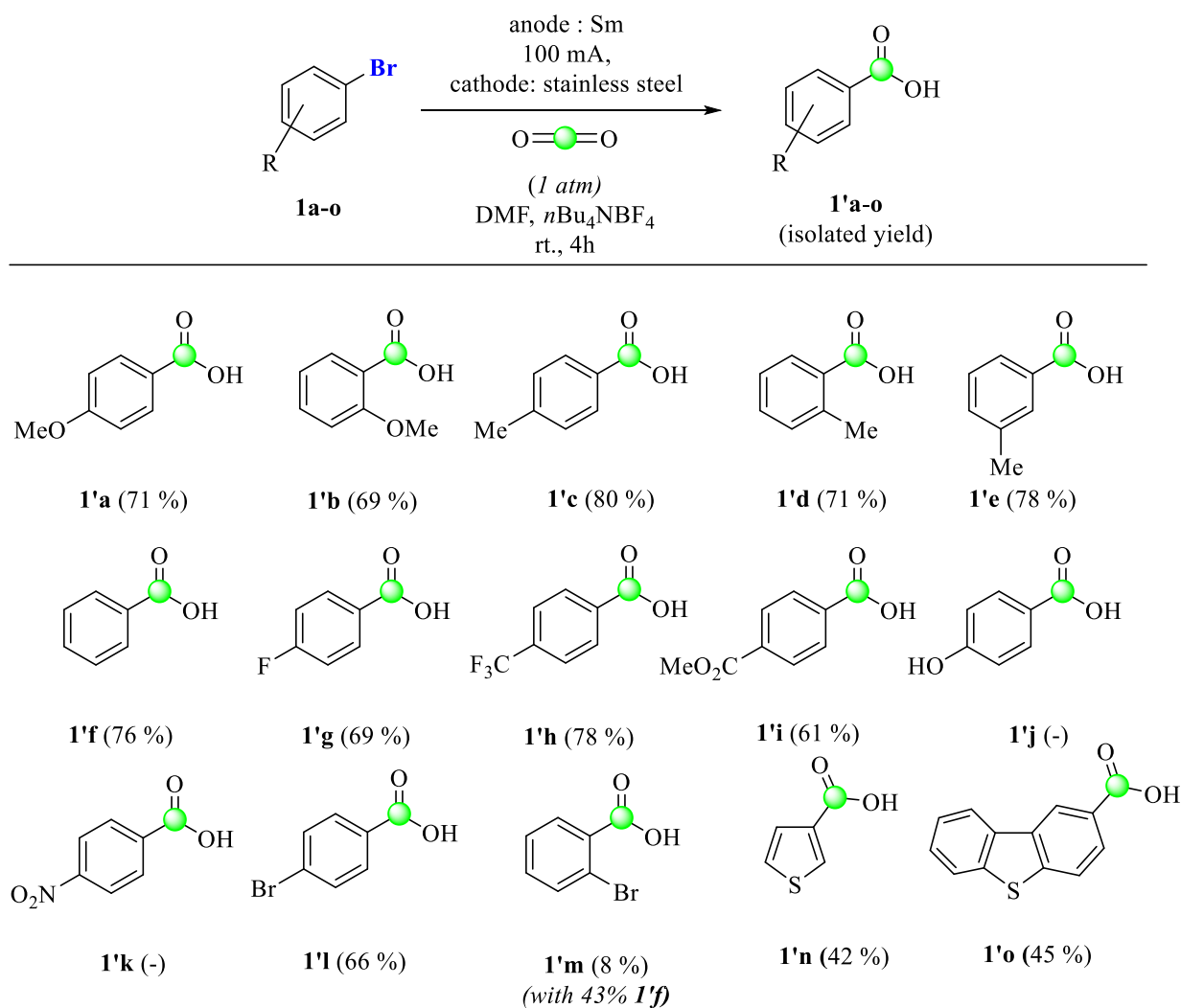


**Figure 43:** Scope of the carboxylation of aryl bromide using electrogenerated Sm(II) in DMF under  $\text{CO}_2$  atmosphere.

Unexpectedly, the carboxylation of dihalogenated substrates did not demonstrate the typical reactivity. Starting with 1,4-dibromobenzene **11**, three compounds were isolated: 4-bromobenzoic acid **1'l** as the main product with a yield of 66% resulting from the monocarboxylation of **11**. This latter also underwent the dicarboxylation to furnish terephthalic acid with a 20% yield. The third compound was the benzoic acid as a minor product Sm coming from the addition of one molecule of  $\text{CO}_2$  while the second bromide was eliminated. In sharp contrast, the benzoic acid was mainly isolated (43%) by starting from 1,2-dibromobenzene **1m**, whereas the yield of the brominated monocarboxylated compound was about 8%. Apparently, the dehalogenation rate is higher when the two bromine atoms are placed in ortho position for each other. We propose that once the first  $\text{CO}_2$  is fixed, the bromine undergoes an elimination assisted by the Sm(II) in the medium via this mechanism (**Figure 44**):

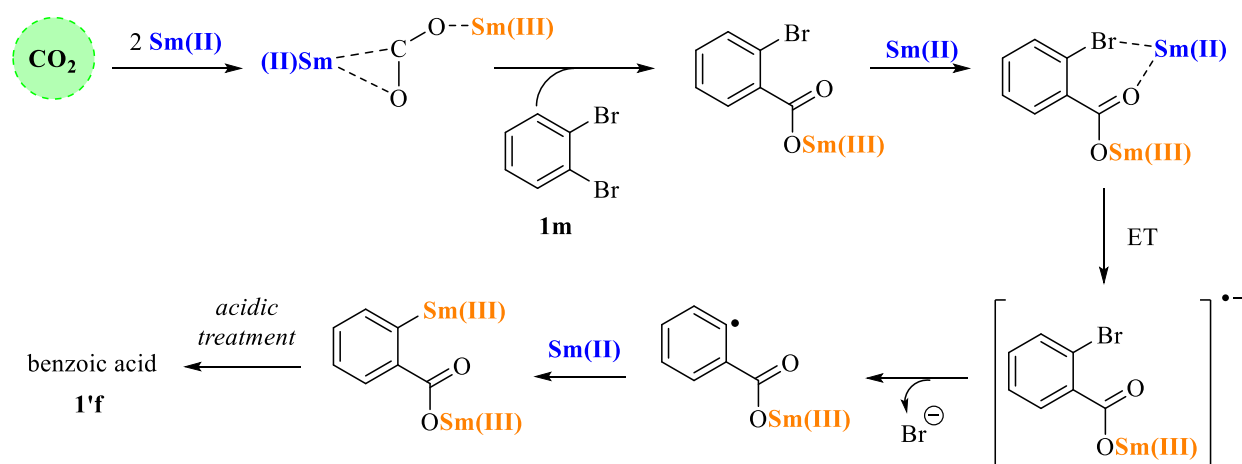


**Figure 44:** Proposed mechanism for halogen elimination mediated by Sm(II).

After the CO<sub>2</sub> fixation step, the bromine atom can interact with the Sm(II) metal center to create a five-membered transition state, favorizing the electron transfer and the reduction of the second bromine. A second electron transfer furnishes the carbanion that after protonation delivers the benzoic acid **1'f**. Following the reaction by <sup>1</sup>H NMR revealed the direct formation of benzoic acid **1'f** while only traces of **1'm** were detected, indicating that dehalogenation and the CO<sub>2</sub> fixation occur at the same time which explains the low yield of **1'm**.

Moreover, the carboxylation of 3-bromothiophene **1n** and 2,8-dibromo dibenzothiophene **1o** was examined. While the former yielded the corresponding carboxylic acid with 42% yield, the latter produced the dibenzothiophene-2-carboxylic acid **1'o** with 45% yield as a unique product. In this case, we believe that this electron-rich structure enhances the dehalogenation, in our conditions, to create a conjugated and stable radical.

After achieving the carboxylation of aryl bromides, we investigated the carboxylation of more challenging aryl chlorides. Fortunately, we isolated the corresponding carboxylic acids, with slightly lower yields starting from the bromide analogs (**Figure 45**). Surprisingly, the dichlorinated substrates (**1p**, **1q**, and **1r**) reacted to produce monocarboxylated products (**1'p**, **1'q**, and **1'r**) without any side reaction. Indeed, the dehalogenation process is much more difficult with these compounds, a hypothesis based on the difference of the bond dissociation energy (BDE) between C-Br (~270 kJ/mol) and C-Cl (~330 kJ/mol).

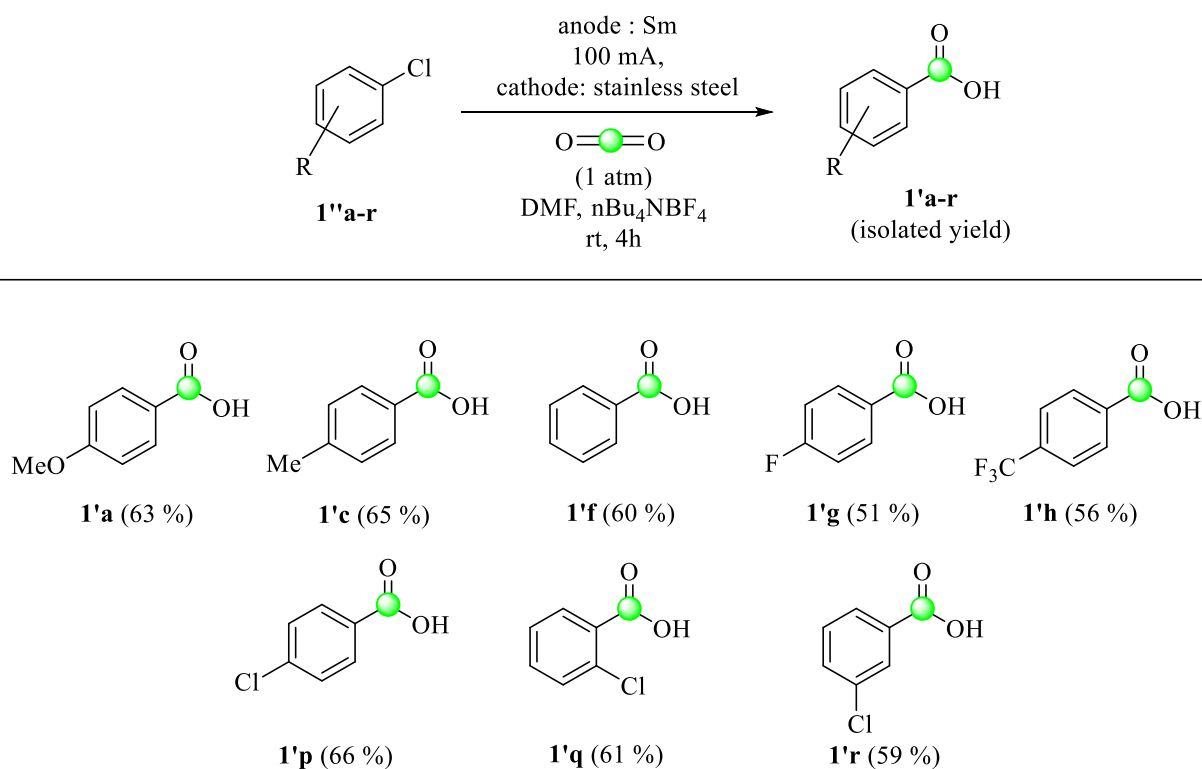


**Figure 45:** Carboxylation of aryl chlorides by electrogenerated Sm(II) in DMF under CO<sub>2</sub> atmosphere.

At this point, we turned our attention to the control experiments aiming to understand the mechanism of the carboxylation of aryl halides.

## 5. Mechanistic studies

### a. Control experiments

Several experiments were conducted under the optimized conditions to get insight into the mechanistic pathway.

After having proved that the samarium can perform a CO<sub>2</sub> reduction to yield the oxalate via dimerization, we tested the behavior of bromo and chlorobenzene alone under continuous electrogeneration of Sm(II). Therefore, we added Ph-Br and Ph-Cl in two separated cells, and we started the electrolysis for 4 hours (**Figure 46**).

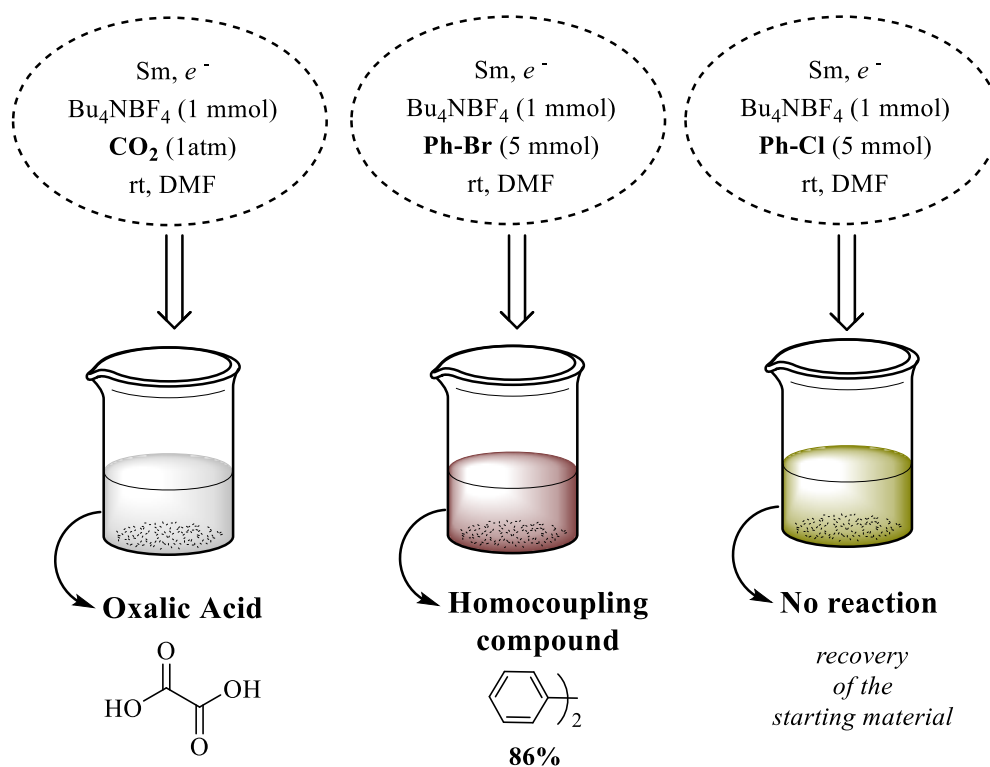


**Figure 46:**  $\text{CO}_2$  only (on the left); Ph-Br (in the middle) and Ph-Cl (on the right) without  $\text{CO}_2$

Starting from Ph-Br, we isolated the homocoupling product (43%) while the rest was the recovered starting material. In the case of Ph-Cl, the substrate did not react at all and was totally recovered. This distinct behavior supports our hypothesis concerning the strength of the C-Cl bond compared to the C-Br, and furthermore, it explains the fast dehalogenation rate observed with the dibrominated substrates.

These findings suggest also that with the bromobenzene, the carboxylation starts with the formation of the  $[\text{CO}_2]^-$  radical anion along with the reduction of the bromine to result in the corresponding  $\text{C}_{sp^2}$  radical, and afterward, a radical coupling provides the benzoic acid.

On the contrary, the inertia of the aryl chloride during the electrolysis supports a radical substitution mechanism initiated by the  $[\text{CO}_2]^-$  radical anion to deliver finally the benzoic acid.

### *b. Kagan's reagent vs. the electrogenerated Sm(II)*

The  $\text{SmI}_2$ , or Kagan's reagent, constitutes one of the most effective reductive reagents and numerous studies highlighted its significant applications in organic chemistry. As previously mentioned, and to our best knowledge, only one photoinduced carboxylation mediated by  $\text{SmI}_2$  is reported in the literature proposing the formation of a  $\text{CO}_2$  radical anion.<sup>47</sup> With this in mind, we tested this reagent under  $\text{CO}_2$  atmosphere.

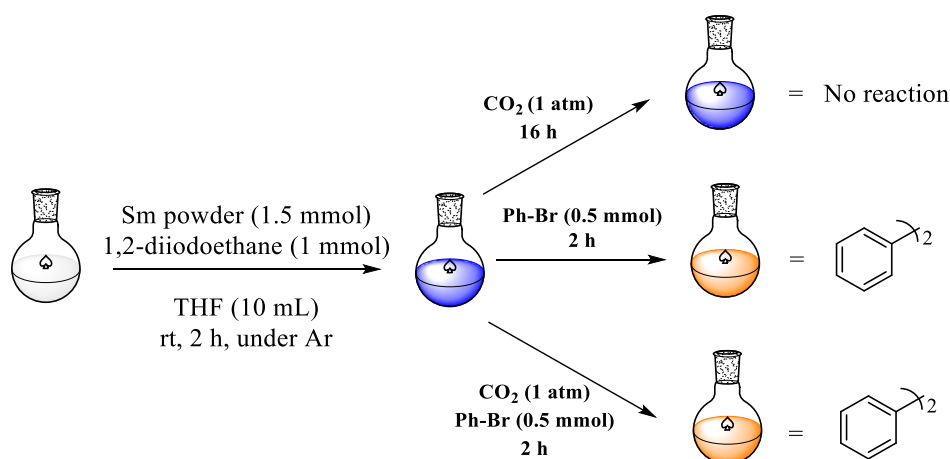


**Figure 47:** Experimental tests using Kagan's reagent.

As shown in **Figure 47**, in a freshly prepared solution of 0.1 M  $\text{SmI}_2$  in THF, the  $\text{CO}_2$  was introduced for 16 hours under inert atmosphere. Remarkably, the solution kept its blue color, which indicates the persistence of divalent samarium species. Nevertheless, the white precipitate was not formed during the reaction, and even after treatment of the reaction mixture, the  $^1\text{H}$  and  $^{13}\text{C}$  NMR spectra did not reveal the formation of oxalic acid.

Next, 0.5 mmol of phenyl bromide was added to another two solutions of  $\text{SmI}_2$  in THF, and the  $\text{CO}_2$  was bubbled in one of them. With or without  $\text{CO}_2$ , we isolated only the homocoupling product would be isolated after 2 hours. This outcome marks certainly, the enormous difference between the reactivity of chemical and electrochemical divalent samarium species.

### c. Radical trapping experiment

Trying to get evidence of the  $[\text{CO}_2]^-$  formation, we added one equivalent of 2,2,6,6-tetramethyl piperidine-1-yl)oxy (TEMPO) as a radical scavenger along with the addition of phenyl bromide and carbon dioxide to the reaction mixture (**Figure 48**, (a)). Unfortunately, we were not able to trap the  $\text{CO}_2$  radical anion (**1's**), and the reaction was inhibited and the bromobenzene was recovered entirely whereas the TEMPO disappeared by the end of the electrolysis. Noteworthy, the treated mixture did not show traces of radical coupling product between the TEMPO and the  $\text{C}_{sp^2}$  radical (**1't**).

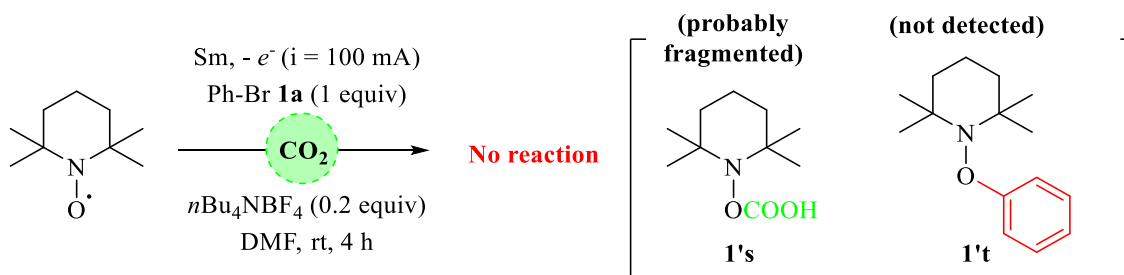


**Figure 48:** Radical trapping experiment with TEMPO.

Based on these observations, we believe that the TEMPO reacted with the  $[\text{CO}_2]^-$  but the intermediate **1**'s was probably highly unstable, and thus it decomposed leaving the starting material Ph-Br intact.

## 6. Electrochemical Studies

### *a. The oxidation of samarium: a noteworthy interaction*

Aiming to confirm the interaction between the samarium and  $\text{CO}_2$ , we evaluated the oxidation of a samarium rod of  $20 \text{ mm}^2$  surface in a solution of  $0.1 \text{ M}$  of  $n\text{Bu}_4\text{NPF}_6$ , in DMF.

The oxidation of  $\text{Sm}(0)$  to  $\text{Sm}(\text{II})$  began at  $-0.5 \text{ V/SCE}$  (**blue curve**). The addition of  $0.025 \text{ M}$  of chlorobenzene in DMF did not furnish a significant variation of potential (**green curve**). However, bubbling the  $\text{CO}_2$  for around 5 minutes before the analysis provoked a significant shift towards the negative direction from  $-0.5 \text{ V}$  to  $-0.8 \text{ V}$  (**red curve**). This shift indicates that adding the  $\text{CO}_2$  facilitated the electrogeneration of samarium (II) and its solubilization in the medium as samarium salts.

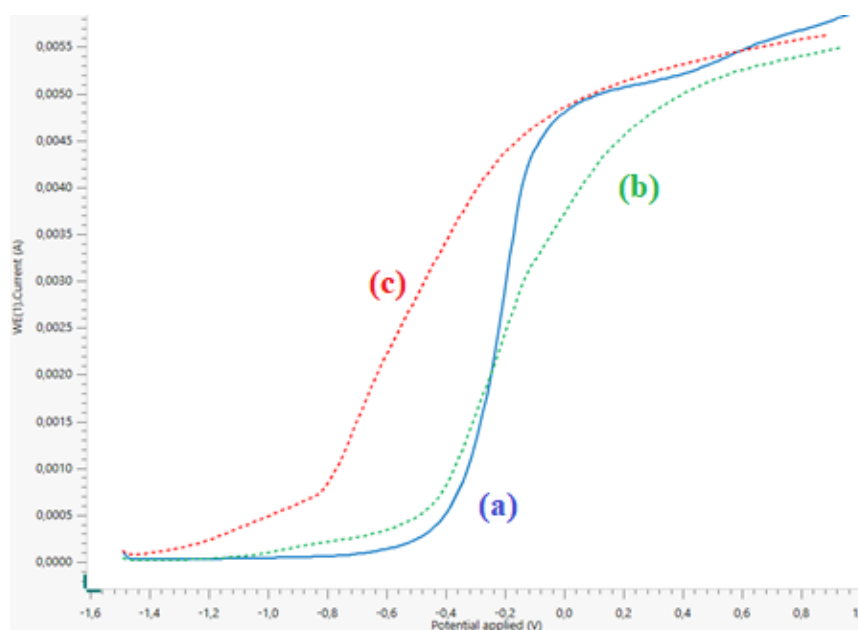


**Figure 49:** Samarium anode oxidation: Sm electrode surface  $20 \text{ mm}^2$ , scanning potential between  $-1.5$  and  $0.9 \text{ V}$  vs. SCE in DMF with  $n\text{Bu}_4\text{NPF}_6$  [ $0.1 \text{ M}$ ]. Scan rate :  $100 \text{ mV}\cdot\text{s}^{-1}$ . (a) blue line: without additive; (b) green line: in the presence of chlorobenzene  $0.025 \text{ M}$ ; (c) Red line: after bubbling  $\text{CO}_2$  in the solution for 5 min.

*b. Sm(II) + CO<sub>2</sub> = CO<sub>2</sub> activation*

The results above encouraged us to conduct a cyclic voltammetry study for the carboxylation of aryl halides. A pre-electrogenerated solution of 0.01 M SmCl<sub>2</sub> in MeCN exhibited a redox couple with a formal potential of -1.5 V/SCE (**green line**). Upon the introduction of CO<sub>2</sub>, the CV revealed a total loss of the Sm(II) to Sm(III) oxidation wave the reduction signal remained at -1.4 V/SCE (**red line**). This remarkable change in the electrochemical behavior of the samarium reveals the evident consumption of Sm(II) by CO<sub>2</sub> and the formation of Sm(III) - CO<sub>2</sub> species.

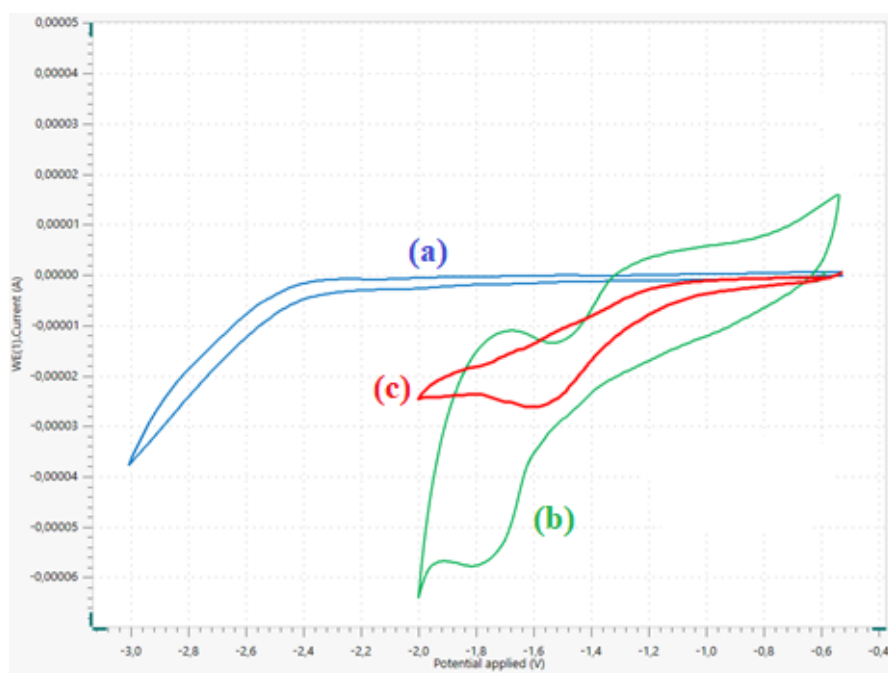


**Figure 50:** Cyclic voltammetry of SmCl<sub>2</sub> before and after adding CO<sub>2</sub>: Glassy carbon electrode surface 20 mm<sup>2</sup>, and platinum wire as counter electrode scanning potential between -0.5 and -3 V vs. SCE in CH<sub>3</sub>CN with *n*Bu<sub>4</sub>NPF<sub>6</sub> [0.1 M]. Scan rate: 100 mV/s. (a): 0.1 M *n*Bu<sub>4</sub>NPF<sub>6</sub>; (b): 0.1 M SmCl<sub>2</sub> in CH<sub>3</sub>CN; (c): 0.1 M SmCl<sub>2</sub> + CO<sub>2</sub>.

Compared to other reagents produced from sacrificial anodes (e.g., Mg<sup>2+</sup>, Al<sup>3+</sup>, Li<sup>+</sup>) that are inert towards the CO<sub>2</sub> reduction, it is noteworthy to highlight the unique reductive character of electrogenerated divalent samarium.

## 7. Proposed mechanism

All these observations suggest two different pathways depending on the nature of the starting material (**Figure 52**):

**Substrate Ar-Br:** The aryl bromides were found to follow a radical coupling mechanism due to the low bond dissociation energy compared to the chloride analogs. Along with the activation of carbon dioxide, the substrate is reduced to form the radical anion. The unstable C<sub>sp2</sub> radical,



generated after the dissociation of the bromide, immediately couples with the CO<sub>2</sub> radical anion in the medium to deliver the corresponding benzoic acid.

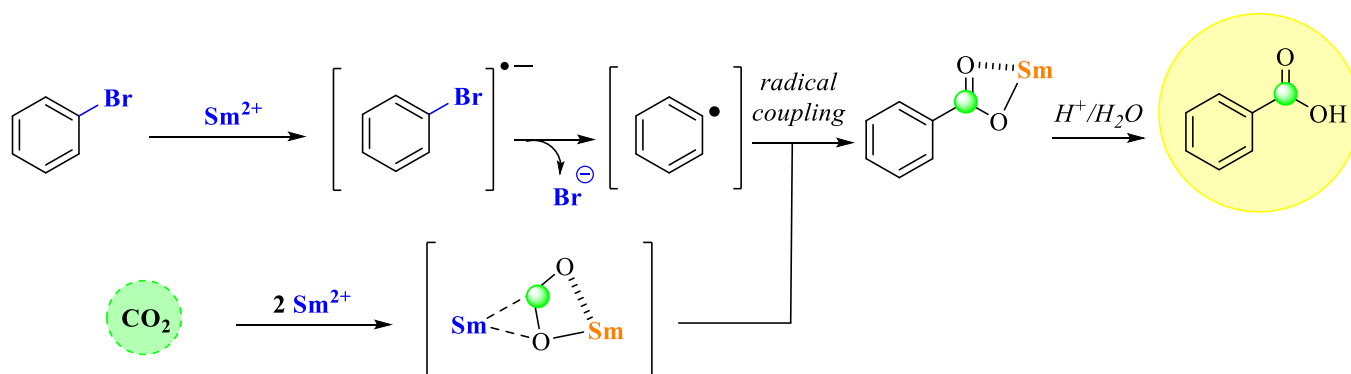


**Figure 51:** Proposed mechanism for the carboxylation of aryl bromides via radical coupling.

**Substrate Ar-Cl:** Aryl chloride derivatives possessing a higher redox potential than the Ar-Br ones, in this case, the CO<sub>2</sub> undergoes exclusively the reduction. The generated radical anion induces then a radical substitution with the substrate in the medium to give the corresponding carboxylic acid.

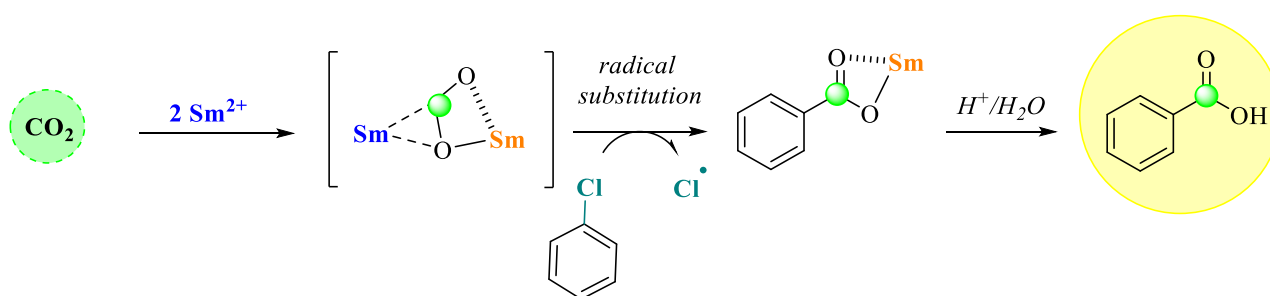


**Figure 52:** Proposed mechanisms for the carboxylation of aryl chlorides via radical substitution.

## 8. Attempts to perform a catalytic reaction

After establishing the stoichiometric procedure, we investigated next the same transformation but with a catalytic loading of divalent samarium.

Different electrolytes were screened to test their reactivity towards the carboxylation of aryl chlorides. The best yield was 16% with the *n*Bu<sub>4</sub>NI using 20 mol% of Sm<sup>2+</sup>, electrogenerated following the electrocatalysis conditions explained in the introduction chapter, in the presence of 3 equiv of TMSCl, as an oxophilic reagent, in DMF.

However, replacing the DMF with other polar solvents furnished only the starting material, which reflects the critical role of the solvent choice in this reaction.

We examined then the effect of the oxophilic reagent, speculating that the TMSCl is not strong enough in this case, probably due to the electron-richness of the carboxylic acid, increased by  $\pi$ -donation from the aromatic ring.

Therefore, we conducted several experiments using compounds well known to form strong bonds with the oxygen atom, such as boron reagents, titanium complexes, phosphines, or other silyl reagents like TMSOTf. Unfortunately, all of these attempts failed, and in the few reactions where we detected the targeted product, the yield remained lower than the catalyst loading. Also, the addition of an organic acid in the medium, such as methanesulfonic acid MsOH, did not yield any carboxylation product.

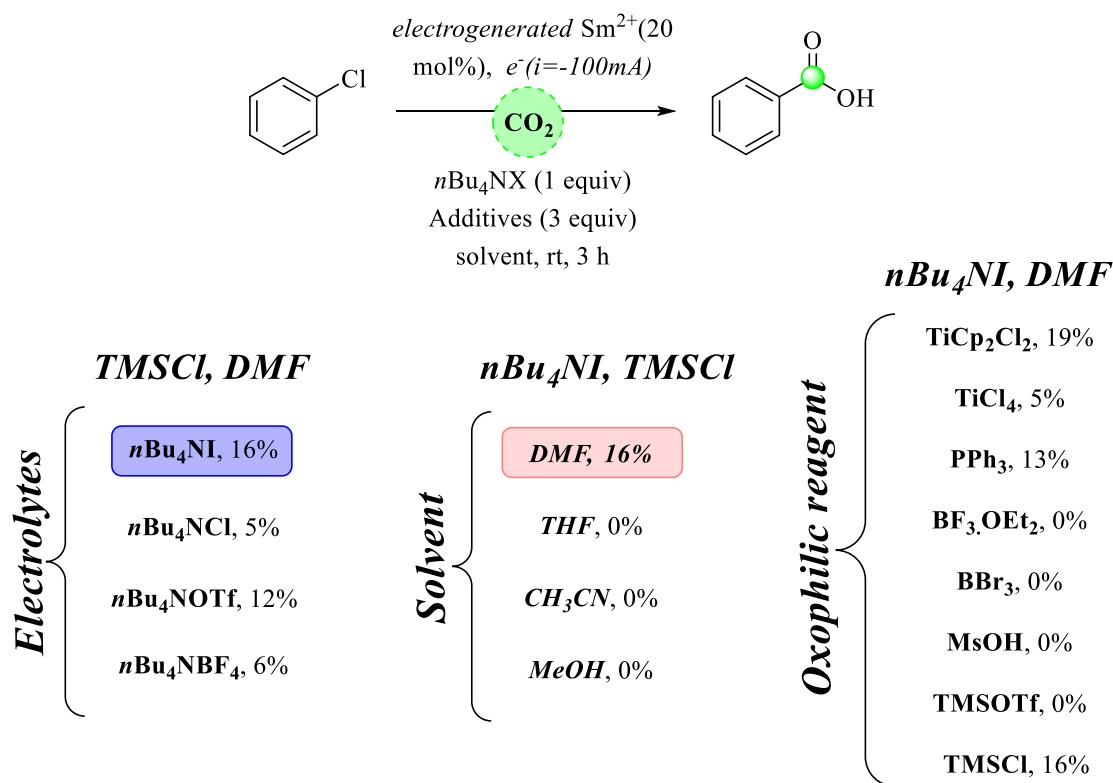


**Figure 53:** Screening catalytic carboxylation of aryl chloride reaction conditions.

We believe that the key-step holding the catalysis back lies in the separation of the Sm(III) from the final product. The successful stoichiometric carboxylation of aryl chlorides in DMF exclusively suggests also that the solvent is somehow involved in this transformation.

## 9. Conclusion and Perspectives

In this chapter, we introduced the CO<sub>2</sub> activation by electrochemically generated Sm(II). The formation of oxalic acid in the absence of any substrate was the indisputable proof of the reduction of CO<sub>2</sub> mediated by this reductive reagent.

Based on this concept, we elaborated the carboxylation of aryl halides via CO<sub>2</sub> activation under CO<sub>2</sub> atmosphere in DMF.

The carboxylation worked with aryl bromide to give the corresponding products with good to excellent yields. Interestingly, dibrominated starting materials showed a fast debromination rate

after the first carboxylation, especially for the ortho-substituted compounds. We attributed this reactivity to the capacity of the samarium to eliminate halogens adjacent to a carbonyl functional group via coordination followed by a sequence of electron-transfer steps.

Luckily, the challenging aryl chlorides were also nicely transformed under our conditions to give the corresponding carboxylic acid in lower yields than the brominated analogs, yet without any elimination product in the case of dichlorinated starting materials.

Several control experiments exposed the crucial role of Sm(II) to run the carboxylation of the aromatic halides in addition to a significant selectivity towards the CO<sub>2</sub> reduction. The radical trapping experiment with TEMPO did not furnish any product and led to the recovery of the starting material.

Lastly, we proved by electrochemical measurements that the introduction of carbon dioxide boosts the release of Sm divalent species, unlike the aryl chloride. Also, the cyclic voltammetry revealed the loss of Sm(II)/Sm(III) wave after bubbling the CO<sub>2</sub> for 5 minutes, indicating the effective chemical interaction between the Sm(II) and CO<sub>2</sub> in solution.

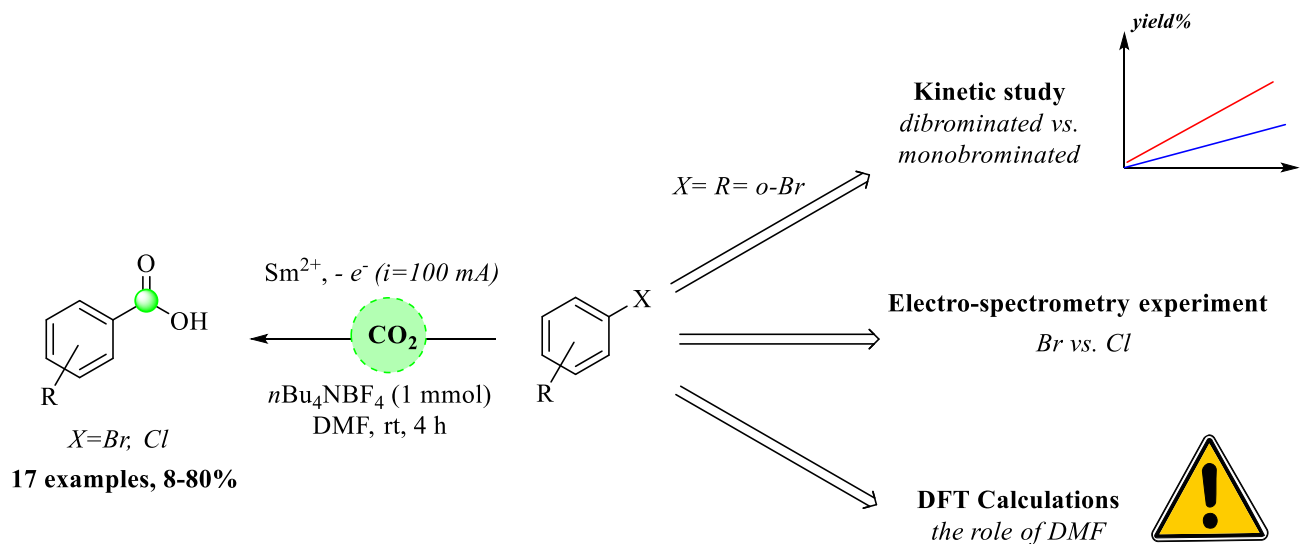


**Figure 54:** required further investigation for the carboxylation of aromatic halides

Further prospects are needed such as a kinetic study of the debromination process vs. carboxylation reaction to explain the reason behind this side reaction. Additionally, an electro-spectrometry could be an efficient method to detect the different species involved in the carboxylation of aryl bromides as well as of aryl chlorides (**Figure 54**).

Further interesting work would be the examination of other substrates such as the carboxylation of activated alkenes as chalcone derivatives and methyl cinnamate under our conditions. Preliminary experiments showed that it is possible to fix the CO<sub>2</sub> on the  $\beta$ -position of an EWG group (**Figure 55**). We also discovered that this reactivity was, similarly to the carboxylation of aromatic halides, solvent-dependant and occurred only in DMF. So, the next step involves understanding the role of DMF in our conditions.

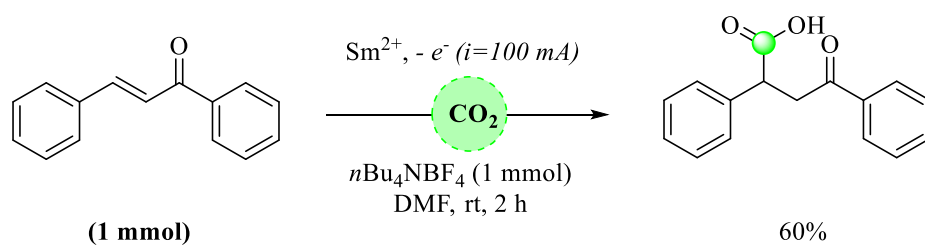


**Figure 55:** Carboxylation of activated alkenes by electrogenerated Sm(II)

Finally, the ultimate goal remains to find convenient conditions to perform such carboxylation reactions efficiently promoted by a catalytic amount of electrogenerated divalent samarium species.



---

# Experimental Part

---

---

## Instrumentation and Chemicals

---

All commercially available reagents were used without further purification unless otherwise stated. All solvents were also used without further purification. Dimethylformamide (DMF) was purchased from Carlo Erba and tetrabutylammonium tetrafluoroborate ( $n\text{Bu}_4\text{NBF}_4$ ) from Fluka. The samarium rod was a 12.7mm diameter, 99.9% (metals basis excluding Ta) rod, purchased from Alfa-Aesar and the stainless-steel grid from Goodfellow. Electrolysis was performed using an EGG Instrument Potentiostat/Galvanostat Model 273 in an undivided cell equipped with a samarium rod as anode and a stainless-steel grid as a cathode. NMR spectra were recorded on Bruker AM 360 (360 MHz), 300 (300 MHz) or AM 250 (250 MHz) in  $\text{CDCl}_3$  with drops of  $\text{CD}_3\text{OD}$  in some cases or totally in  $\text{DMSO-d}_6$  due to the solubility of some products. Data for  $^1\text{H}$  NMR are recorded as follows: chemical shift ( $\delta$ , ppm), coupling constant ( $J$ , Hz), multiplicity (s = singlet, d = doublet, t = triplet, m = multiplet, q = quartet, dd = doublet of doublets, dt = doublet of triplets, td = triplet of doublets, and br = broad signal, integration). Reactions were monitored by thin-layer chromatography (TLC), and column chromatography purifications were carried out using silica gel.

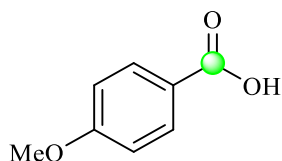
---

## General Procedure for the carboxylation of aryl halides

---

Under  $\text{CO}_2$  (1 atm), the reactions were carried out in an undivided cell containing a magnetic stirring bar, equipped with a samarium rod as anode and a stainless-steel as the cathode. The cell was charged with 322 mg of tetrabutylammonium tetrafluoroborate  $n\text{Bu}_4\text{NBF}_4$  (1 mmol) and the aryl halide (5 mmol) dissolved in 100 mL of DMF. The electrolysis was started using a chronopotentiometry mode with  $i = 100$  mA for 15000 seconds. During the reaction, precipitation was observed, indicating the formation of a samarium carboxylate salt in the medium, insoluble in DMF. When the substrate is no longer detected on the TLC, the reaction was quenched with 6 M HCl aq. (40 mL), slowly added, and the mixture was stirred at room temperature until a homogenous solution was obtained. After dissolution, 300 mL of distilled water was added, and the aqueous solution was extracted with ethyl acetate (3 x 100 mL). The organic phase was extracted with ethyl acetate (5 x 200 mL). The collected organic layer was washed with brine (3 x 100 mL), dried over  $\text{MgSO}_4$ , and concentrated under *vacuo*. The residue was purified by silica gel chromatography using petroleum ether/ethyl acetate (80/20 and then 50/50).

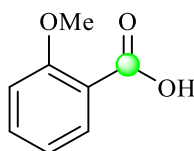
## Characterization of the compounds



**4-methoxybenzoic acid (1'a):** 539 mg (3.55 mmol, yield: 71%,).  $^1\text{H}$  NMR (300 MHz,  $\text{CDCl}_3$ )  $\delta$  8.00 (d,  $J = 8.4$  Hz, 2H), 6.91 (d,  $J = 8.6$  Hz, 2H), 3.85 (s, 3H).

$^{13}\text{C}$  NMR (91 MHz,  $\text{CDCl}_3$ )  $\delta$  169.1, 163.5, 132.0, 122.4, 113.5, 55.4.

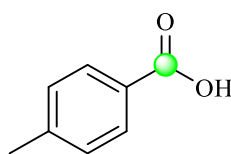
The  $^1\text{H}$  NMR and  $^{13}\text{C}$  NMR spectra are in agreement with those reported in the literature.<sup>67</sup>



**2-methoxybenzoic acid (1'b):** 524 mg (3.45 mmol, yield: 69%).  $^1\text{H}$  NMR (300 MHz,  $\text{DMSO-}d_6$ ):  $\delta$  7.65 (d,  $J = 10.1$  Hz, 1H), 7.49 (td,  $J = 11.3, 4.4$  Hz, 1H), 7.10 (d,  $J = 9.8$  Hz, 1H), 6.97 (td,  $J = 17.4, 10.0$  Hz, 1H), 3.77 (s,  $J = 20.6$  Hz, 3H).

$^{13}\text{C}$  NMR (75 MHz,  $\text{DMSO-}d_6$ ):  $\delta$  167.8, 158.5, 133.4, 131, 121.7, 120.4, 112.8, 56.1.

The  $^1\text{H}$  NMR and  $^{13}\text{C}$  NMR spectra are in agreement with those reported in the literature.<sup>68</sup>



**4-methylbenzoic acid (1'c):** 544 mg (4 mmol, yield: 80%,)  $^1\text{H}$  NMR (360 MHz,  $\text{CDCl}_3$ )  $\delta$  7.89 (d, 2H), 7.20 (d, 2H), 2.36 (s, 3H).

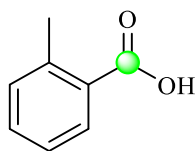
$^{13}\text{C}$  NMR (63 MHz,  $\text{CDCl}_3$ )  $\delta$  169.6, 143.6, 129.7, 128.8, 127.1, 21.2.

The  $^1\text{H}$  NMR and  $^{13}\text{C}$  NMR spectra are in agreement with those reported in the literature.<sup>69</sup>

<sup>67</sup> X. Zhang, W. -Z. Zhang, L. -L. Shi, C. -X. Guo, L. -L. Zhang, X. -B. Lu, *Chem. Commun.* **2012**, 48, 6292.

<sup>68</sup> A. Correa, R. Martín, *J. Am. Chem. Soc.* **2009**, 131, 44, 15974.

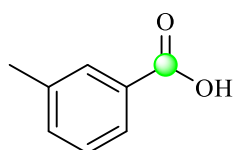
<sup>69</sup> T. Fujihara, K. Nogi, T. Xu, J. Terao, Y. Tsuji, *J. Am. Chem. Soc.* **2012** 134, 22, 9106.



**2-methylbenzoic acid (1'd):** 482 mg (3.55 mmol, yield: 71%).  $^1\text{H}$  NMR (300 MHz,  $\text{CDCl}_3 + \text{CD}_3\text{OD}$ ):  $\delta$  7.83 (d,  $J = 7.5$  Hz, 1H), 7.29 (dd,  $J = 8.3, 6.5$  Hz, 1H), 7.20 – 6.97 (m, 2H), 2.49 (s, 3H).

$^{13}\text{C}$  NMR (91 MHz,  $\text{CDCl}_3 + \text{CD}_3\text{OD}$ )  $\delta$  169.9, 139.9, 131.7, 131.3, 130.5, 129.5, 125.3, 21.3.

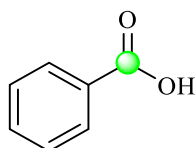
The  $^1\text{H}$  NMR and  $^{13}\text{C}$  NMR spectra are in agreement with those reported in the literature.<sup>69</sup>



**3-methylbenzoic acid (1'e):** 530 mg (3.9 mmol, yield: 78%).  $^1\text{H}$  NMR (300 MHz,  $\text{CDCl}_3$ )  $\delta$  7.93 (m,  $J = 7.3$  Hz, 2H), 7.51 – 7.29 (m, 2H), 2.43 (s, 3H).

$^{13}\text{C}$  NMR (75 MHz,  $\text{CDCl}_3$ )  $\delta$  172.5, 138.3, 134.5, 130.7, 129.2, 128.3, 127.3, 21.2.

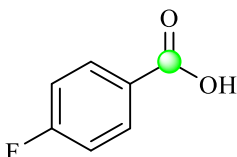
The  $^1\text{H}$  NMR and  $^{13}\text{C}$  NMR spectra are in agreement with those reported in the literature.<sup>69</sup>



**Benzoic acid (1'f):** 464 mg (3.8 mmol, yield: 76%)  $^1\text{H}$  NMR (360 MHz,  $\text{CDCl}_3$ )  $\delta$  7.99 (d,  $J = 7.7$  Hz, 2H), 7.49 (t,  $J = 7.3$  Hz, 1H), 7.37 (t,  $J = 7.5$  Hz, 2H).

$^{13}\text{C}$  NMR (91 MHz,  $\text{CDCl}_3$ )  $\delta$  169.2, 132.9, 130.1, 129.7, 128.2.

The  $^1\text{H}$  NMR and  $^{13}\text{C}$  NMR spectra are in agreement with those reported in the literature.<sup>68</sup>



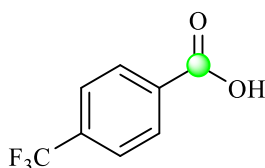


**4-fluorobenzoic acid (1'g):** 483 mg (3.45 mmol, yield: 69%).  $^1\text{H}$  NMR (300 MHz,  $\text{CDCl}_3$ )  $\delta$  7.99 (m, 2H), 7.03 (t, 2H).

$^{13}\text{C}$  NMR (91 MHz,  $\text{CDCl}_3$ )  $\delta$  167.9, 165.7(d,  $J_{\text{C-F}}=250\text{Hz}$ ), 132.3(d,  $J_{\text{C-F}}=9.5\text{Hz}$ ), 126.5, 115.2(d,  $J_{\text{C-F}}=22\text{Hz}$ ).

$^{19}\text{F}$  NMR (75 MHz,  $\text{CDCl}_3$ ):  $\delta$  106.94.

The  $^1\text{H}$  NMR and  $^{13}\text{C}$  NMR spectra are in agreement with those reported in the literature.<sup>70</sup>

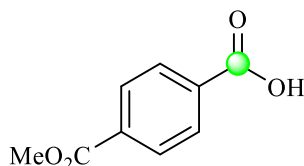


**4-(trifluoromethyl) benzoic acid (1'h):** 741 mg (3.9 mmol, yield: 78%).  $^1\text{H}$  NMR (300 MHz,  $\text{CDCl}_3 + \text{MeOD}$ )  $\delta$  8.02 (d,  $J = 8.1$  Hz, 2H), 7.56 (d,  $J = 8.2$  Hz, 2H).

$^{13}\text{C}$  NMR (63 MHz, DMSO)  $\delta$  166.1, 134.6, 132.5(d,  $J=31$  Hz), 130.1, 125.9, 125.5(q,  $J=272$  Hz).

$^{19}\text{F}$  (282 MHz,  $\text{CDCl}_3$ ):  $\delta$  61.6.

The  $^1\text{H}$  NMR and  $^{13}\text{C}$  NMR spectra are in agreement with those reported in the literature.<sup>69</sup>

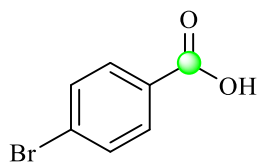


**Methyl 4-carboxybenzoate acid (1'i):** 549 mg (3.05 mmol, yield: 61%).  $^1\text{H}$  NMR (300 MHz,  $\text{CDCl}_3$ )  $\delta$  8.03 (m, 4H), 3.88 (s, 3H).

$^{13}\text{C}$  NMR (91 MHz,  $\text{CDCl}_3$ )  $\delta$  167.8, 166.6, 134.4, 133.6, 129.7, 129.4, 52.3.

The  $^1\text{H}$  NMR and  $^{13}\text{C}$  NMR spectra are in agreement with those reported in the literature.<sup>70</sup>

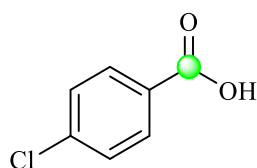
<sup>70</sup> F. Rebih, M. Andreini, A. Moncomble, A. Harrison-Marchand, J. Maddaluno, M. Durandetti, *Chem. Eur. J.* **2016**, *22*, 3758.



**4-bromobenzoic acid (1'm):** 573 mg (2.85 mmol, yield: 57%).  $^1\text{H NMR}$  (300 MHz,  $\text{DMSO-}d_6$ ):  $\delta$  13.19 (s, 1H), 7.86 (d,  $J = 8.5$  Hz, 2H), 7.71 (d,  $J = 8.5$  Hz, 2H).

$^{13}\text{C NMR}$  (75 MHz,  $\text{DMSO-}d_6$ )  $\delta$  167.1, 132.1, 131.7, 130.4, 127.3.

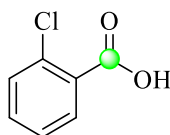
The  $^1\text{H NMR}$  and  $^{13}\text{C NMR}$  spectra are in agreement with those reported in the literature.<sup>71</sup>



**4-chlorobenzoic acid (1'o):** 511.5 mg (3.3 mmol, yield: 66%).  $^1\text{H NMR}$  (300 MHz,  $\text{DMSO}$ )  $\delta$  13.21 (s, 1H), 8.03-7.84 (m, 2H), 7.65-7.41 (m, 2H).

$^{13}\text{C NMR}$  (75 MHz,  $\text{DMSO}$ )  $\delta$  166.5, 133.7, 133.3, 133, 130, 129.3, 128.3.

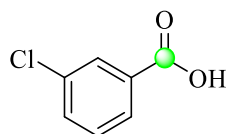
The  $^1\text{H NMR}$  and  $^{13}\text{C NMR}$  spectra are in agreement with those reported in the literature.<sup>71</sup>



**2-chlorobenzoic acid (1'p):** 473 mg (3.05 mmol, 61%).  $^1\text{H NMR}$  (300 MHz,  $\text{DMSO}$ )  $\delta$  13.21 (s, 1H), 7.94 (d, 2H), 7.57 (d, 2H).

$^{13}\text{C NMR}$  (75 MHz,  $\text{DMSO}$ )  $\delta$  166.2, 133.4, 133, 132.7, 130.6, 128.9, 127.9.

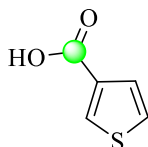
The  $^1\text{H NMR}$  and  $^{13}\text{C NMR}$  spectra are in agreement with those reported in the literature.<sup>71</sup>



**3-chlorobenzoic acid (1'q):** 457 mg (2.95 mmol, 59%).  $^1\text{H NMR}$  (300 MHz,  $\text{CDCl}_3$ )  $\delta$  8.11 (t,  $J = 1.8$  Hz, 1H), 8.05 – 7.97 (dt, 1H), 7.60 (ddd,  $J = 8.0, 2.2, 1.1$  Hz, 1H), 7.44 (t,  $J = 7.9$  Hz, 1H).

$^{13}\text{C}$  NMR (91 MHz,  $\text{CDCl}_3$ )  $\delta$  171.1, 134.7, 133.9, 130.9, 130.3, 129.8, 128.3.

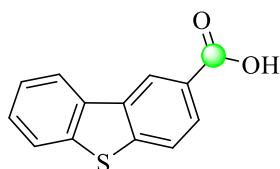
The  $^1\text{H}$  NMR and  $^{13}\text{C}$  NMR spectra are in agreement with those reported in the literature.<sup>71</sup>



**3-thiophenecarboxylic acid (1'n):** 267 mg (2.1 mmol, yield: 42%,).  $^1\text{H}$  NMR (300 MHz,  $\text{CDCl}_3$ )  $\delta$  8.25 (dd,  $J = 3.0, 1.1$  Hz, 1H), 7.58 (dd,  $J = 5.1, 1.1$  Hz, 1H), 7.39 – 7.30 (m, 1H).

$^{13}\text{C}$  NMR (91 MHz,  $\text{CDCl}_3$ )  $\delta$  168.2, 134.6, 132.9, 128.1, 126.3.

The  $^1\text{H}$  NMR and  $^{13}\text{C}$  NMR spectra are in agreement with those reported in the literature.<sup>72</sup>

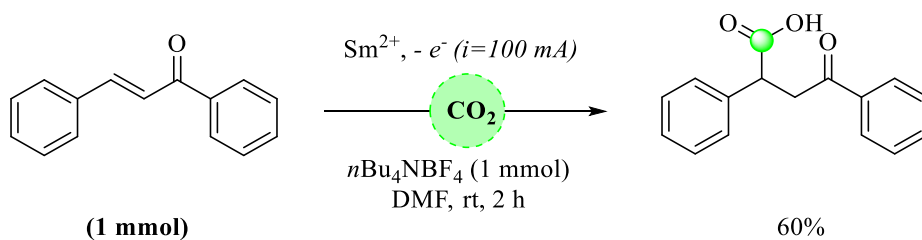


**Dibenzothiophene-2-carboxylic acid (1'o):** 513 mg (2.25 mmol, yield: 45%,).  $^1\text{H}$  NMR (250 MHz, DMSO)  $\delta$  8.91 (d,  $J = 1.1$  Hz, 1H), 8.49 (dd,  $J = 6.4, 1.6$  Hz, 1H), 8.15 (d,  $J = 6.1$  Hz, 1H), 8.07 (m, 2H), 7.61 – 7.52 (m, 2H).

$^{13}\text{C}$  NMR (63 MHz,  $\text{CDCl}_3$ )  $\delta$  167.8, 143.7, 139.4, 135.5, 135, 128.1, 128, 127, 125, 123.6, 123.5, 123.4, 122.8.

ESI (-):  $[\text{M}-\text{H}] = 227.0174$ .

## Carboxylation of chalcone



<sup>71</sup> S. Mukhopadhyay, S. Batra, *Chem. Eur. J.* **2018**, *24*, 14622.

<sup>72</sup> K. Paridala, S. M. Lu, M.M. Wang, C. Li, *Chem. Commun.* **2018**, *54*, 11574.

Under CO<sub>2</sub> (1 atm), the reaction was carried out in an undivided cell containing a magnetic stirring bar, equipped with a samarium rod as anode and a stainless-steel as the cathode. The cell was charged with 322 mg of tetrabutylammonium tetrafluoroborate *n*Bu<sub>4</sub>NBF<sub>4</sub> (1 mmol) and (*E*)-chalcone (208 mg, 1 mmol) dissolved in 50 mL of DMF. The electrolysis was started using a chronopotentiometry mode with *i* = 100 mA for 7200 seconds. When the substrate was no longer detected on the TLC, the reaction was quenched with 2 M HCl aq. (40 mL), slowly added, and the mixture was stirred at room temperature until a homogenous solution was obtained. After dissolution, 50 mL of distilled water was added, and the aqueous solution was extracted with ethyl acetate (3 x 20 mL). The collected organic layer was washed with brine (3 x 20 mL), dried over MgSO<sub>4</sub>, and concentrated under *vacuo*. The residue was purified by silica gel chromatography using petroleum ether/ethyl acetate (80/20 and then 50/50) to deliver 152.4 mg of 4-oxo-2,4-diphenylbutanoic acid (0.6 mmol, 60%).

**4-Oxo-2,4-diphenylbutanoic acid (1'v):** 152.4 mg (0.6 mmol, yield: 60%,). <sup>1</sup>H NMR (360 MHz, CDCl<sub>3</sub>) δ 7.98 (d, *J* = 7.4 Hz, 2H), 7.58 (t, *J* = 7.4 Hz, 1H), 7.47 (t, *J* = 7.7 Hz, 2H), 7.4-7.25 (m, 5H), 4.34 (dd, *J* = 10.1, 4.1 Hz, 1H), 3.93 (dd, *J* = 18.1, 10.1 Hz, 1H), 3.31 (dd, *J* = 18.1, 4.2 Hz, 1H).

<sup>13</sup>C NMR (91 MHz, CDCl<sub>3</sub>) δ 197.6, 179, 137.6, 136.1, 133.4, 129.0, 128.9, 128.3, 128.0, 46.3, 42.2.

The <sup>1</sup>H NMR and <sup>13</sup>C NMR spectra are in agreement with those reported in the literature.<sup>73</sup>

<sup>73</sup> T. Song, S. Arseniyadis, J. Cossy, *Org. Lett.* **2019**, *21*, **3**, 603





Electrogenerated Sm(II)-catalyzed  
the carboxylation of benzyl  
chloride derivatives

---



# Electrogenerated Sm(II)-catalyzed the carboxylation of benzyl chloride derivatives

## 1. Phenylacetic acids: state of the art

In the previous chapter, the synthesis of benzoic acids from organic frameworks was discussed in addition to their numerous applications in fine chemistry. Having one additional carbon atom give rise to phenylacetic acids, an interesting class of carboxylic acids highly valued in pharmaceutical chemistry. More specifically, phenylacetic acids moiety is the reactive center in many non-steroidal anti-inflammatory drugs (NSAIDs) (**Figure 56**).<sup>74</sup>

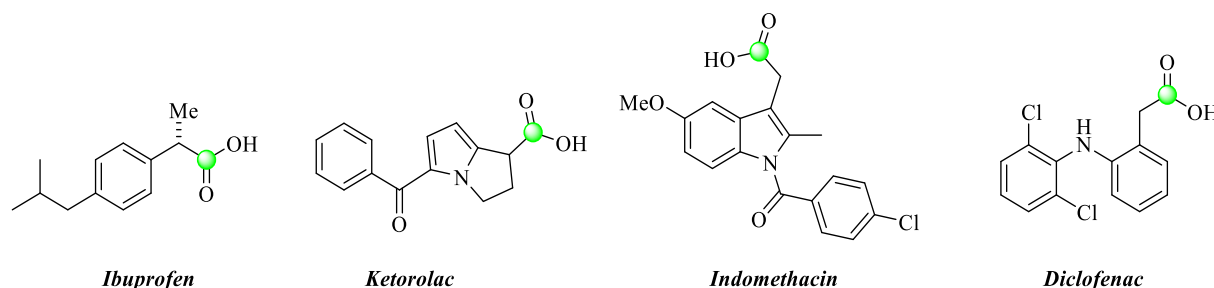


**Figure 56:** Examples of NSAIDs containing the phenylacetic acid motif.

To access these products, many protocols were evaluated, searching for the most economical and efficient pathway and the carboxylation route using CO<sub>2</sub> satisfied these requests.

The electrochemistry was the first to investigate this approach,<sup>21,75</sup> but catalytic carboxylation based on transition metals were also developed to produce phenylacetic acids via Markovnikov hydrocarboxylation of styrene derivatives using CO<sub>2</sub> as C<sub>1</sub>-building block. The stability of η<sup>3</sup>-benzylic metal intermediate allowed the CO<sub>2</sub> insertion to occur selectively on the benzylic position. However, these strategies required the use of an excessive quantity of organometallic reductant and remained limited to unsubstituted styrenes.<sup>76,13</sup> Targeting this point, ongoing efforts based on photoinduced carboxylations of styrene derivatives present a promising method to solve the drawback related to the overuse of co-reductants.<sup>77</sup>

On the other hand, the reductive carboxylation of benzyl halides was recently presented as a shortcut route to obtain substituted phenylacetic acids.<sup>78</sup> Very recently, the carboxylation of other

<sup>74</sup> H. Maag, *Prodrugs of Carboxylic Acids*; Springer: New York, **2007**

<sup>75</sup> O. Sock, M. Troupel, J. Perichon, *Tetrahedron Lett.* **1985**, *26*, 1509

<sup>76</sup> S. Saini, H. Singh, P. K. Prajapati, A. K. Sinha, S. L. Jain., *ACS Sustainable Chem. Eng.* **2019**, *7*, **13**, 11313; W. Butcher, E. J. McClain, T. G. Hamilton, T. M. Perrone, K. M. Kroner, G. C. Donohoe, N. G. Akhmedov, J. L. Petersen, B. V. Popp, *Org. Lett.* **2016**, *18*, 6428.

<sup>77</sup> a) K. Murata, N. Numasawa, K. Shimomaki, J. Takaya, N. Iwasawa, *Chem. Commun.* **2017**, *53*, 3098; b) Q.-Y. Meng, S. Wang, G. S. Huff, B. König, *J. Am. Chem. Soc.* **2018**, *140*, **9**, 3198; c) V.R. Yatham, Y. Shen, R. Martin, *Angew. Chem.* **2017**, *129*, 11055; *Angew. Chem., Int. Ed.* **2017**, *56*, 10915.

<sup>78</sup> Y.-G. Chen, X.-T. Xu, K. Zhang, Y.-Q. Li, L.-P. Zhang, P. Fang, T. -S. Mei, *Synthesis* **2018**, *50*, 35



benzylic derivatives revealed a worth noting reactivity by tolerating tertiary starting materials under mild conditions.<sup>79</sup>

In this introduction, we will focus our study on the reductive carboxylation of organic(pseudo) halides as an interesting alternative for the CO<sub>2</sub> insertion mediated by typical organometallic reagents.

## 2. Catalytic carboxylation of organic (pseudo)halides

### a. Using benzyl halides as starting material

In 2013, Martin's group described the first catalytic carboxylation of benzyl bromides and chlorides using Ni(0) catalysis.<sup>11</sup> After oxidative addition of the benzyl halide, a Ni(I) intermediate was generated via single electron transfer from the zinc powder, added in the medium as a co-reductant (**Figure 57**).

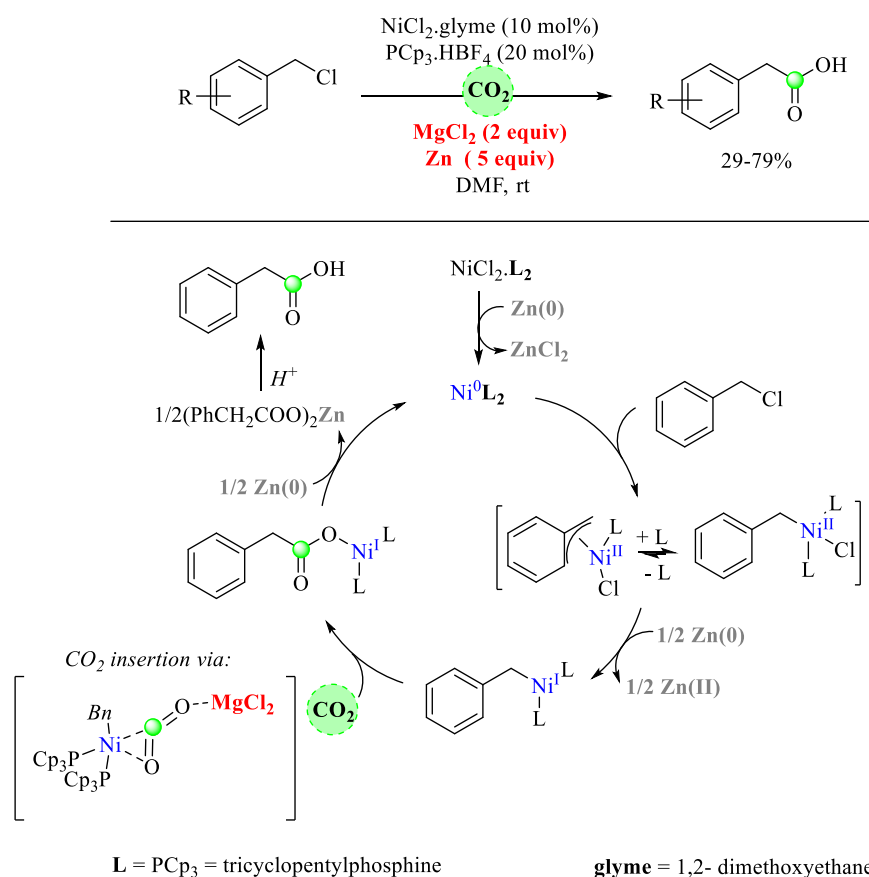


**Figure 57:** Proposed mechanism for the carboxylation of benzyl halides described by Martin's group.

Concerning the scope, the carboxylation of primary benzyl halides was efficiently achieved using this protocol while secondary and tertiary substrates were tested only with benzyl bromides. Overall, the authors described the Ni-based carboxylation as a substitute for previous procedures

<sup>79</sup> a) A. Correa, T. León, R. Martin, *J. Am. Chem. Soc.* **2014**, *136*, 1062; b) T. Moragas, M. Gaydou, R. Martin, *Angew. Chem.* **2016**, *128*, 5137; *Angew. Chem., Int. Ed.* **2016**, *55*, 5053

that suffered from many problems such as low selectivity, the excessive use of co-reductants, and scope limitation. This Ni-based system presented also several drawbacks:

- *The use of zinc powder:* This overly used additive (5 equiv) was crucial for the carboxylation, permitting the generation of the Ni(I)-intermediate so the CO<sub>2</sub> insertion could occur subsequently.
- *Magnesium dichloride MgCl<sub>2</sub> as additive:* The addition of MgCl<sub>2</sub> was a key factor in the CO<sub>2</sub> insertion step, and without it, the yield dropped to 28% (vs. 74% with MgCl<sub>2</sub>). In 2014, Sakaki's DFT calculations explained this behavior by proposing a transition state combining the Ni(I) and MgCl<sub>2</sub>. This latter activates the CO<sub>2</sub> by its Lewis acidity and thus, facilitates the CO<sub>2</sub> insertion into the Ni(I)-C bond.<sup>80</sup>
- *The scope limitation:* Even though the secondary and tertiary benzyl bromides reacted smoothly, but this was not the case with the corresponding chlorides. The scope of challenging benzyl chlorides covered only unsubstituted substrates exposing a major reaction limitation.

Two years later, He and co-workers reported similar conditions, but the carboxylation was mediated by a Pd(0) catalysis with Mn powder as co-reducing agent and also in the presence of MgCl<sub>2</sub> (**Figure 58**).<sup>81</sup> DFT studies proved the existence of a non-innocent interaction between this additive and CO<sub>2</sub>, as similarly described in the Ni-catalysis case.

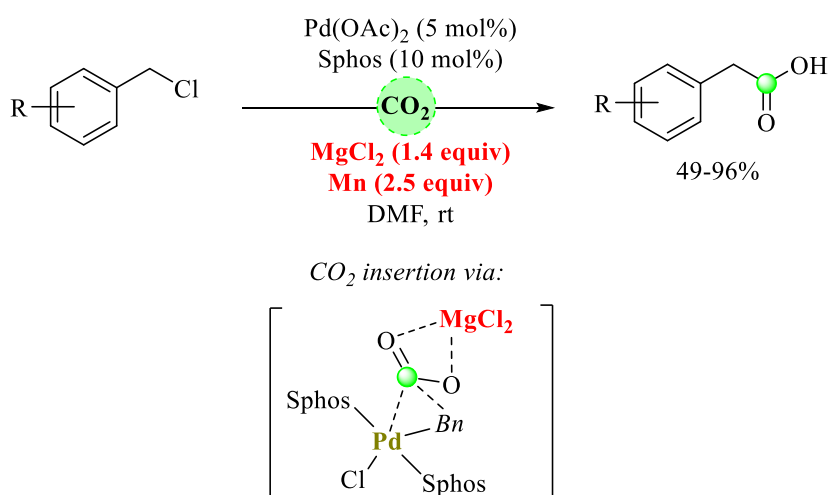


**Figure 58:** Pd-catalyzed the carboxylation of benzyl chlorides.<sup>81</sup>

A worth noting example from Beller's group described the carboxylation of benzyl halides with formic acid to obtain phenylacetic acids.<sup>82</sup> This method consisted in using a Pd(0)/Pd(II) catalytic cycle, and the *in situ* generation of carbon monoxide via the decomposition of formic acid, assisted by the ligand and the *N, N, N', N'*-tetramethylethylenediamine (TMEDA) as a base. After the oxidative addition, an excess of base in the medium triggered the reductive elimination step to yield the acid anhydride. Finally, hydrolysis or the release of CO, allowed the formation of the phenylacetic acids in good yields.

<sup>80</sup> F. B. Sayyed, S. Sakaki, *Chem. Commun.* **2014**, 50, 13026

<sup>81</sup> S. Zhang, W.Q. Chen, A. Yu, L.N. He, *ChemCatChem.* **2015**, 7, 3972

<sup>82</sup> L. Wang, H. Neumann, M. Beller, *Angew. Chem. Int. Ed.* **2018**, 57, 1

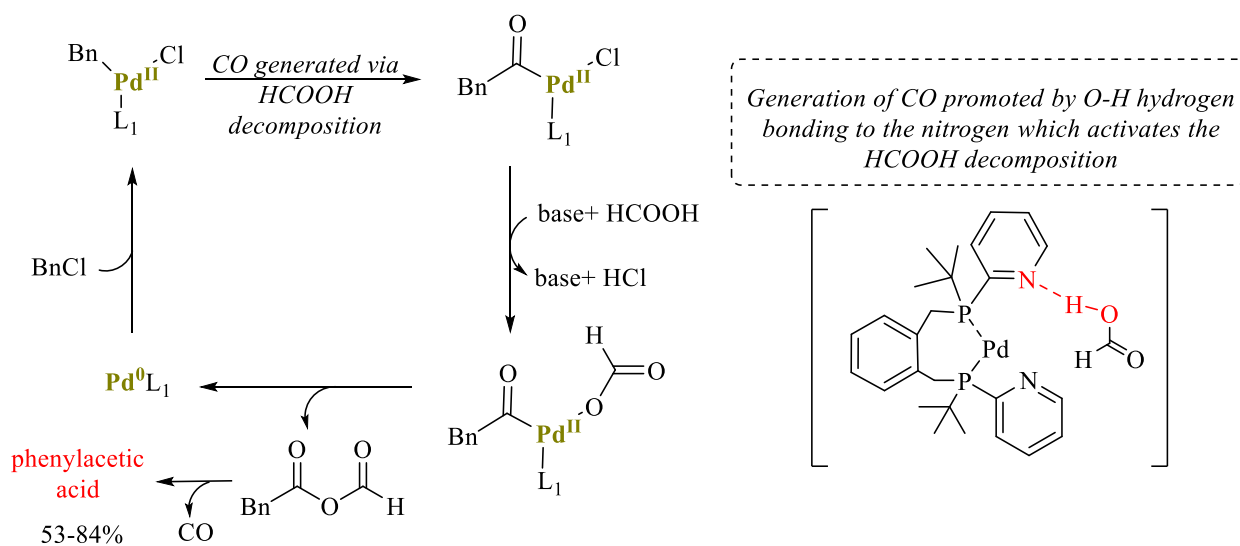


**Figure 59:** Mechanistic pathway for the carboxylation of benzyl halides with formic acid.<sup>82</sup>

Indeed, this approach presented an original path to access this category of carboxylic acids in the absence of a reducing agent. Nevertheless, this transformation was limited to unsubstituted phenyl chlorides due to the bulky ligand, and optimal carboxylation yield was achieved only at high temperature (115°C).

### b. Using benzyl esters derivatives as starting material

The carboxylation using these starting materials goes through  $C_{sp^3}$ -O bond cleavage and it is known as a challenging process due to the high activation energy barrier. Martin's group was also in this case the first to publish the carboxylation of aryl and benzyl esters derivatives using a Ni(II) complex.<sup>79a</sup>

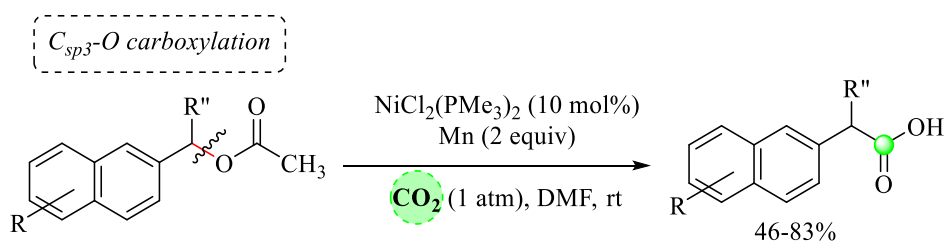


**Figure 60** Ni-catalyzed the carboxylation of  $C_{sp^3}$ -O bonds.<sup>79a</sup>

The optimized conditions tolerated different leaving groups such as pivalates, carbamates, and acetates. Due to its higher atom economy, the acetate derivatives were used to study the scope of this reaction. Remarkably, high yields were observed mainly with  $\pi$ -extended systems like naphthalene or anthracene while simple phenyl-containing substrates did not react as well as expected (**Figure 61, A**). This reactivity was rationalized based on the Dewar-Chatt-Duncanson proposed model, which suggested a  $\eta^2$ -coordination mode between the Ni(0) center and the  $\pi$ -

system.<sup>83</sup> Furthermore, an X-ray structure described by Krüger showed this binding mode between Ni(0) and anthracene.<sup>84</sup>

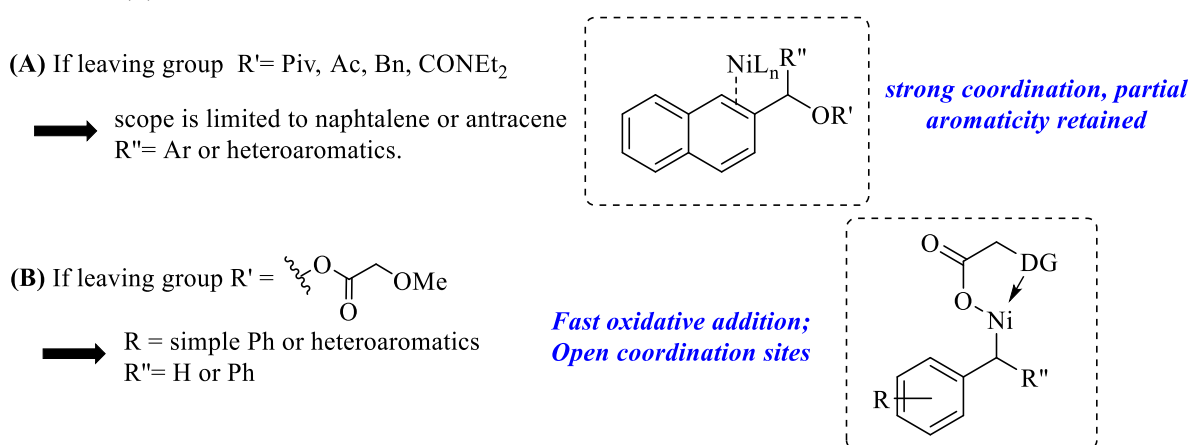


**Figure 61:** Proposed hypothesis for the different behavior observed according to the substrates.<sup>79a</sup>

Apparently, filling a coordinating site on the Ni center had a crucial impact on the reaction. Therefore, the authors conducted a study using traceless directing groups to investigate probable chelation assistance. This test revealed the major role played by the leaving group bearing coordinating frameworks like ethers or pyridyl (**Figure 61, B**). This observation allowed the extension of the scope to benzyl esters derivatives, affording substituted phenylacetic acids in moderate to good yields (up to 79%).

Despite the advance accomplished in this work, the complexity of the parameters affected enormously the sustainability of this transformation. Many compounds were not compatible with the conditions such as substrates bearing halides that underwent dehalogenation processes. Also, substrates containing *ortho* chelating groups (pyrazole, esters, aldehyde...) were inert in all the experimental conditions, and even some compounds furnished the homodimerization product.

### c. Using ammonium salts as starting material

Benzylic ammonium salts form an interesting category of benzylic derivatives that can be easily synthesized from the corresponding amines. The group of Martin reported the carboxylation of benzylic C-N bonds using CO<sub>2</sub> via an electrophilic cross-coupling reaction mediated by Ni-catalysis, combined with 1,10-phenanthroline derivatives, as bench-stable ligands (**Figure 62**).<sup>79b</sup> These compounds demonstrated a high insensitivity to the electronic changes of the aromatic ring and afforded the corresponding carboxylic acids in good to excellent yields. Notably, secondary benzyl ammonium salts also reacted very well under these conditions. The proposed mechanism was based on the generation of a Ni(I) intermediate, produced via a SET from the co-reductant (Mn), similarly to a previous report.<sup>11</sup>

<sup>83</sup> M. J. S. Dewar, *Bull. Soc. Chim. Fr.* **1951**, 18, 79; J. Chatt, L. A. Duncanson, *J. Chem. Soc.* **1953**, 2939; J. Chatt, L. A. Duncanson, L. M. Venanzi, *J. Chem. Soc.* **1955**, 4456.

<sup>84</sup> D. J. Brauer, C. Krueger, *Inorg. Chem.* **1977**, 16, 884.

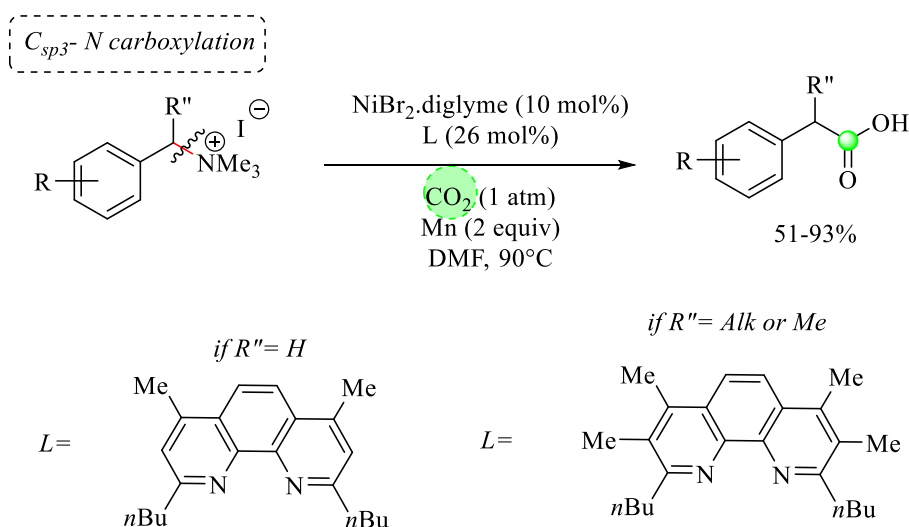


**Figure 62:** First cross-electrophile coupling reaction via unconventional C-N bond cleavage/ $\text{CO}_2$  insertion. <sup>79b</sup>

This approach allowed to overcome the problem of side reactions (dehalogenation, dimerization) and tolerated unusual starting material to produce new carboxylic acids. However, an additional synthetic step was required to access the starting substrates, and high reaction temperature ( $90^\circ\text{C}$ ) was essential as well as long reaction time (72 h) to achieve satisfying yields.

Very recently, an elegant photoinduced cross-electrophile coupling of tetraalkylammonium salts with  $\text{CO}_2$  was introduced by Yu and co-workers. <sup>85</sup> The advantages of this protocol, compared to the previous one, are the compatibility with tertiary substrates and the mild reaction temperature.

#### d. Photocarboxylation of benzylic C–H bonds

Even though no pseudo(halides) carboxylation is used in this protocol, yet it deserves to be discussed as an original pathway to obtain phenylacetic acids. König's group established the photocarboxylation of benzylic C-H bonds as a straightforward tool for the synthesis of carboxylic acids (**Figure 63**). <sup>86</sup> In this strategy, catalytic amounts of the photosensitizer 1,2,3,5-tetrakis(carbazol-9-yl)-4,6-dicyanobenzene 4CzIPN in the presence of triisopropylsilanethiol ( $\text{Pr}_3\text{SiSH}$ ) as a hydrogen atom transfer catalyst were added to achieve the carboxylation. This transformation tolerated different functional groups with good to very good yields. Control experiments proved the formation of 2,3,4,6-tetra(9H-carbazol-9-yl)-5-(1-phenylethyl)benzotrile (4CzPEBN), after the substitution of one cyano group of 4CzIPN by a benzyl moiety. Thus, they proposed the mechanism illustrated below with 4CzPEBN instead of 4CzIPN:

<sup>85</sup> L-L. Liao, G-M. Cao, J-H. Ye, G-Q. Sun, W-J. Zhou, Y-Y. Gui, S.-S. Yan, G. Shen, D-G. Yu, *J. Am. Chem. Soc.* **2018**, *140*, **50**, 17338.

<sup>86</sup> Q.-Y. Meng, T. E. Schirmer, A. L. Berger, K. Donabauer, B. König, *J. Am. Chem. Soc.* **2019** DOI: 10.1021/jacs.9b05360

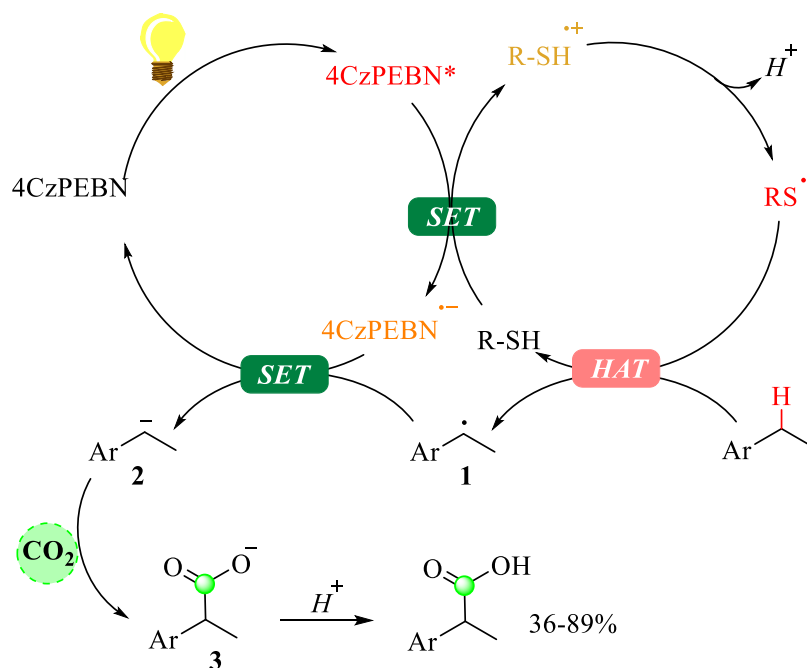


**Figure 63:** Plausible mechanism for the photocarboxylation of benzylic C<sub>sp3</sub>-H bonds.<sup>86</sup>

The visible light enabled the formation of 4CzPEBN\* that underwent a first electron transfer with the HAT catalyst <sup>i</sup>Pr<sub>3</sub>SiSH to form the corresponding 4CzPEBN<sup>•-</sup> and <sup>i</sup>Pr<sub>3</sub>SiSH<sup>•+</sup>. The deprotonation of this latter generated the radical <sup>i</sup>Pr<sub>3</sub>SiS<sup>•</sup>, and this intermediate abstracted furtherly the benzylic hydrogen to furnish the benzyl radical **1**. A second electron transfer between **1** and 4CzPEBN<sup>•-</sup> allowed the regeneration of 4CzPEBN and the formation of the carbanion **2**. The CO<sub>2</sub> was then captured by this benzylic anion to deliver the phenylacetic acid.

Even though this system offered a new perspective for the carboxylation reactions, yet the conditions worked only with secondary benzylic C-H bond.

### 3. Electrocarylation of benzyl chlorides

As previously mentioned, electrochemistry was the first method used to achieve the carboxylation of benzyl chlorides. In a one-compartment electrochemical cell, the electrocarboxylation (or carboxylation assisted by electrochemistry) can occur in two different pathways: direct or indirect electrocarboxylation.

#### *b. Direct Electrocarylation*

In the literature, different electrochemical approaches with various cathode materials were investigated for the direct carboxylation of benzyl chlorides. From mercury to platinum or glassy

carbon, all of the proposed systems imposed a very negative potential (overpotential), which is the principal cause of side reactions (**Figure 64, I**).<sup>87</sup>

Recently, many papers dealing with the electroreduction of organic chlorides at silver cathodes have appeared. In this case, the reduction occurred at a more positive potential than the previously reported ones, probably due to the high affinity of silver for halides (**Figure 64, II**).<sup>88</sup> Still, various side products were described (reduced and dimerized products) and resulting in a complex mixture. On the other hand, an eco-friendly silver-based approach was described by Lu's group using an ionic liquid as an alternative for the massive amount of supporting electrolytes.<sup>89</sup>

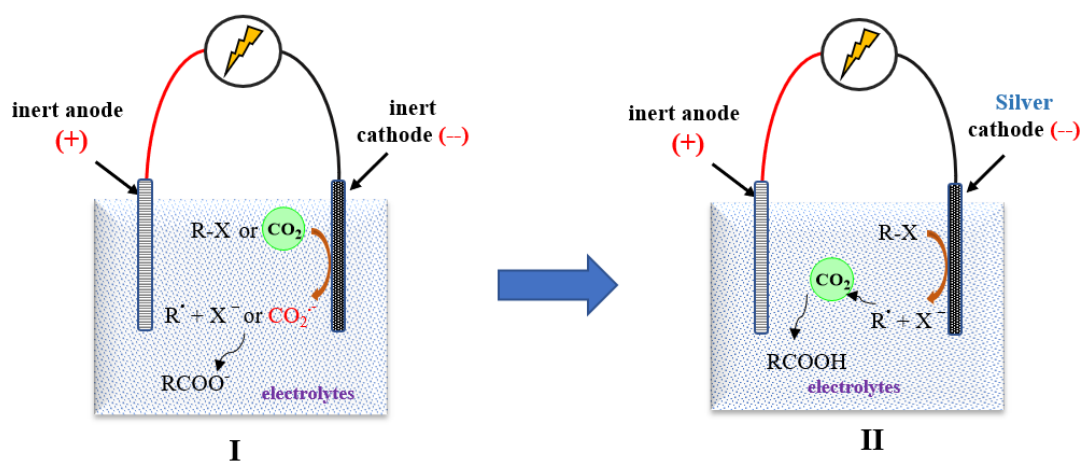


**Figure 64:** Developed systems for direct electrocarboxylation of benzyl chlorides.

Recently, Atobe and co-workers proposed an elegant procedure based on flow electrochemistry.<sup>90</sup> In a microreactor, the electrocarboxylation occurred using a platinum anode and a glassy carbon cathode, with the unstable carboxylate being directly acidified in an acidification region. Therefore, this technique represents an excellent alternative for the sacrificial anodes in addition to the multiple advantages offered by the use of a microreactor such as the important surface-to-volume ratio, the precise temperature control, and the high-speed mixing.

Very recently, a direct electrochemical reduction of benzylic C-N bonds was reported by Manthiram's group.<sup>91</sup> Using platinum as the cathode and glassy carbon as the anode, the authors managed to carboxylate primary and secondary substrates with good to excellent yields.

Meanwhile, some examples reported the use of sacrificial anodes (mainly Mg and Al) to produce phenylacetic acids.<sup>75,92</sup> The primary role of the released metal cation was the stabilization of the generated carboxylate anion and the limitation of its decomposition. However, the distance between the electrodes was critical in these electrochemical transformations. Due to the dissolution

<sup>87</sup> S. Wawzonek, R. C. Duty, J. H. Wagenknecht, *J. Electrochem. Soc.* **1964**, *111*, 74; M. M. Baizer and J. L. Chruma, *J. Org. Chem.* **1972**, *37*, 1951; J. H. Wagenknecht, *J. Electroanal. Chem. Interfacial Electrochem.* **1974**, *52*, 489; D. A. Tyssee, J. H. Wagenknecht, M. M. Baizer, J. L. Chruma, *Tetrahedron Lett.* **1972**, 4809.

<sup>88</sup> A. A. Isse, A. Gennaro, *Chem. Comm.* **2002**, 2798; A. A. Isse, M. G. Ferlin, A. Gennaro, *J. Electroanal. Chem.* **2005**, *581*, 38; O. Scialdone, A. Galia, G. Errante, A. A. Isse, A. Gennaro, G. Filardo, *Electrochimica Acta* **2008**, *53*, 2514.

<sup>89</sup> D. NIU, J. Zhang, K. Zhang, T. Xue, J. Lu, *Chin. J. Chem.*, **2009**, *27*, 1041

<sup>90</sup> H. Tateno, Y. Matsumura, K. Nakabayashi, H. Senbokub, M. Atobe, *RSC Adv.* **2015**, *5*, 98721.

<sup>91</sup> D.-T. Yang, M. Zhu, Z. J. Schiffer, K. Williams, X. Song, X. Liu, K. Manthiram, *ACS Catal.* **2019**, *9*, 4699

<sup>92</sup> G. Silvestri, S. Gambino, G. Filardo, A. Gulotta, *Angew. Chem., Int. Ed. Engl.*, **1984**, *23*, 979; G. Silvestri, S. Gambino, G. Filardo, G. Greco, A. Gulotta, *Tetrahedron Lett.*, **1984**, 25,4307; O. Sock, J. Pouliquen, M. Heintz, O. Sock, M. Troupel, *J. Chem. Educ.* **1986**, *63*, 1013; M. Heintz, O. Sock, C. Saboureaux, J. Perichon, M. Troupel, *Tetrahedron*, **1988**, *44*, 1631. O. Scialdone, A. Galia, G. Silvestri, C. Amatore, L. Thouin, J.-N. Verpeaux, *Chem. -Eur. J.* **2006**, *12*, 7433; S. Chanfreau, P. Cognet, S. Camy, J.-S. Condoret, *J. Supercrit. Fluid.* **2008**, *46*, 156; Y. Hiejima, M. Hayashi, A. Uda, S. Oya, H. Kondo, H. Senbokub, K. Takahashi, *Phys. Chem. Chem. Phys.* **2010**, *12*, 1953.

of the sacrificial anode, the space between the two dipoles increased during the electrolysis, causing a Joule-heating effect which could limit their further industrial application.

### b. Indirect electrocarboxylations of benzyl chloride derivatives

This method consisted in using a homogeneous catalyst exhibiting a reductive power and thus, capable of reducing the benzyl halide or the CO<sub>2</sub> in the mixture. In this context, the electricity served as a reductant to regenerate the active catalyst.

Various transition metal complexes catalyzed this type of transformations. For example, several nickel,<sup>93</sup> palladium,<sup>94</sup> and cobalt<sup>75,95</sup> catalysts achieved the carboxylation of benzyl chlorides with significant current efficiency under mild conditions. Yet these protocols provided phenylacetic acids with low to moderate turnover numbers due to the deactivation of the catalyst after hydrogen abstraction from the solvent or residual water traces.

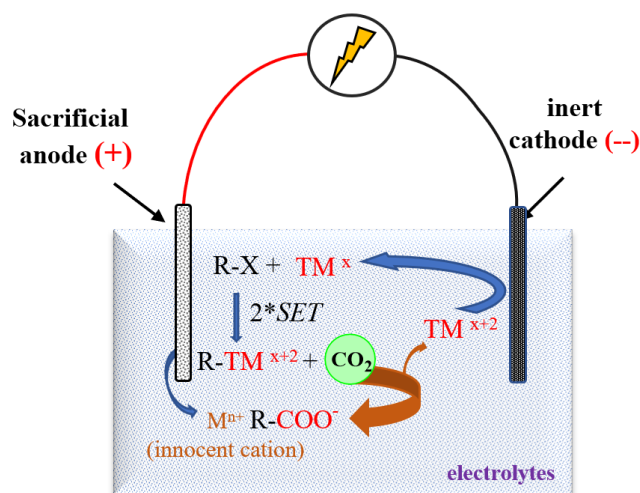


**Figure 65:** Carboxylation of benzyl halides using transition metal catalysts (TM) as chemical mediators.

Whether directly or via a catalyst, the electrocarboxylation pathway followed this mechanism (**Figure 66**): the reaction started first by the reduction of benzyl chloride ( $E_p = -1.62$  V vs. SCE) to generate the benzyl radical  $\text{BnCH}_2^\cdot$ , possessing a lower standard reduction ( $-1.43$  V vs. SCE) with an estimated lifetime around  $10^{-6}$  s. This radical underwent thus a second electron transfer to provide the anionic form  $\text{BnCH}_2^-$ . Along with other side reactions, the  $\text{BnCH}_2^-$  performs a nucleophilic attack to generate the corresponding carboxylic acid.

<sup>93</sup> A. Gennaro, A. A. Isse, F. Maran, *J. Electroanal. Chem.* **2001**, 507, 124; J. F. Fauvarque, Y. De Zelicourt, C. Amatore, A. Jutand, *J. App. Electrochem.* **1990**, 20, 338; J. F. Fauvarque, C. Amatore, A. Jutand, *J. App. Electrochem.* **1988**, 18, 109.

<sup>94</sup> J. Damodar, S. R. K. Mohan, S. R. J. Reddy, *Electrochem. Commun.* **2001**, 3, 762.

<sup>95</sup> W. H. Chung, P. Guo, K. Y. Wong, C. P. Lau, *J. Electroanal. Chem.* **2000**, 486, 32; A. A. Bessel, D. R. Rolison, *J. Am. Chem. Soc.* **1997**, 119, 12673; A. A. Isse, A. Gennaro, E. Vianello, *J. Chem. Soc., Dalton Trans.* **1996**, 1613.



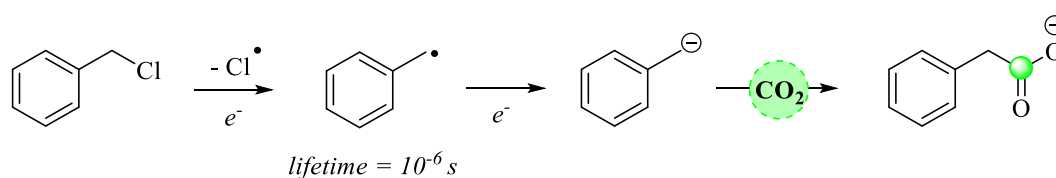


**Figure 66:** General mechanistic pathway for the carboxylation of benzyl chloride.

Noteworthy, the reduction of carbon dioxide to the  $\text{CO}_2$  radical anion was observed in some of these cases but only as an undesirable pathway affecting the efficiency of the electrocarboxylation.

In the previous chapter, the carboxylation of aryl halides via  $\text{CO}_2$  activation mediated by electrogenerated Sm(II)-salts was successfully realized. Aiming to expand the application of this method, the carboxylation of benzyl chlorides was then targeted to produce phenylacetic acids using Sm(II) electrolysis.

#### 4. Carboxylation of benzyl chlorides

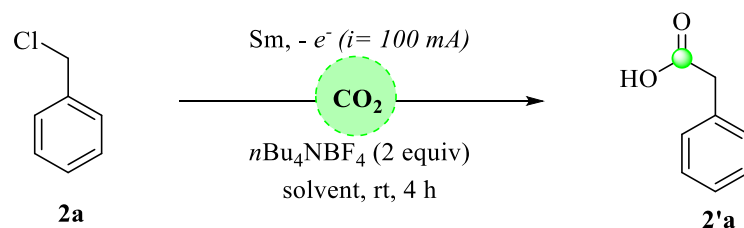
As a preliminary test using electrogenerated Sm(II) complexes, benzyl chloride was added to the electrochemical cell containing ammonium tetrafluoroborate  $n\text{Bu}_4\text{NBF}_4$  as electrolyte in DMF. The current intensity was then fixed at 100 mA, and the electrolysis started along with a constant bubbling of  $\text{CO}_2$  through a fritted glass as previously established for the electrocarboxylation of aryl halides.

After four hours, the phenylacetic acid was isolated with only 11% yield (**Figure 67**, (1)). Replacing DMF by acetonitrile  $\text{CH}_3\text{CN}$  due to the higher  $\text{CO}_2$  solubility in this latter (0.59 M vs. 0.38 M)<sup>96</sup> afforded a higher yield of 29% (**Figure 67**, (2)).

With a green and safe approach in mind, the increase of  $\text{CO}_2$  pressure was not an option, and a practical technique allowing to improve the  $\text{CO}_2$  concentration in the medium was thus required.

Carbon dioxide is available not only as gas but also in the solid-state as dry ice. So, the dry ice was added during the electrolysis as a  $\text{CO}_2$  source. Surprisingly, the phenylacetic acid was isolated, in this case, in quantitative yield after only two hours of electrolysis without any side product (**Figure 67**, (3)). This finding clearly evidenced the intimate interplay between  $[\text{CO}_2]_{\text{soluble}}$  and the efficiency of the electrocarboxylation.

<sup>96</sup> A. Gennaro, A. Isse, E. Vianello, *J. Electroanal. Chem.* **1990**, 289, 203.



- (1) DMF +  $\text{CO}_2(\text{gas})$ , **yield = 11%**  
 (2)  $\text{CH}_3\text{CN} + \text{CO}_2(\text{gas})$ , **yield = 29%**  
 (3)  $\text{CH}_3\text{CN} + \text{dry ice}$ , **yield > 99%** (after 2 h)

**Figure 67:** Carboxylation of benzyl chloride using a stoichiometric amount of electrogenerated divalent Sm in different solvents and different  $\text{CO}_2$  source

To confirm this result, several substrates were engaged under the same conditions (**2a-j**), and moderate to excellent yields were obtained with primary (**2a-h**) and secondary chloride substrates (**2i**), even the *p*-nitrobenzyl chloride **2h** provided the carboxylated product selectively without any reduction of the nitro group as was observed previously starting from nitro-substituted aryl bromide. Triphenylmethyl chloride **2j** furnished the corresponding carboxylic acid **2'j** under these conditions but unfortunately in a low yield, probably due to steric bulk.

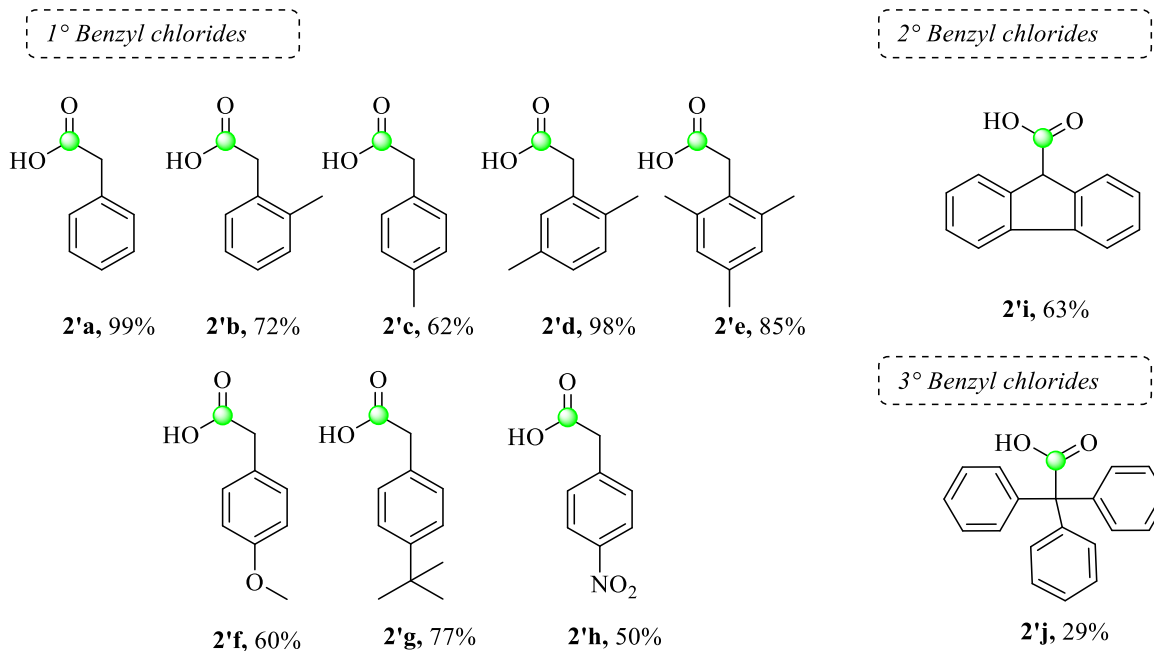
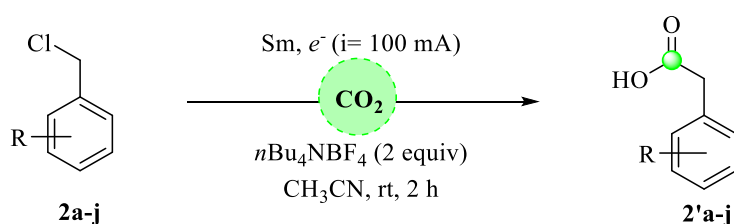


**Figure 68:** Scope of the carboxylation of benzyl chlorides with electrogenerated Sm(II)

Considering these results, we started the investigations seeking the elaboration of catalytic carboxylation conditions using electrogenerated Sm(II) in CH<sub>3</sub>CN.

## 5. Sm(II)-catalyzed carboxylation of benzyl chlorides via CO<sub>2</sub> activation

### a. Optimization & Scope of the catalytic carboxylation

We began our study by generating 20 mol% of Sm<sup>2+</sup> in a solution containing *n*Bu<sub>4</sub>NBF<sub>4</sub> in CH<sub>3</sub>CN. This generation was made using a samarium rod first as an anode with a stainless-steel grid (SS) as the cathode. The required time to generate 20 mol% of Sm(II) was calculated to be 386 seconds under a current intensity equal to 100 mA. After this period, the polarity was reversed and the electrocatalysis was started. Then dry ice was added together with benzyl chloride **2a** and to 3 equivalents of trimethylsilyl chloride (TMSCl). During the electrolysis time (2 hours), the dry ice was introduced each 15 min in small pieces without significantly perturbing the surface of the solvent, to maintain a correct CO<sub>2</sub> concentration during the electrolysis without affecting the temperature of the medium. The treatment of the final mixture provided 60% of phenylacetic acid as isolated yield (**Table 2, entry 1**).

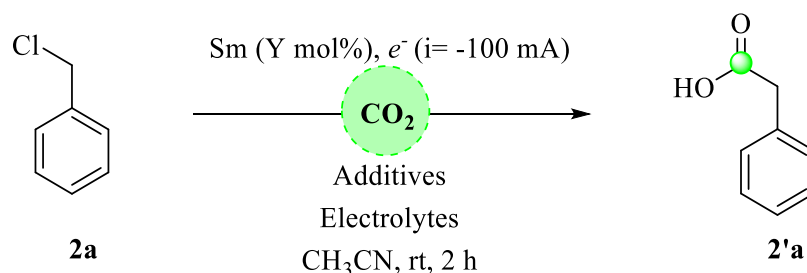


**Table 2:** Screening for the reaction conditions catalytic carboxylation of benzyl chlorides.

Entry	Y mol%	Additives (equiv)	Electrolytes (equiv)	2'a Yield(%) <sup>a</sup>
1	20	TMSCl (3)	<i>n</i> Bu <sub>4</sub> NBF <sub>4</sub> (1)	60
2	20	TMSOTf (3)	<i>n</i> Bu <sub>4</sub> NBF <sub>4</sub> (1)	45
3	20	AcOH, TsOH or MsOH (3)	<i>n</i> Bu <sub>4</sub> NBF <sub>4</sub> (1)	0
4	20	AcOH, TsOH or MsOH (1)	<i>n</i> Bu <sub>4</sub> NBF <sub>4</sub> (1)	0
5	20	TMSCl (3)	<i>n</i> Bu <sub>4</sub> NOTf (1)	59
6	20	TMSCl (3)	<i>n</i> Bu <sub>4</sub> NI (1)	98

7	20	TMSCl (3)	$n\text{Bu}_4\text{NI}$ ( <b>0.25</b> ) + $n\text{Bu}_4\text{NPF}_6$ (0.75)	21
<b>8</b>	<b>20</b>	<b>TMSCl (1.5)</b>	<b><math>n\text{Bu}_4\text{NI}</math> (1)</b>	<b>96</b>
9	10	TMSCl (3)	$n\text{Bu}_4\text{NI}$ (1)	39

<sup>a</sup> Isolated yields

Replacing TMSCl with trimethylsilyl triflate (TMSOTf) decreased the yield to 45% (**entry 2**). The use of organic acids such as acetic acid instead of TMSCl, aiming to produce directly in the medium **2'a**, did not yield any carboxylated product and the starting material was recovered (**entry 3 and 4**). Changing the nature of the electrolyte, knowing that the ligand choice modifies the redox potential Sm(II), to tetrabutylammonium iodide ( $n\text{Bu}_4\text{NI}$ ) yielded **2'a** with 98% yield (**entry 6**). However, using less than one equivalent of  $n\text{Bu}_4\text{NI}$  had a deleterious impact on the reactivity (**entry 7**). In contrast, reducing the amount of TMSCl to half (1.5 equiv) did not significantly affect the yields (**entry 8**). Furthermore, maintaining 20 mol% catalytic loading was critical to obtain a high yield (**entry 9**).

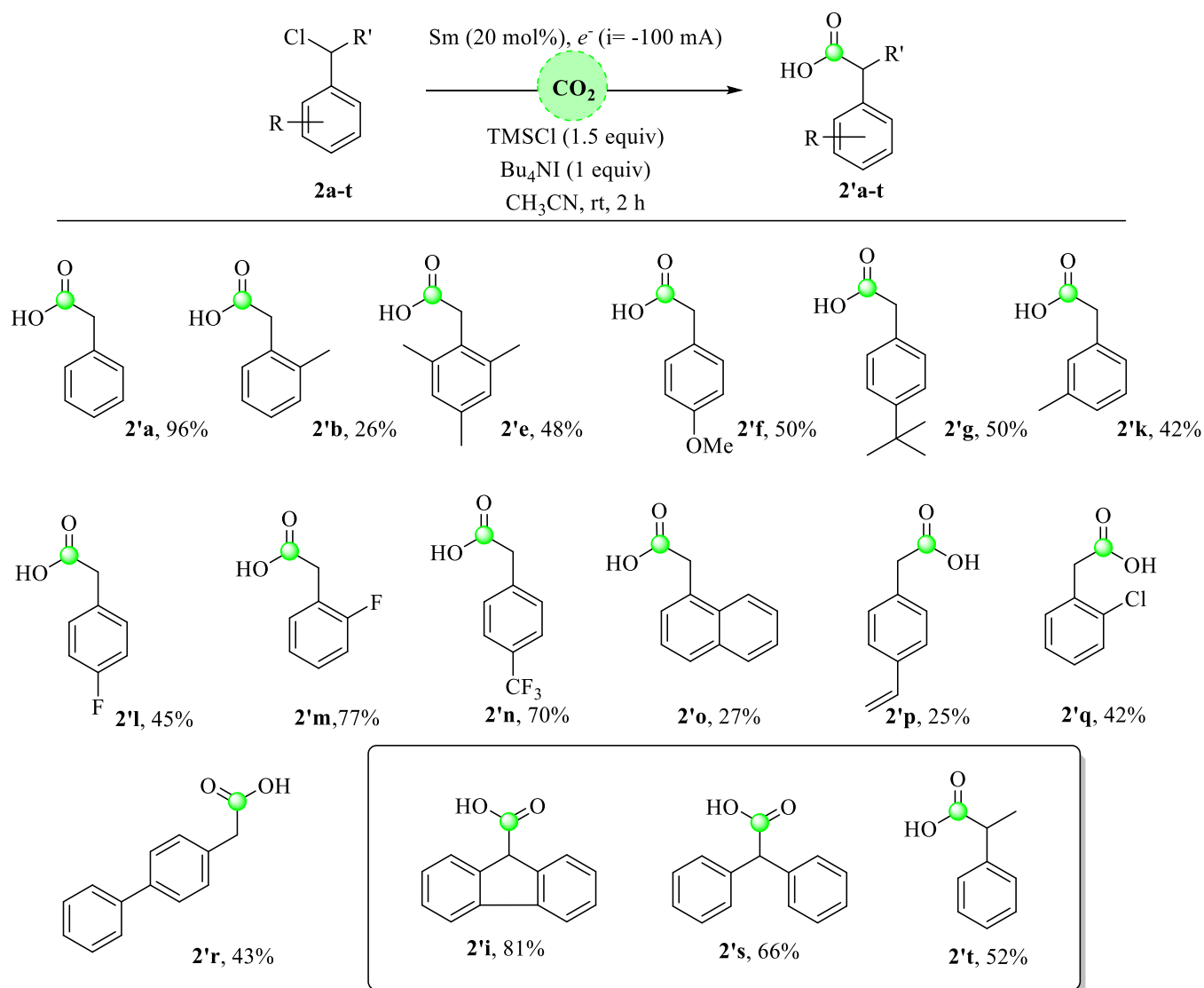


**Figure 69:** Divalent Sm(II)-catalyzed carboxylation of primary and secondary benzyl chlorides.

With these optimized conditions in hands, we next turned our attention to study the scope of the reaction using commercially available benzyl chlorides as substrates (**2a-t**) (**Figure 69**). Diverse primary compounds underwent the carboxylation efficiently with electron-donating (**2b-k**) and electron-withdrawing groups (**2l-n**). Interestingly, p-vinyl benzyl chloride **2p** and 2-chlorobenzyl chloride **2q** reacted selectively to give the corresponding products with 42% (**2'p**) and 25% (**2'q**) respectively, without any dehalogenation or dicarboxylation as side reactions already reported in other approaches. Moreover, under these conditions, the secondary chloride (**2i**, **2s**, and **2t**) furnished the relevant products with good to very good yields (yields up to 81%).

To understand the mechanism of this catalytic reaction, control experiments and mechanistic studies were conducted subsequently.

### b. Mechanistic studies

To reveal whether a benzyl radical or the corresponding anion initiates the nucleophilic attack or indeed the CO<sub>2</sub> radical anion species was formed in the solution before a radical substitution with the benzyl chloride, numerous blank tests were elaborated to get insight into the mechanistic pathway of this transformation (**Figure 70**).

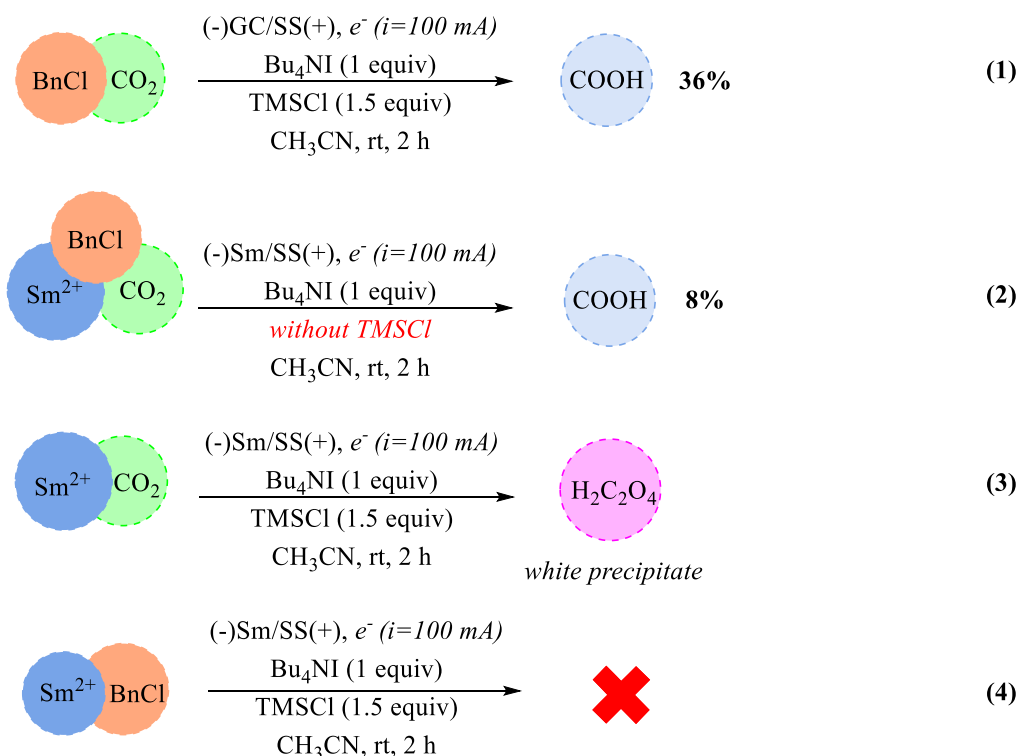


**Figure 70:** Blank tests: (1) without Sm(II); (2) without TMSCl; (3) without benzyl chloride; (4) without CO<sub>2</sub>.

Control experiments showed that substituting the samarium rod with an inert glassy carbon (GC) anode provided, after 2 hours, 36% of the carboxylic acid (**Figure 70**, (1)). This reactivity is associated with the direct electrocarboxylation of the benzyl chloride as reported previously in

2015.<sup>97</sup> In this case, the benzyl radical or anion attacks the CO<sub>2</sub> to yield the carboxylated compound. In fact, this result also proves that the presence of divalent samarium enhances the carboxylation rate almost three times more than the direct electrocarboxylation.

Furthermore, without TMSCl and in the presence of the Sm cathode, **2'a** was isolated with 8% yield (**Figure 70, (2)**). But surprisingly, in the absence of **2a**, white-grey solid precipitation was observed when the electrolysis was conducted with dry ice only (**Figure 70, (3)**). Just as in the previous chapter, the crude <sup>13</sup>C-NMR revealed the formation of oxalic acid, proving undoubtedly that the samarium performed the CO<sub>2</sub> reduction catalytically under these reactions. Indeed, performing the electrolysis without CO<sub>2</sub> which led to the complete recovery of the starting material at the end (**Figure 70, (3)**).

Due to the presence of chloride ions resulting from TMSCl, ion exchange tests between chloride-iodide anion were executed (**Figure 71**).

Other tests allowed the examination of the effect of replacing **2a** by benzyl iodide **2v** as a substrate. After treatment, the purification provided **2'a** with a 52% yield. Second test considered replacing the iodide source (*n*Bu<sub>4</sub>NI) with ammonium hexafluorophosphate (*n*Bu<sub>4</sub>NPF<sub>6</sub>) and using 20 mol% SmCl<sub>3</sub> as a precatalyst. By using this latter, the electrogeneration step is no longer needed, and the electrocatalysis process was directly started. This test furnished the product **2'a** with 75% yield.

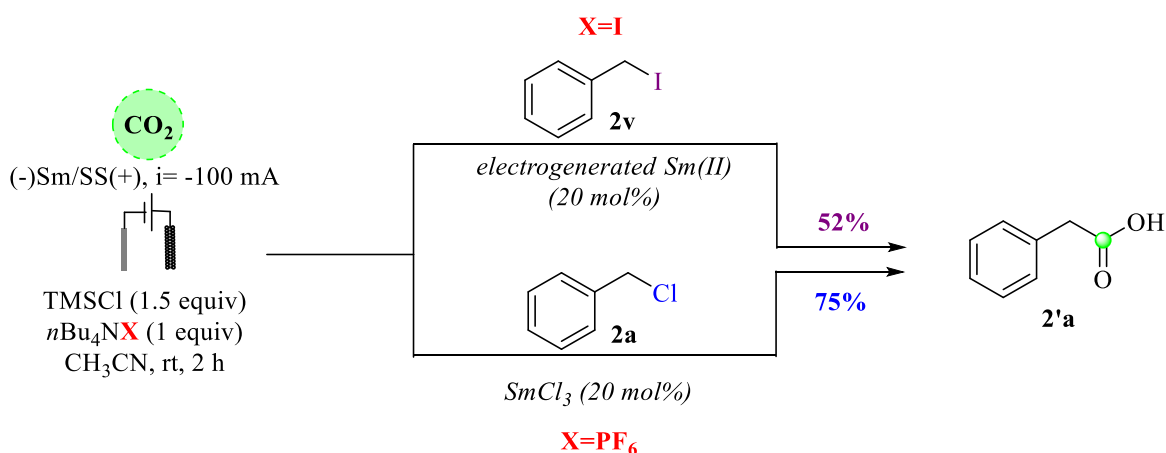


**Figure 71:** Investigating the role of ion exchange.

Comparing these results with the previous ones obtained under optimized conditions, led to the conclusion that the ion exchange did not play a critical role in the carboxylation with the generated *in situ* CO<sub>2</sub> radical anion ability to induce the C-Cl bond dissociation.

As radical species were generated during this process, radical trapping experiments were essential to identify the intermediates involved in this reaction (**Figure 72**). However, similarly to the case encountered with aryl halides, the carboxylic acid **2'a** was not detected in the presence of additional TEMPO. Even though a TEMPO-CO<sub>2</sub> intermediate was not isolated, a radical coupling product between the benzyl radical and the TEMPO was neither obtained. Therefore, we suggest

<sup>97</sup> H. Tateno, Y. Matsumura, K. Nakabayashi, H. Senboku, M. Atobe, *RSC Adv.* **2015**, *5*, 98721.

that the TEMPO trapped the  $\text{CO}_2$  radical anion, and then the unstable intermediate underwent a degradation process, which explains its absence in the reaction mixture.

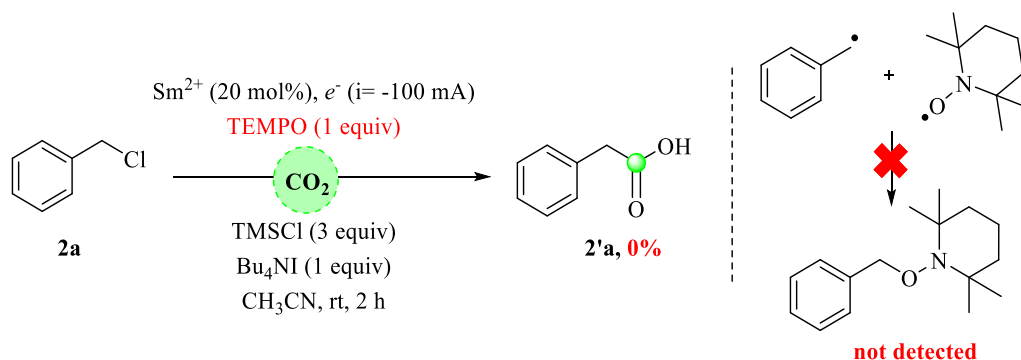


**Figure 72:** Radical trapping attempt using TEMPO as a radical scavenger.

As a compound exhibiting high sensitivity towards radical species,  $\beta$ -pinene was added to the reaction mixture (**Figure 73**).

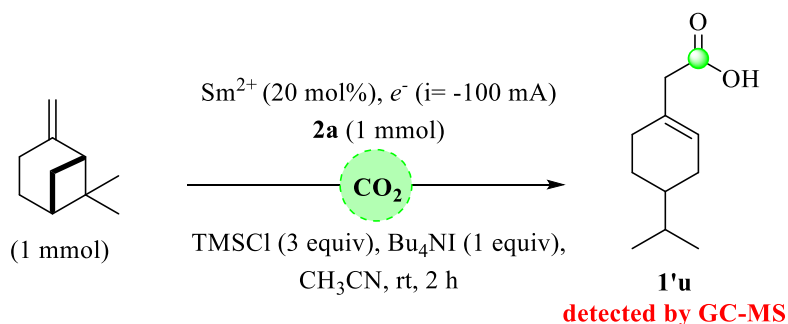


**Figure 73:** Radical trapping experiment using  $\beta$ -pinene as a radical scavenger.

Indeed, the  $\text{CO}_2$  insertion product **1'u** was detected by GC-MS, whereas **2a** was completely recovered. This result offered certain evidence for the formation of the  $\text{CO}_2$  radical anion under the optimized conditions.

To evaluate an electrocatalytic process, the cyclic voltammetry (CV) offers many options such as the evaluation of the redox behavior of the catalyst and the existence of a catalytic current under the optimized conditions. Based on these arguments, cyclic voltammetry studies were conducted to provide further proof for the mechanistic pathway.

*c. Electrochemical studies of the catalytic carboxylation of benzyl chloride*

**Figure 74** presents the cyclic voltammogram of the catalyst obtained in the absence and in the presence of CO<sub>2</sub> in addition to the effect of TMSCl on generating a catalytic current under optimized conditions.

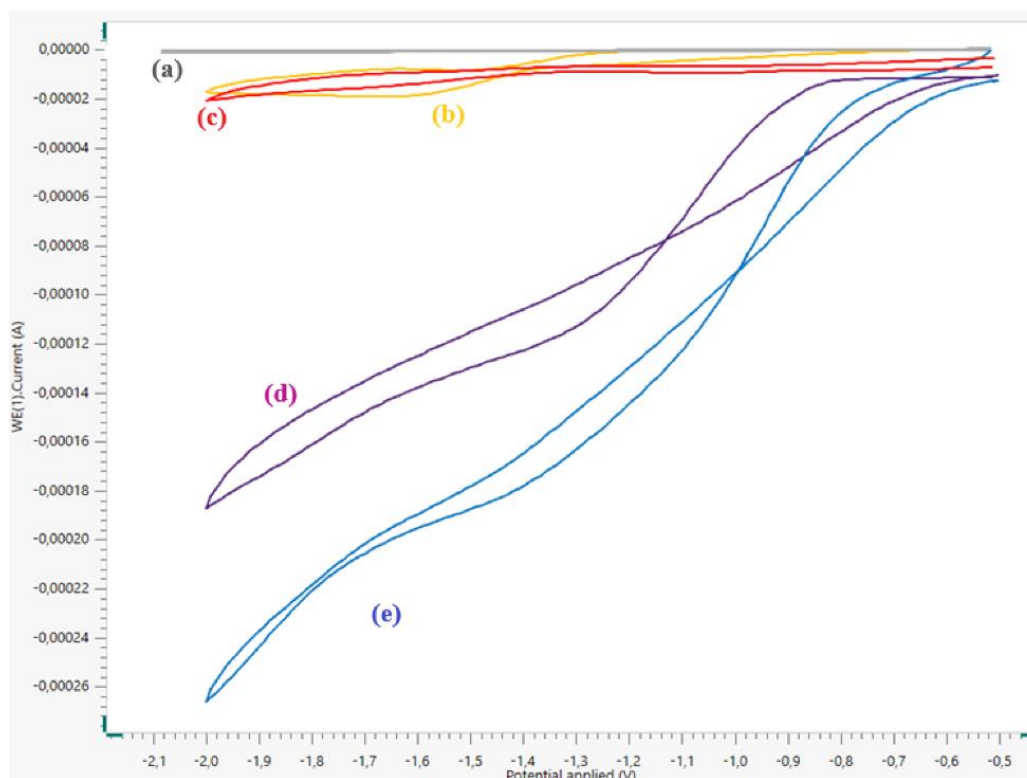


**Figure 74** Cyclic voltammetry analysis of the carboxylation of benzyl chloride: Glassy carbon electrode surface 20 mm<sup>2</sup>, and platinum wire as counter electrode scanning potential between -0.5 and -2 V vs. SCE in CH<sub>3</sub>CN with *n*Bu<sub>4</sub>NPF<sub>6</sub> [0.1 M]. Scan rate: 100 mV/s. (a): 0.1 M *n*Bu<sub>4</sub>NPF<sub>6</sub>; (b): (a) + 0.2 M SmCl<sub>2</sub>; (c): (b) + CO<sub>2</sub>; (d): (c) + 0.5 mL solution of BnCl:TMSCl 1:1.5 in CH<sub>3</sub>CN; (e): (d) + 0.5 mL solution of BnCl:TMSCl 1:1.5.

Without CO<sub>2</sub>, the quasi-reversible system of Sm(III)/Sm(II) was registered effectively at -1.4 V/SCE (b). Once the CO<sub>2</sub> is added, the oxidation wave disappeared, and a weak reduction wave emerged with a cathodic shift towards -1.8 V/SCE (c). The addition of a mixture containing substrate **1a** and TMSCl (1:1.5) triggered a significant reduction wave that started at -0.95 V/SCE while further addition of this mixture magnified this wave (d). Overall, these findings confirm the existence of a catalytic current involving the Sm(III)/Sm(II) redox couple, assisted by TMSCl.

After analyzing all these results, we assume the proposed mechanism below (**Figure 75**):

First, the Sm<sup>2+</sup> reduces the carbon dioxide to the corresponding CO<sub>2</sub><sup>•-</sup> radical anion and forms the complex **A**. This latter then undergoes a radical substitution with **2a** to deliver the samarium carboxylate adduct **B**. After transmetallation with TMSCl, the compound **C** is formed and the oxidized samarium Sm(III) allows the regeneration of the active catalyst Sm(II) via cathodic reduction on the Sm rod. Finally, the carboxylic acid **2'a** is isolated after hydrolytic treatment.



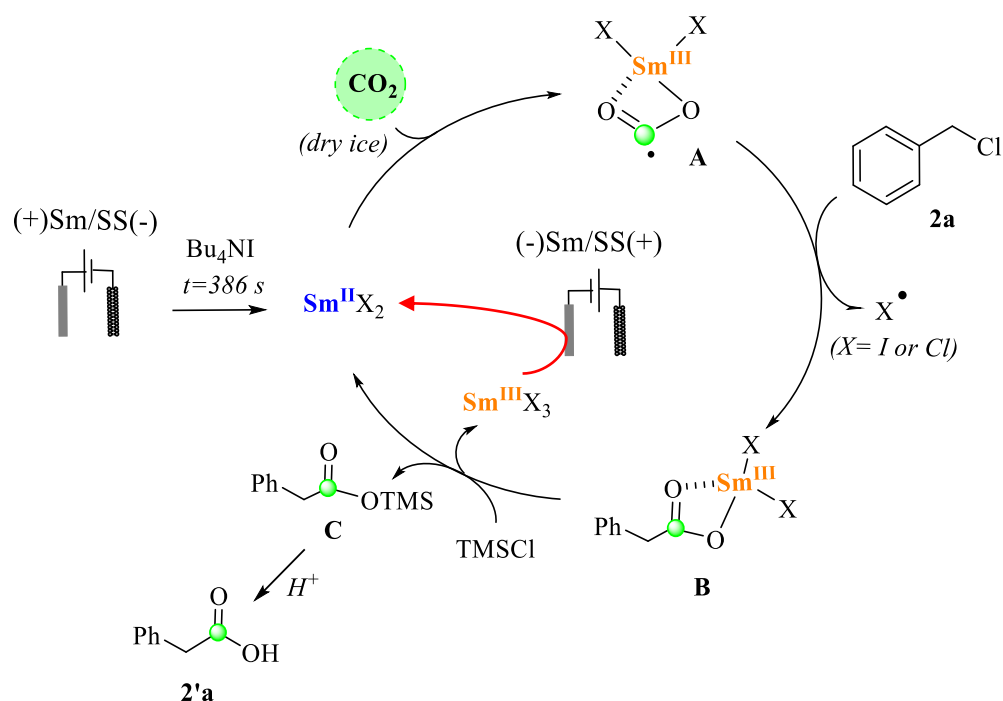


**Figure 75** Proposed mechanism for the carboxylation of benzyl chlorides catalyzed by  $\text{SmI}_2$

## 6. Conclusion and perspectives

In this chapter, we introduced a new catalytic carboxylation of benzyl chlorides based on electrogenerated divalent samarium complexes. This procedure tolerated different functional groups, and even secondary benzyl chlorides reacted well under the optimized conditions. Also, we propose that this process goes through  $\text{CO}_2$  activation to generate radical anion  $[\text{CO}_2]^\cdot-$  that triggers a radical substitution to furnish valuable carboxylic acids.

This method demonstrated a significant advance considering that it is the first carboxylation of benzyl chlorides without additional metal as co-reductant.

This process reveals high efficiency, compared to direct electrocarboxylation on a GC electrode, and it thus offers a great alternative to other methods requiring high overpotential and producing multiple side products.

Moreover, a remarkable selectivity towards the carboxylation at the benzylic position was observed in the absence of any side product from dehalogenation,  $\beta$ -hydrogen elimination or even dimerization as reported in previous cases. Furthermore, the ligand exchange was not behind the observed reactivity, and we assume that the  $\text{SmI}_2$  is the real catalyst for the carboxylation in the medium.

Considering these facts, we wondered about the reason behind the failure to elaborate a catalytic procedure with aryl chlorides. The main difference between both protocols being the solvent, we suggest a catalyst-solvent interplay that dominates the catalytic reactivity. Besides, the electronic character of the benzoic acid, where the oxygen is electron-rich by  $\pi$ -donation making thus the

Sm-O bond stronger, causes a more difficult dissociation requires much more energy than in the case of phenylacetic acid, attached to an  $sp^3$  carbon center. These hypotheses should be extensively studied by DFT calculations to compute the energy barrier for the synthesis of each product and the possible role of the solvent to propose an explanation.

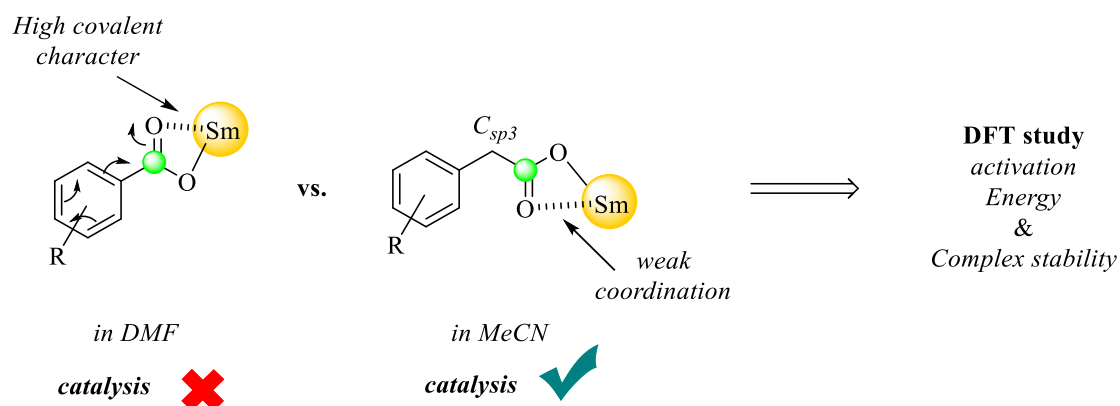


**Figure 76** Comparison between the aromatic carboxylic acid and phenyl carboxylic acid

Furthermore, as a stereogenic center is produced at the end of the carboxylation of racemic secondary benzyl halides, it is worth-studying the reaction simply by starting from a chiral substrate to observe if the chirality is retained after the CO<sub>2</sub> fixation. Subsequently, investigating the carboxylation using a chiral ligand is highly interesting for the direct synthesis of valuable enantio-enriched phenylacetic acid derivatives. Indeed, after the CO<sub>2</sub> activation, the Sm(III) may remain coordinated to the radical surrounded by a chiral environment, to induce the formation of a non-racemic carbon center.

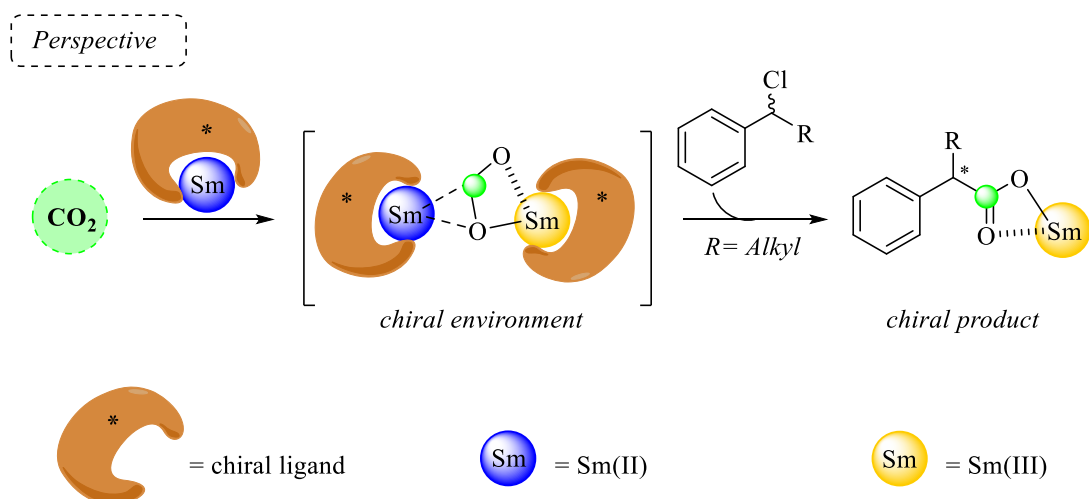


**Figure 77** Enantioselective carboxylation of benzyl chlorides by chiral Sm(II) complex

Having these catalytic conditions in hand, we can now extend the reactivity of this method by testing different substrates suitable for carboxylation reactions, such as unsaturated hydrocarbons.



---

# Experimental Part

---

## Instrumentation and Chemicals

---

All commercially available reagents were used without further purification unless otherwise stated. All solvents were also used without further purification. Dimethylformamide (DMF) and Acetonitrile ( $\text{CH}_3\text{CN}$ ) were purchased from Carlo Erba and VWR chemicals, respectively. Tetrabutylammonium tetrafluoroborate ( $n\text{Bu}_4\text{NBF}_4$ ) and tetrabutylammonium iodide ( $n\text{Bu}_4\text{NI}$ ) were bought from Fluka. The samarium rod was a 12.7mm diameter, 99.9% (metals basis excluding Ta) rod, purchased from Alfa-Aesar and the stainless-steel grid from Goodfellow (AISI 304). Electrolysis was performed using an EGG Instrument Potentiostat/Galvanostat Model 273 in an undivided cell equipped with a samarium rod as anode and a stainless-steel grid as a cathode. NMR spectra were recorded on Bruker AM 360 (360 MHz), 300 (300 MHz) or AM 250 (250 MHz) in  $\text{CDCl}_3$ . Data for  $^1\text{H}$  NMR are recorded as follows: chemical shift ( $\delta$ , ppm), multiplicity (s = singlet, d = doublet, t = triplet, m = multiplet, q = quartet, dd = doublet of doublets, dt = doublet of triplets, td = triplet of doublets, and br = broad signal), coupling constant ( $J$ , Hz) and integration. Reactions were monitored by thin-layer chromatography (TLC) using bromocresol as TLC stain, and column chromatography purifications were carried out using silica gel.

## General Procedure for the stoichiometric carboxylation of benzyl chloride derivatives

---

An undivided cell charged with tetrabutylammonium iodide  $n\text{Bu}_4\text{NI}$  (2 mmol) in acetonitrile (40 mL) was used with a chronopotentiometry mode, the electrolysis of  $\text{Sm}^{2+}$  was performed for 7200 seconds with  $i = 100$  mA, and the dry ice was carefully added to the mixture in small pieces then the substrate (1 mmol). Then, the reaction was left along with adding a small piece of dry ice each 15 min. When the electrolysis stopped, the solvent was evaporated, and a solution of HCl (2 M) was added to obtain the carboxylic acid which was extracted using  $\text{Et}_2\text{O}$  (50 mL). After phase separation, the organic phase was washed with water and brine and dried over anhydrous  $\text{MgSO}_4$ . The crude obtained after the solvent evaporation under *vacuo* was purified by column chromatography on silica gel (90/10 then 50/50 PE/ EtOAc).

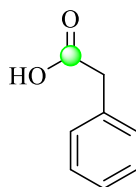
## General Procedure for the catalytic carboxylation of benzyl chloride derivatives

---

In an undivided cell charged with tetrabutylammonium iodide  $n\text{Bu}_4\text{NI}$  (1 mmol) in acetonitrile (40 mL), the electro-generation of  $\text{Sm}^{2+}$  was started by setting the chronopotentiometry mode for 386 seconds with  $i = 100$  mA, which is the required time to produce 20 mol% of  $\text{SmI}_2$  in solution. After this first step, the second one consisted of switching the polarity of the electrodes, so the Sm rod now is playing the role of the cathode where the regeneration of the catalyst is going to take place. At this point, the dry ice was carefully added to the mixture in small pieces followed by the substrate (1 mmol) and the trimethylsilyl chloride  $\text{TMSCl}$  (1.5 mmol). Now, the time was changed to 7200 seconds, and the reaction was left along with adding a small piece of dry ice each 15 min. When the electrolysis stopped, the solvent was evaporated, and a solution of  $\text{HCl}$  (2 M) was added to obtain the carboxylic acid which was extracted using  $\text{Et}_2\text{O}$  (50 mL). After phase separation, the organic phase was washed with water and brine and dried over anhydrous  $\text{MgSO}_4$ . The crude obtained after the solvent evaporation under *vacuo* was purified by column chromatography on silica gel (90/10 then 50/50 PE/ EtOAc).

## Characterization of the compounds

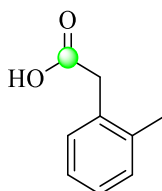
---



**Phenylacetic acid (2'a):** 130 mg (0.96 mmol, 96%).  $^1\text{H NMR}$  (250 MHz,  $\text{CDCl}_3$ )  $\delta$  10.98 (s, 1H), 7.36 (m,  $J = 4.8$  Hz, 5H), 3.70 (s, 2H).

$^{13}\text{C NMR}$  (63 MHz,  $\text{CDCl}_3$ )  $\delta$  178.2, 133.2, 129.4, 128.6, 127.3, 41.1.

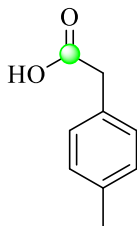
The  $^1\text{H NMR}$  and  $^{13}\text{C NMR}$  spectra are in agreement with those reported in the literature.<sup>11</sup>



**2-(o-tolyl)acetic acid (2'b):** 39 mg (0.26 mmol, 26%).  $^1\text{H NMR}$  (360 MHz,  $\text{CDCl}_3$ )  $\delta$  7.24 (s, 4H), 3.72 (s, 2H), 2.37 (s, 3H).

$^{13}\text{C NMR}$  (91 MHz,  $\text{CDCl}_3$ )  $\delta$  177.9, 137, 132.1, 130.4, 130.2, 127.9, 126.2, 38.9, 19.3.

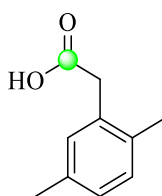
The  $^1\text{H}$  NMR and  $^{13}\text{C}$  NMR spectra are in agreement with those reported in the literature.<sup>82</sup>



**2-(p-tolyl)acetic acid (2'c):** 93 mg (0.62 mmol, 62%).  $^1\text{H}$  NMR (360 MHz,  $\text{CDCl}_3$ )  $\delta$  10.72 (s, 1H), 7.22 (m, 4H), 3.66 (s, 2H), 2.40 (s, 3H).

$^{13}\text{C}$  NMR (63 MHz,  $\text{CDCl}_3$ )  $\delta$  178.2, 137.1, 130.3, 129.4, 129.3, 40.7, 21.2.

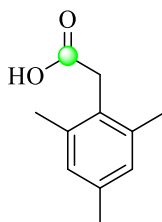
The  $^1\text{H}$  NMR and  $^{13}\text{C}$  NMR spectra are in agreement with those reported in the literature.<sup>81</sup>



**2-(3,5-dimethylphenyl)acetic acid (2'd):** 160 mg (0.98 mmol, 98%).  $^1\text{H}$  NMR (250 MHz,  $\text{CDCl}_3$ )  $\delta$  7.22 – 6.93 (m, 3H), 3.66 (s, 2H), 2.34 (s, 3H), 2.31 (s, 3H).

$^{13}\text{C}$  NMR (63 MHz,  $\text{CDCl}_3$ )  $\delta$  177.7, 135.8, 133.7, 131.7, 131.1, 130.1, 128.5, 38.7, 20.9, 18.8.

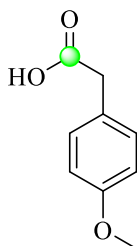
The  $^1\text{H}$  NMR and  $^{13}\text{C}$  NMR spectra are in agreement with those reported in the literature.<sup>98</sup>



**2-(2,4,6-trimethylphenyl)acetic acid (2'e):** 85 mg (0.48 mmol, 48%).  $^1\text{H}$  NMR (250 MHz,  $\text{CDCl}_3$ ) = 6.87 (s, 2H), 3.68 (s, 2H), 2.29 (s, 6H), 2.26 (s, 3H).

$^{13}\text{C}$  NMR (63 MHz,  $\text{CDCl}_3$ )  $\delta$  177.6, 137.1, 136.8, 129.0, 127.9, 34.6, 20.9, 20.1.

The  $^1\text{H}$  NMR and  $^{13}\text{C}$  NMR spectra are in agreement with those reported in the literature.<sup>98</sup>

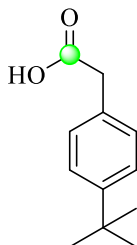


<sup>98</sup> M. She, D. Xiao, B. Yin, Z. Yang, P. Liu, Ji. Li, Z. Shi, *Tetrahedron* **2013**, 69, 7264.

**2-(4-methoxyphenyl)acetic acid (2'f):** 83 mg (0.5 mmol, 50%).  $^1\text{H NMR}$  (250 MHz,  $\text{CDCl}_3$ )  $\delta$  11.97 (s, 1H), 7.30 (d,  $J = 8.3$  Hz, 2H), 6.97 (d,  $J = 8.4$  Hz, 2H), 3.87 (s, 3H), 3.76 (s, 2H).

$^{13}\text{C NMR}$  (63 MHz,  $\text{CDCl}_3$ )  $\delta$  178.5, 158.9, 130.5, 125.4, 114.1, 55.2, 40.2.

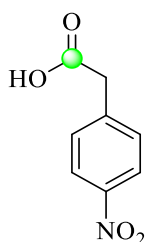
The  $^1\text{H NMR}$  and  $^{13}\text{C NMR}$  spectra are in agreement with those reported in the literature.<sup>11</sup>



**2-(4-(tert-butyl)phenyl)acetic acid (2'g):** 96 mg (0.5 mmol, 50%).  $^1\text{H NMR}$  (250 MHz,  $\text{CDCl}_3$ )  $\delta$  7.40 (d,  $J = 8.3$  Hz, 2H), 7.26 (d,  $J = 8.2$  Hz, 2H), 3.66 (s, 2H), 1.36 (s, 9H).

$^{13}\text{C NMR}$  (63 MHz,  $\text{CDCl}_3$ )  $\delta$  178.1, 150.2, 130.4, 128.7, 125.4, 40.5, 34.6, 31.3.

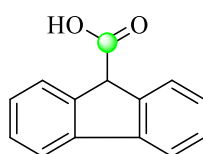
The  $^1\text{H NMR}$  and  $^{13}\text{C NMR}$  spectra are in agreement with those reported in the literature.<sup>11</sup>



**2-(4-nitrophenyl)acetic acid (2'h):** 90.5 mg (0.5 mmol, 50%).  $^1\text{H NMR}$  (300 MHz,  $\text{CDCl}_3$ )  $\delta$  8.16 (d,  $J = 8.5$  Hz, 2H), 7.3 (d,  $J = 8.5$  Hz, 2H), 3.13 (s, 2H).

$^{13}\text{C NMR}$  (75 MHz,  $\text{CDCl}_3$ )  $\delta$  171.7, 148.3, 143.6, 131.8, 124.3, 41.2.

The  $^1\text{H NMR}$  and  $^{13}\text{C NMR}$  spectra are in agreement with those reported in the literature.<sup>99</sup>

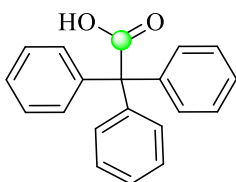


**9H-fluorene-9-carboxylic acid (2'i):** 170 mg (0.81 mmol, 81%).  $^1\text{H NMR}$  (360 MHz,  $\text{CDCl}_3$ )  $\delta$  7.77 (dt,  $J = 7.6$ , 1 Hz, 2H), 7.69 (dt,  $J = 7.5$ , 1.0 Hz, 2H), 7.44 (dt,  $J = 7.5$ , 1.1 Hz, 2H), 7.35 (t,  $J = 7.4$  Hz, 2H), 4.90 (s, 1H).

$^{13}\text{C NMR}$  (91 MHz,  $\text{CDCl}_3$ )  $\delta$  171.8, 141.4, 140.6, 127.5, 127.3, 125.2, 120.3, 53.2.

The  $^1\text{H NMR}$  and  $^{13}\text{C NMR}$  spectra are in agreement with those reported in the literature.<sup>11</sup>

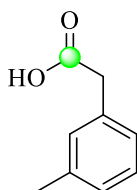
<sup>99</sup> S. M. Cho, H. K. Lee, Q. Liu, M.-W. Wang, H. J. Kwon, *ACS Chem. Biol.* **2019**, *14*, 11.



**2,2,2-triphenylacetic acid (2'j):** 83 mg (0.29 mmol, 29%).  $^1\text{H NMR}$  (360 MHz,  $\text{CDCl}_3$ )  $\delta$  7.35-7.22 (m, 9 H), 7.17-7.15 (m, 6H).

$^{13}\text{C NMR}$  (91 MHz,  $\text{CDCl}_3$ )  $\delta$  174.6, 143.5, 130.4, 128.3, 127.1, 67.2.

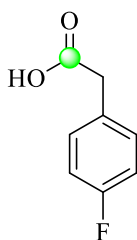
The  $^1\text{H NMR}$  and  $^{13}\text{C NMR}$  spectra are in agreement with those reported in the literature.<sup>11</sup>



**2-(m-tolyl)acetic acid (2'k):** 63 mg (0.42 mmol, 42%).  $^1\text{H NMR}$  (360 MHz,  $\text{CDCl}_3$ )  $\delta$  7.51 – 6.94 (m, 4H), 3.69 (s, 2H), 2.43 (s, 3H).

$^{13}\text{C NMR}$  (91 MHz,  $\text{CDCl}_3$ )  $\delta$  178.5, 138.4, 133.2, 130.2, 128.6, 128.2, 126.4, 41.0, 21.4.

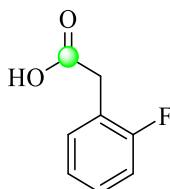
The  $^1\text{H NMR}$  and  $^{13}\text{C NMR}$  spectra are in agreement with those reported in the literature.<sup>98</sup>



**2-(4-fluorophenyl)acetic acid (2'l):** 69 mg (0.45 mmol, 45%).  $^1\text{H NMR}$  (300 MHz,  $\text{CDCl}_3$ )  $\delta$  10.45 (s, 1H), 7.42 – 7.16 (m, 2H), 7.16 – 6.89 (m, 2H), 3.65 (s, 2H).

$^{13}\text{C NMR}$  (91 MHz,  $\text{CDCl}_3$ )  $\delta$  178.1, 162.5 (d,  $J = 246$  Hz), 130.9 (d,  $J = 8.0$  Hz), 128.9 (d,  $J = 3.6$  Hz), 115.6 (d,  $J = 21.6$  Hz), 40.1.

The  $^1\text{H NMR}$  and  $^{13}\text{C NMR}$  spectra are in agreement with those reported in the literature.<sup>11</sup>

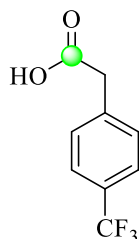


**2-(2-fluorophenyl)acetic acid (2'm):** 118 mg (0.77 mmol, 77%).  $^1\text{H NMR}$  (250 MHz,  $\text{CDCl}_3$ )  $\delta$  11.97 (s, 1H), 7.3-7.25 (m, 2H), 7.17-7.03 (m, 2H), 3.72 (s, 2H).



$^{13}\text{C}$  NMR (63 MHz,  $\text{CDCl}_3$ )  $\delta$  177.4, 160.9 (d,  $J = 254.7$  Hz), 131.4 (d,  $J = 3.9$  Hz), 129.3 (d,  $J = 8.1$  Hz), 124.1 (d,  $J = 3.8$  Hz), 120.5 (d,  $J = 15.9$  Hz), 115.4 (d,  $J = 21.7$  Hz), 34.2 (d,  $J = 3.3$  Hz).

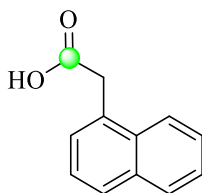
The  $^1\text{H}$  NMR and  $^{13}\text{C}$  NMR spectra are in agreement with those reported in the literature.<sup>98</sup>



**2-(4-(trifluoromethyl)phenyl)acetic acid (2'n):** 143 mg (0.7 mmol, 70%).  $^1\text{H}$  NMR (360 MHz,  $\text{CDCl}_3$ )  $\delta$  11.10 (s, 1H), 7.64 (d,  $J = 8.1$  Hz, 2H), 7.45 (d,  $J = 8.1$  Hz, 2H), 3.76 (s, 2H).

$^{13}\text{C}$  NMR (63 MHz,  $\text{CDCl}_3$ )  $\delta$  176.4, 135.7, 129.6, 129.5 (q,  $J = 32.6$  Hz), 125.3 (q,  $J = 3.8$  Hz), 123.7 (q,  $J = 271.9$  Hz), 40.4.

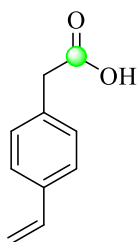
The  $^1\text{H}$  NMR and  $^{13}\text{C}$  NMR spectra are in agreement with those reported in the literature.<sup>11</sup>



**2-(naphthalen-1-yl)acetic acid (2'o):** 50 mg (0.27 mmol, 27%).  $^1\text{H}$  NMR (250 MHz,  $\text{CDCl}_3$ )  $\delta$  8.07 – 7.73 (m, 4H), 7.62 -7.41 (m, 4H), 4.12 (s, 1H).

$^{13}\text{C}$  NMR (63 MHz,  $\text{CDCl}_3$ )  $\delta$  177.6, 133.8, 132.0, 129.7, 128.8, 128.3, 128.2, 126.5, 125.8, 125.4, 123.6, 38.7.

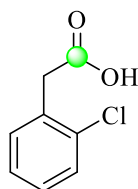
The  $^1\text{H}$  NMR and  $^{13}\text{C}$  NMR spectra are in agreement with those reported in the literature.<sup>98</sup>



**2-(4-vinylphenyl)acetic acid (2'p):** 40.5 mg (0.25 mmol, 25%).  $^1\text{H}$  NMR (360 MHz,  $\text{CDCl}_3$ )  $\delta$  7.4 (d,  $J = 8.2$  Hz, 2H), 7.23 (d,  $J = 8.2$  Hz, 2H), 6.7 (dd,  $J = 17.6, 10.9$  Hz, 1H), 5.75 (dd,  $J = 17.6, 0.9$  Hz, 1H), 5.26 (dd,  $J = 10.8, 0.9$  Hz, 1H), 3.67 (s, 2H).

$^{13}\text{C}$  NMR (91 MHz,  $\text{CDCl}_3$ )  $\delta$  176.9, 136.8, 136.3, 132.7, 129.5, 126.5, 114.0, 40.6.

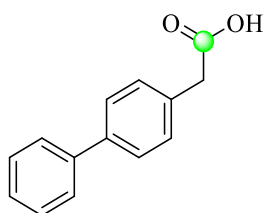
The  $^1\text{H}$  NMR and  $^{13}\text{C}$  NMR spectra are in agreement with those reported in the literature.<sup>81</sup>



**2-(2-chlorophenyl)acetic acid (2'q):** 71.4 mg (0.42 mmol, 42%).  $^1\text{H NMR}$  (250 MHz,  $\text{CDCl}_3$ )  $\delta$  7.44-7.37 (m, 2H), 7.34-7.21 (m, 2H), 3.82 (s, 2H).

$^{13}\text{C NMR}$  (63 MHz,  $\text{CDCl}_3$ )  $\delta$  177.2, 134.6, 131.8, 131.7, 129.6, 129, 127, 38.9.

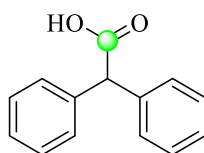
The  $^1\text{H NMR}$  and  $^{13}\text{C NMR}$  spectra are in agreement with those reported in the literature.<sup>11</sup>



**2-([1,1'-biphenyl]-4-yl)acetic acid (2'r):** 91 mg (0.43 mmol, 43%).  $^1\text{H NMR}$  (250 MHz,  $\text{CDCl}_3$ )  $\delta$  7.6 (dd,  $J = 12.6, 7.9$  Hz, 4H), 7.44-7.29 (m, 5H), 3.64 (s, 2H).

$^{13}\text{C NMR}$  (63 MHz,  $\text{CDCl}_3$ )  $\delta$  177.1, 140.7, 140.5, 132.2, 129.8, 128.7, 128.0, 127.4, 127.1, 40.8.

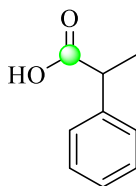
The  $^1\text{H NMR}$  and  $^{13}\text{C NMR}$  spectra are in agreement with those reported in the literature.<sup>82</sup>



**2,2-diphenylacetic acid (2's):** 127 mg (0.6 mmol, 60%).  $^1\text{H NMR}$  (300 MHz,  $\text{CDCl}_3$ )  $\delta$  7.44 – 7.26 (m, 10H), 5.06 (s, 2H).

$^{13}\text{C NMR}$  (91 MHz,  $\text{CDCl}_3$ )  $\delta$  178.5, 137.8, 128.3, 128.2, 127.1, 56.8.

The  $^1\text{H NMR}$  and  $^{13}\text{C NMR}$  spectra are in agreement with those reported in the literature.<sup>11</sup>

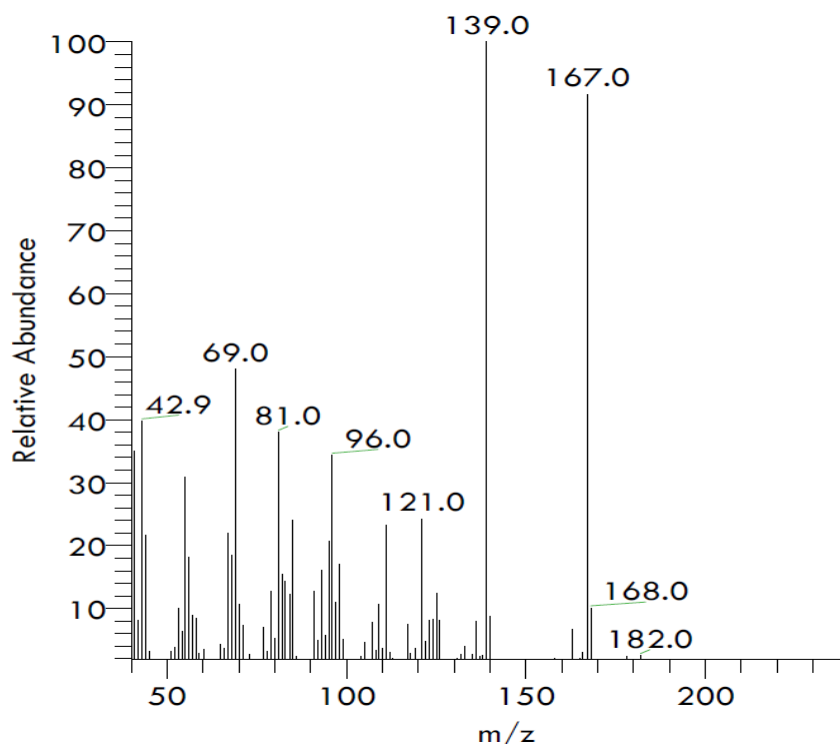
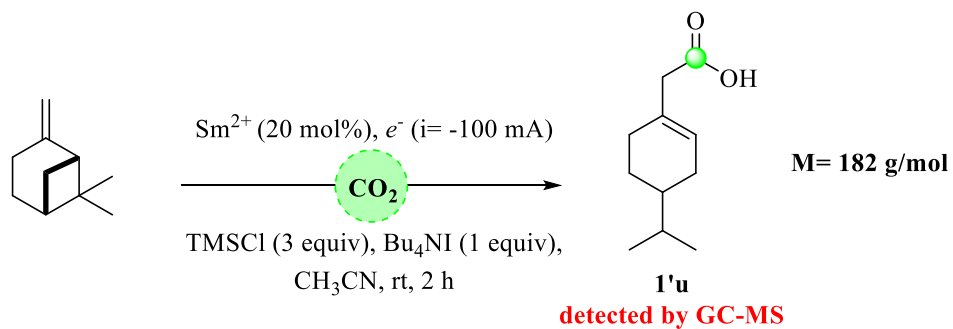


**2-phenylpropanoic acid (2't):** 78 mg (0.52 mmol, 52%).  $^1\text{H NMR}$  (360 MHz,  $\text{CDCl}_3$ )  $\delta$  9.91 (s, 1H), 7.44 – 7.28 (m, 5H), 3.80 (q,  $J = 7.2$  Hz, 1H), 1.57 (d,  $J = 7.2$  Hz, 3H).

$^{13}\text{C NMR}$  (91 MHz,  $\text{CDCl}_3$ )  $\delta$  181.1, 139.8, 128.7, 127.6, 127.4, 45.5, 18.1.

The  $^1\text{H NMR}$  and  $^{13}\text{C NMR}$  spectra are in agreement with those reported in the literature.<sup>11</sup>

## Radical trapping experiment with beta-pinene









Electrogenerated Sm(II)-catalyzed  
the hydrocarboxylation of styrene  
and phenylacetylene derivatives

---



# Electrogenerated Sm(II)-catalyzed the hydrocarboxylation of styrene and phenylacetylene derivatives

## 1. Hydrocarboxylation of styrene and phenylacetylene derivatives: state of the art

The carboxylation of aryl and benzyl halides does not involve a regioselectivity issue due to the existence of an activated bond in these substrates, which is the carbon-halogen one. Despite the significant development in this field, still, the use of unfunctionalized starting material remains tempting. More specifically, unsaturated hydrocarbons present a perfect example for this type of compound, characterized by at least, one  $\pi$ -bond between two carbon centers. The electrons involved in this bond occupy a molecular orbital with a higher energy value than the one implicated in a simple C-C, responsible for the reactivity of these molecules. Besides reaction with ethylene, the reaction with a metal catalyst arises a regioselectivity question using these compounds due to the presence of two active sites. Nevertheless, the addition of a phenyl substituent favors the formation of  $\eta^3$ -benzylic metal intermediate to yield mainly the Markovnikov product (**Figure 78, top**).

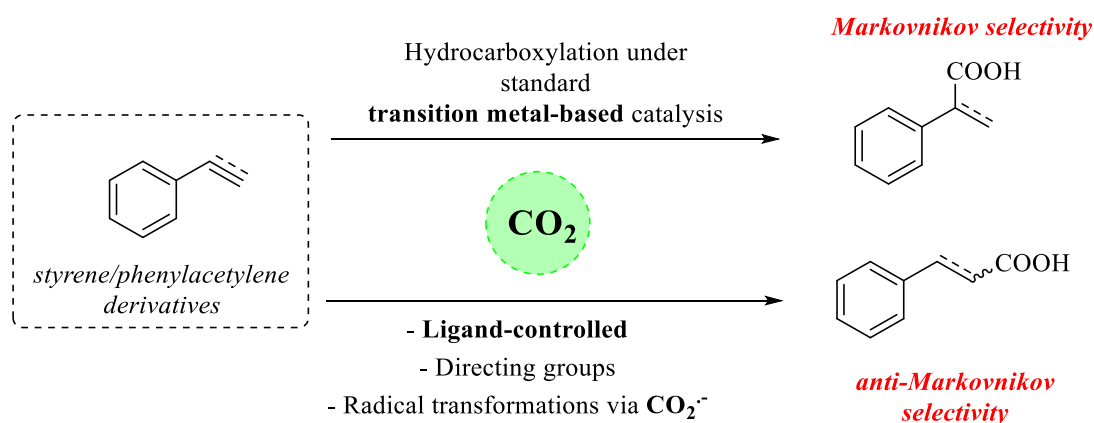


**Figure 78:** The hydrocarboxylation outcome depending on the reactional conditions.

In contrast, the formation of the anti-Markovnikov compound presents a challenging goal for standard transition metal catalysis. Therefore, various strategies mediated by these metals were developed to adjust the selectivity of the reaction towards the  $\beta$ -position (**Figure 78, bottom**). For example, the use of a bulky ligand or the addition of a directing group on the substrate provided



successful pathways to modulate the regioselectivity of the catalyst and achieve the  $\beta$ -CO<sub>2</sub> insertion.

Hydrocarboxylation of styrenes and phenylacetylenes with CO<sub>2</sub> is considered as an atom-economic and straightforward approach to deliver carboxylic acids. As mentioned in the previous chapter, most of the reported methods using styrenes as starting materials led to the formation of branched carboxylic acids via CO<sub>2</sub> insertion on the  $\alpha$ -position.<sup>13,76,77</sup> On the other hand, only a few reports exist in the literature describing the synthesis of linear carboxylic acids, resulting from the direct  $\beta$ -selective hydrocarboxylation and most of them are based on single-electron pathways (Figure 79).<sup>100, 101 77b</sup>

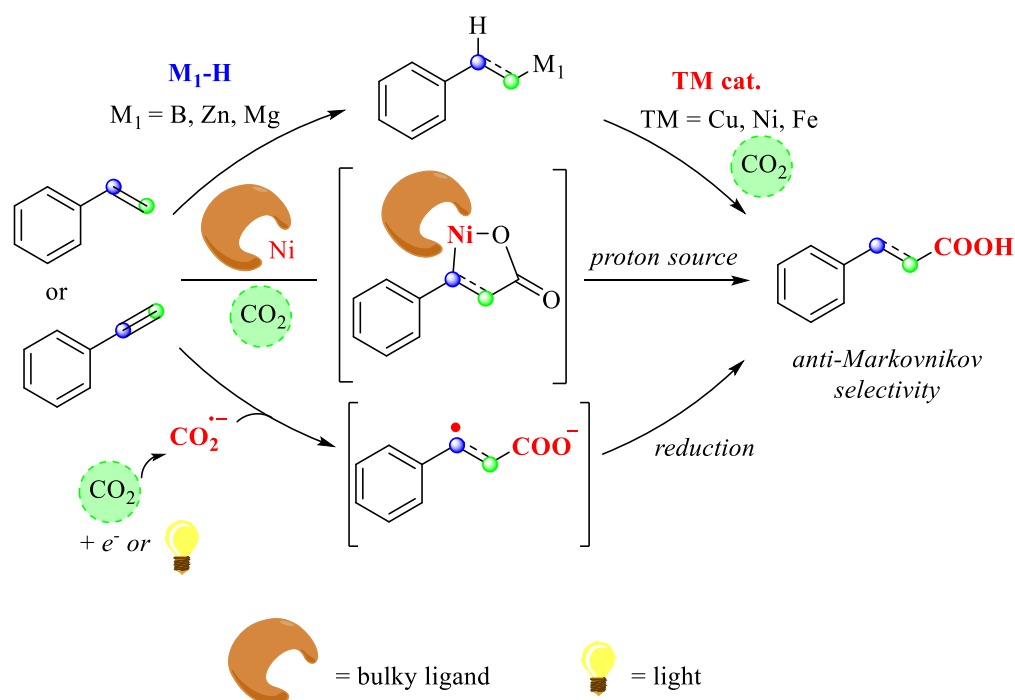


**Figure 79:** Described protocols leading to the anti-Markovnikov hydrocarboxylation

The reason behind this  $\beta$ -selectivity of a radical addition is principally the stability of the generated benzyl radical, which is rapidly reduced, and after protonation, furnishes the anti-Markovnikov product. Considering these facts, the CO<sub>2</sub> activation-based process could offer the right combination to perform the anti-Markovnikov addition with unsaturated substrates such as styrene and phenylacetylene derivatives. The reported methods describing the anti-Markovnikov addition of styrenes and phenylacetylene derivatives, even as a side reaction, will be discussed in the next section (Figure 79).

<sup>100</sup> X. Wang, M. Nakajima, R. Martin, *J. Am. Chem. Soc.* **2015**, *137*, 8924.

<sup>101</sup> H. Seo, A. Liu, T. F. Jamison, *J. Am. Chem. Soc.* **2017**, *139*, 13969.

## 2. Catalytic $\beta$ -hydrocarboxylation of styrene and phenylacetylene derivatives

The principal transition metals allowing the preparation of acrylic acids are nickel, copper, and iron. Höberg investigated first the reaction of alkenes and  $\text{CO}_2$  with a stoichiometric amount of  $\text{Ni}(\text{cod})_2$ .<sup>102</sup> A mixture of branched and linear carboxylic acids was obtained, and the proportion of these two products depended on the reaction temperature and electronic features of the alkenes (**Figure 80**).

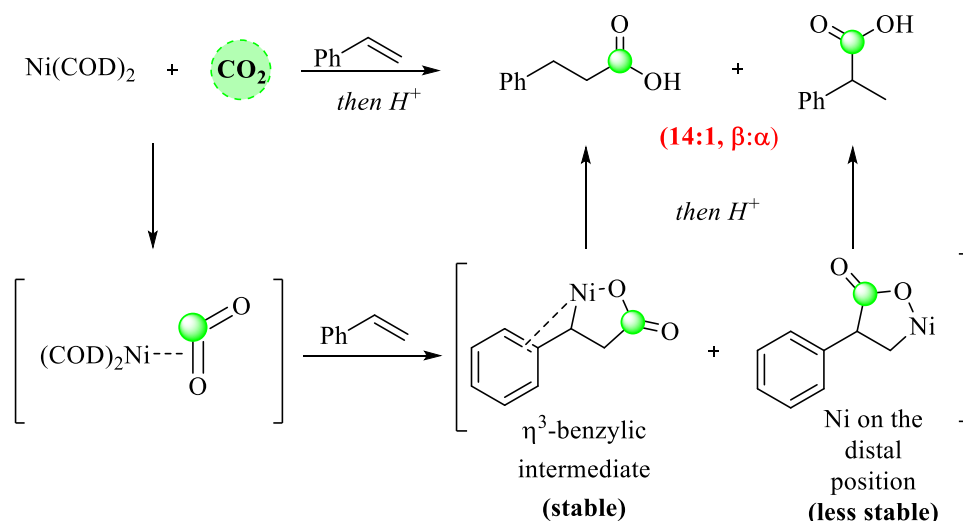


**Figure 80:** Höberg's work on the carboxylation of styrene derivatives

Indeed, these results inspired others to test catalytic approaches based on  $\text{Ni}^0$  complexes. Earlier attempts to generate carboxylic acids selectively from styrenes and phenylacetylenes derivatives were limited to the use of organoboranes, organozinc and Grignard reagents as hydride sources and reductants. After a few years of investigations, direct hydrocarboxylation was achieved using water as proton source but still, the regioselectivity was not as expected. And finally, the use of proper ligand for the metal center and the addition of a suitable proton source allowed the establishment of direct and selective  $\beta$ -hydrocarboxylation of double and triple bonds.<sup>77b, 100</sup>

### a. The use of organoboranes

Boranes are compounds containing an active hydrogen-boron bond capable of reducing a  $\text{C}=\text{C}$ ,  $\text{C}=\text{N}$  or  $\text{C}=\text{O}$  motifs via hydroboration reaction. Interestingly, this reduction follows an anti-Markovnikov *syn*-addition manner where the bulky boron attaches to the less substituted position while the hydrogen reacts with the more substituted one. Thanks to the boron's empty *p* orbital, this group can be easily transmetalated once transformed to boronate by accepting two electrons usually from a base or a halide.

<sup>102</sup> a) H. Höberg, D. Schaefer, *J. Organomet. Chem.* **1982**, 238, 383; b) H. Höberg, D. Schaefer, G. Burkhart, *J. Organomet. Chem.* **1982**, 228, 21; c) G. Burkhart, H. Höberg, *Angew. Chem.* **1982**, 94, 75, *Angew. Chem.* **1982**, 94, 75; *Angew. Chem., Int. Ed.* **1982**, 21, 76; d) H. Höberg, D. Schaefer, *J. Organomet. Chem.* **1982**, 236, 28; e) H. Höberg, D. Schaefer, *J. Organomet. Chem.* **1983**, 51-53; c) H. Höberg, Y. Peres, A. Milchereit, *J. Organomet. Chem.* **1986**, 307, 38.

Based on this characteristic, various  $\beta$ -hydrocarboxylation of unsaturated hydrocarbons were elaborated and catalyzed with transition metals.<sup>5</sup> In the case of styrenes and phenylacetylenes, copper(I) catalysis allowed the preparation of the corresponding carboxylic acids with high regioselectivity.<sup>103</sup>

In 2011, Sawamura<sup>104</sup> and Hou<sup>105</sup> described independently the hydrocarboxylation of alkenes mediated by a Cu-catalyst in two steps (**Figure 81**). First, a hydroboration reaction using 9-BBN permitted the fixation of the boron moiety on the distal position. Secondly, the strong base used as an additive (*t*BuOK or LiOMe) gave rise to the boronate species, facilitating the transmetalation step via a Cu-O-B transition state. Finally, the CO<sub>2</sub> insertion into the Cu-C bond delivered the expected carboxylic acid. Even though this method tolerated unactivated alkenes, the hydrocarboxylation of internal alkenes remained inaccessible and only two examples were highlighted with styrene derivatives.

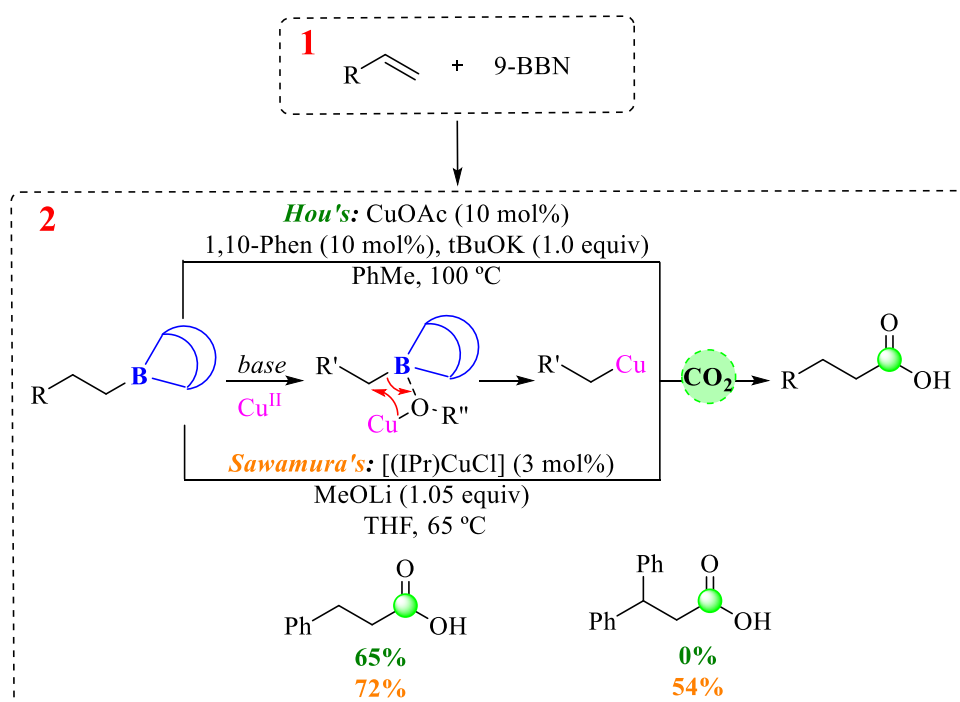


**Figure 81:** Hydrocarboxylation of alkenes catalyzed by Cu-complexes.<sup>104, 105</sup>

Skrydrups's work overcame this barrier by replacing the harsh bases with cesium fluoride (CsF) and elevating the reaction temperature to 120°C (**Figure 82**).<sup>106</sup>

Similarly to the previous examples, the boron-fluoride interaction triggered the transmetalation step between the boronate and the copper catalyst and the subsequent CO<sub>2</sub> insertion into Cu-C bond. Under these conditions, the hydrocarboxylation occurred successfully with different alkenes and alkynes. However, styrenes and stilbenes derivatives delivered a mixture of 2 and 3-propionic acid with poor regioselectivity, except with heteroaromatics. Terminal phenylacetylenes underwent a  $\beta,\beta$ -dicarboxylation, furnishing at the end **malonic acids** instead of acrylic acids.

<sup>103</sup> S. Wang, G. Du, C. Xi, *Org. Biomol. Chem.* **2016**, *14*, 3666.

<sup>104</sup> H. Ohmiya, M. Tanabe, M. Sawamura, *Org. Lett.* **2011**, *13*, 1086.

<sup>105</sup> T. Ohishi, L. Zhang, M. Nishiura, Z. Hou, *Angew. Chem. Int. Ed.* **2011**, *50*, 8114.

<sup>106</sup> M. Juhl, S. L.R. Laursen, Y. Huang, D. U. Nielsen, K. Daasbjerg, T. Skrydstrup, *ACS Catal.* **2017**, *7*, **2**, 1392.

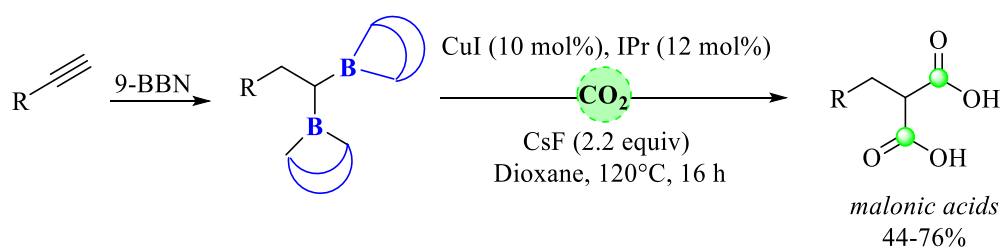


**Figure 82:** Skydrup's hydrocarboxylation of alkynes to produce malonic acids.<sup>106</sup>

### b. The use of organozinc and Grignard reagent

Due to the stability of the  $\eta^3$ -benzylic metal intermediate, hydrocarboxylation approaches based on metal-hydride catalysis contributed typically to the  $\text{CO}_2$  fixation on the  $\alpha$ -position and the subsequent isolation of phenylacetic acids as the main product while the linear carboxylic acid remained a minor impurity. For example, Ma's group described a Ni-catalyzed syn-hydrocarboxylation of alkynes using air-sensitive and pyrophoric  $\text{Et}_2\text{Zn}$  as a hydride source.<sup>107</sup> The optimized conditions gave the phenylacetic acid with 84% yield while less than 3% of linear carboxylic acid was obtained, along with the reduced product. The formation of nickel hydride during the reaction on the  $\beta$ -carbon along with organozinc on the adjacent position furnished the Markovnikov product eventually. However, the single example where the anti-Markovnikov product was isolated majorly with 54% yield was started from 1-phenyl-1-propyne as a substrate. Unfortunately, this inverted reactivity was not further explained (**Figure 83**).

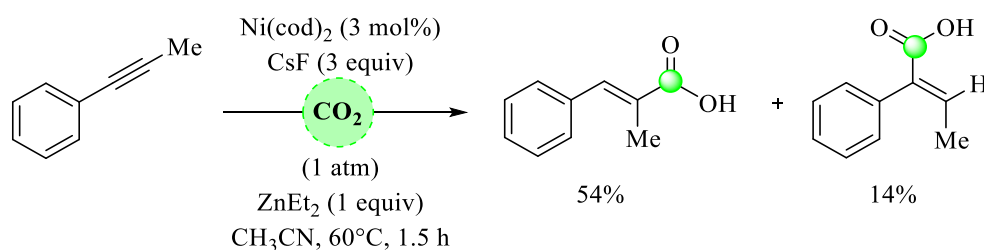


**Figure 83:** Products of the hydrocarboxylation of 1-phenyl-1-propyne using Ma's conditions.<sup>107</sup>

Likewise, Thomas' work used  $\text{FeCl}_2$  as a catalyst mixed with  $\text{EtMgBr}$  to form *in situ* the metal hydride complex for the hydrocarboxylation of styrenes (**Figure 84**).<sup>13b</sup> In most of the screened molecules, the phenylacetic acid remained the primary product. Surprisingly, changing the hydride source from  $\text{EtMgBr}$  to  $\text{CpMgBr}$  reversed the regioselectivity and furnished the linear carboxylic acid in much higher yield (74%, 1/6  $\alpha/\beta$ ) without further explanation.

<sup>107</sup> S. Li, W. Yuan, S. Ma, *Angew. Chem.* **2011**, *123*, 2626; *Angew. Chem. Int. Ed.* **2011**, *50*, 2578

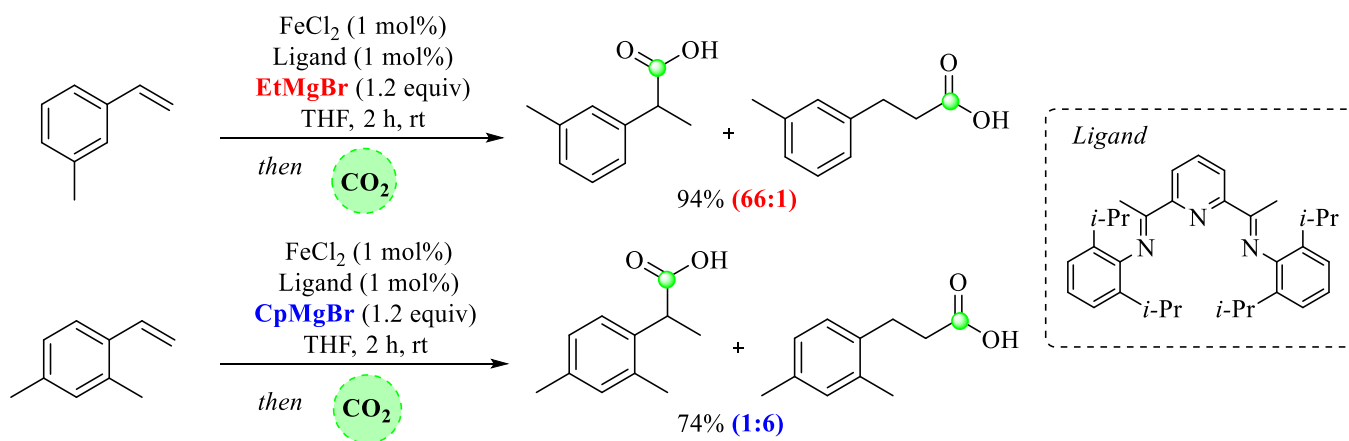


**Figure 84:** Effect of the hydride source on the regioselectivity. <sup>13b</sup>

### c. Ligand-controlled hydrocarboxylation

The first regioselective hydrocarboxylation was reported in Martin's laboratory using a dual-system of bulky  $\text{Ni}^0$  complex with *i*PrOH or *t*-BuOH as a readily available and green proton source for the hydrocarboxylation of alkynes.<sup>100</sup> This approach demonstrated a high regioselectivity profile in favor of the  $\beta$ -position, in most cases, along with very good yields (**Figure 85**).

The proposed mechanism attributed the observed selectivity to the formation of two oxinickelacyclopentene in equilibrium where one of them exhibit a higher steric hindrance between the proton source and the alkyl substituent on the terminal position of the alkyne (**Figure 85**).

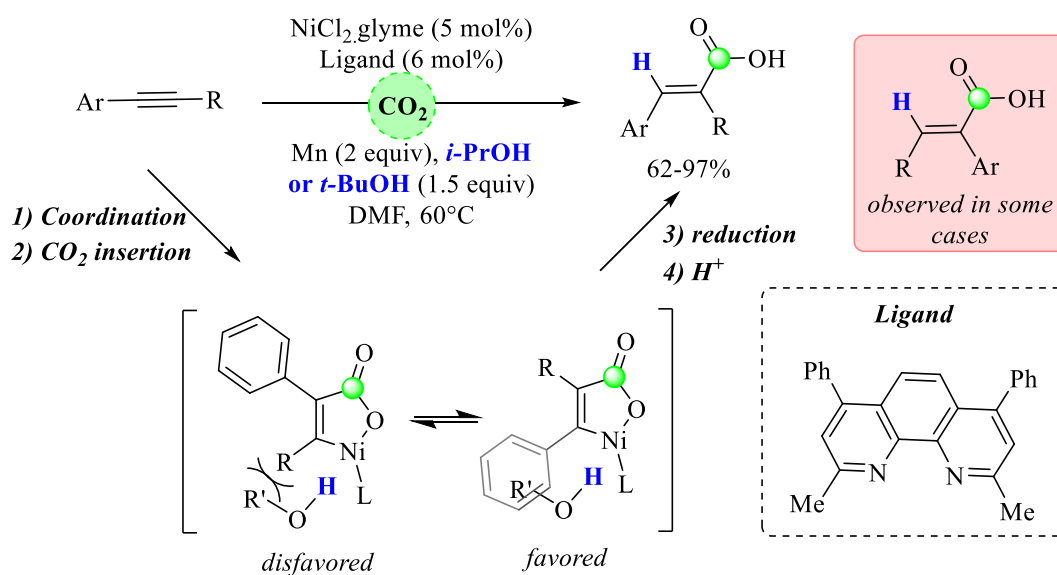


**Figure 85:** Ni-catalyzed selective hydrocarboxylation of alkynes to yield acrylic acids.<sup>100</sup>

Still, substrates bearing large substituent at the terminal position of the alkyne afforded a mixture of the  $\alpha$  and  $\beta$ -carboxylic acids, and in many cases, the authors switched from *i*PrOH to *t*-BuOH to obtain higher regioselectivity.

In 2018, König reported a novel strategy combining photochemistry and Ni-catalysis to achieve a selective hydrocarboxylation (**Figure 86**).<sup>77b</sup> Concerning the reaction conditions, a mixture of 1,2,3,5-tetrakis(carbazol-9-yl)-4,6-dicyanobenzene (4CzIPN) as photosensitizer with Hantzsch ester (HEH) as a terminal reductant in addition to different inorganic salts ( $K_2CO_3$ ,  $LiOOCCH_3$ ) was used to perform this reaction. This method is under ligand control, as a simple ligand like neocuproine led to the branched carboxylic acid while the use of bis(diphenylphosphino)butane (dppb) resulted in the formation of the  $\beta$ -carboxylated product.

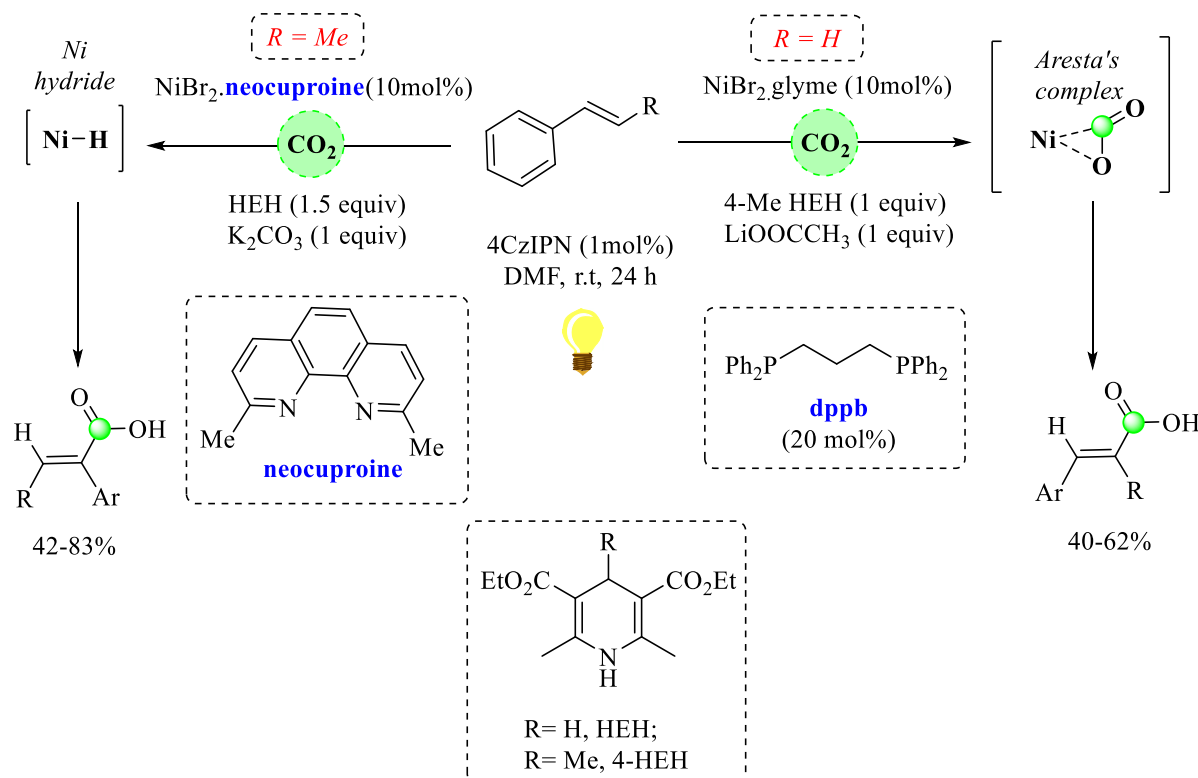


**Figure 86:** Ligand controlled photo-hydrocarboxylation of styrene derivatives reported by König and his co-workers.<sup>77b</sup>

Based on DFT calculations, the authors proposed two pathways depending on the ligand choice:

1- With the neocuproine (**Figure 86, on the left**), a nickel hydride complex was generated after protonation by  $HEH^+$ , which reacted subsequently with the styrene and the Ni(II) occupied the benzylic position. An electron transfer permitted the generation of Ni(I) and the subsequent insertion of  $CO_2$  into the Ni-C bond. Lastly, another electron transfer delivered the branched carboxylic acid.

2- With dppb (**Figure 86, on the right**), the calculation revealed an interaction between the Ni and  $CO_2$ , to form Aresta's complex first. This latter underwent then the styrene insertion, giving rise to the nickelalactone intermediate, similar to the one reported in Martin's work,<sup>100</sup>

where the carboxylate is on the distal site. After double electron transfer, it furnished the desired acrylic acid. However, the  $\beta$ -hydrocarboxylation worked only with unsubstituted styrenes and the need for inorganic salts was not fully explained.

#### d. Site-selectivity controlled by the substrate

This reactivity was described by Ma's group inspired by a recently developed approach based on a Ni-catalysis to achieve the hydrocarboxylation of alkynes (**Figure 87**).<sup>108</sup> While in the previous report, the authors obtained the phenylacetic acid as the main product,<sup>107</sup> the authors reversed the regioselectivity in this work by adding a hydroxyl group as a directing group towards the  $\beta$ -position and producing the desired  $\alpha$ -alkylidene- $\gamma$ -butyrolactones finally.<sup>101b</sup>

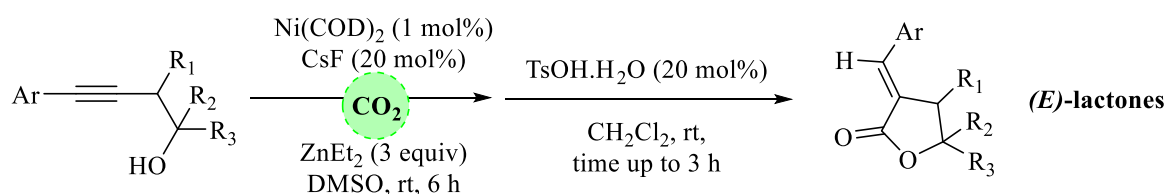


**Figure 87:** Synthesis of lactones via the hydrocarboxylation of alkynes mediated by Ni catalysis

The reaction proceeded precisely the same as in the previous report,<sup>107</sup> but in this case, the Ni center was coordinated to the hydroxy group, forming a much stronger intermediate than the  $\eta^3$ -benzylic metal ones. This coordination dictated subsequently the addition of the metal-hydride complex to the  $\text{CO}_2$  and provides the anti-Markovnikov product.

Another illustration for this type of reaction was reported by Sato and co-workers in 2017.<sup>109</sup> In this example, a Ni-catalyst was used in the presence of water as a proton source for the selective  $\alpha$ -carboxylation of ynamides (**Figure 88**). After reporting the synthesis of  $\beta$ -amino- $\alpha,\beta$ -unsaturated esters where the carboxylation occurred on the  $\beta$ -carbon of the ynamides,<sup>110</sup> the authors were surprised to obtain the  $\alpha$ -selectivity using the Ni- $\text{H}_2\text{O}$  system.

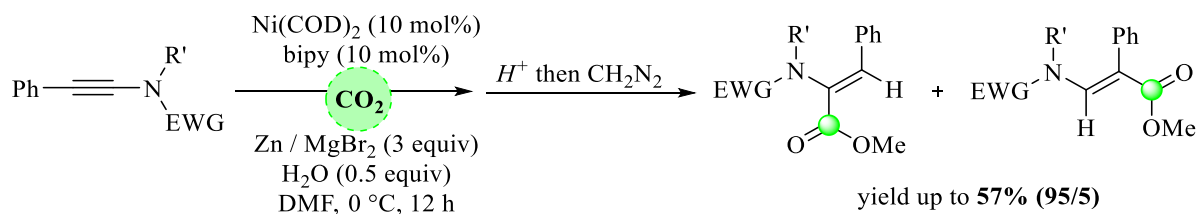


**Figure 88:** Hydrocarboxylation of ynamides to produce  $\beta$ -amino- $\alpha,\beta$ -unsaturated esters.<sup>109110</sup>

<sup>108</sup> S. Li, S. Ma, *Chem. Asian J.* **2012**, 7, 2411.

<sup>109</sup> R. Doi, I. Abdullah, T. Taniguchi, N. Saito, Y. Sato, *Chem. Commun.* **2017**, 53, 7720

<sup>110</sup> N. Saito, I. Abdullah, K. Hayashi, K. Hamada, M. Koyama, Y. Sato, *Org. Biomol. Chem.* **2016**, 14, 10080.

After several investigations, the authors discovered that using the mixture Zn/MgBr<sub>2</sub> was crucial to obtain this selectivity and unlike Martin's work,<sup>100</sup> the steric hindrance was not the critical factor. Therefore, the authors suggested that either a steric repulsion between the Ni-catalyst and the alkyl substituent on the  $\beta$ -position of the ynamides was at the origin of the  $\alpha$ -selectivity, or the coordination of the nitrogen atom of the substrate and the Ni-complex directed the CO<sub>2</sub> addition towards the  $\alpha$ -position.

### 3. $\beta$ -Selective hydrocarboxylation initiated by CO<sub>2</sub><sup>-</sup>

The main difficulty with the CO<sub>2</sub> was the high redox potential, requiring thus harsh conditions and strong organometallics to overcome this barrier. On the other hand, some organic frameworks demonstrated, once activated by light, a high reductive power that could offer a solution for the challenging CO<sub>2</sub> reduction.

Jamison's group adopted this idea and described a  $\beta$ -selective hydrocarboxylation with styrene derivatives via continuous flow using *p*-terphenyl as a photoredox organocatalyst (**Figure 89**).<sup>101</sup> After screening different reductants and proton sources, a mixture of 1,2,2,6,6-pentamethylpiperidine (PMP) and water afforded the best result with 87% yield and a 29:1 ratio of mono- to dicarboxylated product in DMF. Moreover, the hydrocarboxylation furnished the carboxylic acids in good yields, regardless of the styrene substitution.

To get insight into the mechanism, the authors conducted two reactions: one without the CO<sub>2</sub> and the other without the PMP. Even though in both cases no carboxylic acid was detected, still the conversion was 88% without the CO<sub>2</sub>, and ethylbenzene was detected. This result can be rationalized by the reduction of styrene ( $E^\circ = -2.58$  V/SCE in DMF) to the corresponding benzyl radical by the *p*-terphenyl ( $E^\circ = -2.63$  V/SCE in DMF). Furthermore, a deuterium labeling study proved undoubtedly that the water is the proton source in the hydrocarboxylation process.

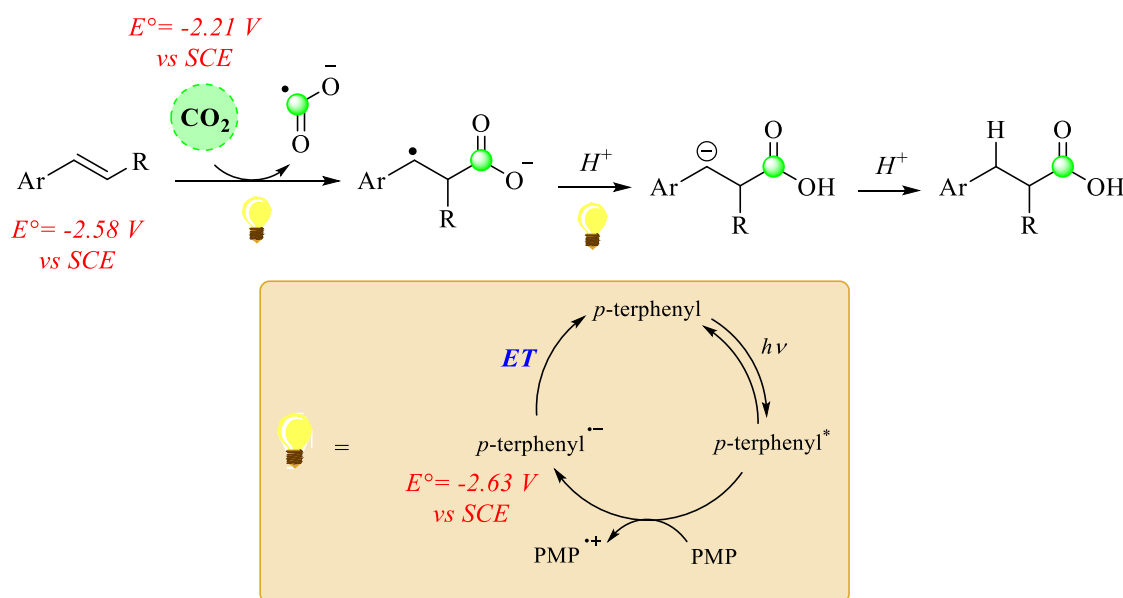


**Figure 89:** *p*-Terphenyl catalyzed the photocatalytic hydrocarboxylation of styrene derivatives.



Concerning the mechanistic pathway, the authors proposed a radical mechanism initiated by the photoexcitation of *p*-terphenyl and its subsequent reduction to the corresponding radical anion via SET from PMP (**Figure 89**). This strong reductant performed the CO<sub>2</sub> reduction to the corresponding radical anion and this latter underwent an anti-Markovnikov addition with the styrene to generate the benzyl radical. As previously mentioned, this radical is unstable and thus the corresponding carbanion is rapidly generated. Lastly, the protonation of this anion yielded the expected β-carboxylic acid, whereas the dicarboxylated product was delivered by trapping a second molecule of CO<sub>2</sub> instead of the proton.

#### 4. Electrocarboxylation of styrene and phenylacetylene derivatives

Different electrochemical strategies addressed the hydrocarboxylation of unsaturated hydrocarbons.<sup>21</sup> Most of the reported approaches with styrenes were based on using a magnesium or an aluminum electrode as a sacrificial anode with different types of cathode material (GC, Pt, Ti, Ni ...). The released cations in these procedures facilitated the electron transfer by decreasing the overpotential and most importantly, stabilizing the obtained carboxylate and limiting its decomposition.

Nevertheless, the investment in chemical mediators, which are usually group d-complexes, allowed the elaboration of much more selective electrocarboxylation by exploiting the capacity of the transitional metal to favor the interaction with one substrate over another, thus enhancing the regioselectivity of the CO<sub>2</sub> fixation process.

##### *a. Electrocarboxylation using sacrificial anodes*

Under these conditions, different possible reactions can occur depending on the reduction potential of the olefin. If  $E^{\circ}_{CO_2} > E^{\circ}_{styrene}$ , this indicates that the CO<sub>2</sub> undergoes the reduction first to yield the [CO<sub>2</sub>]<sup>-</sup> that attacks the double bond and generates the carboxylate anion. As side products, the CO<sub>2</sub> dimerization to oxalate, CO, or even carbonate can be obtained in proportions determined by the experimental conditions. If  $E^{\circ}_{CO_2} \approx E^{\circ}_{styrene}$ , in this case, depending on the concentration of the reaction components, an electron transfer between the styrene and CO<sub>2</sub> is considered the primary step in this process. Usually, this type of electrocarboxylations led to low yields. If  $E^{\circ}_{CO_2} < E^{\circ}_{styrene}$ , the styrene receives first the electron to produce the radical anion species which then acts as a nucleophile towards CO<sub>2</sub> and delivers the corresponding radical anion.

Even if in most cases, the succinic acid is the primary product,<sup>111</sup> various parameters affect the electrocarboxylation of styrenes like the electrode material, the concentration of the substrate,

<sup>111</sup> H. Senboku, H. Komatsu, Y. Fujimura, M. Tokuda, *Synlett* **2001**, 3, 418; H. Wang, M.-Y. Lin, H.-J. Fang, T.-T. Chen, J.-X. Lu, *Chin. J. Chem.* **2007**, 25, 913; G.-Q. Yuan, H.-F. Jiang, C. Lin, S.-J. Liao, *Electrochimica Acta* **2008**, 53, 2170

the proton donor choice. Changing any factor alters significantly the efficiency of the electrocarboxylation, and leads to different product distributions.

Addressing this problem, an important study of the electrochemical carboxylation of styrene was conducted by Silvestri and his co-workers using Al sacrificial anode (**Figure 90**).<sup>112</sup> The authors discussed the different side reactions resulting from each component. For example, the styrene undergoes the reduction to ethylbenzene via hydrogen transfer from water traces in DMF or the exothermic polymerization if its concentration exceeded 0.8 M.

Furthermore, the cathode material had a high impact on the reaction. While the use of Zn, Cu or mercury as cathodes enhances the styrene polymerization even at low concentration, the use of vitreous carbon resulted in the isolation of monocarboxylic acid in high yield along with 3,4-diphenyl adipic acid in addition to causing high overpotential and low Faradic efficiency.

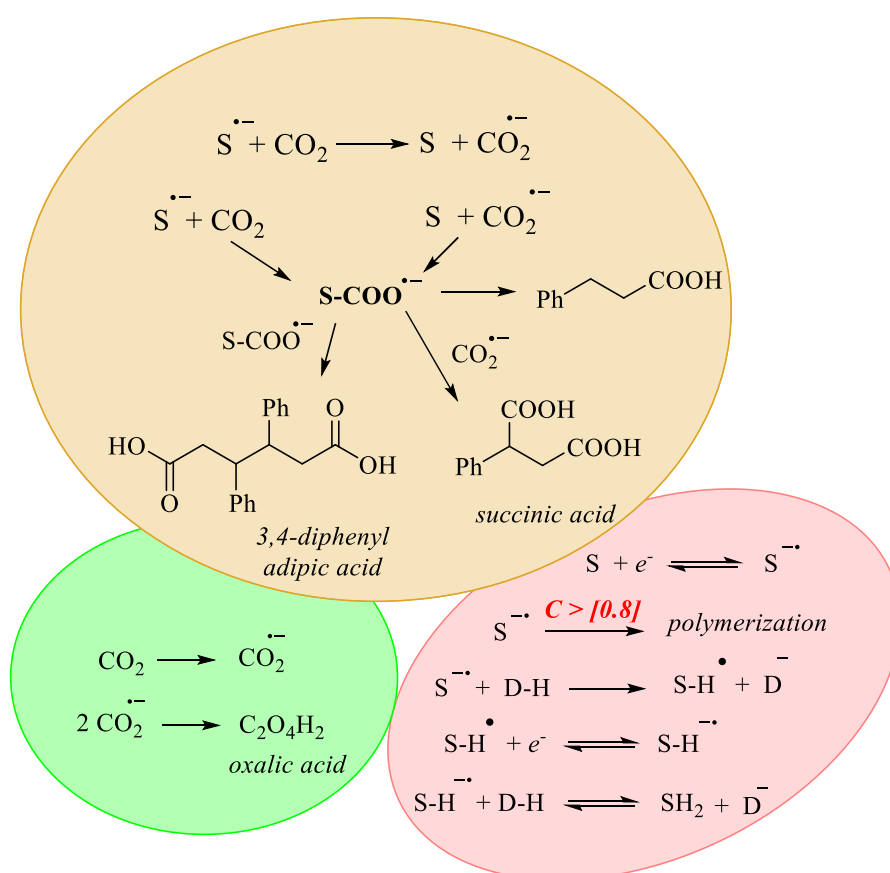


**Figure 90:** Possible transformations of styrene and carbon dioxide in an electrochemical process. S= styrene, D-H: proton donor.<sup>112</sup>

On the other hand, the addition of a proton donor like water or phenol led to a dramatic change in the composition of the mixture. The use of water led to an increase in the protonation rate of the styrene ( $10^4 \text{ M}^{-1} \cdot \text{s}^{-1}$ ) and thus the yield of the phenyl propionic acid raised significantly. However, the phenol revealed a higher reactivity by elevating the rate to more than  $10^5 \text{ M}^{-1} \cdot \text{s}^{-1}$ . This difference can be attributed to the interaction of water with DMF, and the higher proton transfer efficiency of phenol with respect to H<sub>2</sub>O.

<sup>112</sup> S. Gambino, A. Gennaro, G. Filardo, G. Silvestri, E. Vianello, *J. Electrochem. Soc.* **1987**, *134*, **9**, 2172

Furthermore, the authors proved that the formation of ethylbenzene via protonation became disfavored upon the addition of CO<sub>2</sub> even under high concentration of proton source, and the carboxylation of the styrene occurred smoothly to furnish phenylsuccinic acids and/or phenyl propionic acid.

As for the phenylacetylene, its transformation into carboxylic acids was not well investigated without the addition of transitional metals in the medium. In the literature, only one approach introduced the electrocarboxylation of phenylacetylene to produce maleic acid as the main product (**Figure 91**).<sup>113</sup>

The combination of a Ni cathode with an Al anode using *n*Bu<sub>4</sub>NBr as conducting salts in DMF under 4 MPa CO<sub>2</sub> pressure was crucial to obtain an excellent yield of phenyl maleic anhydride (88%) along with 5% of dicarboxylic acid.

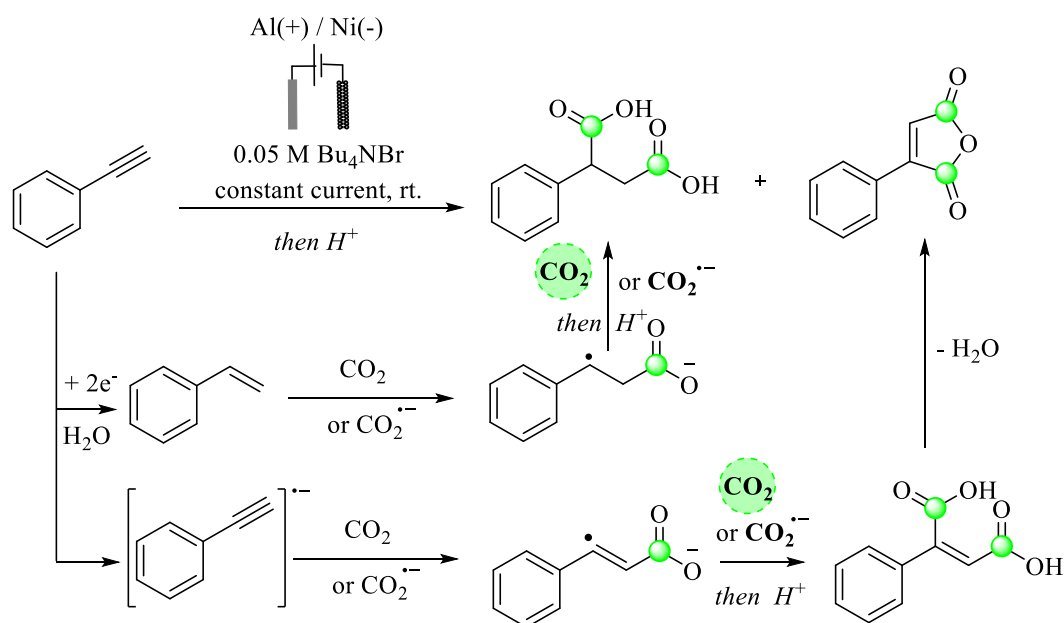


**Figure 91:** Electrocarboxylation of phenylacetylene derivatives using a Ni-cathode.<sup>113</sup>

However, the addition of water reversed these results in favor of the formation of the dicarboxylic acid for which the yield increased from 4% in a dry solvent to 90% after the addition of 0.3 mL of H<sub>2</sub>O. The authors proposed that the water provided protons, favoring the reduction of phenylacetylene into styrene, and finally delivering the saturated phenylsuccinic acid.

Recently, the same group reported an interesting electrosynthesis of saturated tricarboxylic acids besides dicarboxylic acids just by adding CuI as a catalyst to activate the double bond of phenyl maleic anhydride and subsequently to trigger a third CO<sub>2</sub> fixation (**Figure 92**).<sup>114</sup>

<sup>113</sup> G.-Q. Yuan, C. Lin, H.-F. Jiang, *Tetrahedron* **2008**, *64*, 5866.

<sup>114</sup> C. Li, G. Yuan, H. Jiang, *Chin. J. Chem.* **2010**, *28*, 1685

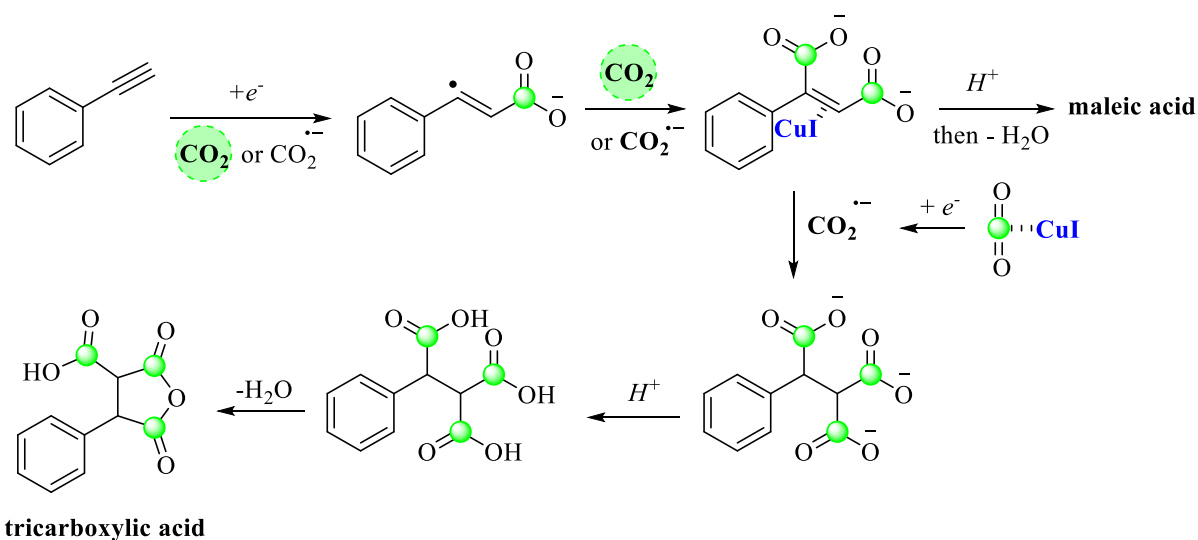


**Figure 92:** The effect of adding CuI on the electrocarboxylation of alkynes.<sup>114</sup>

### b. Carboxylations via chemical mediators

Besides lowering the overpotential, the addition of a chemical mediator can favor the electrocarboxylation over other side reactions regardless of the parameters mentioned above. A remarkable example based on a Fe<sup>I</sup>-complex [CpFe(CO)<sub>2</sub>]<sub>2</sub> (Fp<sub>2</sub>) was presented in 2000, using an aluminum foil as a cathode and Hg pool as an anode for the carboxylation of styrenes.<sup>115</sup> This Fe-complex activated the CO<sub>2</sub> selectively to form the CO<sub>2</sub><sup>•-</sup> that performed then a radical addition with styrene delivering mainly the dicarboxylic acid while the low amount of 3-phenyl propionic acid came from the water traces in DMF. Finally, cyclic voltammetry studies demonstrated the definite interaction between the Fp<sub>2</sub> and CO<sub>2</sub> because, after the addition of this latter, the oxidation wave disappeared whereas the reduction one multiplied.

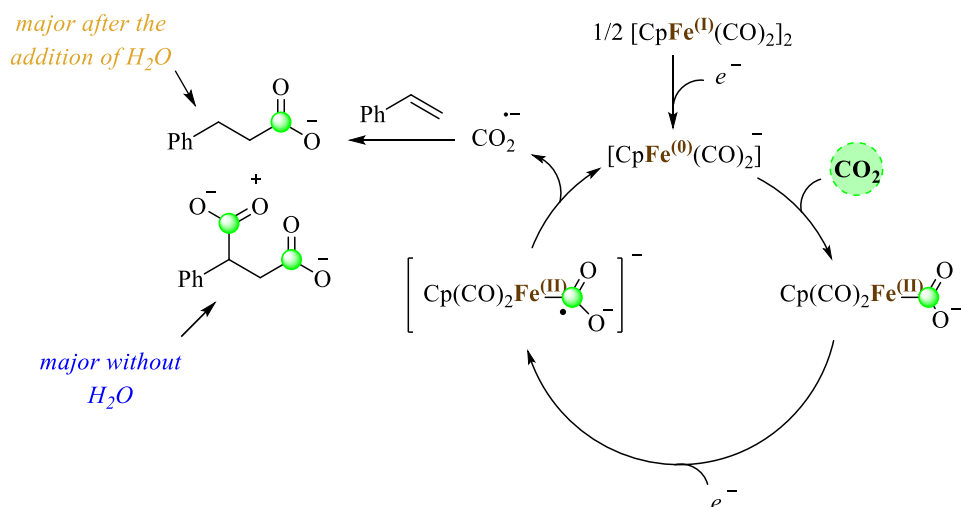


**Figure 93:** Fe-catalyzed carboxylation of styrene derivatives via CO<sub>2</sub> activation.<sup>115</sup>

<sup>115</sup> D. Ballivet-Tkatchenko, J.-C. Folest, J. Tanji, *Appl. Organometal. Chem.* **2000**, *14*, 847

In the case of phenylacetylene, the carboxylation was mainly reported with Ni-bipyridine complexes, by Périchon and his co-workers under mild conditions. The electricity serves as a clean reductant by transforming  $\text{Ni}^{\text{II}}$  to  $\text{Ni}^0$  complex, which is the active catalyst in this reaction. Inspired by Hoberg's work<sup>116</sup>, the authors elaborated the reductive electrocarboxylation of alkynes catalyzed by Ni complexes using Mg as a sacrificial anode. In their initial work, only the  $\alpha$ -acrylic acid was obtained with terminal alkynes.<sup>116</sup> However, the use of phenylpropene gave 65% of a mixture of monocarboxylic acid with  $\alpha/\beta$  regioselectivity of 62/38 with 7% of the corresponding dicarboxylic acid (**Figure 94**).<sup>117</sup>

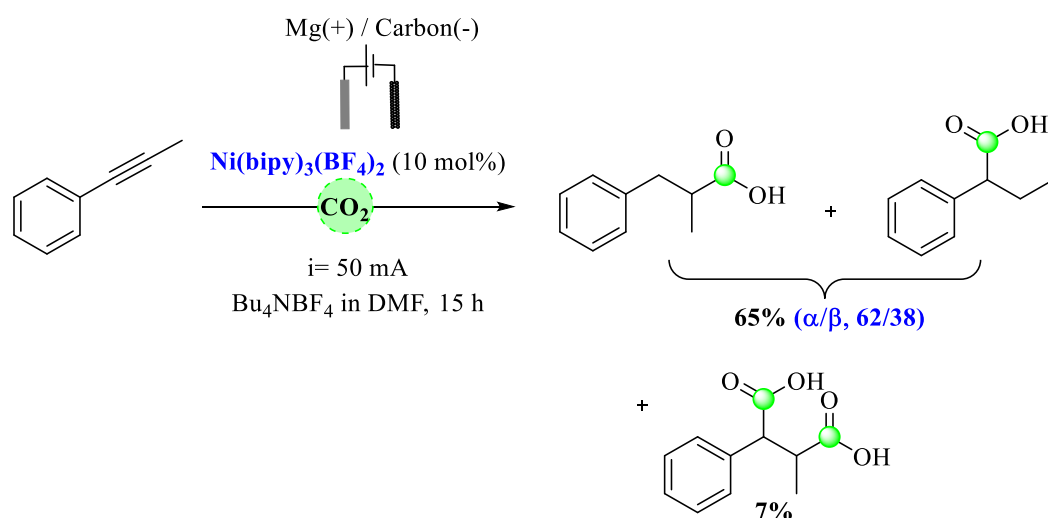


**Figure 94:** Carboxylation of phenylpropene and the isolated mixture of carboxylic acids reported by Périchon's group.<sup>117</sup>

This result made the authors realize the steric hindrance effect on the regioselectivity. A few years later, they highlighted the role of  $\text{Mg}^{2+}$  as it allows the  $\text{Ni}^{2+}$  cleavage from the final product, leaving it free to regenerate the  $\text{Ni}^0$  via cathodic reduction.

As far as we know, a sustainable electrochemical procedure delivering the  $\beta$ -carboxylation of styrenes and phenylacetylenes selectively does not exist in the literature. Therefore, the electrocatalytic strategy developed in our group to generate *in situ*  $\text{Sm}^{2+}$  as a strong monoelectronic reductant from soluble samarium anode that, unlike the unreactive  $\text{Mg}^{2+}$  and  $\text{Al}^{3+}$ , reacts as a catalyst and reduces the  $\text{CO}_2$  to  $\text{CO}_2^-$  presents a worth-trying option for the hydrocarboxylation of unsaturated substrates to produce selectively the anti-Markovnikov product.

<sup>116</sup> E. Duñach, J. Périchon, *J. Organomet. Chem.* **1988**, 352, 239

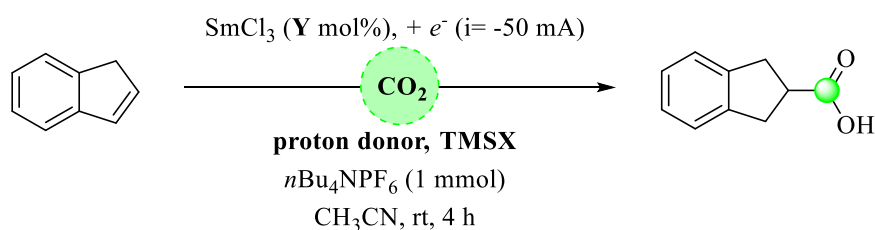
<sup>117</sup> E. Duñach, S. Dérien, J. Périchon, *J. Organomet. Chem.* **1989**, 364, 33

## 5. Catalytic hydrocarboxylation of styrene and phenylacetylene derivatives mediated by electrogenerated Sm(II)

### a. Hydrocarboxylation of styrene derivatives

For the optimization, indene **3w** was chosen as a starting material to test the carboxylation using  $\text{SmCl}_3$  as a precatalyst for the reaction along with a samarium rod as a cathode and a stainless steel grid as the anode (**Table 3**). Indeed and according to our preliminary tests with benzyl chlorides in the precedent chapter, the electrogeneration step was not performed and the electrocatalysis process was directly started in acetonitrile. Of note, dry ice was added as  $\text{CO}_2$  source along with  $\text{TMSCl}$  as an oxophilic reagent. As for the proton donor, water was firstly chosen after the reported accomplishments using the  $\text{SmI}_2\text{-H}_2\text{O}$  system for the reduction of challenging functional groups.<sup>118</sup> Even though a large quantity of the starting material was recovered, still the monocarboxylic acid was isolated with 35% yield (**entry 1**). However, at the end of the electrolysis, the Sm electrode was covered with a black layer.  $\text{H}_2\text{O}$  was thus replaced with simple alcohols, leading to a clear solution, and slightly higher yields were observed with MeOH and EtOH (**entry 2-3**). The addition of *t*-BuOH gave 50% of the monocarboxylic acid, revealing the essential function played by the proton source choice (**entry 4**). Due to its ever-increasing applications in organic chemistry and catalysis, hexafluoroisopropanol (HFIP) was added to the electrochemical medium as a potential proton donor.<sup>119</sup> However, the desired product was delivered but only with 22% yield along with a great amount of degradation (**entry 5**).

Next, we found that decreasing the number of equivalents of *t*-BuOH led to a lower amount of the desired product, accompanied by traces of phenylsuccinic acid (**entry 6-7**). Similarly, a large amount of  $\text{TMSCl}$  was required for this transformation (**entry 8-9**). Eventually, a mixture of 10 equiv of *t*-BuOH and 8 equiv of  $\text{TMSCl}$  afforded, after four hours of electrolysis, the highest yield about 62% (**entry 10**). It is worth noting that increasing the catalyst loading to 20 mol% did not furnish any further improvement of the yield (**entry 12**). On the contrary, inferior results were obtained with 5 mol% of  $\text{SmCl}_3$  with no significant side reaction (**entry 13**). Lastly, using dry ice (**entry 14**) and maintaining a diluted medium (**entry 15**) were beneficial for the carboxylation.



<sup>118</sup> M. Szostak, M. Spain, D. Parmar, D. J. Procter, *Chem. Commun.* **2012**, 48, 330

<sup>119</sup> I. Colomer, A. E. R. Chamberlain, M. B. Haughey, T. J. Donohoe, *Nat. Rev. Chem.* **2017**, DOI: 10.1038/s41570-017-0088.

**Table 3** Screening of the reaction conditions for the hydrocarboxylation of alkenes

Entry	Y mol%	Proton donor (equiv)	TMSX (equiv)	Yield(%) <sup>a</sup>
1	10	H <sub>2</sub> O (20)	TMSCl (6)	35
2	10	MeOH (20)	TMSCl (6)	37
3	10	EtOH (20)	TMSCl (6)	42
4	10	<i>t</i> -BuOH (20)	TMSCl (6)	50
5	10	HFIP (20)	TMSCl (6)	22
6 <sup>b</sup>	10	<i>t</i> -BuOH ( <b>3</b> )	TMSCl (6)	39
7 <sup>b</sup>	10	<i>t</i> -BuOH ( <b>5</b> )	TMSCl (6)	51
8	10	<i>t</i> -BuOH ( <b>10</b> )	TMSCl (6)	56
9	10	<i>t</i> -BuOH (10)	TMSCl ( <b>3</b> )	38
<b>10</b>	<b>10</b>	<b><i>t</i>-BuOH (10)</b>	<b>TMSCl (8)</b>	<b>62</b>
11	10	<i>t</i> -BuOH ( <b>10</b> )	TMSOTf (6)	N.R
12	<b>20</b>	<i>t</i> -BuOH (10)	TMSCl (8)	60
13	<b>5</b>	<i>t</i> -BuOH (10)	TMSCl (8)	27
14 <sup>c</sup>	10	<i>t</i> -BuOH (10)	TMSCl (8)	35
15 <sup>d</sup>	10	<i>t</i> -BuOH (10)	TMSCl (8)	53

<sup>a</sup> Isolated yields. <sup>b</sup> traces of succinic acid were detected by <sup>1</sup>H NMR. <sup>c</sup> dry ice was replaced by CO<sub>2(g)</sub> (1 atm). <sup>d</sup> 15 mL instead of 35 mL of CH<sub>3</sub>CN.

The best results were eventually obtained using 10 mol% of SmCl<sub>3</sub> with a 1/10/8 mixture of the alkene, *t*-BuOH, and TMSCl, respectively in the presence of CO<sub>2</sub> added to the reaction as dry ice.

Encouraged by these findings, we started investigating the scope of Sm<sup>II</sup>-catalyzed regioselective hydrocarboxylation of styrene derivatives (**Figure 95**). Initially, different unsubstituted styrenes were tested. Electron-deficient (**3c**) and -rich motifs (**3g-h**) afforded the corresponding acrylic acids with yields up to 95% with total regioselectivity. This successful carboxylation of electron-rich compounds (e.g. **3g** and **3h**), known for their high reduction potential, presents strong evidence that the CO<sub>2</sub> is predominantly reduced by the divalent samarium. Substrates bearing a chlorine substituent (**3d** and **3j**) caused a dramatic decrease in the conversion and in the yield. This behavior was attributed to the previously reported reactivity of aryl chlorides with CO<sub>2</sub> using Sm(II) complex (see **chapter 2**), although no aryl carboxylic acid was detected in the mixture. When a substrate bearing a phenyl (**3f**) or a methyl group (**3i**) on the benzylic position was tested, the reaction delivered the desired product successfully with moderated yields (50% and 60%, respectively). To our delight, a (hetero)aromatic reagent such as 2-vinylbenzofuran (**3k**) was also

tolerated under our conditions and gave 3-(1-benzofuran-2-yl)propionic acid (**3'k**) with 52% yield. Lastly, substrates bearing an –OH (**3l**), or –CN (**3m**) group inhibited the reaction. This observation can be rationalized with the high tendency of the low valent lanthanides to coordinate to such electron-donating substituents which may lead to catalyst quenching.

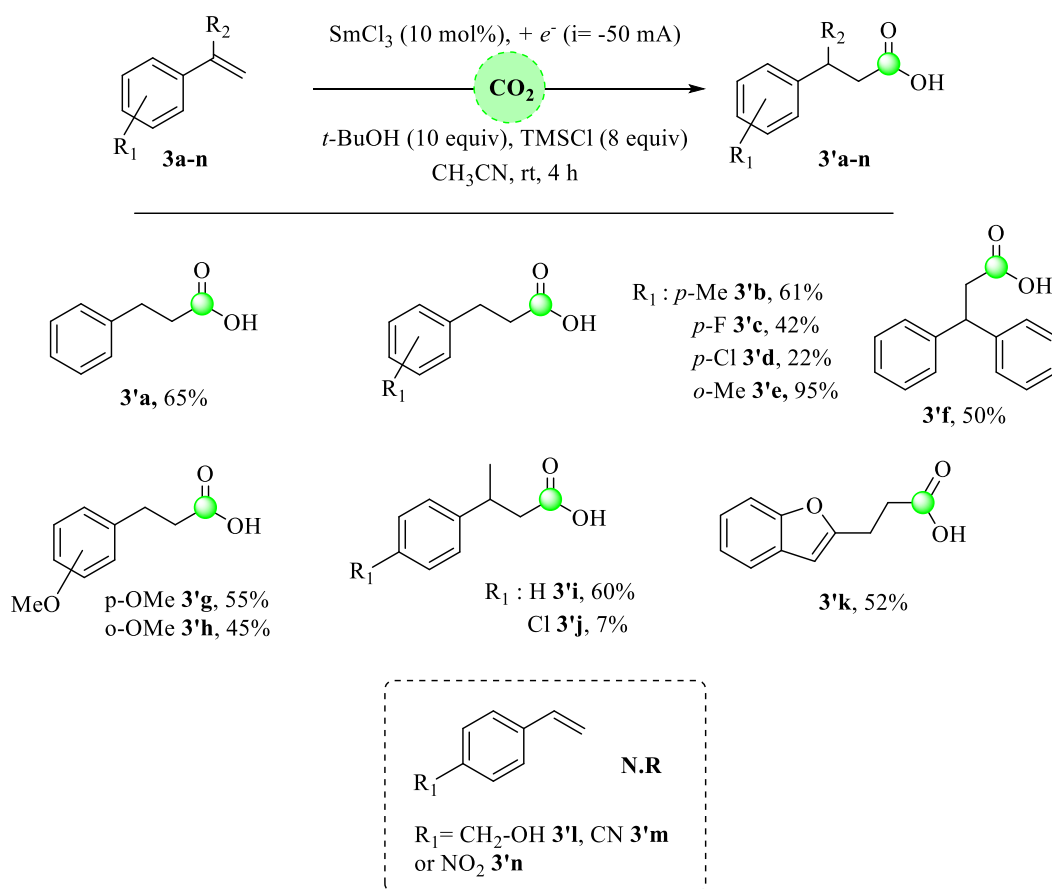


**Figure 95:** Substrate scope of styrene derivatives.

Interestingly, vinyl bromides (**3o** and **3p**) were unstable under the electrochemical conditions, furnishing **3'a** as a final product with comparable yields to the one obtained from styrene (**3a**) (**Figure 96**).

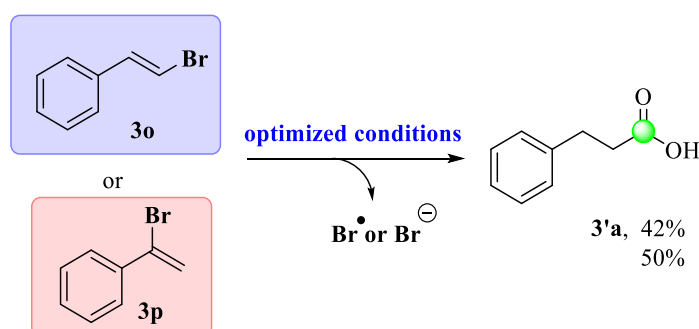


**Figure 96:** hydrocarboxylation of bromovinyl benzene as a substrate.



The electrochemical hydrocarboxylation conditions were also compatible with a range of 1,2-disubstituted olefins. As shown in **Figure 97**, the hydrocarboxylation of alkenes with a methyl substituent (**3q-t**) delivered the corresponding carboxylic acids (**3'q-t**) in moderate to excellent yields (45-95%). Also, stilbenes derivatives (**3w-x**) underwent smoothly the transformation, and furnished the desired linear carboxylic acids (**3'w-x**), albeit in lower yields, probably due to steric hindrance.

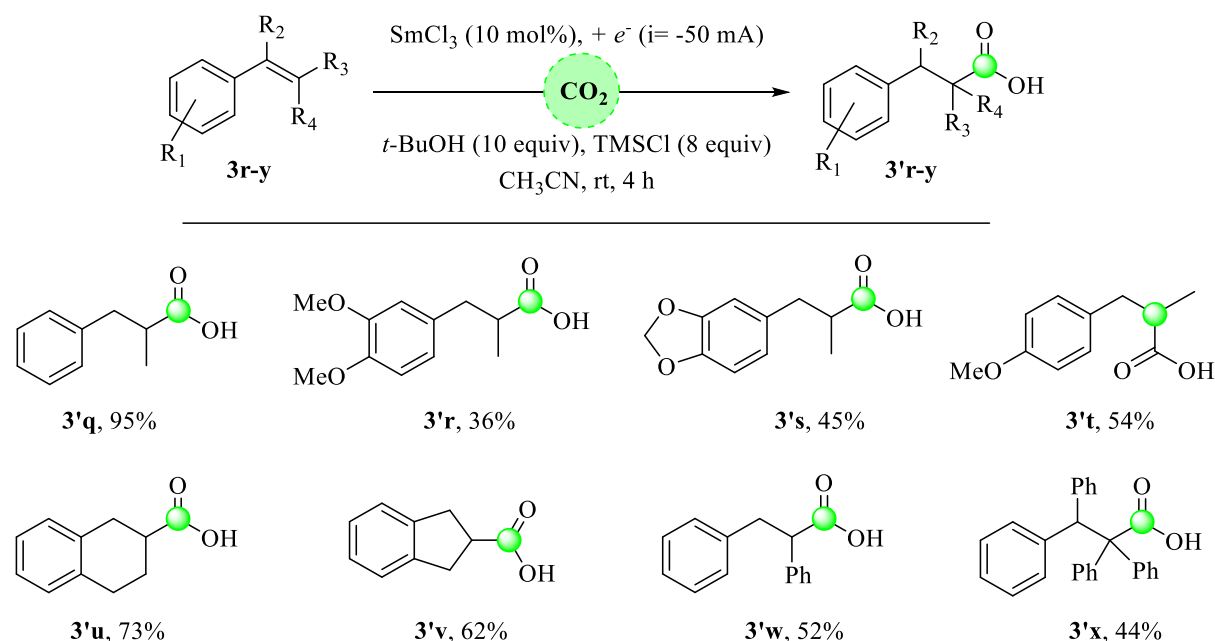


**Figure 97:** Substrate scope of 1,2 disubstituted styrene derivatives.

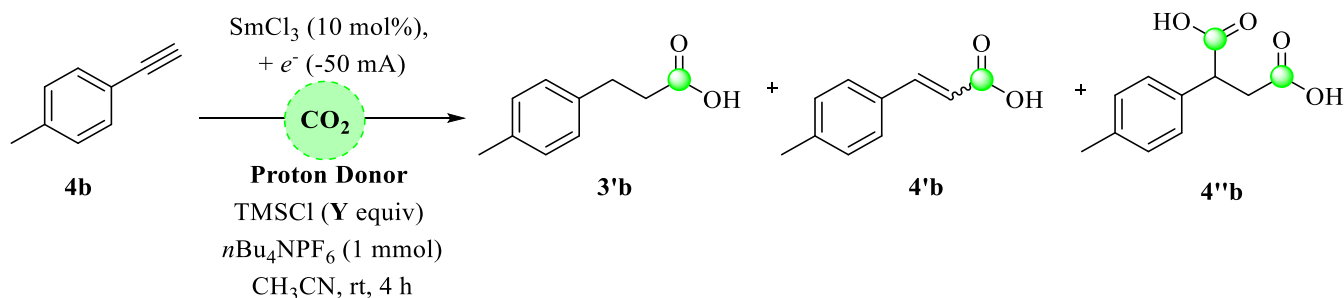
Compared to the previously reported hydrocarboxylation strategies, the use of electrogenerated divalent samarium from  $\text{SmCl}_3$  demonstrated a remarkable  $\beta$ -selectivity by furnishing exclusively the product of the anti-Markovnikov addition in all cases described above. Encouraged by these results, we decided to extend the hydrocarboxylation conditions to the aryl acetylene derivatives, aiming to produce the corresponding acrylic acids.

### *b. Hydrocarboxylation of phenylacetylene derivatives*

We started our investigation with the alkynes based on the optimized conditions established for the styrenes derivatives (**Table 4**). Starting from 4-ethynyltoluene **4b** and using 10 mol% of  $\text{SmCl}_3$ , 10 equiv of  $t\text{-BuOH}$ , and 8 equiv of  $\text{TMSCl}$  in acetonitrile along with the addition of dry ice as a  $\text{CO}_2$  source, we identified, after four hours of electrolysis, three different products: 3-(*p*-tolyl)propanoic acid **3'b** as the main product (60%), 3-(*p*-tolyl)acrylic acid **4'b** as a secondary product (19%, *E/Z* 1/4), and traces of 2-(*p*-tolyl)succinic acid **4''b** (10%) (**entry 1**). The increase of  $t\text{-BuOH}$  to 20 equiv disfavored the formation of dicarboxylic acid **4''b** but enhanced the cinnamic acid yield to become 28% (*E/Z* 1/4) while the unsaturated carboxylic acid remained the

major product with 64% yield (**entry 2**). Any decrease in TMSCl to less than 6 equiv caused a considerable drop in the hydrocarboxylation yield (**entry 4**).

**Table 4** Optimization of the hydrocarboxylation of alkynes reaction conditions.



Entry	Proton donor (equiv)	Y equiv of TMSCl	Yield(%) <sup>a</sup> (3'b:4'b:4''b) <sup>b</sup>
1	<i>t</i> -BuOH (10)	8	79% (60:19:10)
2	<i>t</i> -BuOH (20)	8	92 (64:28:0)
<b>3</b>	<b><i>t</i>-BuOH (20)</b>	<b>6</b>	<b>91 (66:25:0)</b>
4	<i>t</i> -BuOH (20)	<b>3</b>	36 (30:6:0)
5	MeOH (20)	6	25 (25:0:0)
6	EtOH (20)	6	31 (31:0:0)
7	PhOH or PhSH (20)	6	0
8	Et <sub>3</sub> SiH or Ph <sub>3</sub> SiH (1, 3 or 5)	0	0
9	MsOH or AcOH (3)	6	0
10 <sup>c</sup>	<i>t</i> -BuOH (20)	6	12 (6:5:1)
11 <sup>d</sup>	<i>t</i> -BuOH (20)	6	0
12 <sup>e</sup>	<i>t</i> -BuOH (20)	6	92 (70:22:0)

<sup>a</sup> Isolated yields. <sup>b</sup> Due to the unsuccessful separation of the unsaturated product from the saturated one, the proportions are determined by <sup>1</sup>H NMR. <sup>c</sup> THF was used as a solvent. <sup>d</sup> MeOH was used as a solvent. <sup>e</sup> electrocatalysis for 8 hrs.

The use of other alcohols like MeOH, EtOH instead of *t*-BuOH furnished exclusively the unsaturated carboxylic acid but with a low yield (22% and 35% respectively) (**entry 5-6**). Interestingly, adding phenol or thiophenol, aiming to trigger a hydrogen atom abstraction (HAT), resulted in the full recovery of **4b** (**entry 7**). Furthermore, we evaluated the reaction with silanes such as Et<sub>3</sub>SiH or Ph<sub>3</sub>SiH as hydrogen donors and oxophilic reagents. However, only the reduction of the triple bond was detected without any CO<sub>2</sub> insertion in this case (**entry 8**). As observed with aryl and phenyl chlorides, the use of organic acids (MsOH or AcOH) inhibited the carboxylation (**entry 9**).

Regarding the solvent effect, the use of THF instead of MeCN decreased the yield to 12% (**entry 10**). Moreover, the MeOH was not a suitable solvent for this reaction (**entry 11**).

Increasing the time to 8 hours instead of 5 hours resulted in a slight change of the products mixture towards the formation of **3'b** (70%) isolated together with 22% of **4'b** (**entry 12**).

After all these optimizations, we decided to adopt the best conditions to perform the hydrocarboxylation of phenylacetylene derivatives (**Table 4, entry 3**). The scope of this method showed better yields than the ones obtained with the styrene derivatives, which is consistent with the higher reactivity of alkynes vs. alkenes.

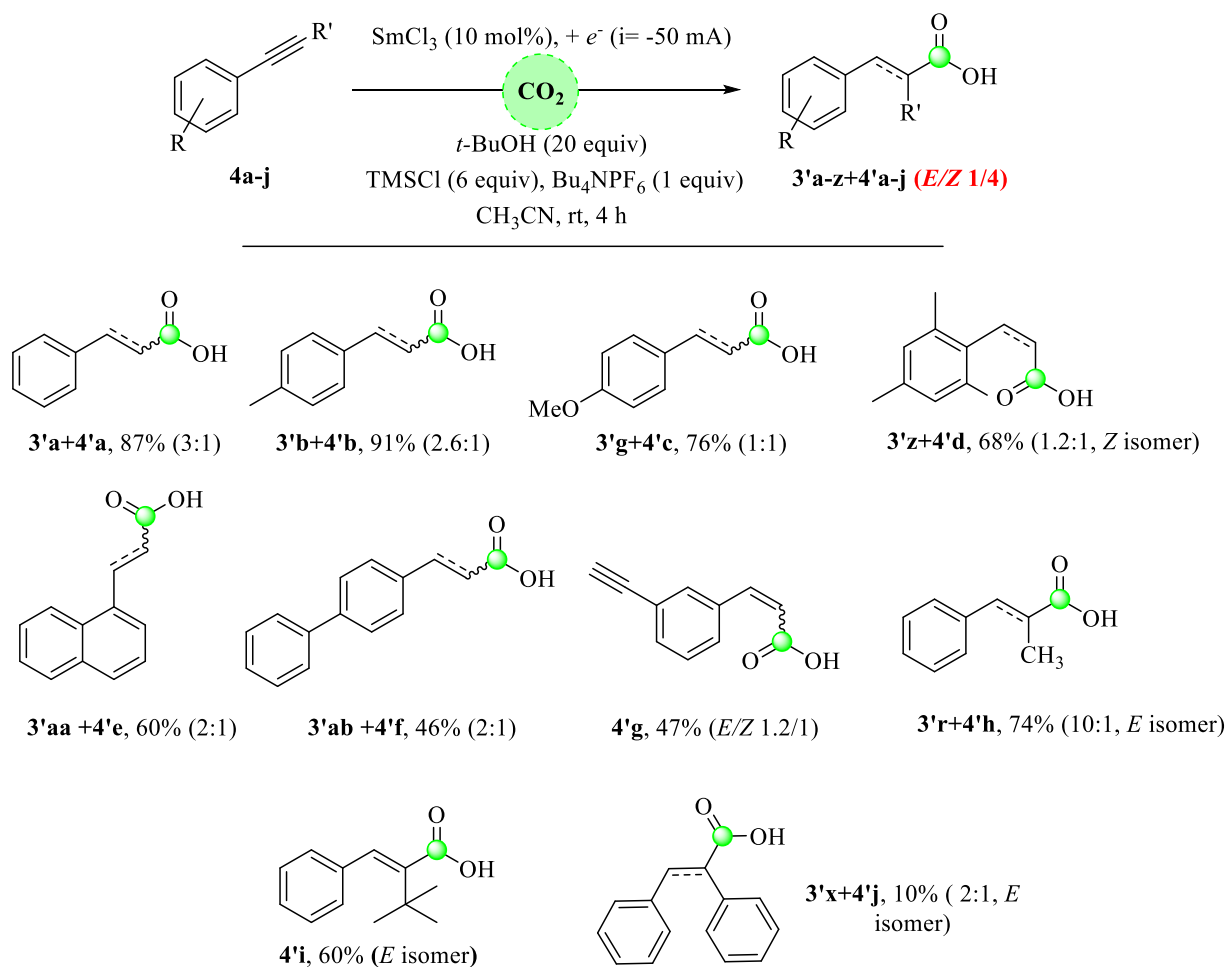


**Figure 98:** Scope of the hydrocarboxylation of phenylacetylene derivatives

A remarkable substituent effect was observed in the case of alkynes. Compared to the substrate **4a**, the electron-rich substituents (**4b-d**) favored the formation of the corresponding cinnamic acids (**4'b-d**) on the detriment of the saturated products (**3'b-z**). Only one alkyne moiety of the use of 1,3-diethynylbenzene (**4g**) reacted to afford exclusively 3-(3-ethynylphenyl) acrylic acid **4'g** without notable diastereoselectivity. The hydrocarboxylation of internal alkynes was also possible under our electrochemical conditions with good yields (**4h-i**) and *E*-selectivity. Lastly, the 1,2-diphenylethyne (**4j**) furnished a mixture of **3'x** and **4'j** (*E*) but only with a yield of 10%.

We next turned our attention to the hydrocarboxylation of protected alkynes. The optimized electrochemical conditions tolerated a trimethylsilyl group and led to the exclusive preparation of the analogous acrylic acids in good yields (**Figure 99**).

All the tested substrates (**4k-o**) produced the desired carboxylic acids (**4'k-o**) with yields up to 60% but unfortunately, without any significant diastereoselectivity.

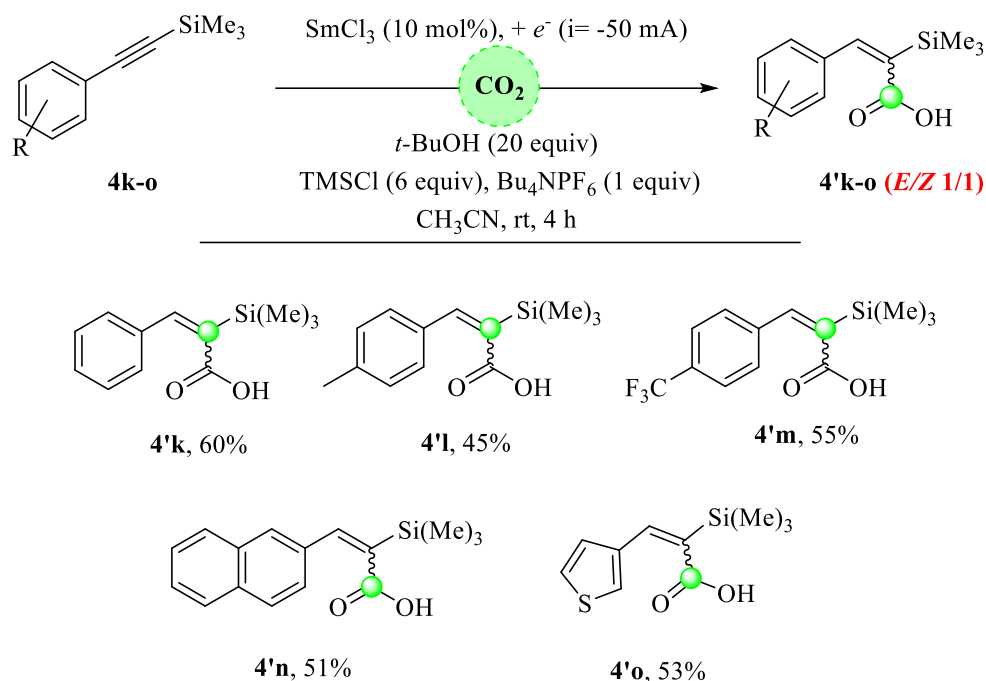


**Figure 99:** Scope of the hydrocarboxylation of protected alkynes

This new class of acrylic acids bearing TMS group in the  $\alpha$ -position could provide access to new products via post-functionalization strategies such as fluorination or C-C coupling reactions.

However, when the *para* substituent was a powerful electron-donating group such as a methoxy (**4p**) or a dimethylamine (**4q**) (**Figure 100**), a mixture of products was isolated, similarly to the case of unprotected alkynes with total elimination of the TMS group.

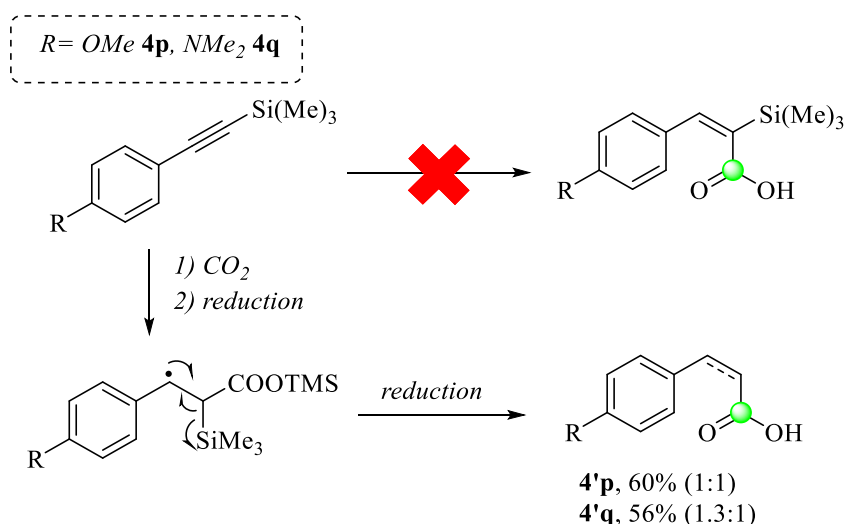


**Figure 100:** Hydrocarboxylation with strong electron-rich substrates

We speculated that the elimination of the TMS group occurred after the formation of an unstable benzyl radical that triggered a radical elimination of the silyl moiety and the subsequent regeneration of the double bond.

All these findings in this part prompted many questions about the mechanistic pathway leading to this reactivity, especially with the hydrocarboxylation of alkynes.

### *c. Mechanistic studies*

#### **A. Control experiments**

Our studies were first focused on assigning the role of each component present in the cell (**Figure 101**). Without the catalyst or *t*-BuOH **Eq. (1)**, the transformation of the alkenes and alkynes failed and low yields were obtained in the absence of TMSCl **Eq. (2)**. While the alkynes demonstrated inertia towards direct electrocarboxylation, the alkenes on the other side showed a considerable degradation but without any formation of carboxylic acid **Eq. (3)**.

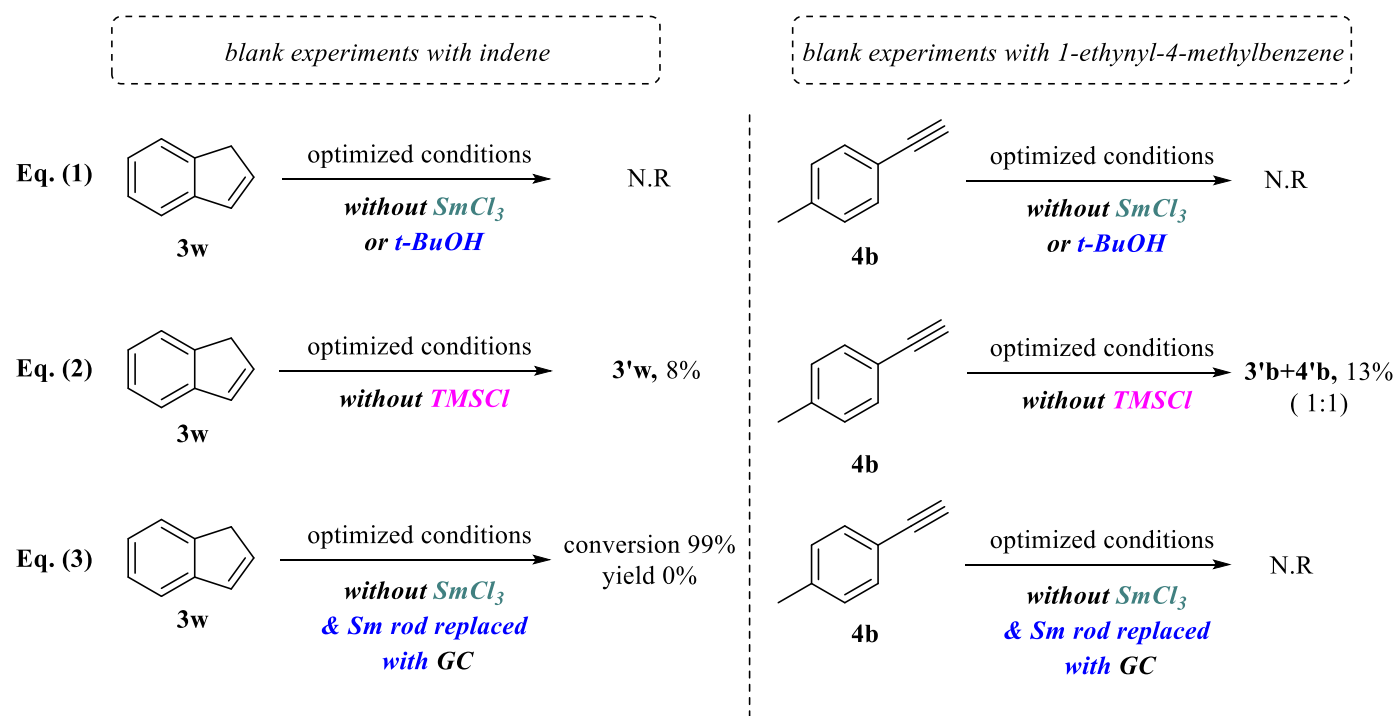


**Figure 101:** Blank experiments with styrene and phenylacetylene derivatives.

These tests are clear proof that without the  $\text{CO}_2$  activation by  $\text{SmCl}_3$ , the carboxylation of such unsaturated products is not possible under typical electrochemical conditions.

## **B. Stoichiometric tests**

In order to understand the reason behind the obtained mixture of saturated and unsaturated carboxylic acids, stoichiometric trials were conducted (**Figure 102**). The continuous electrogeneration of  $\text{Sm}^{2+}$  (**Eq. 4, Condition A**) and the addition 4 equiv of  $\text{SmCl}_3$  (**Eq. 4, Condition B**) led, after 2 hours of electrolysis, to the total conversion of **4b** to 3-phenylpropionic acid **3'b** in excellent yields, without any trace of 4-methylcinnamic acid **4'b**. We speculate that the reduction of the double bond could be the rate-determining step, which could rationalize the outcome under catalytic conditions after 8 h (**Table 4, entry 12**).

After omitting the TMSCl (**Eq. 5**), even with a stoichiometric amount of electrogenerated divalent Sm, the yield dropped to 37% with a mixture of **3'b:4'b** around 12:1, calculated from  $^1\text{H}$  NMR spectra.

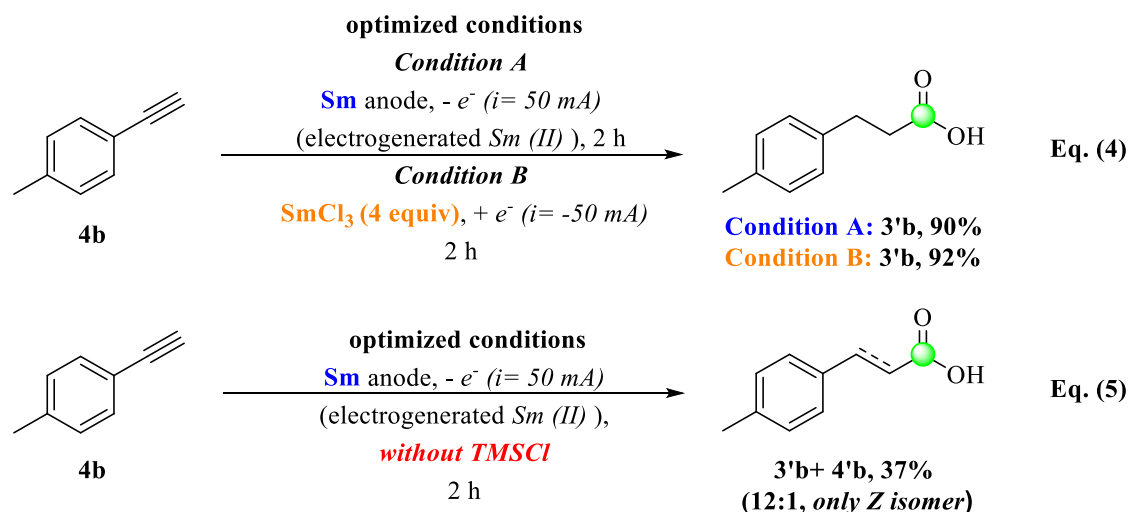


**Figure 102:** Stoichiometric tests starting from 4-ethynyltoluene

This significant decrease in yield signified that TMSCl has another crucial role in the mechanistic pathway, besides the dissociation of the Sm(III) from the final product.

### C. Deuterium-labeling experiments

To identify the definitive proton source in our conditions, we chose styrene **3a** and phenylacetylene **4a** as model substrates to conduct the deuterium-labeling experiments (**Figure 103**).

We explored first the hydrocarboxylation of **3a** under our conditions and followed by DCl quench, which led to the isolation of **3'a** without any deuterium fixation (**Eq. 6**). Surprisingly, the addition of t-BuOD, supposed to be the proton donor, delivered the deuterium-free product (**Eq. 7**). Based on these results, we investigated the CO<sub>2</sub> fixation in CD<sub>3</sub>CN and **3'aa** was isolated with >80% deuterium incorporation on the benzylic position (**Eq. 8**).

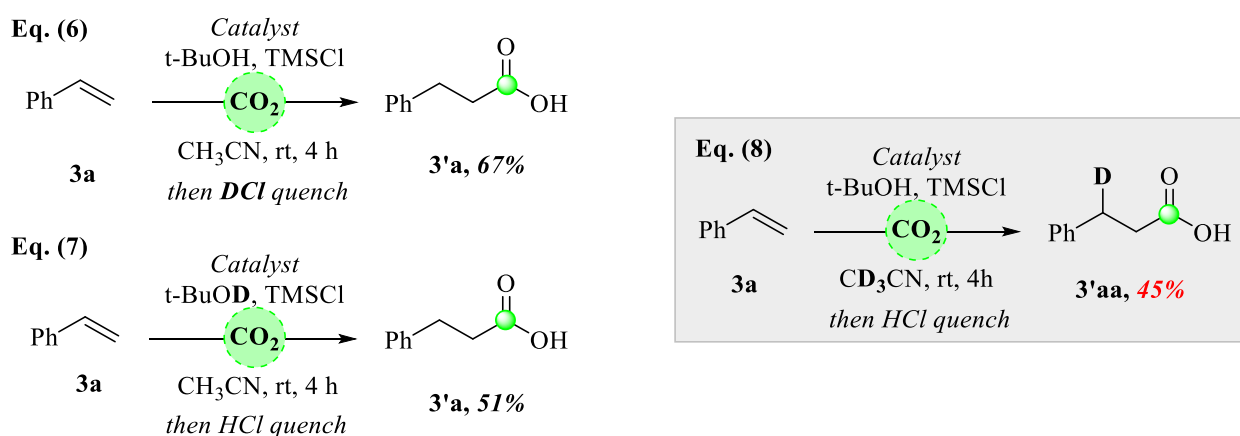


**Figure 103:** Deuterium labeling experiments with styrene derivatives

The same tests were applied to the hydrocarboxylation of phenylacetylene (**Figure 104**). Similarly to the case of styrene, the DCI quench did not trigger any deuterium fixation (**Eq. 9**). The result obtained in **Eq. 10** indicated undoubtedly that the carboxylation did not start by the deprotonation of the alkyne. The outcome of the **Eq. 11 and 12** confirmed that the proton source in the hydrocarboxylation of alkenes and alkynes is the solvent ( $\text{CH}_3\text{CN}$ ).

*Deuterium labeling experiments of the phenylacetylene*

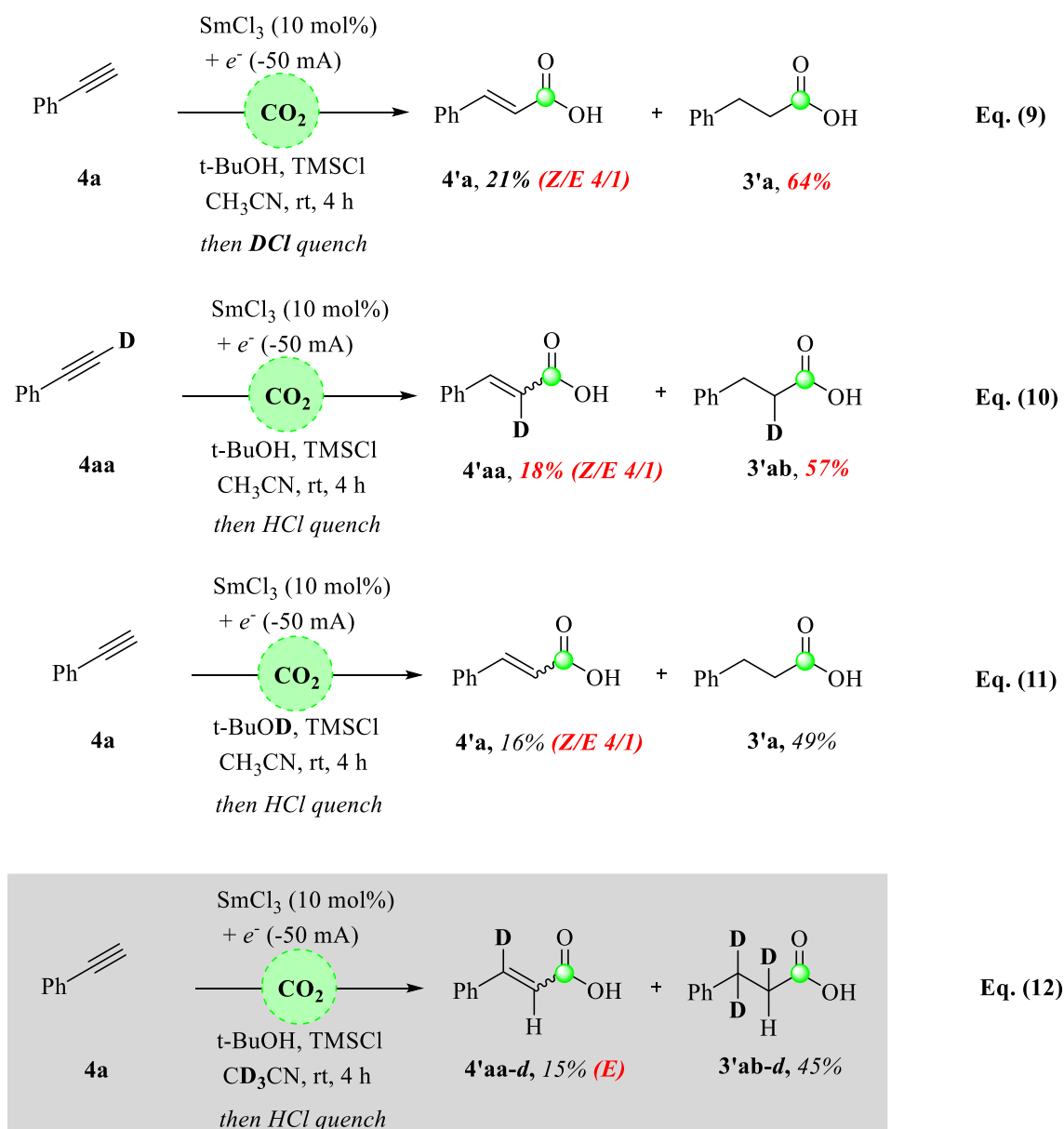


**Figure 104:** Deuterium labeling experiments with phenylacetylene.

At this point, we speculated that: (1) the unique C-H activation of the acetonitrile is triggered by its coordination to the Sm(II), which renders the protons much more acidic and thus explains the observed proton donor character that we observed. Noteworthy, this behavior was also described



with transition-metal based catalysts.<sup>120</sup> (2) The role played by the *t*-BuOH in the medium appeared to be not the proton donor, but it remains an essential additive in the protocol as we showed in the previous blank experiments (**Figure 101**).

We believe that after the deprotonation of CH<sub>3</sub>CN, the simple coordination of Sm(II) via the nitrogen (Sm-NCCH<sub>3</sub>) to a strong Sm-CH<sub>2</sub>CN bond (**Figure 105**). At this stage, the *t*-BuOH, known as non-coordinating alcohol,<sup>36</sup> is activated by TMSCl, and can, therefore, be deprotonated by the generated carbanion, thus leading to the dissociation of the Sm(III). This hypothesis explains the low or absent reactivity without these two additives and how the acetonitrile acts as an H-source under our conditions.

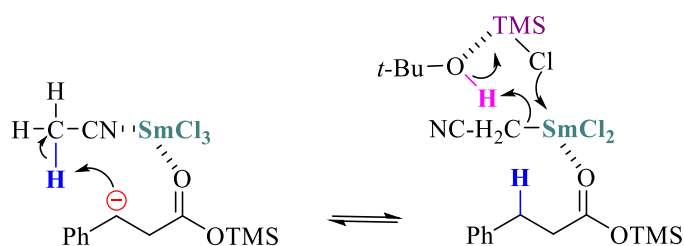


**Figure 105:** Suggested intermediates interpreting the D-labeling results

#### **D. Reaction with a radical clock**

To further clarify the mechanism of our protocol, a *radical clock* substrate was added to the reaction mixture (**Figure 106**). Under optimized conditions, an inseparable combination of two ring-opening products was obtained and analyzed by <sup>1</sup>H NMR and HRMS. The primary compound is the monocarboxylated one (**I**), demonstrating the reduction of the double bond. The product (**II**) resulted from the dicarboxylation reaction. Overall, this outcome proves the generation of benzyl radical from the addition of CO<sub>2</sub> radical anion to the alkene.

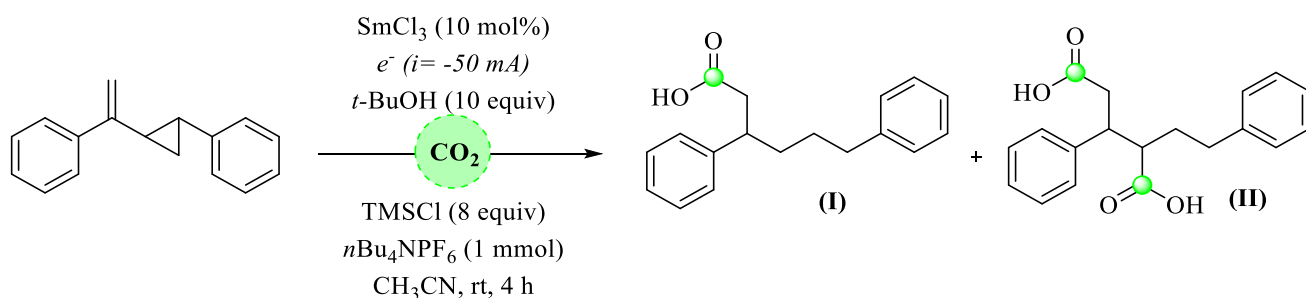


**Figure 106:** Radical clock experiment.

#### **E. Trapping with TEMPO**

<sup>120</sup> A. C. Bissember, M. G. Gardiner, T. S. Wierenga, *J. Organomet. Chem.* **2018**, 869, 213.

After confirming that the hydrocarboxylation goes through several radical species, a radical scavenger was added to the cell, aiming to quench a radical intermediate.

However, adding the TEMPO did not only decrease the yield of the reaction but the hydrocarboxylation of indene (**Figure 107, Eq. 13**) and 4-ethynyltoluene (**Figure 107, Eq. 14**) was utterly inhibited upon adding 2 equiv and 10 equiv of TEMPO, respectively. Extending the reaction time to 8 hours of electrocatalysis resulted in the restoration of reactivity, and finally, the expected products were isolated with the same yield as without TEMPO.

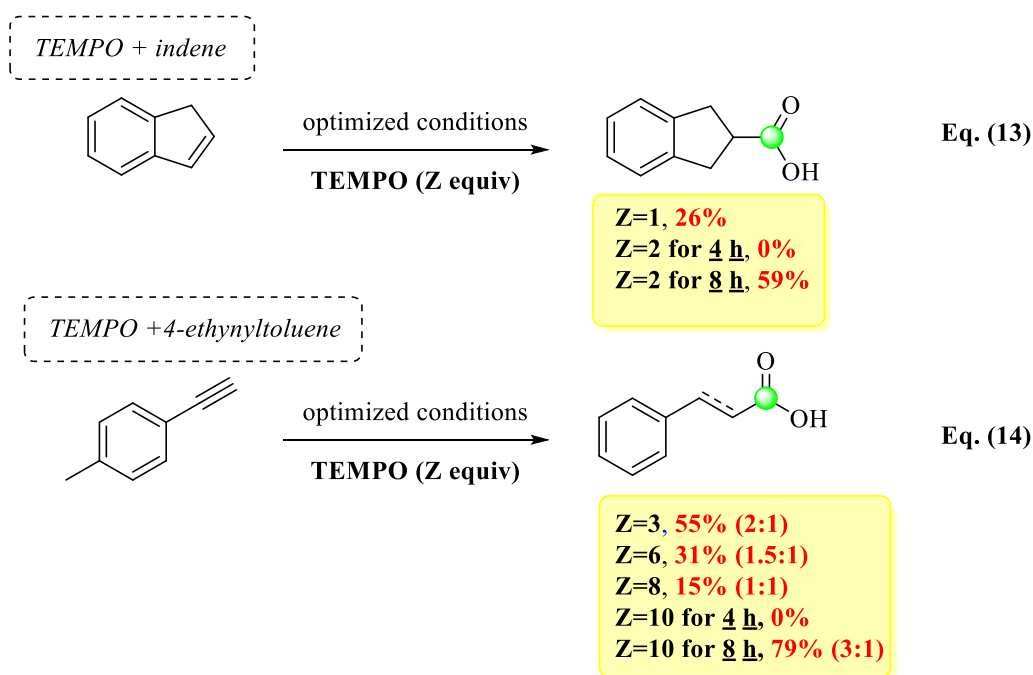


**Figure 107:** Radical trapping experiments of indene and 4-ethynyltoluene with TEMPO

This result shows that the radical scavenger did not deactivate the catalyst. We propose that it was neutralized by the formed  $\text{CO}_2^{\cdot-}$  to lead to an unstable, not isolable intermediate. This hypothesis also explains the restored reactivity after the complete consumption of TEMPO.

Based on these facts, we assume that the number of equivalents of TEMPO reveals the amount of  $\text{CO}_2$  radical anion involved in the hydrocarboxylation reaction and leading eventually to the formation of the products.

## **F. Electrochemical analysis**

- *In the case of the hydrocarboxylation of styrene derivatives (indene 3v)*

To gain insight into the electrochemical behavior of the present species in the solution, we carried out a series of cyclic voltammetry (**Figure 108**). These studies were initiated by determining the behavior of each reactant in the electrochemical medium. The cyclic voltammogram of  $\text{SmCl}_2$  electrogenerated from  $\text{SmCl}_3$  in  $\text{CH}_3\text{CN}$  containing tetrabutylammonium hexafluorophosphate  $n\text{Bu}_4\text{NPF}_6$  as supporting electrolyte is presented in the figure below. It shows a quasi-reversible system with a redox potential around  $-1.4$  V/SCE. The addition of  $\text{CO}_2$  caused the loss of the oxidation wave of  $\text{SmCl}_2$  while the reduction wave persisted with a slight cathodic shift to  $-1.6$  V/SCE. This result indicates that a chemical reaction takes place between the  $\text{CO}_2$  and  $\text{Sm(II)}$ , releasing another  $\text{Sm(III)}$  complex.

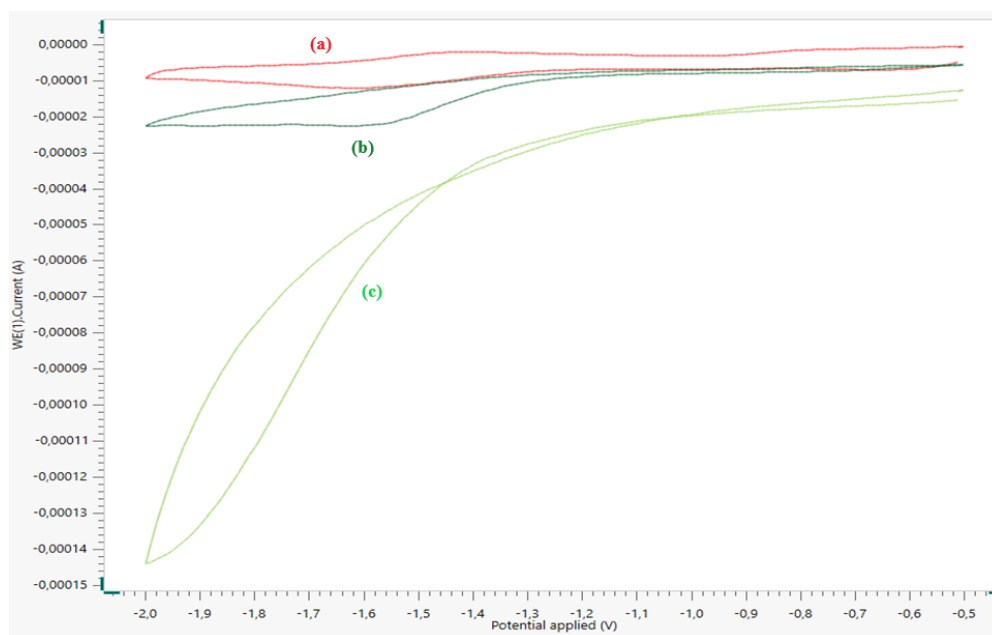


**Figure 108:** Cyclic Voltammetry analysis of hydrocarboxylation of alkenes: Glassy carbon electrode surface  $20 \text{ mm}^2$ , and platinum wire as counter electrode scanning potential between  $-0.5$  and  $-2$  V vs. SCE in  $\text{CH}_3\text{CN}$  with  $n\text{Bu}_4\text{NPF}_6$  [0.1 M]. Scan rate:  $100 \text{ mV/s}$ . (a):  $0.1 \text{ M}$  electrogenerated  $\text{SmCl}_2$  in  $0.1 \text{ M}$   $n\text{Bu}_4\text{NPF}_6$  in  $\text{CH}_3\text{CN}$ ; (b): (a) +  $\text{CO}_2$ ; (c): (b) +  $1 \text{ mL}$   $t\text{BuOH}:\text{TMSCl}:\text{indene}$  (10:8:1)

Moreover, upon the addition of  $1 \text{ mL}$  of a solution containing  $1 \text{ mmol}$  indene,  $10$  equiv  $t\text{-BuOH}$  and  $8$  equiv of  $\text{TMSCl}$ , a massive reduction wave emerged. This electrochemical response signifies that the analysis electrode is detecting a larger quantity of  $\text{SmCl}_3$  while the amount of this latter did not change. This behavior indicates the existence of a catalytic current and proves that the hydrocarboxylation is catalyzed by  $\text{SmCl}_2$ .

➤ *In the case of the hydrocarboxylation of phenylacetylene derivatives (ethynylbenzene 4a)*

Likewise, the hydrocarboxylation of the phenylacetylene was investigated by cyclic voltammetry to check if it follows the same potential regime as the indene (**Figure 109**). Indeed, the CO<sub>2</sub> changed the quasi-reversible behavior of SmCl<sub>2</sub> to an irreversible reduction wave.

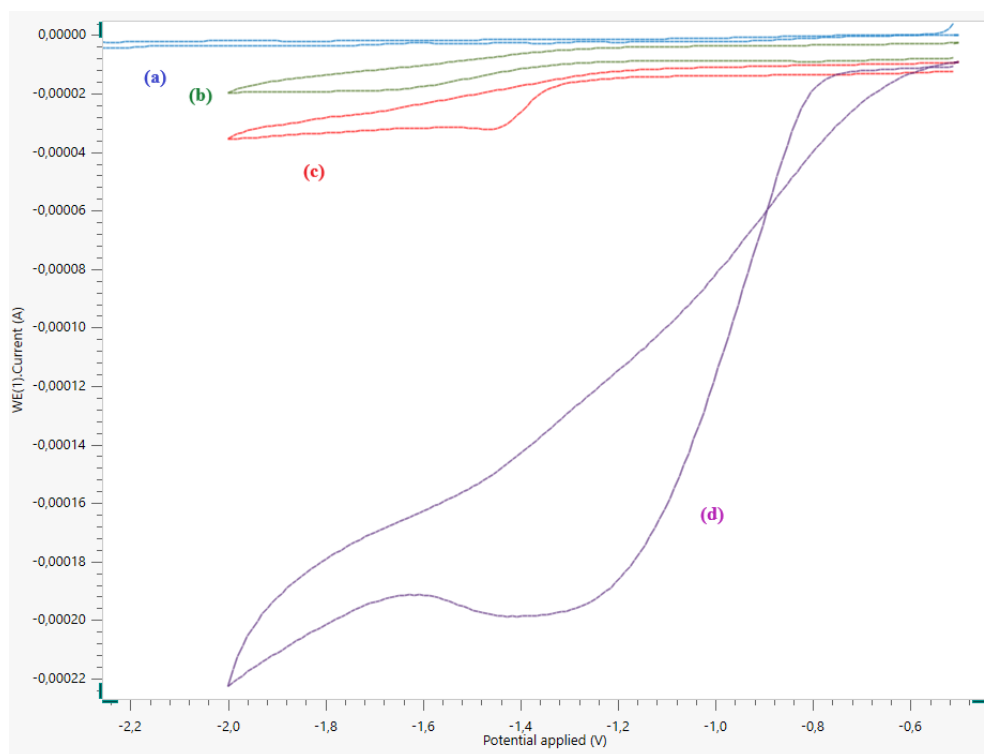


**Figure 109:** Cyclic voltammetry study of hydrocarboxylation of phenylacetylene: Glassy carbon electrode surface 20 mm<sup>2</sup>, and platinum wire as counter electrode scanning potential between -0.5 and -2 V vs. SCE in CH<sub>3</sub>CN with nBu<sub>4</sub>NPF<sub>6</sub> [0.1 M]. Scan rate: 100 mV/s. (a): 0.1 M nBu<sub>4</sub>NPF<sub>6</sub>; (b): (a) + 0.1 M electrogenerated SmCl<sub>2</sub>; (c): (b) + CO<sub>2</sub>; (d): (c) + 1 mL *t*BuOH:TMSCl:phenylacetylene (20:6:1)

The addition of a mixture of 1 mmol of phenylacetylene, 20 equiv of *t*-BuOH and 6 equiv of TMSCl triggered a catalytic current similar to the case of indene as previously described.

➤ *Electrochemical study for silylated product and cinnamic acid*

In the case of alkynes, the hydrocarboxylation of phenylacetylene derivatives resulted in a mixture of linear carboxylic acid and the acrylic acid, whereas the hydrocarboxylation of substrates protected by a TMS terminal group yielded the corresponding acrylic acid exclusively. Therefore, electrochemical investigations were essential to reveal this distinct behavior.

After conducting the cyclic voltammetry study for cinnamic acid **4'a** and for the silylated product **4'l**, we found that electrochemically, these two products behaved differently. In a cell containing 0.2 mmol of cinnamic acid in a solution of 0.1 M TBAP in CH<sub>3</sub>CN, the CV furnished two reduction waves at -1.4 V and -1.8 V vs. SCE, present in the redox potential window of Sm(III)/Sm(II). On the other hand, the silylated product showed no sign of reduction and remained inert against any electron transfer. This behavior could explain the outcome obtained with this type of substrates.

According to all our realized tests in addition to the electrochemical analyses, we propose the following mechanism for the hydrocarboxylation of alkenes and alkynes (**Figure 110**):

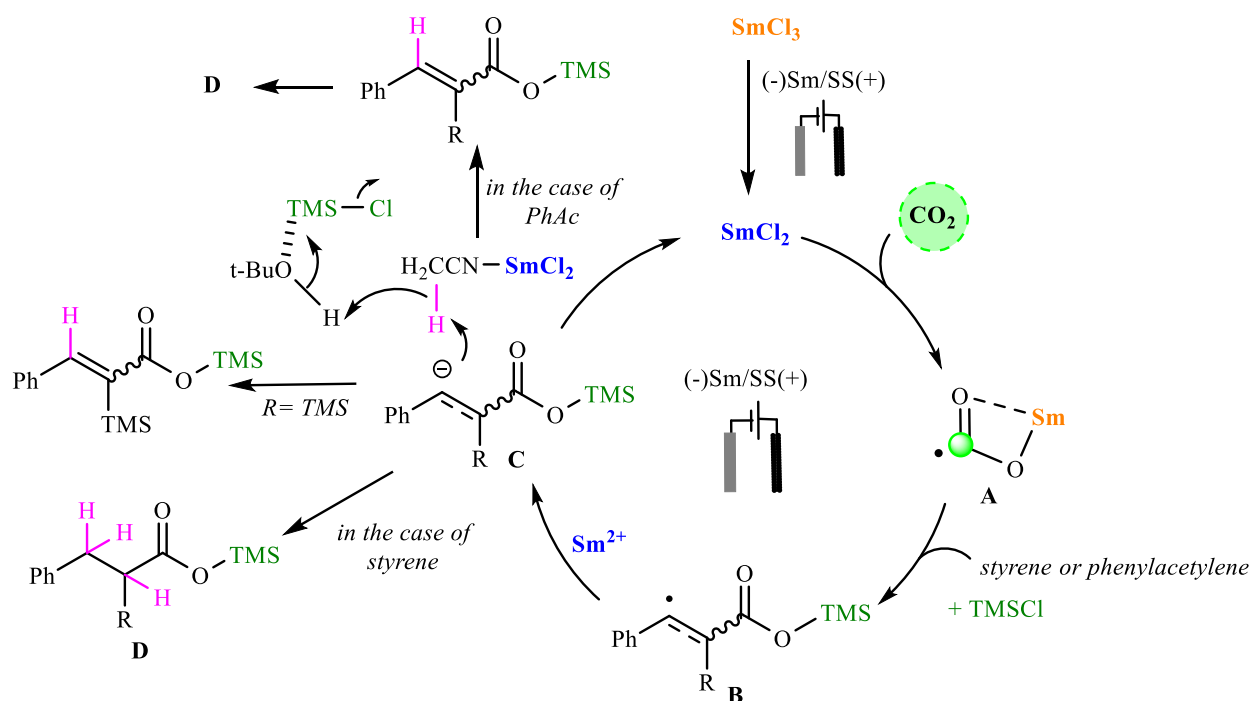


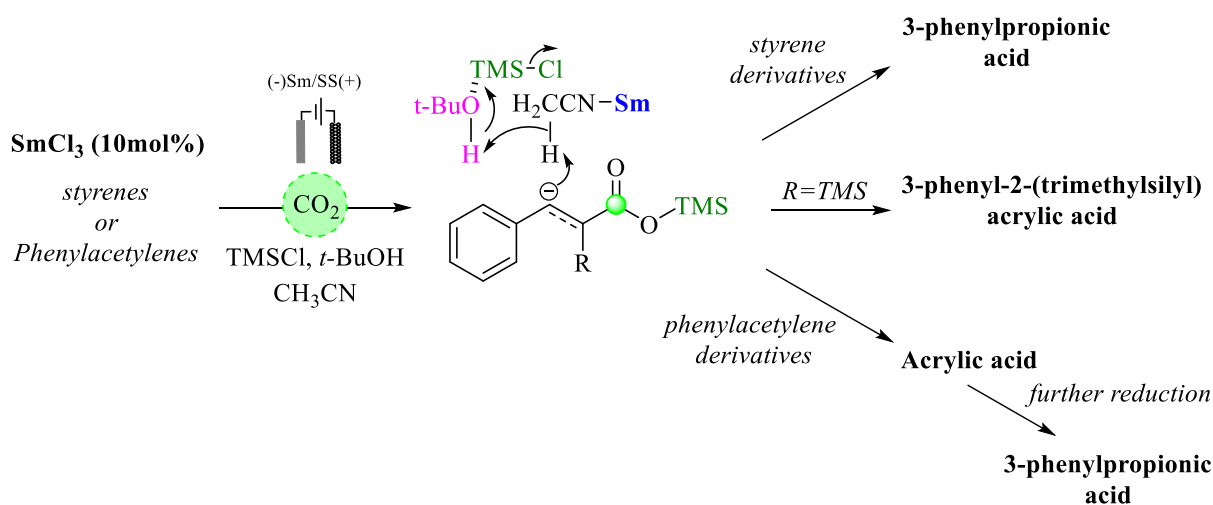
**Figure 110:** Suggested mechanism for the carboxylation of alkenes catalyzed by  $\text{SmCl}_2$  complex

Firstly, the  $\text{Sm(II)}$  activates the  $\text{CO}_2$  and generates the corresponding radical anion **A**. This latter then undergoes an anti-Markovnikov addition with the alkene or the alkyne to produce the benzylic radical **B** which is rapidly reduced to the carbanion **C**. In the solution, the  $t\text{-BuOH}$ , activated by  $\text{TMSCl}$ , is essential for the reaction. Therefore, we suggested a mechanism displaying two successive proton donations: the first one involves the solvent  $\text{CH}_3\text{CN}$  that after its activation by the catalyst, transfers one proton to form the product **D** (in the case of styrene). The  $\text{CH}_2\text{CN}^-$  anion abstracts the nearest activated proton, from the  $t\text{-BuOH-TMSCl}$  adduct, to restore its original structure and dissociate the  $\text{Sm(III)}$  to be regenerated on the cathode. In the case of phenylacetylene, further reduction/protonation steps of the acrylic acid furnish the mixture of two carboxylic acids.

## 6. Conclusion and Perspectives

In this chapter, we developed the regioselective hydrocarboxylation of styrene and phenylacetylene derivatives via  $\text{CO}_2$  activation, catalyzed by a reductive  $\text{SmCl}_2$  complex in acetonitrile. This reaction showed a remarkable anti-Markovnikov selectivity in both cases and occurred even with the reduction-resistant rich substrates to give selectively the aliphatic carboxylic acids with the alkenes, and majorly with the alkynes in good to excellent yields. Also,

protected alkynes achieved the carboxylation with good yields to afford the corresponding acrylic acids solely.



Several experimental investigations permitted the identification of the role of each species present in this reaction. Foremost,  $\text{SmCl}_2$  was proved to catalyze this reaction by different blank tests and after adding the *ter*-butanol as a proton donor, our deuterium labeling studies showed that the real proton source is the acetonitrile.

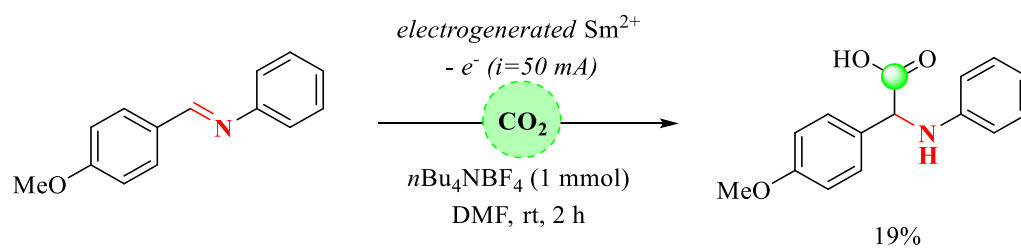
On the other hand, the exclusive formation of acrylic acids from protected alkynes was attributed to the resistance of the generated silylated product to reduction, as a conclusion deduced after examination of its electrochemical behavior.

Electrochemical measurements of both systems led us to confirm the existence of a catalytic current after the addition of  $\text{TMSCl}$  proving the transmetalation step between  $\text{Sm}(\text{III})$  and  $\text{TMSCl}$ .

Nevertheless, this unprecedented method requires further electrochemical investigations such as electro-spectrometry experiments to identify the species concerned, mainly with the protected alkynes due to their unique reactivity depending on the substitution.

Investing in the new *C-H* activation of acetonitrile by the samarium chemistry looks also promising as a new tool combining the role of solvent and proton donor. To our knowledge, it's the first report describing this kind of reactivity with an  $\text{Sm}$  complex. Applying this protocol to other transformations such as the carboxylation of imines is worth trying for selective access to original amino acids.

Targeting this subject, we conducted preliminary studies starting from (*p*-methoxybenzylidene)aniline to test the feasibility of this transformation. However, the hydrocarboxylation always resulted in the hydrolysis of the imine in  $\text{MeCN}$ . Finally, we were able to isolate 19% of the corresponding amino-acid after 2 hours of electrolysis, under electrogenerated  $\text{Sm}(\text{II})$  stoichiometric conditions using a 0.02 M solution of  $n\text{Bu}_4\text{NBF}_4$  in  $\text{DMF}$ .



The hydrolysis of the imine in these conditions was the main obstacle for the hydrocarboxylation. This perspective opens another new level of reactions in samarium chemistry, and hence, it is worth a whole research topic dedicated to examining this novel reactivity.

Similarly to the previous chapter, our reaction yielded the formation of a stereogenic carbon center, which presents an excellent opportunity to evaluate asymmetric catalysis with divalent samarium complexes.







## General conclusion

**F**or many years, the divalent samarium was used for typical stoichiometric reactions such as the reduction of functional groups or the C-C bond formation via radical cascades for instance. Looking at the fast progress in chemistry, raising the bar of creativity is the core of research today. In this thesis, we did not stick to the rules of divalent samarium, and we decided to invest its unique monoelectronic reactivity in a hot topic of current environmental, industrial and chemical research, the activation of carbon dioxide.

As we reported in this manuscript, risking and defying the norms resulted in the introduction of a whole new episode of samarium chemistry by combining three fundamental concepts: (1) The electrochemistry as a clean source of electrons and as a promising tool towards greener chemistry; (2) the catalysis based on Sm(II) complexes which was, not far ago, a huge challenge and (3) most importantly, the CO<sub>2</sub> activation, one of the most discussed topics in chemistry, to produce economy-growing class of products, the carboxylic acids.

Our principal aim concerned using commercially available starting material to keep this chemistry affordable and accessible for everyone. Besides, the use of dry ice offered easy access and danger-free CO<sub>2</sub> source compared to the standard usage of CO<sub>2</sub> bottles under pressure.

We started this work using CO<sub>2</sub> gas for the carboxylation of aromatic bromides and chlorides to deliver benzoic acids under stoichiometric conditions (**Figure 111**). Primarily, this first chapter demonstrated the formation of oxalic acid as evidence of the reduction of CO<sub>2</sub> by the electrogenerated divalent samarium. Also, it turned our attention to the impact of the solvent choice not only on the desired transformation but also on the establishment of a catalytic process.

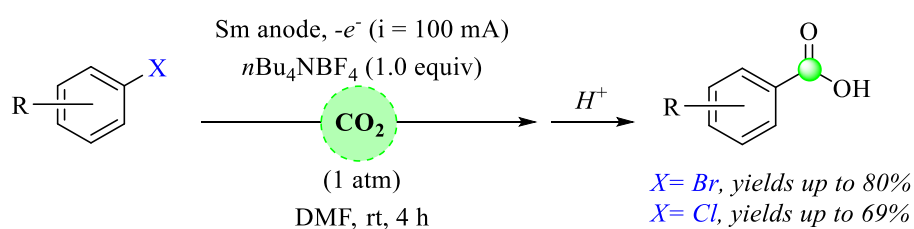


**Figure 111:** Carboxylation of aryl halides mediated by electrogenerated Sm(II) complex.

Based on the assembled information, we focused on optimizing catalytic conditions for the carboxylation of benzyl chlorides, motivated by the high pharmaceutical value of the corresponding phenylacetic acids (**Figure 112**). After successful catalytic attempts using dry ice as CO<sub>2</sub> source, the reaction provided a series of carboxylic acids, giving us hope that other applications may find its way relying on this new reactivity.

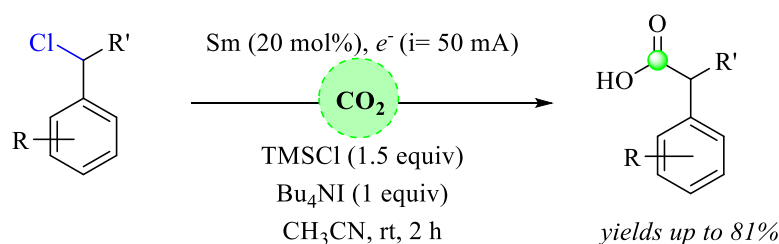


**Figure 112:** Catalytic carboxylation of benzyl chloride derivatives initiated by Sm(II) complexes.

Unactivated hydrocarbons are considered as a challenging material to deal with due to their stability and the absence of any significant functional group suitable for chemical transformations. Looking for an original goal, we tested the hydrocarboxylation of styrene and phenylacetylene analogs as starting materials to generate acrylic and aliphatic carboxylic acids (**Figure 113**).

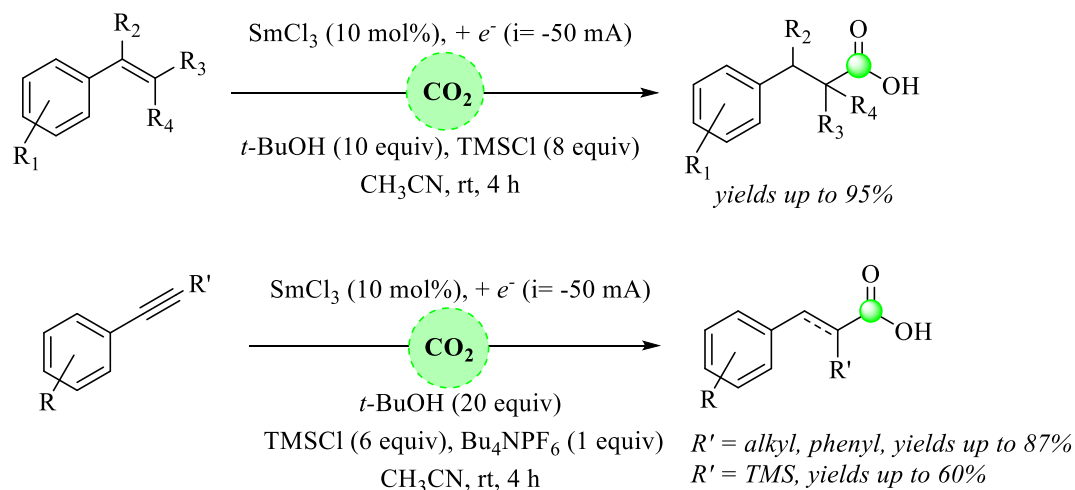


**Figure 113:** Carboxylation of styrene and phenylacetylene derivatives catalyzed by electrogenerated Sm(II) complexes.

We were amazed by the  $\beta$ -selectivity of this method, which encouraged us to dig deeper into the mechanistic pathway. Several experiments revealed surprisingly that the solvent, which is acetonitrile, reacted as a proton donor in this case. The activation of  $\text{CH}_3\text{CN}$  by samarium complexes can be exploited in another type of reaction and can reveal an unexplored section of samarium applications.

Despite the significant advance, the next challenge to overcome remains the asymmetric catalysis using divalent Samarium complexes. The radical reducing nature of these species and their high number of coordination sites complicate its use in this field.<sup>42</sup> Still, it is worth investing time and resources to solve this mystery because once exposed, another horizon of samarium chemistry begins.



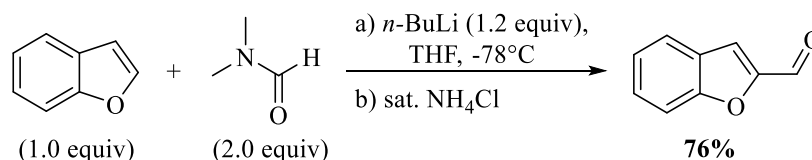


# Experimental Part

## Instrumentation and Chemicals

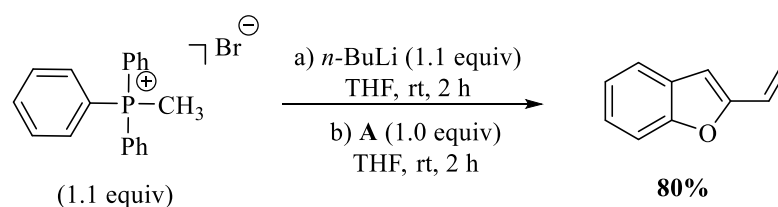
All commercially available reagents were used without further purification unless otherwise stated. All solvents were also used without further purification. CH<sub>3</sub>CN was purchased from VWR chemicals and tetrabutylammonium hexafluorophosphate (*n*Bu<sub>4</sub>NPF<sub>6</sub>) from TCI. The samarium rod was a 12.7mm diameter, 99.9% (metals basis excluding Ta) rod, purchased from Alfa-Aesar and the stainless-steel grid from Goodfellow (AISI 304). Electrolysis and electrochemical studies were performed using an EGG Instrument Potentiostat/Galvanostat Model 273. The electrolysis was conducted in an undivided cell equipped with a samarium rod as anode and a stainless-steel grid as a cathode. NMR spectra were recorded on Bruker AM 400 (400 MHz), 360 (360 MHz), 300 (300 MHz) or AM 250 (250 MHz) in CDCl<sub>3</sub>. Data for <sup>1</sup>H NMR are recorded as follows: chemical shift ( $\delta$ , ppm), multiplicity (s = singlet, d = doublet, t = triplet, m = multiplet, q = quartet, dd = doublet of doublets, dt = doublet of triplets, td = triplet of doublets, and br = broad signal), coupling constant (*J*, Hz) and integration. Reactions were monitored by thin-layer chromatography (TLC), using bromocresol as TLC stain and column chromatography purifications were carried out using on silica gel.

## Synthesis of 2-vinylbenzofuran (3k)



Following a reported procedure in the literature,<sup>121</sup> to a solution of benzofuran (500 mg, 1.0 equiv) in dry THF (20 mL) cooled at -78 °C under Ar was added *n*-BuLi (3.16 mL, 1.6 M in hexane, 1.2 equiv), dropwise. After stirring the mixture for 1 h at -78°C, DMF (0.63 mL, 2 equiv) was added dropwise and stirred for another 4.5 h at -78°C. After the complete consumption of benzofuran, the reaction was quenched with sat. NH<sub>4</sub>Cl. The aqueous layer was extracted with EtOAc (3x) and the combined organic layer was dried over MgSO<sub>4</sub>, filtered, concentrated *in vacuo*. The resultant crude residue was purified by column chromatography (0-100% EtOAc/cyclohexane) and the benzofuran-2-carbaldehyde was isolated in 76% yield (504 mg, 3.2 mmol).

<sup>121</sup> S. Senaweera, J. D. Weaver, *Chem. Commun.* **2017**, 53, 7545.

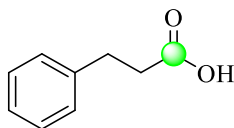


Following a reported procedure in the literature,<sup>101</sup> to a solution of methyltriphenylphosphonium bromide (1.25 g, 1.1 equiv) in THF (20 mL) was slowly added *n*-BuLi (1.4 mL, 2.5 M solution in hexanes, 1.1 equiv) at room temperature. The mixture was stirred for 2 h at room temperature before adding a solution of aldehyde (540 mg, 1.0 equiv) in THF (5 mL) dropwise and leave the reaction for another 2 h at room temperature. The reaction mixture was quenched with water, and the aqueous portion was extracted with diethyl ether. The combined organic layers were washed with brine, dried over anhydrous magnesium sulfate, filtered, and concentrated under reduced pressure. The crude mixture was purified by column chromatography (100% cyclohexane) to afford the 2-vinylbenzofuran **3k** (2.56 mmol, 80%).

## General Procedure for the catalytic carboxylation of styrene derivatives

An undivided cell charged with tetrabutylammonium hexafluorophosphate  $n\text{Bu}_4\text{NPF}_6$  (1 mmol) in acetonitrile (40 mL), equipped with a samarium rod as the cathode and a stainless-steel as the anode, was used. The electro-generation of  $\text{Sm}^{2+}$  from  $\text{SmCl}_3$  (0.1 equiv) was started by setting the chronopotentiometry mode for 15000 seconds with  $i = -50$  mA. The dry ice was carefully added to the mixture in small pieces followed by the alkene (1.0 mmol), the *ter*-butanol *t*-BuOH (10 equiv) the trimethylsilyl chloride  $\text{TMSCl}$  (8 equiv). During the electrolysis, small pieces of dry ice were added each 15 min. After 4 hours of electrolysis, the reaction was quenched with diethyl ether  $\text{Et}_2\text{O}$  (10 mL), and the solvent was evaporated. To the obtained solid, a solution of HCl (2 M) was added and the aqueous solution was extracted with  $\text{Et}_2\text{O}$  (2\*30 mL). The combined organic phase was washed with water and brine and dried over anhydrous  $\text{MgSO}_4$ . The solvent evaporation under *vacuo* furnished the product that was purified by column chromatography on silica gel (90/10 then 50/50 PE/ EtOAc).

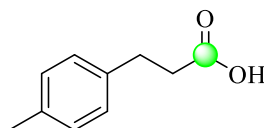
## Characterization of the compounds



**3-phenylpropanoic acid (3'a):** 97.5 mg (0.65 mmol, 65%).  $^1\text{H NMR}$  (360 MHz,  $\text{CDCl}_3$ )  $\delta$  11.31 (br, 1H), 7.42-7.32 (m, 5H), 3.08 (t,  $J = 7.5$  Hz, 2H), 2.80 (t,  $J = 7.6$  Hz, 2H).

$^{13}\text{C NMR}$  (75 MHz,  $\text{CDCl}_3$ )  $\delta$  177.8, 140.1, 128.5, 128.2, 126.3, 35.3, 30.5.

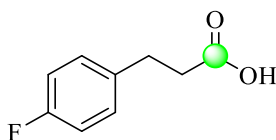
The  $^1\text{H NMR}$  and  $^{13}\text{C NMR}$  spectra are in agreement with those reported in the literature.<sup>101</sup>



**3-(p-tolyl)propanoic acid (3'b):** 100 mg (0.61, 61%).  $^1\text{H NMR}$  (360 MHz,  $\text{CDCl}_3$ )  $\delta$  7.19 (m, 4H), 3.00 (t,  $J = 7.8$  Hz, 2H), 2.74 (t,  $J = 7.8$  Hz, 2H), 2.41 (s, 3H).

$^{13}\text{C NMR}$  (91 MHz,  $\text{CDCl}_3$ )  $\delta$  179.6, 137.1, 135.9, 129.3, 128.2, 35.8, 30.2, 21.0.

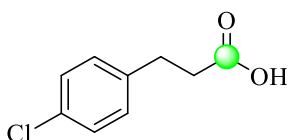
The  $^1\text{H NMR}$  and  $^{13}\text{C NMR}$  spectra are in agreement with those reported in the literature.<sup>101</sup>



**3-(4-fluorophenyl)propanoic acid (3'c):** 70.5 mg (0.42, 42%).  $^1\text{H NMR}$  (360 MHz,  $\text{CDCl}_3$ )  $\delta$  7.22 – 7.11 (m, 2H), 7.04 – 6.91 (m, 2H), 2.93 (t,  $J = 7.7$  Hz, 2H), 2.67 (t,  $J = 7.7$  Hz, 2H).

$^{13}\text{C NMR}$  (91 MHz,  $\text{CDCl}_3$ )  $\delta$  179.2, 161.4 (d,  $J = 257.6$  Hz), 135.7 (d,  $J = 3.6$  Hz), 129.6 (d,  $J = 7.9$  Hz), 115.3 (d,  $J = 21.2$  Hz), 35.6, 29.6.

The  $^1\text{H NMR}$  and  $^{13}\text{C NMR}$  spectra are in agreement with those reported in the literature.<sup>101</sup>

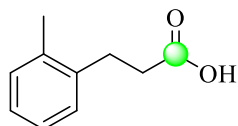


**3-(4-chlorophenyl)propanoic acid (3'd):** 40.5 mg (0.22, 22%).  $^1\text{H NMR}$  (360 MHz,  $\text{CDCl}_3$ )  $\delta$  7.42 – 7.15 (m, 4H), 3.02 (t,  $J = 7.8$  Hz, 2H), 2.70 (t,  $J = 7.8$  Hz, 2H).

$^{13}\text{C NMR}$  (91 MHz,  $\text{CDCl}_3$ )  $\delta$  178.6, 140.1, 128.5, 128.2, 126.3, 35.5, 30.5.



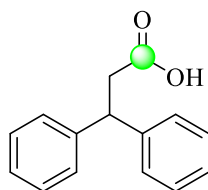
The  $^1\text{H}$  NMR and  $^{13}\text{C}$  NMR spectra are in agreement with those reported in the literature.<sup>122</sup>



**3-(o-tolyl)propanoic acid (3'e):** 156 mg (0.95, 95%).  $^1\text{H}$  NMR (300 MHz,  $\text{CDCl}_3$ )  $\delta$  11.56 (br, 1H), 7.24 (m, 4H), 3.05 (t,  $J = 7.0$  Hz, 2H), 2.80 – 2.67 (t,  $J = 7.0$  Hz, 2H), 2.42 (s, 3H).

$^{13}\text{C}$  NMR (75 MHz,  $\text{CDCl}_3$ )  $\delta$  179.8, 138.3, 136.0, 130.4, 128.5, 126.6, 126.2, 34.4, 28.0, 19.3.

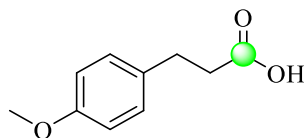
The  $^1\text{H}$  NMR and  $^{13}\text{C}$  NMR spectra are in agreement with those reported in the literature.<sup>122</sup>



**3,3-diphenylpropanoic acid (3'f):** 113 mg (0.5 mmol, 50%).  $^1\text{H}$  NMR (360 MHz,  $\text{CDCl}_3$ )  $\delta$  7.55 – 7.08 (m, 10H), 4.58 (t,  $J = 7.9$  Hz, 1H), 3.14 (d,  $J = 7.9$  Hz, 2H).

$^{13}\text{C}$  NMR (75 MHz,  $\text{CDCl}_3$ )  $\delta$  178.0, 143.2, 128.6, 128.1, 128.0, 127.6, 126.6, 46.6, 40.4.

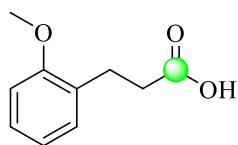
The  $^1\text{H}$  NMR and  $^{13}\text{C}$  NMR spectra are in agreement with those reported in the literature.<sup>101</sup>



**3-(4-methoxyphenyl)propanoic acid (3'g):** 99 mg (0.55 mmol, 55%).  $^1\text{H}$  NMR (360 MHz,  $\text{CDCl}_3$ )  $\delta$  7.17 (d,  $J = 8.6$  Hz, 2H), 6.88 (d,  $J = 8.5$  Hz, 2H), 3.83 (s, 3H), 2.94 (t,  $J = 7.7$  Hz, 2H), 2.68 (t,  $J = 7.7$  Hz, 2H).

$^{13}\text{C}$  NMR (75 MHz,  $\text{CDCl}_3$ )  $\delta$  177.4, 159.0, 130.5, 125.4, 114.2, 55.4, 40.1.

The  $^1\text{H}$  NMR and  $^{13}\text{C}$  NMR spectra are in agreement with those reported in the literature.<sup>101</sup>

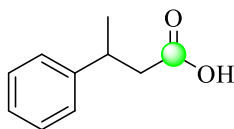


**3-(2-methoxyphenyl)propanoic acid (3'h):** 81 mg (0.45 mg, 45%).  $^1\text{H}$  NMR (300 MHz,  $\text{CDCl}_3$ )  $\delta$  7.30 – 7.14 (m, 2H), 6.90 (dd,  $J = 14.3, 7.6$  Hz, 2H), 3.85 (s, 3H), 2.98 (t,  $J = 7.7$  Hz, 2H), 2.69 (t,  $J = 7.7$  Hz, 2H).

<sup>122</sup> S. M. Kim, H. Y. Shin, D. W. Kim, J. W. Yang, *ChemSusChem* **2016**, 9, 241.

$^{13}\text{C}$  NMR (75 MHz,  $\text{CDCl}_3$ )  $\delta$  179.8, 157.4, 129.9, 128.4, 127.7, 120.4, 110.2, 55.1, 34.0, 25.8.

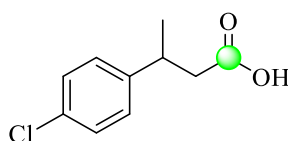
The  $^1\text{H}$  NMR and  $^{13}\text{C}$  NMR spectra are in agreement with those reported in the literature.<sup>123</sup>



**3-phenylbutanoic acid (3'i):** 94.5 mg (0.6 mmol, 60%).  $^1\text{H}$  NMR (360 MHz,  $\text{CDCl}_3$ )  $\delta$  7.49 – 7.13 (m, 5H), 3.41 – 3.24 (m, 1H), 2.76 – 2.59 (m, 2H), 1.37 (d,  $J = 7.0$  Hz, 3H).

$^{13}\text{C}$  NMR (91 MHz,  $\text{CDCl}_3$ )  $\delta$  178.7, 145.4, 128.5, 126.7, 126.5, 42.6, 36.1, 21.8.

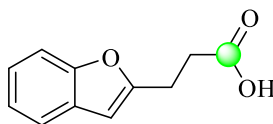
The  $^1\text{H}$  NMR and  $^{13}\text{C}$  NMR spectra are in agreement with those reported in the literature.<sup>101</sup>



**3-(4-chlorophenyl)butanoic acid (3'j):** 13 mg (0.07 mmol, 7%).  $^1\text{H}$  NMR (360 MHz,  $\text{CDCl}_3$ )  $\delta$  7.35 – 7.30 (m, 2H), 7.27 – 7.22 (m, 2H), 3.35 – 3.24 (m, 1H), 2.75 – 2.55 (m, 2H), 1.35 (d,  $J = 6.9$  Hz, 3H).

$^{13}\text{C}$  NMR (91 MHz,  $\text{CDCl}_3$ )  $\delta$  178.5, 144.0, 132.4, 128.9, 128.3, 42.6, 35.8, 22.1.

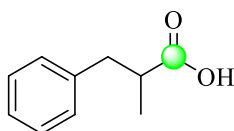
The  $^1\text{H}$  NMR and  $^{13}\text{C}$  NMR spectra are in agreement with those reported in the literature.<sup>124</sup>



**3-(benzofuran-2-yl)propanoic acid (3'k):** 99mg (0.52 mmol, 52%).  $^1\text{H}$  NMR (360 MHz,  $\text{CDCl}_3$ )  $\delta$  7.52 – 7.45 (m, 1H), 7.41 (d,  $J = 7.7$  Hz, 1H), 7.20 (td,  $J = 14.1, 7.1$  Hz, 2H), 6.45 (s, 1H), 3.13 (t,  $J = 7.5$  Hz, 2H), 2.84 (t,  $J = 7.5$  Hz, 2H).

$^{13}\text{C}$  NMR (91 MHz,  $\text{CDCl}_3$ )  $\delta$  177.2, 156.8, 154.6, 128.5, 123.4, 122.6, 120.5, 110.8, 102.6, 31.8, 23.7.

The  $^1\text{H}$  NMR and  $^{13}\text{C}$  NMR spectra are in agreement with those reported in the literature.<sup>101</sup>



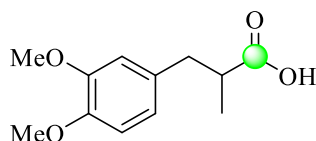
**2-methyl-3-phenylpropanoic acid (3'r):** 156 mg (0.95 mmol, 95%).  $^1\text{H}$  NMR (360 MHz,  $\text{CDCl}_3$ )  $\delta$  10.70 (br, 1H), 7.50 – 7.14 (m, 5H), 3.14 (dd,  $J = 13.3, 6.2$  Hz, 1H), 2.82 (dq,  $J = 13.2, 6.8$  Hz, 1H), 2.73 (dd,  $J = 13.3, 8.0$  Hz, 1H), 1.23 (d,  $J = 6.9$  Hz, 3H).

$^{13}\text{C}$  NMR (91 MHz,  $\text{CDCl}_3$ )  $\delta$  182.8, 139.1, 129.0, 128.5, 126.5, 41.3, 39.3, 16.5.

<sup>123</sup> S. Shabbi, S. Lee, M. Lim, H. Lee, H. Ko, Y. Lee, H. Rhee, *J. Organom. Chem.* **2017**, *846*, 296.

<sup>124</sup> Y. Wang, W. Ren, J. Li, H. Wang, Y. Shi, *Org. Lett.* **2014**, *16*, 5960.

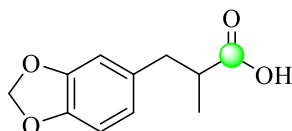
The  $^1\text{H}$  NMR and  $^{13}\text{C}$  NMR spectra are in agreement with those reported in the literature.<sup>101</sup>



**3-(3,4-dimethoxyphenyl)-2-methylpropanoic acid (3's):** 80 mg (0.36 mmol, 36%).  $^1\text{H}$  NMR (360 MHz,  $\text{CDCl}_3$ )  $\delta$  6.76 (m, 3H), 3.85 (s, 6H), 3.01 (dd,  $J = 13.4, 6.5$  Hz, 1H), 2.73 (dq,  $J = 13.5, 6.9$  Hz, 1H), 2.63 (dd,  $J = 13.4, 7.8$  Hz, 1H), 1.18 (d,  $J = 6.9$  Hz, 3H).

$^{13}\text{C}$  NMR (91 MHz,  $\text{CDCl}_3$ )  $\delta$  182.3, 148.7, 147.5, 131.5, 121.0, 112.1, 111.1, 55.8, 55.7, 41.4, 38.9, 16.4.

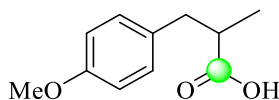
The  $^1\text{H}$  NMR and  $^{13}\text{C}$  NMR spectra are in agreement with those reported in the literature.<sup>125</sup>



**3-(benzo[d][1,3]dioxol-5-yl)-2-methylpropanoic acid (3't):** 93 mg (0.45 mmol, 45%).  $^1\text{H}$  NMR (360 MHz,  $\text{CDCl}_3$ )  $\delta$  6.69 (m, 3H), 5.94 (s, 2H), 3.00 (dd,  $J = 13.4, 6.5$  Hz, 1H), 2.71 (m, 1H), 2.62 (dd,  $J = 13.4, 7.8$  Hz, 2H), 1.19 (d,  $J = 6.9$  Hz, 3H).

$^{13}\text{C}$  NMR (91 MHz,  $\text{CDCl}_3$ )  $\delta$  182.4, 147.6, 146.1, 132.7, 121.9, 109.3, 108.1, 100.8, 41.4, 39.0, 16.4.

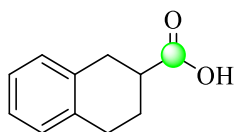
The  $^1\text{H}$  NMR and  $^{13}\text{C}$  NMR spectra are in agreement with those reported in the literature.<sup>126</sup>



**3-(4-methoxyphenyl)-2-methylpropanoic acid (3'u):** 105 mg (0.54 mmol, 54%).  $^1\text{H}$  NMR (360 MHz,  $\text{CDCl}_3$ )  $\delta$  7.14 (d,  $J = 8.6$  Hz, 2H), 6.87 (d,  $J = 8.6$  Hz, 2H), 3.83 (s, 3H), 3.05 (dd,  $J = 13.3, 6.3$  Hz, 1H), 2.85 – 2.71 (m, 1H), 2.67 (dd,  $J = 13.3, 7.8$  Hz, 1H), 1.21 (d,  $J = 6.8$  Hz, 3H).

$^{13}\text{C}$  NMR (91 MHz,  $\text{CDCl}_3$ )  $\delta$  182.4, 158.2, 131.1, 129.9, 113.9, 55.2, 41.4, 38.4, 16.4.

The  $^1\text{H}$  NMR and  $^{13}\text{C}$  NMR spectra are in agreement with those reported in the literature.<sup>127</sup>



<sup>125</sup> J. P. Cueva, A. Gallardo-Godoy, J. I. Juncosa, P. A. Vidi, M. A. Lill, V. J. Watts, D. E. Nichols, *J. Med. Chem.* **2011**, *54*, **15**, 5508.

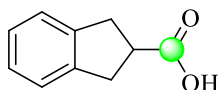
<sup>126</sup> M. Schulze, *Synthetic Communications* **2010**, *40*, **10**, 1461.

<sup>127</sup> Y. Zhu, X. Chen, C. Yuan, G. Li, J. Zhang, Y. Zhao, *Nature Comm.* **2017**, *8*, 14904.

**1,2,3,4-tetrahydronaphthalene-2-carboxylic acid (3'v):** 126 mg (0.73 mmol, 73%).  $^1\text{H NMR}$  (300 MHz,  $\text{CDCl}_3$ )  $\delta$  11.42 (s, 1H), 7.38 – 7.03 (m, 4H), 3.13 (d,  $J = 7.3$  Hz, 2H), 3.01 – 2.81 (m, 3H), 2.34 (m, 1H), 1.98 (m, 1H).

$^{13}\text{C NMR}$  (63 MHz,  $\text{CDCl}_3$ )  $\delta$  181.4, 135.6, 134.6, 129.1, 128.9, 126.0, 125.9, 39.7, 31.3, 28.4, 25.6.

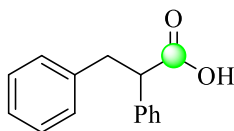
The  $^1\text{H NMR}$  and  $^{13}\text{C NMR}$  spectra are in agreement with those reported in the literature.<sup>101</sup>



**2,3-dihydro-1H-indene-2-carboxylic acid (3'w):** 100 mg (0.62 mmol, 62%).  $^1\text{H NMR}$  (360 MHz,  $\text{CDCl}_3$ )  $\delta$  7.35 – 7.13 (m, 2H), 3.49 – 3.23 (m, 3H).

$^{13}\text{C NMR}$  (63 MHz,  $\text{CDCl}_3$ )  $\delta$  182.0, 141.3, 126.7, 124.4, 43.4, 36.0.

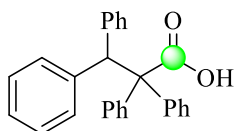
The  $^1\text{H NMR}$  and  $^{13}\text{C NMR}$  spectra are in agreement with those reported in the literature.<sup>101</sup>



**2,3-diphenylpropanoic acid (3'x):** 158 mg (0.7 mmol, 70%).  $^1\text{H NMR}$  (300 MHz,  $\text{CDCl}_3$ )  $\delta$  10.16 (br, 1H), 7.65 – 6.97 (m, 10H), 3.94 (t,  $J = 7.7$  Hz, 1H), 3.49 (dd,  $J = 13.8, 8.3$  Hz, 1H), 3.11 (dd,  $J = 13.8, 7.1$  Hz, 1H).

$^{13}\text{C NMR}$  (75 MHz,  $\text{CDCl}_3$ )  $\delta$  179.6, 138.7, 137.9, 128.9, 128.7, 128.4, 128.1, 127.6, 126.5, 53.5, 39.3.

The  $^1\text{H NMR}$  and  $^{13}\text{C NMR}$  spectra are in agreement with those reported in the literature.<sup>86</sup>



**2,2,3,3-tetraphenylpropanoic acid (3'y):** 166 mg (0.44 mmol, 44%).  $^1\text{H NMR}$  (300 MHz,  $\text{CDCl}_3$ )  $\delta$  8.06 – 6.54 (m, 15H), 5.08 (s, 1H).

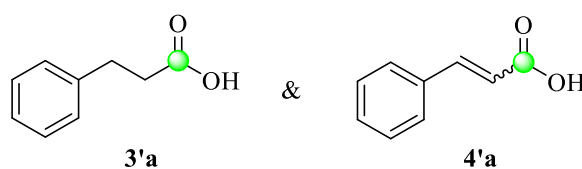
$^{13}\text{C NMR}$  (75 MHz,  $\text{CDCl}_3$ )  $\delta$  177.7, 137.9, 128.6, 128.3, 127.5, 77.2, 56.9.

**HRMS (m/z)  $[\text{M} + \text{Na}]^+$  calculated 401.1512 found 401.1520.**

## General Procedure for the catalytic carboxylation of phenylacetylene derivatives

An undivided cell charged with tetrabutylammonium hexafluorophosphate  $n\text{Bu}_4\text{NPF}_6$  (1 mmol, 1.0 equiv) in acetonitrile (40 mL), equipped with a samarium rod as the cathode and a stainless-steel as the anode, was used. The electro-generation of  $\text{Sm}^{2+}$  from  $\text{SmCl}_3$  (0.1 equiv) was started by setting the chronopotentiometry mode for 15000 seconds with  $i = -50$  mA. After a few minutes, the dry ice was carefully added to the mixture in small pieces followed by the alkyne (1 mmol), the *ter*-butanol *t*-BuOH (20 equiv) the trimethylsilyl chloride TMSCl (6.0 equiv). During the electrolysis, small pieces of dry ice were added each 15 min. After 4 hours of electrolysis, the reaction was quenched with diethyl ether  $\text{Et}_2\text{O}$  (10 mL), and the solvent was evaporated. To the obtained solid, a solution of HCl (2 M) was added and the aqueous solution was extracted with  $\text{Et}_2\text{O}$  (2\*30 mL). The combined organic phase was washed with water and brine and dried over anhydrous  $\text{MgSO}_4$ . The solvent evaporation under *vacuo* furnished the product that was purified by column chromatography on silica gel (90/10 then 50/50 PE/ EtOAc).

### Characterization of the compounds

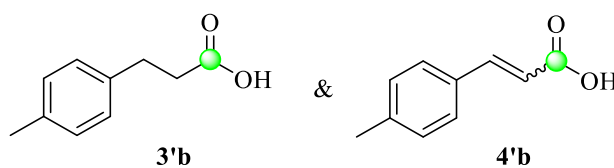


87% (**3'a**:**4'a** 3:1, *E/Z* 1/4).

**3-phenylacrylic acid (4'a):**  $^1\text{H NMR}$  (300 MHz,  $\text{CDCl}_3$ ) 7.63 – 7.21 (m, 5H), 6.48 (d,  $J = 15.9$  Hz, 1H) (*E*), 6.01 (d,  $J = 12.6$  Hz, 1H) (*Z*).

$^{13}\text{C NMR}$  (75 MHz,  $\text{CDCl}_3$ ): 171.8, 143.2, 135.2, 130.2, 128.5, 127.9, 116.4.

The  $^1\text{H NMR}$  and  $^{13}\text{C NMR}$  spectra are in agreement with those reported in the literature.<sup>128</sup>



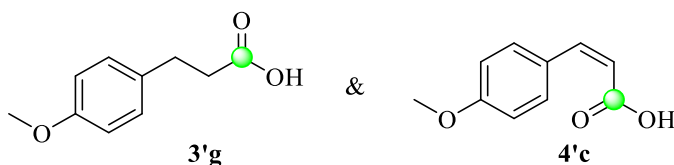
91% (**3'b**:**4'b** 2.6:1, *E/Z* 1/4)

<sup>128</sup> D. Wang, W. Liu, F. Bian, W. Yu, *New J. Chem.* **2015**, 39, 2052.

**3-(p-tolyl)acrylic acid (4'b):**  $^1\text{H NMR}$  (360 MHz,  $\text{CDCl}_3$ )  $\delta$  7.80 (d,  $J = 15.9$  Hz, 1H) (*E*), 7.59 (d,  $J = 8.1$  Hz, 2H) (*Z*), 7.49 (d,  $J = 8.1$  Hz, 2H) (*E*), 7.25 (d,  $J = 7.9$  Hz, 2H) (*E*), 7.21 (d,  $J = 7.9$  Hz, 2H) (*Z*), 7.07 (d,  $J = 12.7$  Hz, 1H) (*Z*), 6.44 (d,  $J = 15.9$  Hz, 1H) (*E*), 5.95 (d,  $J = 12.7$  Hz, 2H) (*Z*), 2.43 (s, 3H) (*E*), 2.41 (s, 3H) (*Z*).

$^{13}\text{C NMR}$  (91 MHz,  $\text{CDCl}_3$ )  $\delta$  172.6, 147.1, 141.3, 131.3, 129.7, 128.4, 116.2, 21.5.

The  $^1\text{H NMR}$  and  $^{13}\text{C NMR}$  spectra are in agreement with those reported in the literature.<sup>128</sup>

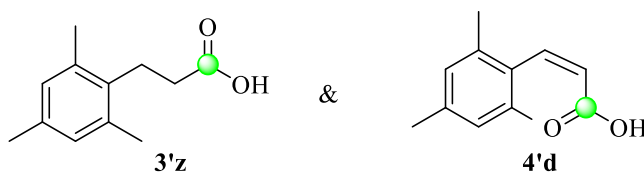


76% ( $3'g:4'c$  1:1, *Z* isomer).

**(Z)-3-(4-methoxyphenyl)acrylic acid (4'c):**  $^1\text{H NMR}$  (360 MHz,  $\text{CDCl}_3$ )  $\delta$  7.73 (d,  $J = 8.7$  Hz, 2H), 6.99 (d,  $J = 12.8$  Hz, 1H), 6.91 (d,  $J = 8.8$  Hz, 2H), 5.86 (d,  $J = 12.8$  Hz, 1H), 3.86 (s, 3H).

$^{13}\text{C NMR}$  (91 MHz,  $\text{CDCl}_3$ )  $\delta$  172.1, 160.6, 145.9, 132.6, 126.9, 115.9, 113.5, 55.2.

The  $^1\text{H NMR}$  and  $^{13}\text{C NMR}$  spectra are in agreement with those reported in the literature.<sup>128</sup>



68% ( $3'z:4'd$  1.2:1, *Z* isomer)

**3-mesitylpropanoic acid (3'z):**  $^1\text{H NMR}$  (360 MHz,  $\text{CDCl}_3$ )  $\delta$  6.85 (s, 2H), 2.97 (t,  $J = 8.4$  Hz, 2H), 2.49 (t,  $J = 8.4$  Hz, 2H), 2.31 (s, 6H), 2.25 (s, 3H).

$^{13}\text{C NMR}$  (91 MHz,  $\text{CDCl}_3$ )  $\delta$  179.8, 136.2, 135.9, 133.9, 129.3, 33.7, 24.7, 21.0, 19.8.

The  $^1\text{H NMR}$  and  $^{13}\text{C NMR}$  spectra are in agreement with those reported in the literature.<sup>129</sup>

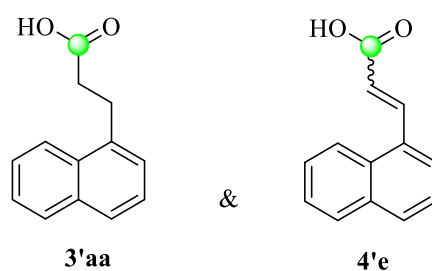
**(Z)-3-mesitylacrylic acid (4'd):**  $^1\text{H NMR}$  (360 MHz,  $\text{CDCl}_3$ )  $\delta$  7.14 (d,  $J = 11.9$  Hz, 1H), 6.88 (d,  $J = 13.2$  Hz, 2H), 6.13 (d,  $J = 12.1$  Hz, 1H), 2.29 (s, 3H), 2.18 (s, 6H).

$^{13}\text{C NMR}$  (91 MHz,  $\text{CDCl}_3$ )  $\delta$  171.1, 146.2, 136.9, 134.4, 131.9, 127.8, 122.0, 20.8, 20.0.

The  $^1\text{H NMR}$  and  $^{13}\text{C NMR}$  spectra are in agreement with those reported in the literature.<sup>130</sup>

<sup>129</sup> W. Liu, W. Ren, J. Li, Y. Shi, W. Chang, Y. Shi, *Org. Lett.* **2017**, *19*, **7**, 1748.

<sup>130</sup> T. Hashimoto, S. Kutubi, T. Izumi, A. Rahman, T. Kitamura, *Tetrahedron* **2011**, *696*, **1**, 99.



60% (3'aa:4'e 2:1, E/Z 1/4)

**3-(naphthalen-1-yl)propanoic acid (3'aa):**  $^1\text{H NMR}$  (300 MHz,  $\text{CDCl}_3$ )  $\delta$  8.03 (d,  $J = 8.3$ , 1H), 7.87 (d,  $J = 7.9$ , 1H), 7.75 (d,  $J = 7.9$ , 1H), 7.52 (m, 2H), 7.44 – 7.29 (m, 2H), 3.52 – 3.4 (m, 2H), 2.90 – 2.77 (m, 2H).

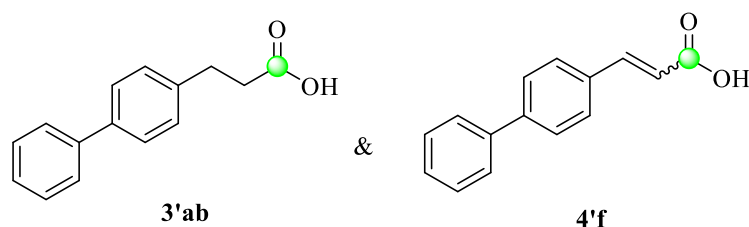
$^{13}\text{C NMR}$  (75 MHz,  $\text{CDCl}_3$ )  $\delta$  178.2, 136.0, 133.8, 131.5, 128.9, 127.2, 126.1, 125.9, 125.6, 125.5, 123.2, 34.7, 27.8.

The  $^1\text{H NMR}$  and  $^{13}\text{C NMR}$  spectra are in agreement with those reported in the literature.<sup>131</sup>

**3-(naphthalen-1-yl)acrylic acid (4'e):**  $^1\text{H NMR}$  (360 MHz,  $\text{CDCl}_3$ )  $\delta$  8.52 (d,  $J = 16.0$  Hz, 1H) (*E*), 8.15-8.20 (m, 1H), 7.79-7.95 (m, 3H), 7.72 (d,  $J = 11.6$  Hz, 1H) (*Z*), 7.46-7.61 (m, 3H), 6.54 (d,  $J = 16.0$  Hz, 1H) (*E*), 6.30 (d,  $J = 11.3$  Hz, 1H) (*Z*).

$^{13}\text{C NMR}$  (91 MHz,  $\text{CDCl}_3$ )  $\delta$  170.1, 143.1, 135.3, 132.7, 131.7, 129.8, 128.0, 127.4, 126.6, 126.1, 124.1, 122.0.

The  $^1\text{H NMR}$  and  $^{13}\text{C NMR}$  spectra are in agreement with those reported in the literature.<sup>132</sup>



46% (3'ab:4'f 2:1, E/Z 1/4)

**3-([1,1'-biphenyl]-4-yl)propanoic acid (3'ab):**  $^1\text{H NMR}$  (300 MHz,  $\text{CDCl}_3$ )  $\delta$  7.60-7.55 (m, 2H), 7.55-7.50 (m, 2H), 7.47-7.39 (m, 2H), 7.36-7.31 (m, 1H), 7.31-7.27 (m, 2H), 3.01 (t,  $J = 7.6$  Hz, 2H), 2.73 (t,  $J = 8.0$  Hz, 2H).

$^{13}\text{C NMR}$  (75 MHz,  $\text{CDCl}_3$ )  $\delta$  179.1, 141.1, 139.6, 139.4, 129.0, 128.9, 127.5, 127.4, 127.2, 35.7, 30.4.

The  $^1\text{H NMR}$  and  $^{13}\text{C NMR}$  spectra are in agreement with those reported in the literature.<sup>124</sup>

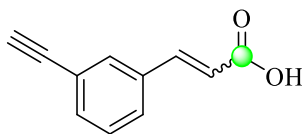
**3-([1,1'-biphenyl]-4-yl)acrylic acid (4'f):**  $^1\text{H NMR}$  (300 MHz,  $\text{CDCl}_3$ )  $\delta$  7.85 (d,  $J = 16.0$  Hz, 1H) (*E*), 7.76–7.29 (m, 9H), 7.12 (d,  $J = 12.7$  Hz, 1H) (*Z*), 6.51 (d,  $J = 15.9$  Hz, 1H) (*E*), 6.03 (d,  $J = 12.7$  Hz, 1H) (*Z*).

<sup>131</sup> M. Lemhadri, H. Doucet, M. Santell, *Tetrahedron* **2004**, *60*, **50**, 11533.

<sup>132</sup> X. Zhao, H. Alper, Z. Yu, *J. Org. Chem.* **2006**, *71*, **10**, 3988.

$^{13}\text{C}$  NMR (91 MHz,  $\text{CDCl}_3$ )  $\delta$  167.5, 143.3, 141.6, 139.2, 133.3, 128.9, 128.8, 127.9, 127.0, 126.6, 119.2.

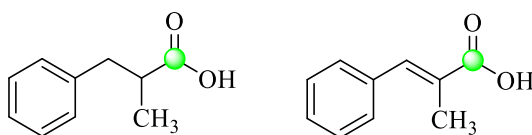
The  $^1\text{H}$  NMR and  $^{13}\text{C}$  NMR spectra are in agreement with those reported in the literature.<sup>133</sup>



**3-(3-ethynylphenyl)acrylic acid (4'g):** 81 mg (0.47 mmol, 47%, *E/Z* 1.2/1).  $^1\text{H}$  NMR (300 MHz,  $\text{CDCl}_3$ )  $\delta$  7.76 (d,  $J = 16.0$  Hz, 1H) (*E*), 7.70 (s, 1H), 7.55 (m, 2H), 7.41 (d,  $J = 7.7$  Hz, 1H), 7.05 (d,  $J = 12.5$  Hz, 1H) (*Z*), 6.48 (d,  $J = 16.0$  Hz, 1H) (*E*), 6.04 (d,  $J = 12.6$  Hz, 1H) (*Z*), 3.14 (s, 1H).

$^{13}\text{C}$  NMR (75 MHz,  $\text{CDCl}_3$ )  $\delta$  170.7, 145.8, 134.3, 134.0, 131.8, 129.0, 128.5, 122.6, 118.1, 82.4, 78.1.

HRMS (m/z)  $[\text{M} + \text{Na}]^+$  calculated 195.0417 found 195.0409.



3'r

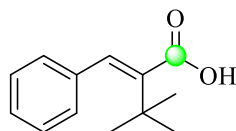
4'h

74% (3'r:4'h 10:1, *E* isomer)

**(E)-2-methyl-3-phenylacrylic acid (4'h):**  $^1\text{H}$  NMR (300 MHz,  $\text{CDCl}_3$ )  $\delta$  7.85 (q,  $J = 1.3$  Hz, 1H), 7.45 (m, 5H), 2.17 (d,  $J = 1.4$  Hz, 3H).

$^{13}\text{C}$  NMR (101 MHz,  $\text{CDCl}_3$ )  $\delta$  174.2, 141.1, 135.7, 129.8, 128.7, 128.3, 127.6, 13.9.

The  $^1\text{H}$  NMR and  $^{13}\text{C}$  NMR spectra are in agreement with those reported in the literature.<sup>134</sup>



**(E)-2-benzylidene-3,3-dimethylbutanoic acid (4'i):** 123 mg (0.6 mmol, 60%, only *E* isomer).  $^1\text{H}$  NMR (360 MHz,  $\text{CDCl}_3$ )  $\delta$  7.39 – 7.25 (m, 5H), 6.61 (s, 1H), 1.36 – 1.22 (m, 9H).

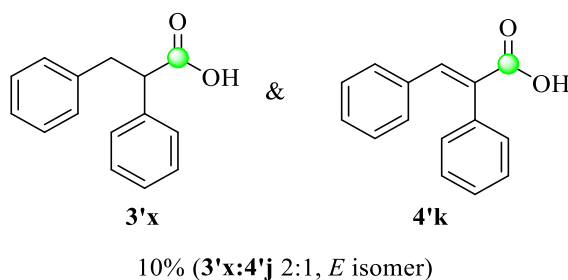
$^{13}\text{C}$  NMR (91 MHz,  $\text{CDCl}_3$ )  $\delta$  175.8, 143.9, 136.1, 128.4, 127.8, 127.7, 127.2, 35.2, 29.4.

HRMS (m/z)  $[\text{M} + \text{Na}]^+$  calculated 227.1043 found 227.1051.

<sup>133</sup> J. J. Matasi, J. P. Caldwell, J. Hao, B. Neustadt, L. Arik, C. J. Foster, J. Lachowicz, D. B. Tulshian, *Biorganic and Medicinal Chem. Lett.* **2005**, *15*, 5, 1333.

<sup>134</sup> Z.-G. Wang, L. Chen, J. Chen, J.-F. Zheng, W. Gao, Z. Zeng, H. Zhou, X. Zhang, P.-Q. Huang, Y. Su, *European Journal of Medicinal Chemistry* **2013**, *62*, 632.





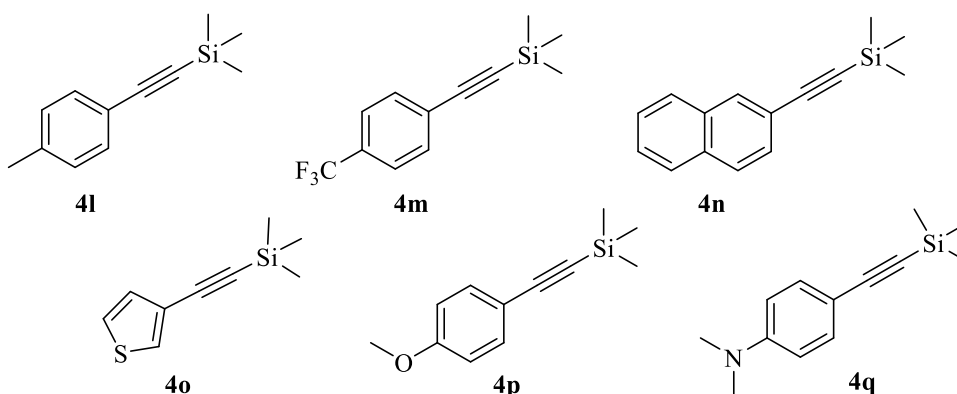
**(E)-2,3-diphenylacrylic acid (4'j):**  $^1\text{H NMR}$  (300 MHz,  $\text{CDCl}_3$ )  $\delta$  7.96 (s, 1 H), 7.50-7.32 (m, 3H), 7.30-7.12 (m, 5H), 7.07 (d,  $J = 7.2$  Hz, 2H).

$^{13}\text{C NMR}$  (75 MHz,  $\text{CDCl}_3$ )  $\delta$  173.1, 142.4, 135.3, 134.3, 131.6, 130.8, 129.7, 129.5, 128.7, 128.3, 128.0.

The  $^1\text{H NMR}$  and  $^{13}\text{C NMR}$  spectra are in agreement with those reported in the literature.<sup>135</sup>

## General Procedure for the synthesis of silyl protected acetylene derivatives

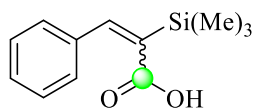
Following a reported procedure in the literature,<sup>136</sup> to a solution of aryl halide (bromide or iodide) (5 mmol, 1.0 equiv), copper iodide  $\text{CuI}$  (0.04 equiv) and  $\text{Pd}(\text{PPh}_3)_2\text{Cl}_2$  (0.02 equiv) in triethylamine  $\text{Et}_3\text{N}$  (5 mL) was added trimethylsilylacetylene (1.2 equiv) dropwise under inert atmosphere. The mixture was heated under an Ar atmosphere at 80 °C for 24 h. After completion of the reaction, it was filtered and the filtrate was treated with water and extracted with DCM (3 \* 20 mL). The combined organic layers were washed with brine, dried over anhydrous  $\text{MgSO}_4$  and concentrated under *vacuo* to yield the crude product. The crude product was purified by column chromatography (0-10%  $\text{EtOAc}/\text{PE}$ ) to give silyl protected acetylene derivatives.



<sup>135</sup> J. Hou, J.-H. Xie, Q.-L. Zhou, *Angew. Chem. Int. Ed.* **2015**, *54*, 6302.

<sup>136</sup> P. Kumar, R. Panyam, R. Sreedharan, T. Gandhi, *Org. Biomol. Chem.* **2018**, *16*, 4357.

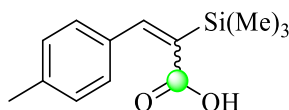
## Characterization of the compounds



**3-phenyl-2-(trimethylsilyl)acrylic acid (4'k):** 132 mg as a white solid (0.6 mmol, 60%).  $^1\text{H NMR}$  (360 MHz,  $\text{CDCl}_3$ )  $\delta$  8.35 (s, 1H) (**Z**), 7.55 – 7.21 (m, 5H) (**E**), 6.89 (s, 1H) (**E**), 0.29 (s, 9H) (**E**), 0.10 (s, 9H) (**Z**).

$^{13}\text{C NMR}$  (101 MHz,  $\text{CDCl}_3$ )  $\delta$  176.7, 155.0, 137.5, 136.5, 128.5, 128.4, 128.0, 0.3.

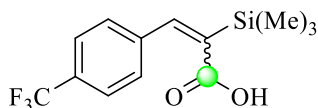
**HRMS (m/z) [M + Na]<sup>+</sup> calculated 243.0812 found 243.0807.**



**3-(p-tolyl)-2-(trimethylsilyl)acrylic acid (4'l):** 105 mg as a white solid (0.45 mmol, 45 %).  $^1\text{H NMR}$  (360 MHz,  $\text{CDCl}_3$ )  $\delta$  8.31 (s, 1H) (**Z**), 7.26 – 7.07 (m, 4H), 6.86 (s, 1H) (**E**), 2.39 (s, 3H) (**Z**), 2.35 (s, 3H) (**E**), 0.11(s, 9H) (**E**), 0.09 (s, 9H) (**Z**).

$^{13}\text{C NMR}$  (101 MHz,  $\text{CDCl}_3$ )  $\delta$  176.5, 155.3, 138.7, 135.7, 134.7, 128.7, 128.6, 21.3, 0.4.

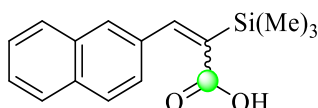
**HRMS (m/z) [M + Na]<sup>+</sup> calculated 257.0968 found 257.0963.**



**3-(4-(trifluoromethyl)phenyl)-2-(trimethylsilyl)acrylic acid (4'm):** 158.5 mg as a yellow solid (0.55 mmol, 55%).  $^1\text{H NMR}$  (360 MHz,  $\text{CDCl}_3$ )  $\delta$  8.30 (s, 1H) (**Z**), 7.7-7.41 (m, 4H), 6.89 (s, 1H) (**E**), 0.3 (s, 9H) (**E**), 0.09 (s, 9H) (**Z**).

$^{13}\text{C NMR}$  (101 MHz,  $\text{CDCl}_3$ )  $\delta$  173.5, 152.8, 138.3, 129.8 (q,  $J = 31.9$  Hz), 128.9, 125.7 (q,  $J = 3.7$  Hz), 124.0 (q,  $J = 272.2$  Hz), 122.2, -2.31.

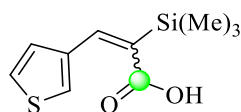
**HRMS (m/z) [M + Na]<sup>+</sup> calculated 311.0686 found 311.0678.**



**3-(naphthalen-2-yl)-2-(trimethylsilyl)acrylic acid (4'n):** 138 mg as a yellow solid (0.51 mmol, 51%).  $^1\text{H NMR}$  (300 MHz,  $\text{CDCl}_3$ )  $\delta$  9.00 (s, 1H) (**Z**), 8.48-7.51 (m, 7H), 6.67 (s, 1H) (**E**), 0.34 (s, 9H) (**E**), 0.32 (s, 9H) (**Z**).

$^{13}\text{C}$  NMR (101 MHz,  $\text{CDCl}_3$ )  $\delta$  175.1, 152.3, 133.8, 133.6, 133.5, 133.2, 128.7, 128.2, 128.1, 127.8, 126.4, 126.0, 125.7, 0.5.

HRMS (m/z)  $[\text{M} + \text{Na}]^+$  calculated 293.0968 found 293.0950.

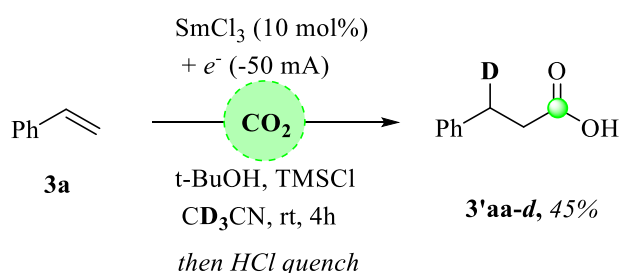


**3-(thiophen-3-yl)-2-(trimethylsilyl)acrylic acid (4'o):** 120 mg as a white solid (0.53 mmol, 53%).  $^1\text{H}$  NMR (300 MHz,  $\text{CDCl}_3$ )  $\delta$  8.17 (s, 1H) (**Z**), 7.52 – 7.45 (m, 1H), 7.34 (dd,  $J = 4.9, 3.0$  Hz, 1H), 7.08 (dd,  $J = 4.9, 1.2$  Hz, 1H), 6.85 (s, 1H) (**E**), 0.28 (s, 9H) (**E**), 0.15 (s, 9H) (**Z**).

$^{13}\text{C}$  NMR (101 MHz,  $\text{CDCl}_3$ )  $\delta$  177.35, 138.03, 135.97, 134.68, 127.29, 126.7, 125.8, -1.6.

HRMS (m/z)  $[\text{M} + \text{Na}]^+$  calculated 249.0376 found 249.0372.

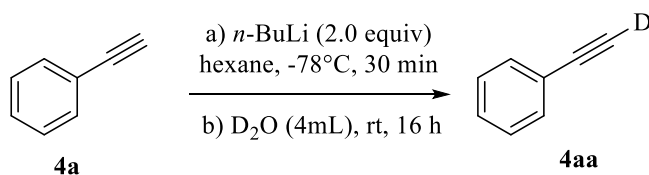
## Deuterium labeling experiments



Following the general procedure for the hydrocarboxylation of styrene derivatives, using **3a** (0.5 mmol),  $\text{SmCl}_3$  (12.25 mg, 0.1 equiv),  $t\text{-BuOH}$  (0.5 mL, 10 equiv) and  $\text{TMSCl}$  (0.5 mL, 8.0 equiv) in 20 mL deuterated acetonitrile  $\text{CD}_3\text{CN}$ . The isolated product **3'aa-d** was obtained with 45% yield, with >90% deuterium incorporation at the  $\alpha$ -position of the hydrocarboxylated products.

**3'aa-d:**  $^1\text{H}$  NMR (300 MHz,  $\text{CDCl}_3$ )  $\delta$  7.38 – 7.18 (m, 5H), 2.96 (m, 1H), 2.71 (d,  $J = 7.6$  Hz, 2H).

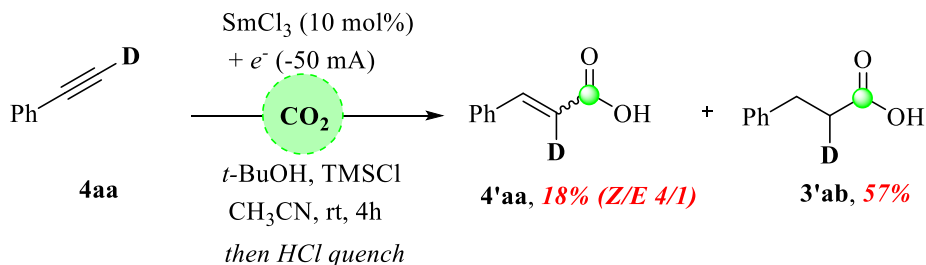
HRMS (m/z)  $[\text{M} + \text{Na}]^+$  calculated 174.0636 found 174.0634.



Following a reported procedure in the literature,<sup>137</sup> to a solution of phenylacetylene **4a** (0.55 mL, 5 mmol) in dry hexane (10 ml) was added  $n\text{-BuLi}$  (5.2 mL, 1.6 M in hexane solution, 2.0 equiv),

<sup>137</sup> J.-S. Zhang, J.-Q. Zhang, T. Chen, L.-B. Han, *Org. Biomol. Chem.* **2017**, *15*, 5462

dropwise, at  $-78^{\circ}\text{C}$  under argon atmosphere. After being stirred at the same temperature for 30 min,  $\text{D}_2\text{O}$  (4 mL) was added at the room temperature and the reaction was stirred continuously at the same temperature for 16 h. The organic layer was separated and the aqueous layer was extracted with  $\text{CH}_2\text{Cl}_2$  (3\*10 mL). The combined organic layer was dried over  $\text{MgSO}_4$  and filtered. The filtrate was concentrated *in vacuo* to afford the (ethynyl-d)benzene **4aa** with 99% deuterium incorporation.



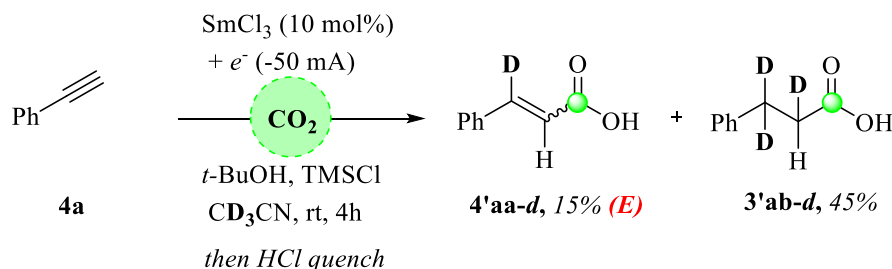
Following the general procedure for the hydrocarboxylation of phenylacetylene derivatives, using **4aa** (1 mmol),  $\text{SmCl}_3$  (0.1 equiv), *t*-BuOH (20 equiv) and TMSCl (6.0 equiv) in 40 mL acetonitrile. The isolated products **4'aa** and **4'ab** were obtained 75% yield, with >98% deuterium incorporation at the  $\beta$ -position of the hydrocarboxylated products.

**4'aa**:  $^1\text{H NMR}$  (300 MHz,  $\text{CDCl}_3$ )  $\delta$  7.82 (s, 1H), 7.68-7.52 (m, 2H), 7.47-7.28 (m, 3H), 7.11 (s, 1H).

**HRMS** (m/z)  $[\text{M} + \text{Na}]^+$  calculated 172.0479 found 172.0530.

**3'ab**:  $^1\text{H NMR}$  (300 MHz,  $\text{CDCl}_3$ ) 7.37-7.21 (m, 5H), 3.01 (d,  $J = 7.5$  Hz, 2H), 2.73 (t,  $J = 7.5$  Hz, 1H).

**HRMS** (m/z)  $[\text{M} + \text{Na}]^+$  calculated 174.0636 found 174.065.



Following the general procedure for the hydrocarboxylation of phenylacetylene derivatives, using **4a** (0.5 mmol),  $\text{SmCl}_3$  (0.1 equiv), *t*-BuOH (20 equiv) and TMSCl (6.0 equiv) in 20 mL deuterated acetonitrile  $\text{CD}_3\text{CN}$ . The isolated products **4'aa-d** and **3'ab-d** were obtained 60% yield, with >80% deuterium incorporation at the  $\alpha$  and  $\beta$ -positions of the hydrocarboxylated products.

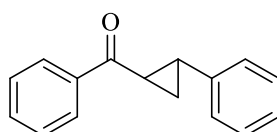
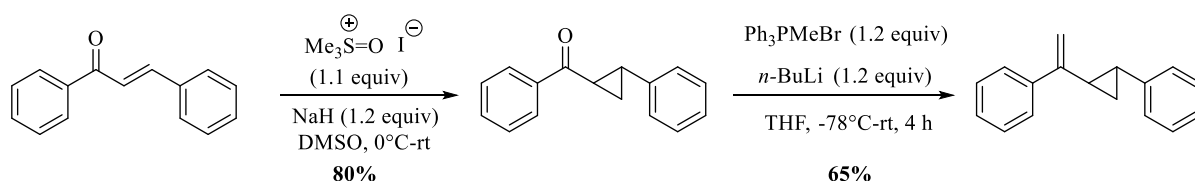
**4'aa-d**:  $^1\text{H NMR}$  (360 MHz,  $\text{CDCl}_3$ )  $\delta$  7.6-7.2 (m, 5H), 6.46 (s, 1H) (*E*), 2.98 (s, 0.4H), 2.69 (s, 1H).

**HRMS** (m/z)  $[\text{M} - \text{H}]^-$  calculated 148.0514 found 148.2449.

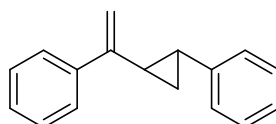
**3'ab-d**:  $^1\text{H NMR}$  (360 MHz,  $\text{CDCl}_3$ )  $\delta$  7.36 – 7.17 (m, 5H), 2.98 (s, 0.41H), 2.68 (s, 1H).

**HRMS** (m/z)  $[\text{M} - \text{H}]^-$  calculated 152.0796 found 152.2692.

## Radical clock experiment

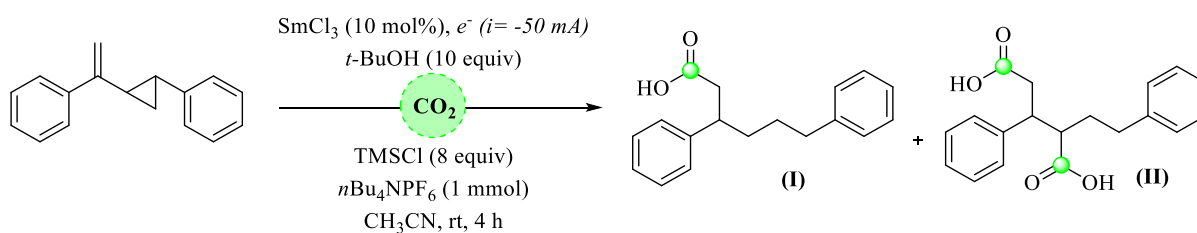
**Synthesis of (1-(2-Phenylcyclopropyl)vinyl)benzene:** <sup>138</sup>

To a two-necked round flask, sodium hydride (6.0 mmol, 1.2 equiv) was added. In dry DMSO (17 mL,) trimethylsulfoxonium iodide (5.5 mmol, 1.1 equiv) was added to the flask under argon atmosphere. The flask was immersed in an ice bath and a solution of chalcone (5 mmol, 1.0 equiv) in dry DMSO (5 mL) was added to the reaction mixture. After completion, the reaction mixture was extracted with ether. The crude product was purified by flash column chromatography with eluent (petroleum ether/ethyl acetate = 10:1) to afford phenyl(2-phenyl cyclopropyl)methanone with 80% yield.

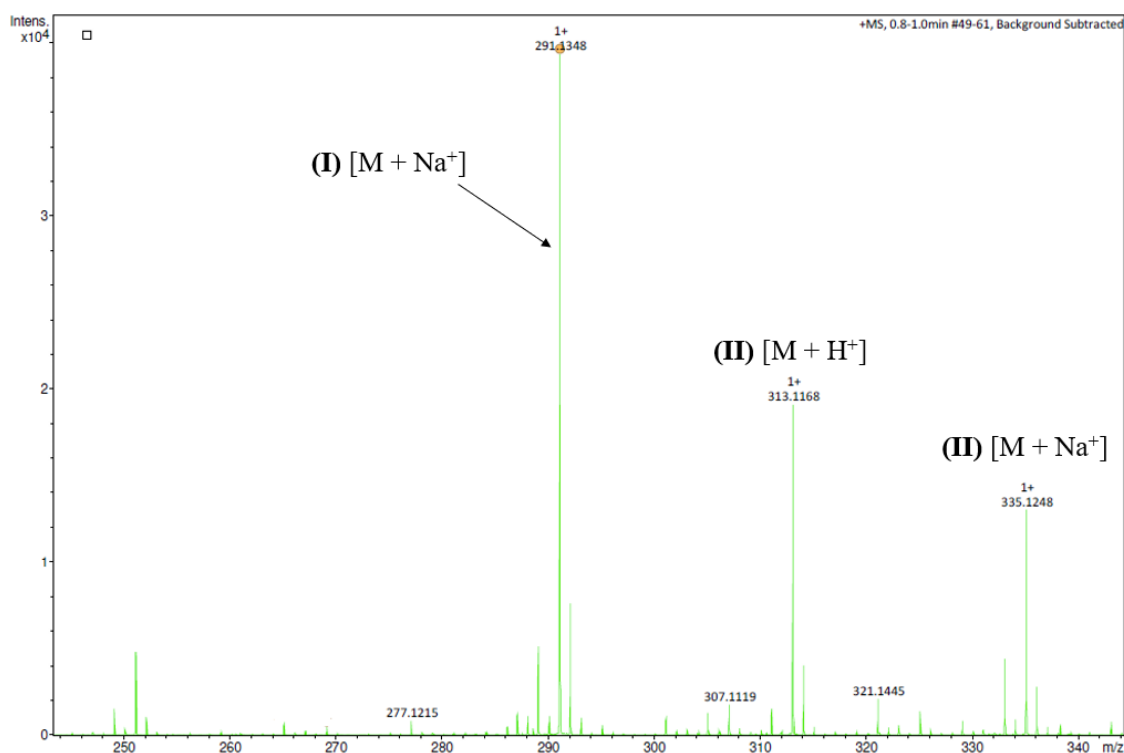


The reaction vessel was charged with phosphonium salt (1.2 equiv) in dry THF. To the stirred mixture, *n*-BuLi (1.2 equiv) was added under argon atmosphere at -78 °C. The mixture was stirred at 0° C for 5 mins and then substituted phenyl(2-phenyl cyclopropyl)methanone (1.0 equiv) in dry THF was added dropwise over 15 min. After stirring at rt for 4 h, the mixture was quenched with saturated NH<sub>4</sub>Cl, then was extracted with CH<sub>2</sub>Cl<sub>2</sub> (3\*15 mL). The combined organic layers were dried over anhydrous sodium sulfate, concentrated and purified by column chromatography (100% PE) to give the (1-(2-Phenylcyclopropyl)vinyl)benzene with 65% yield.

**Radical Clock experiment:**



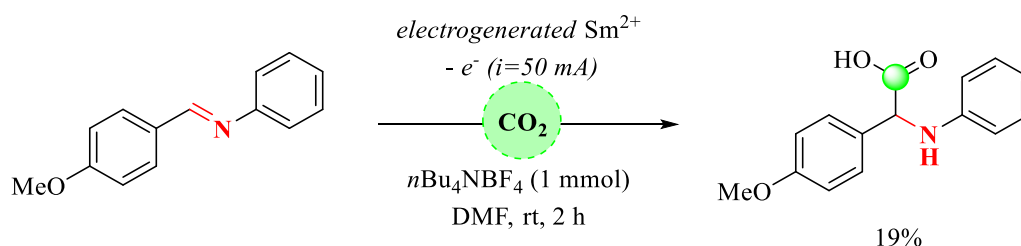
Following the general procedure for the hydrocarboxylation of styrene derivatives, using 1-(2-Phenylcyclopropyl)vinyl)benzene (1 mmol),  $\text{SmCl}_3$  (0.1 equiv),  $t\text{-BuOH}$  (10 equiv) and  $\text{TMSCl}$  (8.0 equiv) in 40 mL acetonitrile for 4 hours. After treatment, the obtained crude was analyzed by **HRMS** and gave the spectra below:



**HRMS (I) [M + Na<sup>+</sup>] calculated 291.1356 found 291.1348**

**HRMS (II) [M + H<sup>+</sup>] calculated 313.1434 found 313.1168; HRMS (II) [M + Na<sup>+</sup>] calculated 335.1254 found 335.1248**

## Synthesis of 2-(4-methoxyphenyl)-2-(phenylamino)acetic acid using electrogenerated divalent samarium



The reaction was carried out in an undivided cell containing a magnetic stirring bar, equipped with a samarium rod as anode and a stainless-steel as the cathode. The cell was charged with 322 mg of tetrabutylammonium tetrafluoroborate  $n\text{Bu}_4\text{NBF}_4$  (1 mmol) and (*E*)-1-(4-methoxyphenyl)-*N*-phenylmethanimine (211 mg, 1 mmol) dissolved in 50 mL of DMF. The electrolysis was started using a chronopotentiometry mode with  $i = 50 \text{ mA}$  for 7200 seconds. When the substrate was no longer detected on the TLC, the reaction was quenched with  $\text{Et}_2\text{O}$  and the DMF was evaporated under *vacuo*. 1 M NaOH (30 mL) was added to the obtained solid and the mixture was extracted with  $\text{Et}_2\text{O}$  (3\*30 mL). the aqueous phase was then acidified with 2 M HCl to pH=4, a yellow solid precipitated. The obtained precipitation was filtered and dried under *vacuo* to obtain 40 mg of the 2-(4-methoxyphenyl)-2-(phenylamino)acetic acid (0.019 mmol, 19%).

$^1\text{H NMR}$  (360 MHz,  $\text{C}_6\text{D}_6$ )  $\delta$  7.41 (d,  $J = 8.7 \text{ Hz}$ , 2H), 7.19 – 7.11 (m, 3H), 6.80 – 6.76 (m, 2H), 6.57 (dd,  $J = 8.2, 4.0 \text{ Hz}$ , 2H), 5.03 (s, 1H), 3.31 – 3.25 (m, 3H).

$^{13}\text{C NMR}$  (63 MHz, DMSO)  $\delta$  173.6, 159.4, 147.4, 130.8, 129.1, 129.0, 116.9, 114.3, 113.5, 59.5, 55.5.

**HRMS (m/z) [M - H]<sup>-</sup> calculated 256.0979 found 256.0985.**





**Titre: Activation électrochimique du CO<sub>2</sub> initié par le samarium divalent : Applications dans la synthèse des acides carboxyliques.**

**Mots clés :** Réduction du CO<sub>2</sub>, Samarium divalent, Electrochimie, Catalyse, Acides Carboxyliques

**Résumé:** La réduction du CO<sub>2</sub> est considérée comme une des approches les plus intéressantes pour convertir ce gaz en produits chimique d'intérêt tels que les acides carboxyliques. Le marché de ces composés devrait augmenter considérablement au cours des prochaines années, d'où la nécessité de trouver des méthodes de production durables et respectueuses de l'environnement.

Les complexes de samarium divalents sont reconnus pour leur fort pouvoir réducteur monoélectronique, ce qui en fait des réactifs de choix pour la réduction de certains groupes fonctionnels difficiles à réduire tels que le CO<sub>2</sub>. Cependant, dans la littérature, bien que ce réactif ait été utilisé en association avec le CO<sub>2</sub>, prouvant ainsi que la réduction du CO<sub>2</sub> est possible, mais jamais à notre connaissance pour des applications synthétiques.

Nous rapportons ici l'activation du CO<sub>2</sub> initiée par le samarium bivalent électrogénéré. Grâce à notre méthode, récemment mise au point, pour la production électrochimique *in situ* d'espèces divalentes de samarium, la synthèse de dérivés de l'acide benzoïque a été réalisée avec succès. De plus, les conditions d'activation electrocatalytique du CO<sub>2</sub> ont été établies dans ce travail et appliquées non seulement à la préparation des acides phénylacétiques à partir de dérivés du chlorure de benzyle, mais également à l'hydrocarboxylation régiosélective des analogues du styrène et du phénylacétylène. Ce protocole à base de Sm (II) électrogénéré offre la prochaine génération de systèmes durables pour la transformation du CO<sub>2</sub> en molécules de haute valeur sous des conditions douces et sans l'ajout de co-réducteurs.

**Title:** Electrogenated divalent samarium for CO<sub>2</sub> activation: applications in carboxylic acid synthesis.

**Keywords:** CO<sub>2</sub> activation, divalent samarium, electrocatalytic carboxylation, hydrocarboxylation.

**Abstract:** CO<sub>2</sub> activation is considered one of the most attractive tools to convert this cheap, abundant and non-toxic gas into valuable chemical feedstocks such as carboxylic acids. The market value of these compounds is expecting a significant increase in the next few years, thus the urgent need for sustainable and eco-friendly production pathways.

Divalent samarium complexes are known for their strong mono-electronic reductive power that made them the perfect choice for the reduction of some challenging functional groups. Indeed, in the literature, this reagent has been used in combination with CO<sub>2</sub> but only to achieve the reductive disproportionation of CO<sub>2</sub> while no example reported C-C bond formation via CO<sub>2</sub> activation using the Sm(II) complexes.

Herein, we report the CO<sub>2</sub> activation initiated by electrogenerated divalent samarium. Taking advantage of our recently developed method for the *in situ* generation of Sm(II) species, the synthesis of benzoic acid derivatives was successfully achieved. Furthermore, electrocatalytic CO<sub>2</sub> activation conditions were established in this work and applied not only for the preparation of phenylacetic acids from benzyl chloride derivatives but also for the regioselective hydrocarboxylation of styrene and phenylacetylene analogs. This electrochemical Sm(II)-based protocol offers the next generation of sustainable system to transform CO<sub>2</sub> into highly valued molecules under mild conditions and without the addition of co-reductants.